Universidad de Concepción
Dirección de Postgrado
Facultad de Ciencias Físicas y Matemáticas
Programa de Doctorado en Ciencias Aplicadas
con Mención en Ingeniería Matemática

MÉTODOS DE GALERKIN DISCONTINUOS EN MECÁNICA DEL MEDIO CONTINUO

(DISCONTINUOUS GALERKIN METHODS IN CONTINUUM MECHANICS)

Tesis para optar al grado de Doctor en Ciencias
Aplicadas con mención en Ingeniería Matemática

Felipe Ricardo Vargas Martínez
concepción-chile
2018

Profesor Guía: Manuel Solano Palma
CI^{2}MA y Departamento de Ingeniería Matemática,
Universidad de Concepción, Chile.

Cotutor: Jay Gopalakrishnan
Fariborz Maseeh Department of Mathematics and Statistics,
Portland State University, Portland, OR, USA.

Discontinuous Galerkin Methods in Continuum Mechanics

Felipe Ricardo Vargas Martínez

Directores de Tesis: Manuel Solano P., Universidad de Concepción, Chile.
Jay Gopalakrishnan, Portland State University, Portland, OR, USA.

Director de Programa: Rodolfo Rodríguez A., Universidad de Concepción, Chile.

Comisión evaluadora

Prof. Erik Burman, University College London, UK.

Prof. Sander Rhebergen, University of Waterloo, Canada.

Prof. Filánder Sequeira, Universidad Nacional, Costa Rica.

Prof. Ke Shi, Old Dominion University, USA.

Comisión examinadora

Firma: _____
Prof. Rodolfo Araya, Universidad de Concepción, Concepción, Chile.

Firma: _____
Prof. Ricardo Oyarzúa, Universidad del Bío-Bío, Concepción, Chile.

Firma: _____
Prof. Manuel Sánchez–Uribe, Pontificia Universidad Católica de Chile, Santiago, Chile.

Calificación: _____

Concepción, Diciembre de 2018

Abstract

This thesis addresses two main topics. First, we apply and analyse a high order hybridizable discontinuous Galerkin (HDG) method to two interesting problems in the context of fluid mechanics, which are Stokes problem and Oseen equations. The novelty of this part is that curved domains are considered instead of polyhedral domains. The analysis is based on approximating the curved domain by a polyhedral computational subdomain where an HDG solution can be computed. To obtain a high order approximation of the Dirichlet boundary data in the computational domain, we employ a transferring technique based on integrating the approximation of the gradient of the velocity. In addition, we first seek for a discrete pressure having zero-mean in the computational domain and then the zero-mean condition in the entire domain is recovered by a post-process that involves an extrapolation of the discrete pressure. Since the problems we are interested on are modelled by similar sets of equations (there is only one additional term in Oseen equations), the treatment of the boundary condition and pressure is the same for both problems. We prove that the method provides optimal order of convergence for the approximations of the pressure, the velocity and its gradient, that is, order h^{k+1} if the local discrete spaces are constructed using polynomials of degree k and the meshsize is h. Numerical experiments validating the method are presented.
Secondly, we also present a dispersion analysis of HDG methods. Considering the Helmholtz system, we quantify the discrepancies between the exact and discrete wavenumbers. In particular, we obtain an analytic expansion for the wavenumber error for the lowest order Single Face HDG (SFH) method. The novel result of this part is that the expansion shows that the SFH method exhibits convergence rates of the wavenumber errors comparable to that of the mixed hybrid Raviart–Thomas (HRT) method. In addition, the same behavior for the higher order cases is observed in numerical experiments.

Resumen

Esta tesis aborda dos temas principales. Primero, aplicamos y analizamos un método de Galerkin Discontinuo Hybridizado (HDG, por sus siglas en inglés) a dos problemas interesantes en el contexto de la Mecánica de Fluidos, que son el Problema de Stokes y las Ecuaciones de Oseen. La novedad de esta parte es que se consideran dominios curvos en vez de dominios poliédricos. El análisis está basado en aproximar el dominio curvo por un subdominio poliédrico en el que se puede calcular una solución numérica. Para obtener una aproximación de alto orden del dato Dirichlet en la frontera computacional, empleamos una técnica de transferencia basada en integrar la aproximación del gradiente de la velocidad. Además, primero buscamos una presión discreta que tenga media nula en el dominio computacional y la condición de media nula en el dominio completo es recuperada a través de un post–proceso. Dado que los problemas en los que estamos interesados son modelados por conjuntos de ecuaciones similares (sólo hay un término adicional en las Ecuaciones de Oseen), el tratamiento de la condición de frontera y de la presión es el mismo para ambos problemas. Demostramos que el método entrega órdenes de convergencia óptimos para las aproximaciones de la presión, velocidad y su gradiente, esto es, orden h^{k+1} si los espacios discretos locales se construyen usando polinomios de grado k y el tamaño de la malla es h. Se presentan ensayos numéricos que validan el método.
En segundo lugar, presentamos también un análisis de dispersión de métodos HDG. Considerando el sistema de Helmholtz, cuantificamos las diferencias entre los números de onda exacto y aproximado. En particular, obtenemos una expansión analítica para el error del número de onda para el método Single Face HDG (SFH) del orden más bajo. El resultado novedoso de esta parte es que la expansión muestra que el método SFH entrega órdenes de convergencia del número de onda que son comparables a las del método mixto Raviart–Thomas híbrido (HRT). Además, el mismo comportamiento se observa en ensayos numéricos para los casos de órdenes más altos.

Agradecimientos

En primer lugar, agradezco a Dios por su infinita bondad. Él es el dueño de todo el conocimiento, la ciencia y la sabiduría, y nada sucede sin que Él lo permita. Él es quien da dones y talentos a las personas, y todo lo que yo pueda lograr es gracias a su infinita misericordia para conmigo.

En segundo lugar, agradezco a mi familia: mi abuelita Ruth, mi mamá Cristina, mi hermano Adolfo y mi papá Adolfo. No ha sido un camino corto, no ha sido fácil, han sido años de lejanía física, y agradezco el apoyo espiritual y emocional que siempre me han brindado. Los amo mucho y deseo que el Señor nos bendiga como familia siempre, y extienda esta bendición a nuestros demás familiares que no menciono aquí, pero que también de una u otra forma me han acompañado en estos años.

Igualmente, agradezco mucho a mis profesores guía: a Manuel, por tantas horas de trabajo, reuniones, tiempo invertido en explicarme códigos computacionales, y tratando también muchas veces de encontrar errores en los que yo intentaba hacer; eres un gran académico, y también una gran persona. No tengo más que excelentes deseos para ti. Y también agradezco especialmente al Dr. Jay Gopalakrishnan, quien tuvo la disposición primero de ser co–director de esta tesis doctoral, y posteriormente de recibirme como visitante en Portland. Haber podido trabajar con alguien con tanto renombre como usted en el área de métodos HDG ha sido realmente un privilegio, y espero poder continuar haciéndolo.

No puedo dejar de agradecer al Departamento de Ingeniería Matemática de la Universidad de Concepción, por permitir integrarme al grupo de docentes part–time y poder así financiar parcialmente mis últimos meses de estudio, y también al Centro de Investigación en Ingeniería Matemática (CI^2MA) por la formación entregada durante estos años; en particular, a los profesores Raimund Bürger, por su labor como docente, y especialmente por su excelente gestión como director del programa de doctorado en los años en que desempeñó ese cargo; al profesor Gabriel Gatica, como director del Centro CI^2MA, por proveernos de un excelente lugar, con cómodas oficinas y condiciones que no en todos lados se dan (cuando uno sale a pasantías se da cuenta de cómo es la realidad en otros lugares). Y también a los profesores Leonardo Figueroa, Mauricio Sepúlveda y Rodolfo Rodríguez, con quienes tomé ramos durante mis años de estudiante de doctorado.

Agradezco a Conicyt–Chile, que a través de su programa de Formación de Capital Humano Avanzado y Proyecto Fondecyt No. 1160320; y proyecto AFB170001 del Programa PIA: Concurso Apoyo a Centros Científicos y Tecnológicos de Excelencia con Financiamiento Basal, han financiado parcial-

mente mis estudios a lo largo de todos estos años.

No quiero dejar fuera a todos mis amigos, hermanos en la fe, y también a mis compañeros de doctorado, por tantos buenos ratos de compañerismo, tantos buenos momentos jugando fútbol, basketball, y últimamente también en los almuerzos. A la Sra. Lorena Carrasco, funcionaria del Centro CI^{2}MA, por su excelente disposición cuando uno le pedía alguna ayuda.

También, agradezco a mis tíos Rogers y Nena, y a su familia, por haberme permitido vivir con ellos cerca de dos años y medio. Fue de mucha tranquilidad para mi familia y para mí haber podido estar en un hogar cálido y de confianza, donde me sentía como uno más de casa.

Finalizo agradeciendo también a mi Vivi, que ha venido a alegrar mi vida en estos últimos meses, y a su acogedora familia, que me han integrado y considerado como uno más de ellos.

Sinceramente,

Felipe Ricardo Vargas Martínez.

Contents

List of Tables

List of Figures

Introduction

Discontinuous Galerkin (DG) methods have been extensively studied and used to solve different kind of problems. In particular, Hybridizable Discontinuous Galerkin (HDG) methods have been proposed in [17]. Hybridization of Discontinuous Galerkin (DG) methods arises as an alternative to reduce the number of globally coupled degrees of freedom of DG methods. In the context of diffusion problems, [17] introduced a unifying framework for hybridization of DG methods, where the only globally coupled degrees of freedom are those of the numerical traces on the inter–element boundaries and the remaining unknowns are obtained by solving local problems on each element. Since then, HDG methods have been widely used to approximate the solution of a variety of problems. In the context of fluid mechanics, they have been introduced for Stokes flow equations [16, 18, 22, 52], quasi–Newtonian Stokes flow [34, 35], Stokes–Darcy coupling [36], Brinkman problem [4, 33, 37], Oseen equations [11] and Navier–Stokes equations [12, 53, 56, 57, 61, 63], among others.
In the first part of this thesis, we will present a high order HDG method to numerically solve the Stokes equations of an incompressible fluid flow occupying a region $\Omega \subset \mathbb{R}^d$ not necessarily polygonal ($d = 2$) or polyhedral ($d = 3$) with boundary $\Gamma := \partial\Omega$ compact, Lipschitz and piecewise $\mathcal{C}^2$. More precisely, denoting by $\boldsymbol{u}$ the velocity of the fluid, p the pressure, $\nu > 0$ a constant viscosity, $\boldsymbol{f} \in [L^2(\Omega)]^d$ a source term and $\boldsymbol{g} \in [L^2(\Gamma)]^d$ the prescribed velocity at the boundary satisfying the compatibility condition $\int_\Gamma \boldsymbol{g} \cdot \boldsymbol{n} = 0$ ($\boldsymbol{n}$ is the outward unit normal to Ω), the equations to solve are

$$\mathrm{L} - \nabla \boldsymbol{u} = 0 \quad \text{in } \Omega, \tag{1a}$$
$$-\nabla \cdot (\nu \mathrm{L}) + \nabla p = \boldsymbol{f} \quad \text{in } \Omega, \tag{1b}$$
$$\nabla \cdot \boldsymbol{u} = 0 \quad \text{in } \Omega, \tag{1c}$$
$$\boldsymbol{u} = \boldsymbol{g} \quad \text{on } \Gamma, \tag{1d}$$
$$\int_\Omega p = 0. \tag{1e}$$

Following this, the next step is to solve the incompressible Ossen equations, given by

$$\mathrm{L} - \nabla \boldsymbol{u} = 0 \quad \text{in } \Omega, \tag{2a}$$
$$-\nu \nabla \cdot \mathrm{L} + (\boldsymbol{\beta} \cdot \nabla)\boldsymbol{u} + \nabla p = \boldsymbol{f} \quad \text{in } \Omega, \tag{2b}$$
$$\nabla \cdot \boldsymbol{u} = 0 \quad \text{in } \Omega, \tag{2c}$$
$$\boldsymbol{u} = \boldsymbol{g} \quad \text{on } \Gamma, \tag{2d}$$
$$\int_\Omega p = 0, \tag{2e}$$

where the convective velocity is assumed to satisfy $\boldsymbol{\beta} \in [W^{1,\infty}(\Omega)]^d$ and to be divergence free.

In both cases, we have to deal with a curved domain. The main idea is to approximate Ω by a polyhedral computational domain where the boundary data $\boldsymbol{g}$ is properly transferred to the computational boundary. We follow the approach proposed by [23] and analyzed in [21] that consists of integrating the approximation of the gradient along *transferring paths* connecting the computational boundary and Γ. This technique allows us to obtain a high order approximation of the boundary data in the computational domain which leads to a high order accuracy of the discrete solution. More precisely, if polynomials of degree k are used to construct the local discrete spaces, the error in the variables L, $\boldsymbol{u}$ and p, measured in L^2-norm, will be of order h^{k+1}, where h is the meshsize. This technique has been recently applied to several problems and shown to perform properly. However, to the best of our knowledge, this is the first work that applies it to the Stokes flow problem where the main difference with previous work is the treatment of the approximated pressure in the computational domain. One of the first ideas based on this transferring technique was introduced by [20] for the one-dimensional case and then extended to higher dimensions for pure diffusion [21, 23] and convection-diffusion [24] equations. In all these work, Dirichlet boundary data was considered and the mesh does not fit the domain. It was shown that high order accuracy is obtained if the distance between the computational domain and the boundary is of only order h. Recently, a similar approach was proposed and studied numerically for Neumann boundary conditions and elliptic interface problems [62]. There, the Neumann data cannot be treated in the same way as Dirichlet data and the computational boundary/interface in [62] must be of order h^2 away from the true boundary/interface in order to obtain optimal results. Roughly speaking, the Neumann data in [62] is imposed by extrapolating the discrete gradient, whereas the Dirichlet data is imposed by performing a line integration of the discrete gradient. This integral is over a segment of length proportional to h, hence it provides a power of h that overcomes the fact that the distance between Γ and the computational boundary is of only of order h.

Let us briefly discuss some of the literature related to numerical methods for differential equations involving curved boundaries or interfaces. In general, these methods can be classified as *fitted* or *unfitted*. In *fitted* methods, the discretization of the domain resolves the boundary/interface, up to some degree of accuracy. For instance, this is the case of isoparametric finite elements [48] where the mapping from the reference element to a physical element is a polynomial whose degree is the same as the polynomial degree of the finite element space. In this direction, [6] considers a finite element approximation for smooth elliptic interfaces where optimal convergence rates are obtained if the mesh isoparemetrically fits the interface. For piecewise linear approximation of a Dirichlet boundary value problem, [8] approximates data at the computational boundary Γ_h by transferring the boundary data g in a *natural way*. That is, for $x \in \Gamma_h$ and a suitably defined $\bar{x} \in \Gamma$ such that $|x - \bar{x}|$ is of order h^2, the computational boundary data, $\widetilde{g}$, is set as $\tilde{g}(x) := g(\bar{x})$. The same idea was extended later to interface problems [9]. As we will see in (1.2), in some sense our technique can be seen as a generalization where we add an additional term to the *natural way* of transferring. For a high order H-div-conforming method to solve elliptic interface problems we refer to [50]. There, the curved interface is locally interpolated by splines and optimal convergence is obtained for a suitable chosen spline degree. Fitted methods have been also applied to control problems in curved domains [29], where only polynomials of degree one are considered. In general, one of the main advantages of fitted methods is that the prescribed data at the boundary/interface can be easily imposed. However, the construction of the meshes might be difficult, especially in complicated geometries. On the other hand, the attractive

feature of unfitted methods is that the mesh is not adjusted to the domain and even Cartesian grids can be considered. However, it is not straightforward to develop a high order unfitted method, mainly because of imposition of the boundary/interface data away from the true boundary/interface. In the context of finite differences, one of the most popular unfitted method is the Immersed Boundary (IB) method introduced by [58] in 1972. For the two dimensional case, [51] showed that it is a first order method for the velocity of a Stokes flow and second order accuracy can be achieved away from the interface. Later, in the same direction, LeVeque and Li developed the Immersed Interface method [49], which is second order accurate. In the context of finite element method, [7] proposed an unfitted method based on Nitsche's approach [54] with the polygonal domain approximation method [67]. There, the numerical scheme is posed in a polygonal domain and a correction term is added to Nitsche's bilinear form in order to obtain high order accuracy. Recently, a high-order finite element method was proposed to solve elliptic interface problems [44]. It is also based on a term involving a piecewise polynomial correction function which is added to the functional at the right hand side. This correction function is suitable constructed a priori using the information provided by the equation and the transmission conditions at the interface. Similarly, an HDG method based also on pre–computing a correction function was proposed and analyzed in [32]. Finally, we would like to mention an alternative approach, the Composite Finite Elements [59, 60], that deals with complicated domains involving rough boundaries or small holes inside. However, to the best of our knowledge, it has not been developed for high order approximations.

Our aim is to develop a method that combines the flexibility of the mesh construction of unfitted methods with the high order accuracy of fitted methods. In fact, the main advantage of our technique is that the computational domain is easy to build and there is no need to adjust it to the actual domain. Moreover, the way we transfer the Dirichlet data allows us to consider high order polynomials in the discrete spaces and obtain high order accuracy. On the other hand, one of the drawbacks of our method compared to others is that it relies on two aspects of the PDE: (1) $\nabla \boldsymbol{u}$ must be part of the equation and (2) $\boldsymbol{u} = \boldsymbol{g}$ at Γ. In addition, the resulting global matrix is not symmetric in our case. Symmetrizing the method is subject of future work. We believe our technique is, in principle, independent on the numerical method, as long the gradient is properly approximated and the PDE has the aforementioned characteristics. In fact, mixed methods for diffusion problems have also been successfully combined with this transferring technique [55].

Chapter 2 of this thesis shows the details of the results obtained when applying this technique to the Stokes problem (1). This work has been accepted for publicaction in the Journal of Scientific Computing. A pre-print is available in

[65] M. Solano and F. Vargas, *A high order HDG method for Stokes flow in curved domains.* https://www.ci2ma.udec.cl/publicaciones/prepublicaciones/prepublicacion.php?id=227, (2016).

On the other hand, Chapter 3 of this thesis contains the results of the application of our technique to Oseen equations (2). These results will be submitted to an ISI journal in a few days.

The other focus of this thesis is to perform a dispersion analysis of HDG methods for the Helmholtz

equation, which is given by

$$ik\boldsymbol{u} + \nabla\phi = \boldsymbol{0} \quad \text{in } \Omega, \tag{3a}$$

$$ik\phi + \nabla \cdot \boldsymbol{u} = f \quad \text{in } \Omega, \tag{3b}$$

$$\phi = 0 \quad \text{on } \partial\Omega, \tag{3c}$$

where $0 \neq k \in \mathbb{C}$ is the wavenumber, $\Omega \subset \mathbb{R}^2$, $\boldsymbol{u} : \Omega \to \mathbb{R}^2$ is a vector unknown, $\phi : \Omega \to \mathbb{R}$ is a scalar unknown, and $f \in L^2(\Omega)$ is a given source term. When solving the Helmholtz system using a numerical method, the so-called "pollution effect" [5] manifests itself in discrepancies between the method's discrete wavenumber and the exact k. Dispersion analyses have long been used to determine these discrepancies for standard methods (see [1, 30] and the bibliography therein).

In a dispersion analysis, one attempts to propagate a wave of exact wavenumber k using a numerical method on an infinite uniform mesh of grid size $h > 0$. The equations of the method then show that the numerical solution can be viewed as a wave of a possibly different wavenumber k^h. Thus, the difference between k and k^h quantifies the wavenumber error of the method. It is traditional to study these differences in the following three forms: "dispersive error" $\mathrm{Re}(kh - k^h h)$, "dissipative error" $\mathrm{Im}(kh - k^h h)$, and the "total error" $|kh - k^h h|$. The behaviour of these quantities as kh goes to 0 gives us valuable insights into the method.

Many previous works have focused on dispersion analyses of various numerical methods [1, 30]. Dispersion relations of some discontinuous Galerkin (DG) methods were obtained in [2]. Here as well as in [64], the dispersive and dissipative errors of DG methods applied to linear advection were studied. In an earlier work [45], the dispersive and dissipative properties of DG methods were analysed in the context of the one-dimensional scalar advection equation as well as the two-dimensional wave equation. This was followed by [3], where the dispersive and dissipative errors of the Interior Penalty Discontinuous Galerkin (IP-DG) method applied to the second-order wave equation were studied. They also studied a more general family of schemes applied to the corresponding first order system. A dispersion analysis of the IP-DG method applied to elastic wave propagation was conducted in [28]. More recently, dispersion analysis of other non-conforming methods have received attention. This includes dispersion analysis of the Discontinuous Petrov–Galerkin (DPG) method [41] and the Plane Wave Discontinuos Galerkin (PWDG) method [39].

The purpose of this part of the thesis is to use dispersion analysis to quantify the wavenumber discrepancies of certain HDG methods. These methods have been applied by many to solve the Helmholtz system – see e.g., [25, 38, 43]. The first work to perform a dispersion analysis of an HDG method was [40]. That work considered one of the standard HDG methods, namely what is called the LDG-H method in [17], studied the influence of its stabilization parameter τ on the dispersion errors, and compared the HDG errors to those of the mixed HRT (hybrid Raviart-Thomas) method. The results in [40] were limited to the lowest order case ($p = 0$) and the next higher order case ($p = 1$). Based on these, the convergence rate of wavenumber errors when $\tau = 1$ was estimated to be $|kh - k^h h| = O((kh)^{2p+2})$. These results made it clear that the HRT method surpassed the LDG-H method by yielding higher order wavenumber errors as $h \to 0$. Therefore, it was natural to ask if any other flavor of the HDG method can possibly achieve rates comparable to the HRT method. That is the reason why we study the Single Face HDG (SFH) method, which uses exactly the same stabilization as the LDG-H method, but applies it in such a way that $\tau = 0$ in all but one edge of every mesh element.

The SFH method was one of the first HDG methods to be analyzed [15]. Its construction and analysis was motivated by [17] (even though [15] was published before [17]). Due to its 'minimal' stabilization domain, one may view the SFH method as the HDG method that is in some sense 'closest' to the mixed method.

Our results on dispersion analysis are shown in Chapter 4 of this thesis, and gave rise to the publication

[42] J. Gopalakrishnan, M. Solano and F. Vargas, *Dispersion analysis of HDG methods.* Journal of Scientific Computing, 77 (2018), pp. 1703–1735.

Introducción

Los métodos de Galerkin Discontinuos (DG) han sido extensivamente estudiados y usados para resolver diferentes tipos de problemas. En particular, el método de Galerkin Discontinuo Hibridizable (HDG) fue propuesto en [17]. La Hibridización de métodos de Galerkin Discontinuos surge como una alternativa para reducir el número de grados de libertad globalmente acoplados de los métodos DG. En el contexto de problemas de difusión, [17] introdujo un marco teórico unificado para hibridización de métodos DG, donde los únicos grados de libertad globalmente acoplados son los de las trazas numéricas en las fronteras entre elementos, y las demás incógnitas se obtienen resolviento problemas locales en cada elemento. Desde entonces, los métodos HDG han sido ampliamente usados para aproximar la solución de una variedad de problemas. En el contexto de Mecánica de Fluidos, han sido introducidos para ecuaciones de flujo de Stokes [16, 18, 22, 52], flujo de Stokes cuasi–Newtoniano [34, 35], acoplamiento Stokes–Darcy [36], problema de Brinkman [4, 33, 37], ecuaciones de Oseen [11] y las ecuaciones de Navier– Stokes [12, 53, 56, 57, 61, 63], entre otros.

En la primera parte de esta tesis, presentaremos un método HDG de alto orden para resolver numéricamente las ecuaciones de Stokes de un fluido ocupando una región $\Omega \subset \mathbb{R}^d$, no necesariamente poligonal ($d = 2$) o poliédrica ($d = 3$) con frontera $\Gamma := \partial\Omega$ compacta, Lipschitz y $\mathcal{C}^2$ por tramos. Más precisamente, denotando por $\boldsymbol{u}$ la velocidad del fluido, p la presión, $\nu > 0$ una viscosidad constante, $\boldsymbol{f} \in [L^2(\Omega)]^d$ un término fuente y $\boldsymbol{g} \in [L^2(\Gamma)]^d$ la velocidad prescrita en la fontera cumpliendo la condición de compatibilidad $\displaystyle\int_\Gamma \boldsymbol{g} \cdot \boldsymbol{n} = 0$ ($\boldsymbol{n}$ es el vector normal unitario exterior a Ω), las ecuaciones a resolver son

$$
\begin{aligned}
\mathrm{L} - \nabla \boldsymbol{u} &= 0 \quad && \text{in } \Omega, \\
-\nabla \cdot (\nu \mathrm{L}) + \nabla p &= \boldsymbol{f} \quad && \text{in } \Omega, \\
\nabla \cdot \boldsymbol{u} &= 0 \quad && \text{in } \Omega, \\
\boldsymbol{u} &= \boldsymbol{g} \quad && \text{on } \Gamma, \\
\int_\Omega p &= 0.
\end{aligned}
$$

A continuación, el siguiente paso es resolver las ecuaciones de Oseen incompresibles, dadas por

$$\begin{aligned} \mathrm{L} - \nabla \boldsymbol{u} &= 0 && \text{in } \Omega, \\ -\nu \nabla \cdot \mathrm{L} + (\boldsymbol{\beta} \cdot \nabla)\boldsymbol{u} + \nabla p &= \boldsymbol{f} && \text{in } \Omega, \\ \nabla \cdot \boldsymbol{u} &= 0 && \text{in } \Omega, \\ \boldsymbol{u} &= \boldsymbol{g} && \text{on } \Gamma, \\ \int_\Omega p &= 0, \end{aligned}$$

donde se asume que la velocidad convectiva satisface $\boldsymbol{\beta} \in [W^{1,\infty}(\Omega)]^d$ y que tiene divergencia nula.

En ambos casos, debemos lidiar con un dominio curvo. La idea principal es aproximar Ω por un dominio computacional poliédrico en el cual el dato de frontera $\boldsymbol{g}$ es transferido apropiadamente a la frontera computacional. Para ello, seguimos la aproximación propuesta por [23] y analizada en [21] que consiste en integrar la aproximación del gradiente a lo largo de *transferring paths* que conectan la frontera computacional con Γ. Esta técnica nos permite obtener una aproximación de alto orden del dato de frontera en el dominio computacional, que conduce a una precisión de alto orden de la solución discreta. Más precisamente, si los espacios discretos son construidos usando polinomios de grado k, el error en las variables L, $\boldsymbol{u}$ y p, medidos en la norma L^2, serán de orden h^{k+1}, donde h es el tamaño de la malla. Esta técnica a sido aplicada recientemente a varios problemas y se ha mostrado que funciona apropiadamente. Sin embargo, según nuestro conocimiento, esta es la primera vez que esta técnica es aplicada al problema de Stokes y a las ecuaciones de Oseen. En ambos casos, la principal diferencia con los trabajos previos es el tratamiento de la aproximación de la presión en el dominio computacional. Una de las primeras ideas basadas en esta técnica de transferencia fue introducida por [20] para el caso unidimensional y luego fue extendida a dimensiones más altas para difusión pura [21, 23] y ecuaciones convección–difusión [24]. En todos estos trabajos, se consideró dato de frontera de Dirichlet, y una malla que no se ajusta al dominio. Se mostró que se obtiene precisión de alto orden si la distancia entre el dominio computacional y la frontera es sólo de orden h. Recientemente, una aproximación similar fue propuesta y estudiada numéricamente para condiciones de frontera de Neumann y problemas elípticos de interface [62]. Allí, el dato de frontera de Neumann no puede ser tratado de la misma manera que el dato de frontera Dirichlet y la frontera/interface computacional en [62] debe estar a una distancia de orden h^2 de la frontera/interface real, a fin de obtener resultados óptimos. En términos simples, el dato Neumann en [62] se impone extrapolando el gradiente discreto, mientras que el dato Dirichlet se impone calculando una integral de línea del gradiente discreto. Esta integral es sobre un segmento de longitud proporcional a h, lo cual provee una potencia de h que permite corregir el hecho de que la distancia entre Γ y la frontera computacional es sólo de orden h.

Discutamos ahora brevemente algo sobre la literatura relacionada a métodos numéricos para ecuaciones diferenciales en que hay involucradas fronteras o interfaces curvas. En general, estos métodos pueden clasificarse como *fitted* o *unfitted*. En métodos fitted, la discretización del dominio se ajusta a la frontera/interface, hasta un cierto nivel de precisión. Por ejemplo, éste es el caso de los Elementos Finitos isoparamétricos [48] en los que el mapeo desde el elemento de referencia a un elemento físico es un polinomio cuyo grado es el mismo que el grado polinomial del espacio de Elementos Finitos. En esta dirección, [6] considera una aproximación por Elementos Finitos para interfaces elípticas suaves donde se obtienen tasas de convergencia óptimas si la malla se ajusta isoparamétricamente a la interface. Para

una aproximación lineal a trozos de un problema de valores de frontera Dirichlet, [8] aproxima el dato en la frontera computacional Γ_h transfiriendo el dato de frontera g de *manera natural*. Esto eso, para $x \in \Gamma_h$ y un $\bar{x} \in \Gamma$ definido convenientemente de modo tal que $|x - \bar{x}|$ es de orden h^2, entonces el dato de frontera g se define como $\tilde{g}(x) := g(\bar{x})$. La misma idea fue extendida después al caso de problemas de interface [9]. Como veremos en (1.2), en algún sentido nuestra técnica puede ser vista como una generalización donde añadimos un término adicional a la *manera natural* de transferencia. Para un método H-div conforme de alto orden para resolver problemas elípticos de interface, nos remitimos a [50]. En ese trabajo, la interface curva es interpolada localmente por *splines* y se obtiene convergencia ópitma cuando el grado de las *splines* es elegido apropiadamente. Métodos *fitted* también han sido aplicados a problemas de control en dominios curvos [29], en los que se ha considerado sólo polinomios de grado uno. En general, una de las principales ventajas de métodos *fitted* es que el dato prescrito en la frontera/interface puede ser impuesto fácilmente. Sin embargo, la construcción de mallas puede ser difícil, especialmente en geometrías complicadas. Por otro lado, el aspecto atractivo de los métodos *unfitted* es que la malla no está ajustada al dominio e inlcuso se pueden usar mallas Cartesianas. Sin embargo, no es directo desarrollar un método *unfitted* de alto orden, principamente por la imposición de la condición de frontera/interface lejos de la frontera/interface real. En el contexto de diferencias finitas, uno de los métodos *unfitted* más populares es el método Immersed Boundary (IB) introducido por [58] en 1972. Para el caso bidimensional, [51] mostró que IB es un método de primer orden para la velocidad de un flujo de Stokes y que una precisión de segundo orden se puede alcanzar lejos de la interface. Más tarde, en la misma dirección, LeVeque y Li desarrollaron el método Immersed Interface [49], que es de una precisión de segundo orden. En el contexto de Elementos Finitos, [7] propuso un método *unfitted* basado en la aproximación de Nitsche [54] con el método de aproximación del dominio poligonal [67]. Allí, el esquema numérico es planteado en un dominio poligonal y se añade un término de corrección a la forma bilineal de Nitsche a fin de obtener precisión de alto orden. Recientemente, un método de elementos finitos de alto orden fue propuesto para resolver problemas elípticos de interface [44]. También está basado en un término que incluye una función de corrección, polinomial a trozos, que es añadida al funcional del lado derecho. Esta función de corrección se construye apropiadamente usando información entregada por la ecuación y las condiciones de transmisión en la interface. Similarmente, un método HDG basado en calcular previamente una función de corrección fue propuesto y analizado en [32]. Finalmente, nos gustaría mencionar una aproximación alternativa, los *Composite Finite Elements* [59, 60], que lidian con dominios complicados, incluyendo fronteras ásperas o con pequeños hoyos dentro. Sin embargo, según nuestro conocimiento, no ha sido desarrollado para aproximaciones de alto orden.

Nuestro objetivo es desarrollar un método que combine la flexibilidad de la construcción de la malla de los métodos *unfitted* con la precisión de alto orden de los métodos *fitted*. En efecto, la principal ventaja de nuestra técnica es que el dominio computacional es fácil de construir no hay necesidad de ajustarlo al verdadero dominio. Más aún, la manera en que la condición de frontera Dirichlet es transferida nos permite considerar polinomios de grado polinomial alto en los espacios discretos y obtener precisión de alto orden. Por otro lado, uno de los inconvenientes de nuestro método al comprararlo con otros es que se apoya en dos aspectos de la Ecuación Diferencial Parcial: (1) $\nabla \boldsymbol{u}$ debe ser parte de la ecuación, y (2) $\boldsymbol{u} = \boldsymbol{g}$ en Γ. Además, la matriz global resultante no es simétrica en nuestro caso. Simetrizar la matriz es trabajo futuro. Creemos que nuestra técnica es, en principio, independiente del método numérico que se use, siempre y cuando el gradiente es aproximado

adecuadamente y que la Ecuacuón Diferencial Parcial tenga las condiciones ya mencionadas. En efecto, esta técnica ya se ha combinado exitosamente con métodos mixtos para problemas de difusión [55].

El Capítulo 2 de esta tesis muestra los detalles de los resultados obtenidos al aplicar esta técnica al problema de Stokes (1). El artículo que se originó a partir de estos resultados ha sido aceptado para publicación en el Journal of Scientific computing. La pre-publicación asociada están disponible en

[65] M. Solano and F. Vargas, *A high order HDG method for Stokes flow in curved domains.*. https://www.ci2ma.udec.cl/publicaciones/prepublicaciones/prepublicacion.php?id=227, (2016)

Por otro lado, el Capítulo 3 contiene los resultados de la aplicación de nuestra técnica a las ecuaciones de Oseen (2). Estos resultados serán enviados a una revista ISI en pocos días.

El otro enfoque de esta tesis es realizar un análisis de dispersión de métodos HDG para la ecuación de Helmholtz, que está dada por

$$\begin{aligned} ik\boldsymbol{u} + \nabla\phi &= \mathbf{0} \quad \text{in } \Omega, \\ ik\phi + \nabla\cdot\boldsymbol{u} &= f \quad \text{in } \Omega, \\ \phi &= 0 \quad \text{on } \partial\Omega, \end{aligned}$$

donde $0 \neq k \in \mathbb{C}$ es el número de onda, $\Omega \subset \mathbb{R}^2$, $\boldsymbol{u} : \Omega \to \mathbb{R}^2$ es una incógnita vectorial, $\phi : \Omega \to \mathbb{R}$ es una incógnita escalar y $f \in L^2(\Omega)$ es un término fuente dado. Cuando se resuelve el sistema de Helmholtz usando un método numérico, el así llamado "efecto de polución" [5] se manifiesta a través de diferencias entre el número de onda entregado por el método y el valor exacto de k. Los análisis de dispersión han sido muy usados para determinar estas diferencias para métodos estándar (ver [1, 30] y la bibliografía en ellos).

En un análisis de dispersión, se trata de propagar una onda con un número de onda exacto k usando un método numérico en una malla uniforme infinita de tamaño de cuadrícula $h > 0$. Luego, las ecuaciones del método muestran que la solución numérica puede ser vista como una onda con un número de onda k^h posiblemente diferente a k. Así, la diferencia entre k y k^h cuantifica el error del número de onda del método. Es tradicional estudiar estas diferencias en las tres formas siguientes: "error dispersivo" $\mathrm{Re}(kh - k^h h)$, "error disipativo" $\mathrm{Im}(kh - k^h h)$, y el "error total" $|kh - k^h h|$. El comportamiento de estas cantidades cuando kh tiende a 0 nos entrega una valiosa intuición acerca del método.

Muchos trabajos previos se han enfocado en análisis de dispersión de varios métodos numéricos [1, 30]. Relaciones de dispersión de algunos métodos DG han sido obtenidas en [2]. Aquí, al igual que en [64], se han estudiado los errores dispersivos y disipativos de métodos DG aplicados a advección lineal. En un trabajo previo [45], se analizaron las propiedades dispersivas y disipativas de métodos DG en el contexto de la ecuación de advección en una dimensión, y en la ecuación de la onda bidimensional. Esto fue seguido por [3], en que se estudió los errores dispersivo y disipativo del método de Galerkin Discontinuo de Penalización Interior (IP–DG) aplicado a la ecuación de la onda de segundo orden. Ellos estudiaron también una familia de esquemas más general aplicada al correspondiente esquema de primer orden. En [28], se presentó el análisis de dispersión del método IP–DG aplicado a propagación de ondas elásticas. Más recientemente, análisis de dispersión de otros métodos no conformes ha recibido

atención. Esto incluye análisis de dispersión del Método de Petrov–Galerkin Discontinuo (DPG) [41] y el método *Plane Wave Discontinuous Galerkin* (PWDG) [39].

El propósito de esta parte de la tesis es usar análisis de dispersión para cuantificar las discrepancias entre ciertos métodos HDG. Estos métodos han sido muy aplicados para resolver el sistema de Helmholtz (ver, por ejemplo, [25, 38, 43]). El primer trabajo que realizó un análisis de dispersión de un método HDG fue [40]. Ese trabajo consideró uno de los métodos HDG estándar, el que es llamado LDG–H en [17]. En él, se estudió la influencia de su parámetro de estabilización τ sobre los errores de dispersión, y se compararon esos errores con los del método Raviar–Thomas híbrido (HRT). Los resultados en [40] fueron limitados al caso del orden más bajo ($p = 0$) y el siguiente orden más alto ($p = 1$). Basado en ellos, la tasa de convergencia de los errores del número de onda cuando $\tau = 1$ fue estimado en $|kh - k^h h| = O((kh)^{2p+2})$. Estos resultados dejaron en claro que el método HRT superó al método LDG–H al entregar tasas de convergencia del error de número de onda más altas cuando $h \to 0$. Por lo tanto, era natural preguntarse si algún otro tipo de método HDG podía lograr tasas comparables a las del método HRT. Esa es la razón por la cual estudiamos el método Single Face HDG (SFH), el cual usa exactamente la misma estabilización que el método LDG–H, pero la aplica de modo tal que $\tau = 0$ en todos salvo un lado de cada elemento de la malla. El método SFH fue uno de los primeros métodos HDG en ser analizado [15]. Su construcción y análisis fue motivado por [17] (aun cuando [15] fue publicado antes que [17]). Debido a que su estabilización se hace en un "dominio menor", uno podría ver al método SFH como el método HDG que es en cierto sentido "más cercano" al método mixto HRT.

Nuestros resultados obtenidos en análisis de dispersión se muestran en el Capítulo 4 de esta tesis, y dieron origen al artículo

[42] J. Gopalakrishnan, M. Solano and F. Vargas, *Dispersion analysis of HDG methods.* Journal of Scientific Computing, 77 (2018), pp. 1703–1735.

CHAPTER 1

Preliminaries

In this chapter we introduce the notation related to the mesh, inner products, norms and discrete spaces, typically used in the context of HDG methods, and then we state some preliminary results that will be used in the following chapters.

1.1 Notation and General Assumptions

In this section we introduce notation associated to the computational domain and to the family of paths that will allow us to transfer the boundary data from Γ to the computational boundary Γ_h. Moreover, we establish a set of assumptions under which the analysis in chapters 2 and 3 holds.

1.1.1 The mesh

Given $h > 0$, we denote by D_h an open polyhedral computational domain, with boundary Γ_h, meshed by a triangulation T_h of meshsize h, consisting of simplices K that are uniformly shape-regular, that is,

(D.1) there exists $\gamma > 0$, independent of h, such that $h_K \leq \gamma \rho_K$,

where ρ_K is the radius of the largest ball contained in K and h_K is the diameter of K. We assume

(D.2) $\max\limits_{K \in \mathsf{T}_h} h_K \leq h$.

For a simplex K, we denote its outward unit normal by $\boldsymbol{n}_K$, writing $\boldsymbol{n}$ instead of $\boldsymbol{n}_K$ when there is no confusion. Similarly, for a face e, we write $\boldsymbol{n}$ instead of $\boldsymbol{n}_e$ to refer to its normal vector. We also consider, by simplicity, that the triangulation does not have hanging nodes.

In addition, we suppose that

(D.3) $\overline{\mathsf{D}_h} \subset \overline{\Omega}$.

The set of inner faces and boundary faces of T_h are denoted by $\mathcal{E}_h^i$ and $\mathcal{E}_h^\partial$, respectively, and $\mathcal{E}_h = \mathcal{E}_h^i \cup \mathcal{E}_h^\partial$ is the set of all the faces of T_h. We also define the non-meshed region $\mathsf{D}_h^c := \Omega \setminus \overline{\mathsf{D}_h}$.

On the other hand, let $\mathcal{P}_r(K)$ denote the space of polynomials of total degree at most r defined on K, $\boldsymbol{\mathcal{P}}_r(K) := [\mathcal{P}_r(K)]^d$ and $\mathrm{P}_r(K) := [\mathcal{P}_r(K)]^{d\times d}$. Given a region $D \subset \mathbb{R}^d$, we denote by $(\cdot,\cdot)_D$ and $\langle\cdot,\cdot\rangle_{\partial D}$ the $L^2(D)$ and $L^2(\partial D)$ inner products, respectively. The L^2-norms over D and ∂D will be denoted by $\|\cdot\|_D$ and $\|\cdot\|_{\partial D}$.

For each scalar-valued function η and ζ, we define

$$(\eta,\zeta)_{\mathsf{T}_h} := \sum_{K\in\mathsf{T}_h} (\eta,\zeta)_K \quad \text{and} \quad \langle\eta,\zeta\rangle_{\partial\mathsf{T}_h} := \sum_{K\in\mathsf{T}_h} \langle\eta,\zeta\rangle_{\partial K}.$$

Vector-valued functions are boldfaced and, for $\boldsymbol{\eta}$ and $\boldsymbol{\zeta}$, we write

$$(\boldsymbol{\eta},\boldsymbol{\zeta})_{\mathsf{T}_h} := \sum_{i=1}^d (\eta_i,\zeta_i)_{\mathsf{T}_h} \quad \text{and} \quad \langle\boldsymbol{\eta},\boldsymbol{\zeta}\rangle_{\partial\mathsf{T}_h} := \sum_{i=1}^d \langle\eta_i,\zeta_i\rangle_{\partial\mathsf{T}_h}.$$

Tensor-valued functions are in Roman letters and, for N and Z, we write

$$(\mathrm{N},\mathrm{Z})_{\mathsf{T}_h} := \sum_{i,j=1}^d (\mathrm{N}_{ij},\mathrm{Z}_{ij})_{\mathsf{T}_h} \quad \text{and} \quad \langle\mathrm{N},\mathrm{Z}\rangle_{\partial\mathsf{T}_h} := \sum_{i,j=1}^d \langle\mathrm{N}_{ij},\mathrm{Z}_{ij}\rangle_{\partial\mathsf{T}_h}.$$

We use the standard notation for Sobolev spaces and their associated norms and seminorms. Finally, to avoid proliferation of constants, we will write $a \lesssim b$ instead of $a \le Cb$, where C is a constant independent of h.

1.1.2 Treatment of the curved boundary

As we explained in the Introduction, the aim of the first part of the thesis is to solve some problems in curved domains. The main idea is to approximate the curved domain by a polyhedral computational domain denoted by D_h, where a numerical method can be applied. Since the problem will be solved in D_h, we must specify a suitable boundary data on the computational boundary Γ_h. To this end, we consider the idea proposed by [23] and transfer the boundary data $\boldsymbol{g}$ from Γ to Γ_h through transferring paths. That is, let $e \in \mathcal{E}_h^\partial$ with normal unit vector $\boldsymbol{n}$. For each $\boldsymbol{x} \in e$, we set $\bar{\boldsymbol{x}} \in \Gamma$ as the closest intersection between Γ and the ray of tangent vector $\boldsymbol{n}$ starting at $\boldsymbol{x}$. We denote by $\sigma_{\boldsymbol{n}}(\boldsymbol{x})$ the segment joining $\bar{\boldsymbol{x}}$ and $\boldsymbol{x}$, which is referred as *transferring path*. The length of this segment, $l(\boldsymbol{x}) := |\bar{\boldsymbol{x}} - \boldsymbol{x}|$, is assumed to satisfy

(D.4) $l(\boldsymbol{x}) \lesssim h$.

We notice that this assumption implies that $\mathrm{dist}(\Gamma_h,\Gamma) \lesssim h$. In addition, we observe that if $\boldsymbol{x}$ is a vertex in Γ_h, then it has associated two different transferring paths. In other words, the functions $\bar{\boldsymbol{x}} = \bar{\boldsymbol{x}}(\boldsymbol{x})$ and $l(\boldsymbol{x})$ are double-valued on the boundary vertices.
Let $e \in \mathcal{E}_h^\partial$ and K^e the element where it belongs. We define

$$K_{ext}^e := \{\boldsymbol{x} + s\boldsymbol{n} : 0 \le s \le l(\boldsymbol{x}),\ \boldsymbol{x} \in e\}$$

and assume that,

(D.5) for each point $\boldsymbol{x} \in e$, the intersection of the ray $\{\boldsymbol{x} + \eta\boldsymbol{n} : \eta > 0\}$ and Γ is unique.

We denote by $H_e^\perp$ the largest distance of a point in K_{ext}^e to the plane determined by e and $h_e^\perp$ be the distance between e and the vertex of K^e opposite to e, as Fig. 1.1 shows. We set $r_e = H_e^\perp / h_e^\perp$ and $R = \max_{e \in \mathcal{E}_h^\partial} r_e$. This ratio will be important in our estimates and assumptions, since it indicates how far is Γ from the computational boundary relative to the mesh size. If the domain were polygonal and the mesh fits its boundary, this ratio would be zero.

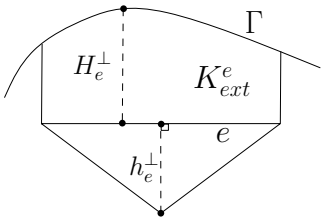

Figure 1.1: Example of a region K_{ext}^e and the distances $H_e^\perp$ and $h_e^\perp$.

Through chapters 2 and 3, Assumptions (D) will be assumed valid, without mention it explicitly.

1.1.3 Transferring of the boundary condition

We are now in position to explain how to transfer the boundary condition from Γ to Γ_h. Let $e \in \mathcal{E}_h^\partial$ with outward normal unit vector $\boldsymbol{n}$ and $\boldsymbol{x} \in e$. Integrating component-wise $\mathrm{L} = \nabla \boldsymbol{u}$ along $\sigma_{\boldsymbol{n}}(\boldsymbol{x})$ we obtain

$$u(\boldsymbol{x}) = u(\bar{\boldsymbol{x}}) - \int_0^{l(\boldsymbol{x})} \mathrm{L}(\boldsymbol{x} + \boldsymbol{n}s)\, \boldsymbol{n}\, ds.$$

Denoting by $\widetilde{\boldsymbol{g}}$ the trace of $\boldsymbol{u}$ at e and noticing that $\boldsymbol{u}(\bar{\boldsymbol{x}}) = \boldsymbol{g}(\bar{\boldsymbol{x}})$, from previous identity we get

$$\widetilde{\boldsymbol{g}}(\boldsymbol{x}) = \boldsymbol{g}(\bar{\boldsymbol{x}}) - \int_0^{l(\boldsymbol{x})} \mathrm{L}(\boldsymbol{x} + \boldsymbol{n}s)\, \boldsymbol{n}\, ds. \tag{1.1}$$

In other words, (1.1) provides an expression to obtain the boundary data at Γ_h in terms of the unknown L. We point out that, according to Lemma B.1 in [21], $\widetilde{\boldsymbol{g}}$ is well-defined if Γ is compact, Lipschitz and piecewise $\mathcal{C}^2$.

In order to construct a discrete approximation of $\widetilde{\boldsymbol{g}}$, denoted by $\widetilde{\boldsymbol{g}}_h$, we consider a *local extrapolation* of polynomials, i.e., given G a polynomial defined on K^e, with $e \in \mathcal{E}_h^\partial$, we extrapolate it from K^e to K_{ext}^e. Thus, the expression in (1.1) suggests the following approximation

$$\widetilde{\boldsymbol{g}}_h(\boldsymbol{x}) := \boldsymbol{g}(\bar{\boldsymbol{x}}) - \int_0^{l(\boldsymbol{x})} \mathrm{L}_h(\boldsymbol{x} + \boldsymbol{n}s)\boldsymbol{n}\, ds, \tag{1.2}$$

where L_h is the local extrapolation of the HDG approximation of L.

We end this section be defining the norms

$$\|\zeta\|_{\mathsf{D}_h^c,h^\perp} := \left\{ \sum_{e\in\mathcal{E}_h^\partial} h_e^\perp \|\zeta\|_{K_{ext}^e}^2 \right\}^{1/2}, \quad \|\boldsymbol{\mu}\|_{\partial\mathsf{T}_h,\alpha} := \left\{ \sum_{K\in\mathsf{T}_h} \langle \alpha_{\partial K}\zeta,\zeta\rangle_{\partial K} \right\}^{1/2},$$

$$\|\zeta\|_{\Gamma_h,\alpha} := \left\{ \sum_{e\in\mathcal{E}_h^\partial} \alpha_e \|\zeta\|_e^2 \right\}^{1/2}, \quad \text{and} \quad \|\boldsymbol{\mu}\|_h := \left\{ \sum_{K\in\mathsf{T}_h} h_K \langle \boldsymbol{\mu},\boldsymbol{\mu}\rangle_{\partial K} \right\}^{1/2}$$

where $\alpha_e := \alpha|_e$ and $\alpha_{\partial K} := \alpha|_{\partial K}$.

1.2 Useful estimates and other definitions

We end this chapter by introducing some other previous tools and results that will be used in the analysis presented in chapters 2 and 3. First of all, we define an auxiliary function and a norm that will help to carry out several of the estimates in this thesis. Let $e \in \mathcal{E}_h^\partial$, a point $\boldsymbol{x}$ lying on e with outer unit normal vector $\boldsymbol{n}$ and a tensor-valued function G. We define the function

$$\delta_{\mathrm{G}}(\boldsymbol{x}) := \frac{1}{l(\boldsymbol{x})} \int_0^{l(\boldsymbol{x})} \big(\mathrm{G}(\boldsymbol{x}+s\boldsymbol{n}) - \mathrm{G}(\boldsymbol{x})\big)\boldsymbol{n}\, \mathrm{d}s. \tag{1.3}$$

If G is a polynomial, the estimates in Lemma 5.2 of [21] states that

$$\|l^{1/2}\delta_{\mathrm{G}}\|_e \le 3^{-1/2} r_e^{3/2} C_{ext}^e C_{inv}^e \|\mathrm{G}\|_{K^e}, \tag{1.4}$$

where

$$C_{ext}^e := \frac{1}{\sqrt{r_e}} \sup_{\mathrm{G}\in\mathrm{P}_k(K^e)\setminus\{0\}} \frac{\|\mathrm{G}\|_{K_{ext}^e}}{\|\mathrm{G}\|_{K^e}} \tag{1.5}$$

and

$$C_{inv}^e := h_e^\perp \sup_{\mathrm{G}\in\mathrm{P}_k(K^e)\setminus\{0\}} \frac{\|\partial_{\boldsymbol{n}}\mathrm{G}\|_e}{\|\mathrm{G}\|_{K^e}}. \tag{1.6}$$

The constants C_{ext}^e and C_{inv}^e do not depend on the meshsize, but depend on the polynomial degree and shape-regularity constant as can be deduced from Lemma A.2 in [21]. C_{ext}^e is what we call *extrapolation constant* because it allows us to bound the L^2-norm of the extrapolation of the polynomial G in terms of $\|\mathrm{G}\|_{K^e}$. Similarly, C_{inv}^e can be seen as the constant of an inverse-type estimate that allows us to control the L^2-norm of the directional derivative of the extrapolation of the polynomial G in terms of $\|\mathrm{G}\|_{K^e}$. Finally, we recall the discrete trace inequality (Lemma 1.46 in [31]): If φ is a scalar, vector or tensor-valued polynomial in K^e, then

$$\|\varphi\|_e \le C_{tr}^e h_e^{-1/2} \|\varphi\|_{K^e}, \tag{1.7}$$

where C_{tr}^e is independent of the meshsize but depends on the polynomial degree.

CHAPTER 2

A high order HDG method for Stokes flow in curved domains

In this chapter we present a high order HDG method to numerically solve the Stokes problem in a region not necessarily polyhedral/polygonal. We prove that the discrete problem is well–posed, then we prove the error estimates which lead to optimal orders of convergence of the variables, and validate the theoretical estimates with numerical examples.

2.1 Introduction

Let $\Omega \subset \mathbb{R}^d$ be a region not necessarily polygonal ($d = 2$) or polyhedral ($d = 3$), with compact, Lipschitz and piecewise $\mathcal{C}^2$ boundary $\Gamma := \partial\Omega$. The Stokes equations of an incompressible fluid flow occupying Ω are given by

$$\mathrm{L} - \nabla \boldsymbol{u} = 0 \quad \text{in } \Omega, \tag{2.1a}$$

$$-\nabla \cdot (\nu \mathrm{L}) + \nabla p = \boldsymbol{f} \quad \text{in } \Omega, \tag{2.1b}$$

$$\nabla \cdot \boldsymbol{u} = 0 \quad \text{in } \Omega, \tag{2.1c}$$

$$\boldsymbol{u} = \boldsymbol{g} \quad \text{on } \Gamma, \tag{2.1d}$$

$$\int_\Omega p = 0, \tag{2.1e}$$

where $\boldsymbol{u}$ is the velocity of the fluid, p the pressure, $\nu > 0$ a constant viscosity, $\boldsymbol{f} \in [L^2(\Omega)]^d$ a source term and $\boldsymbol{g} \in [L^2(\Gamma)]^d$ the prescribed velocity at the boundary satisfying the compatibility condition $\int_\Gamma \boldsymbol{g} \cdot \boldsymbol{n} = 0$ ($\boldsymbol{n}$ is the outward unit normal to Ω). The curved domain Ω will be approximated by a computational domain D_h, as explained in chapter 1. We will introduce the method in the next Section 2.2. The error estimates will be stated in Section 2.3, whereas 2.4 is devoted to their proofs. In Section 2.5 we propose an approximation of the solution outside the computational domain and provide the corresponding error estimates. Section 2.6 shows numerical experiments validating these results. We end this chapter with concluding remarks.

2.2 The HDG method

We proceed now to introduce the numerical method on the computational domain D_h. First of all, we decompose

$$p = \overline{p}^{\mathsf{D}_h} + \widetilde{p}, \tag{2.2}$$

where $\overline{p}^{\mathsf{D}_h} := \dfrac{1}{|\mathsf{D}_h|}\displaystyle\int_{\mathsf{D}_h} p$ and $\widetilde{p} \in L^2_0(\mathsf{D}_h)$ ($L^2(\mathsf{D}_h)$-functions with zero mean in D_h). Since now the problem is posed in a polyhedral domain, we consider the standard HDG method ([18, 52]) that seeks an approximation $(\mathrm{L}_h, \boldsymbol{u}_h, \widetilde{p}_h, \widehat{\boldsymbol{u}}_h)$ of the solution $(\mathrm{L}, \boldsymbol{u}, \widetilde{p}, \boldsymbol{u}|_{\mathcal{E}_h})$ in the space $\mathrm{G}_h \times \boldsymbol{V}_h \times P_h \times \boldsymbol{M}_h$ given by

$$\begin{aligned}
\mathrm{G}_h &= \{\mathrm{G} \in \mathrm{L}^2(\mathsf{T}_h) : \quad G|_K \in \mathrm{P}_k(K) \quad \forall K \in \mathsf{T}_h\}, && \text{(2.3a)}\\
\boldsymbol{V}_h &= \{\boldsymbol{v} \in \boldsymbol{L}^2(\mathsf{T}_h) : \quad \boldsymbol{v}|_K \in \boldsymbol{\mathcal{P}}_k(K) \quad \forall K \in \mathsf{T}_h\}, && \text{(2.3b)}\\
P_h &= \{q \in L^2(\mathsf{T}_h) : \quad q|_K \in \mathcal{P}_k(K) \quad \forall K \in \mathsf{T}_h\}, && \text{(2.3c)}\\
\boldsymbol{M}_h &= \{\boldsymbol{\mu} \in \boldsymbol{L}^2(\mathcal{E}_h) : \quad \boldsymbol{\mu}|_e \in \boldsymbol{\mathcal{P}}_k(e) \quad \forall e \in \mathcal{E}_h\}. && \text{(2.3d)}
\end{aligned}$$

As we will see in Section 2.2.1, this approximation is the only solution of

$$\begin{aligned}
(\mathrm{L}_h, \mathrm{G})_{\mathsf{T}_h} + (\boldsymbol{u}_h, \nabla\cdot \mathrm{G})_{\mathsf{T}_h} - \langle \widehat{\boldsymbol{u}}_h, \mathrm{G}\boldsymbol{n}\rangle_{\partial\mathsf{T}_h} &= 0, && \text{(2.4a)}\\
(\nu\mathrm{L}_h, \nabla\boldsymbol{v})_{\mathsf{T}_h} - (\widetilde{p}_h, \nabla\cdot\boldsymbol{v})_{\mathsf{T}_h} - \langle \widehat{\nu\mathrm{L}}_h\boldsymbol{n} - \widehat{p}_h\boldsymbol{n}, \boldsymbol{v}\rangle_{\partial\mathsf{T}_h} &= (\boldsymbol{f}, \boldsymbol{v})_{\mathsf{T}_h}, && \text{(2.4b)}\\
-(\boldsymbol{u}_h, \nabla q)_{\mathsf{T}_h} + \langle \widehat{\boldsymbol{u}}_h\cdot\boldsymbol{n}, q\rangle_{\partial\mathsf{T}_h} &= 0, && \text{(2.4c)}\\
\langle \widehat{\boldsymbol{u}}_h, \boldsymbol{\mu}\rangle_{\Gamma_h} &= \langle \widetilde{\boldsymbol{g}}_h, \boldsymbol{\mu}\rangle_{\Gamma_h}, && \text{(2.4d)}\\
\langle \widehat{\nu\mathrm{L}}_h\boldsymbol{n} - \widehat{p}_h\boldsymbol{n}, \boldsymbol{\mu}\rangle_{\partial\mathsf{T}_h\setminus\Gamma_h} &= 0, && \text{(2.4e)}\\
(\widetilde{p}_h, 1)_{\mathsf{D}_h} &= 0, && \text{(2.4f)}
\end{aligned}$$

for all $(\mathrm{G}, \boldsymbol{v}, q, \boldsymbol{\mu}) \in \mathrm{G}_h \times \boldsymbol{V}_h \times P_h \times \boldsymbol{M}_h$, where we emphasize that $\widetilde{\boldsymbol{g}}_h$ depends on L_h (c.f. (1.2)),

$$\widehat{\nu\mathrm{L}}_h\boldsymbol{n} - \widehat{p}_h\boldsymbol{n} = \nu\mathrm{L}_h\boldsymbol{n} - \widetilde{p}_h\boldsymbol{n} - \tau\nu(\boldsymbol{u}_h - \widehat{\boldsymbol{u}}_h) \qquad \text{on } \partial\mathsf{T}_h, \tag{2.4g}$$

and τ is a non-negative piecewise constant stabilization parameter defined on $\partial\mathsf{T}_h$. In order to simplify notation, we assume τ to be constant on $\partial\mathsf{T}_h$. The choice of τ is not crucial in our method. For other values of τ we refer to [18].

2.2.1 Well-posedness of the method

In this section we show that the discrete scheme (2.4) with the approximated boundary data (1.2) is well-posed. The steps that will lead to this statement will be very similar to those needed to obtain the error estimates in Section 2.4. The main result of this section is the following.

Theorem 2.1. *Under the assumptions of Lemmas 2.2 and 2.3 (stated and proved below), the scheme (2.4) with the boundary data (1.2) has a unique solution.*

The proof of this Theorem will be a consequence of the two following Lemmas.

Lemma 2.2. *Let* $(\mathrm{L}_h, \boldsymbol{u}_h, \widetilde{p}_h, \widehat{\boldsymbol{u}}_h) \in \mathrm{G}_h \times \boldsymbol{V}_h \times P_h \times \boldsymbol{M}_h$ *be the solution of* (2.4) *with the boundary data in* (1.2). *Let us suppose that* $\boldsymbol{f} = \boldsymbol{0}$ *and* $\boldsymbol{g} = \boldsymbol{0}$. *In addition, for every* $e \in \mathcal{E}_h^\partial$, *we assume that*

(A.1) $r_e^3 (C_{ext}^e)^2 (C_{inv}^e)^2 \leq 1/8$ *and*

(A.2) $r_e h_e^\perp \tau \leq 1/8$.

Then,

$$\|\mathrm{L}_h\|_{\mathsf{D}_h} + \|\boldsymbol{u}_h - \widetilde{\boldsymbol{u}}_h\|_{\partial \mathsf{T}_h, \tau} + \|\widetilde{\boldsymbol{g}}_h\|_{\Gamma_h, l^{-1}} \leq 2\sqrt{6}\nu^{-1} \|\widetilde{p}_h\|_{\Gamma_h, l}. \tag{2.5}$$

Before going through the proof, let us comment on these assumptions. If the domain is polygonal and the mesh fits its boundary, then $r_e = 0$ and all the assumptions are satisfied. In that case we recover the standard HDG method [18]. On the other hand, the constants C_{ext}^e, C_{inv}^e and C_{tr}^e are proportional to $(k+1)^{8/3}$ as stated in Lemma A.2 of [21]. Then, if the ratio r_e is small enough, (A.1) and (A.2) hold. In other words, the larger is the polynomial degree, the smaller this ratio must be to guarantee well-posedness of the scheme.

Let us continue with the proof of Lemma 2.2.

Proof. By taking $\mathrm{G} = \nu \mathrm{L}_h$, $\boldsymbol{v} = \boldsymbol{u}_h$, $q = \widetilde{p}_h$ and $\boldsymbol{\mu} = \widetilde{\boldsymbol{u}}_h$ in the first four equations of (2.4) and adding them up we obtain

$$\|\mathrm{L}_h\|_{\mathsf{D}_h}^2 + \|\boldsymbol{u}_h - \widetilde{\boldsymbol{u}}_h\|_{\partial \mathsf{T}_h, \tau}^2 = \nu^{-1} \langle \nu \widehat{\mathrm{L}}_h \boldsymbol{n} - \widehat{p}_h \boldsymbol{n}, \widetilde{\boldsymbol{g}}_h \rangle_{\Gamma_h}. \tag{2.6}$$

Now, let $e \in \mathcal{E}_h^\partial$ and $\boldsymbol{x} \in e$. According to (1.2) and (1.3) we can write

$$l(\boldsymbol{x})^{-1} \widetilde{\boldsymbol{g}}_h(\boldsymbol{x}) \;=\; -\delta_{\mathrm{L}_h}(\boldsymbol{x}) - \mathrm{L}_h(\boldsymbol{x})\boldsymbol{n}.$$

From this identity we obtain an expression for $\mathrm{L}_h(\boldsymbol{x})\boldsymbol{n}$ and, by (2.4g), we write:

$$\begin{aligned} \nu^{-1} \langle \nu \widehat{\mathrm{L}}_h \boldsymbol{n} - \widehat{p}_h \boldsymbol{n}, \widetilde{\boldsymbol{g}}_h \rangle_{\Gamma_h} &= \langle \mathrm{L}_h \boldsymbol{n}, \widetilde{\boldsymbol{g}}_h \rangle_{\Gamma_h} - \nu^{-1} \langle \widetilde{p}_h \boldsymbol{n}, \widetilde{\boldsymbol{g}}_h \rangle_{\Gamma_h} - \langle \tau(\boldsymbol{u}_h - \widehat{\boldsymbol{u}}_h), \widetilde{\boldsymbol{g}}_h \rangle_{\Gamma_h} \\ &= -\langle l^{-1} \widetilde{\boldsymbol{g}}_h, \widetilde{\boldsymbol{g}}_h \rangle_{\Gamma_h} - \langle \delta_{\mathrm{L}_h}, \widetilde{\boldsymbol{g}}_h \rangle_{\Gamma_h} \\ &\quad -\nu^{-1} \langle \widetilde{p}_h \boldsymbol{n}, \widetilde{\boldsymbol{g}}_h \rangle_{\Gamma_h} - \langle \tau(\boldsymbol{u}_h - \widehat{\boldsymbol{u}}_h), \widetilde{\boldsymbol{g}}_h \rangle_{\Gamma_h}. \end{aligned}$$

Replacing this in (2.6), using Cauchy-Schwarz and Young's inequalities; and moving to the left hand side the terms involving $\widetilde{\boldsymbol{g}}_h$, we get

$$\begin{aligned} \|\mathrm{L}_h\|_{\mathsf{D}_h}^2 \;+\; & \|\boldsymbol{u}_h - \widetilde{\boldsymbol{u}}_h\|_{\partial \mathsf{T}_h, \tau}^2 + \|\widetilde{\boldsymbol{g}}_h\|_{\Gamma_h, l^{-1}}^2 \\ &\leq 4\|\delta_{\mathrm{L}_h}\|_{\Gamma_h, l}^2 + \frac{4}{\nu^2} \|\widetilde{p}_h\|_{\Gamma_h, l}^2 + 4\|\tau(\boldsymbol{u}_h - \widehat{\boldsymbol{u}}_h)\|_{\Gamma_h, l}^2. \end{aligned} \tag{2.7}$$

By (1.7), (1.4), assumptions $(A.1)$ and $(A.2)$, the fact that $l(\boldsymbol{x}) \leq H_e^\perp = r_e h_e^\perp$ and $h_e^\perp \leq \gamma h_e$, we obtain

$$\|\delta_{\mathrm{L}_h}\|_{\Gamma_h, l}^2 \leq \frac{1}{3} \max_{e \in \mathcal{E}_h^\partial} r_e^3 (C_{ext}^e)^2 (C_{inv}^e)^2 \|\mathrm{L}_h\|_{\mathsf{D}_h}^2 \leq \frac{1}{24} \|\mathrm{L}_h\|_{\mathsf{D}_h}^2$$

and

$$\|\tau(\boldsymbol{u}_h - \widehat{\boldsymbol{u}}_h)\|_{\Gamma_h, l}^2 \leq \max_{e \in \mathcal{E}_h^\partial} r_e h_e^\perp \tau \|\boldsymbol{u}_h - \widehat{\boldsymbol{u}}_h\|_{\partial \mathsf{T}_h, \tau}^2 \leq \frac{1}{8} \|\boldsymbol{u}_h - \widehat{\boldsymbol{u}}_h\|_{\partial \mathsf{T}_h, \tau}^2.$$

These two inequalities, together with (2.7), imply (2.5).

□

In order to deal with the term at the right hand side of (2.5), we consider the L^2-projection onto $\boldsymbol{M}_h$, denoted by $\mathbf{P}_M$, and the following assumption: for each $e \in \mathcal{E}_h^\partial$.

(A.3) $2\sqrt{6}\beta M\gamma^{1/2}C_{tr}^e r_e^{1/2} < \dfrac{1}{2}$, where $M := \max\left\{1, (\tau h)^{1/2}\right\}$

and $\beta > 0$ is the constant, independent of h, appearing in next lemma.

Lemma 2.3. *Suppose assumptions of Lemma 2.2 and (A.3) hold. Then* $\widetilde{p}_h = 0$.

Proof. We adapt the proof of Proposition 3.4 in [18] to our setting. Since $\widetilde{p}_h \in L_0^2(\mathsf{D}_h)$, there exists $\beta > 0$, independent of h, such that

$$\|\widetilde{p}_h\|_{\mathsf{D}_h} \leq \beta \sup_{\boldsymbol{w}\in\boldsymbol{H}_0^1(\mathsf{D}_h)\setminus\{\mathbf{0}\}} \frac{(\widetilde{p}_h, \nabla\cdot\boldsymbol{w})_{\mathsf{D}_h}}{\|\boldsymbol{w}\|_{\boldsymbol{H}^1(\mathsf{D}_h)}}. \tag{2.8}$$

On the other hand, let $\boldsymbol{P} : \boldsymbol{H}^1(\mathsf{T}_h) \to \boldsymbol{V}_h$ be any projection such that $(\boldsymbol{P}\boldsymbol{w} - \boldsymbol{w}, \boldsymbol{v})_K = 0$ for all $\boldsymbol{v} \in \boldsymbol{\mathcal{P}}_{k-1}(K)$, for all $K \in \mathsf{T}_h$.

Now, we will work on the numerator of the right hand side of (2.8). Integrating by parts and using the projection $\boldsymbol{P}$, we have

$$\begin{aligned}(\widetilde{p}_h, \nabla\cdot\boldsymbol{w})_{\mathsf{D}_h} &= -(\nabla\widetilde{p}_h, \boldsymbol{w})_{\mathsf{T}_h} + \langle\widetilde{p}_h\boldsymbol{n}, \boldsymbol{w}\rangle_{\partial\mathsf{T}_h}\\ &= -(\nabla\widetilde{p}_h, \boldsymbol{P}\boldsymbol{w})_{\mathsf{T}_h} + \langle\widetilde{p}_h\boldsymbol{n}, \boldsymbol{w}\rangle_{\partial\mathsf{T}_h}.\end{aligned} \tag{2.9}$$

Integrating by parts again and using (2.4b) with $\boldsymbol{v} := \boldsymbol{P}\boldsymbol{w}$, we obtain

$$\begin{aligned}-(\nabla\widetilde{p}_h, \boldsymbol{P}\boldsymbol{w})_{\mathsf{T}_h} &= (\widetilde{p}_h, \nabla\cdot\boldsymbol{P}\boldsymbol{w})_{\mathsf{T}_h} - \langle\widetilde{p}_h\boldsymbol{n}, \boldsymbol{P}\boldsymbol{w}\rangle_{\partial\mathsf{T}_h}\\ &= (\nu\mathrm{L}_h, \nabla\boldsymbol{P}\boldsymbol{w})_{\mathsf{T}_h} - \langle\nu\widehat{\mathrm{L}}_h\boldsymbol{n} - \widehat{p}_h\boldsymbol{n}, \boldsymbol{P}\boldsymbol{w}\rangle_{\partial\mathsf{T}_h} - \langle\widetilde{p}_h\boldsymbol{n}, \boldsymbol{P}\boldsymbol{w}\rangle_{\partial\mathsf{T}_h}.\end{aligned}$$

Using the definition of the numerical flux (2.4g), we can write

$$-(\nabla\widetilde{p}_h, \boldsymbol{P}\boldsymbol{w})_{\mathsf{T}_h} = (\nu\mathrm{L}_h, \nabla\boldsymbol{P}\boldsymbol{w})_{\mathsf{T}_h} - \langle\nu\mathrm{L}_h\boldsymbol{n}, \boldsymbol{P}\boldsymbol{w}\rangle_{\partial\mathsf{T}_h} + \langle\tau\nu(\boldsymbol{u}_h - \widehat{\boldsymbol{u}}_h), \boldsymbol{P}\boldsymbol{w}\rangle_{\partial\mathsf{T}_h}.$$

Integrating by parts we observe that

$$(\nu\mathrm{L}_h, \nabla\boldsymbol{P}\boldsymbol{w})_{\mathsf{T}_h} - \langle\nu\mathrm{L}_h\boldsymbol{n}, \boldsymbol{P}\boldsymbol{w}\rangle_{\partial\mathsf{T}_h} = -(\nu\nabla\cdot\mathrm{L}_h, \boldsymbol{P}\boldsymbol{w})_{\mathsf{T}_h}.$$

Using the projection $\boldsymbol{P}$ and integrating by parts once again, we obtain

$$-(\nu\nabla\cdot\mathrm{L}_h, \boldsymbol{P}\boldsymbol{w})_{\mathsf{T}_h} = -(\nu\nabla\cdot\mathrm{L}_h, \boldsymbol{w})_{\mathsf{T}_h} = (\nu\mathrm{L}_h, \nabla\boldsymbol{w})_{\mathsf{T}_h} - \langle\nu\mathrm{L}_h\boldsymbol{n}, \boldsymbol{w}\rangle_{\partial\mathsf{T}_h}.$$

Hence, we have that

$$-(\nabla\widetilde{p}_h, \boldsymbol{P}\boldsymbol{w})_{\mathsf{T}_h} = (\nu\mathrm{L}_h, \nabla\boldsymbol{w})_{\mathsf{T}_h} - \langle\nu\mathrm{L}_h\boldsymbol{n}, \boldsymbol{w}\rangle_{\partial\mathsf{T}_h} + \langle\tau\nu(\boldsymbol{u}_h - \widehat{\boldsymbol{u}}_h), \boldsymbol{P}\boldsymbol{w}\rangle_{\partial\mathsf{T}_h}.$$

Replacing this into (2.9), we conclude that

$$(\widetilde{p}_h, \nabla\cdot\boldsymbol{w})_{\mathsf{D}_h} = (\nu\mathrm{L}_h, \nabla\boldsymbol{w})_{\mathsf{T}_h} + \langle\tau\nu(\boldsymbol{u}_h - \widehat{\boldsymbol{u}}_h), \boldsymbol{P}\boldsymbol{w}\rangle_{\partial\mathsf{T}_h} - \langle\nu\mathrm{L}_h\boldsymbol{n} - \widetilde{p}_h\boldsymbol{n}, \boldsymbol{w}\rangle_{\partial\mathsf{T}_h}.$$

Adding and subtracting the term $\langle \tau\nu(\boldsymbol{u}_h - \widehat{\boldsymbol{u}}_h), \boldsymbol{w}\rangle_{\partial \mathsf{T}_h}$, we can rewrite this equation as

$$\begin{aligned}(\widetilde{p}_h, \nabla\cdot\boldsymbol{w})_{\mathsf{D}_h} &= (\nu \mathrm{L}_h, \nabla\boldsymbol{w})_{\mathsf{T}_h} + \langle \tau\nu(\boldsymbol{u}_h - \widehat{\boldsymbol{u}}_h), \boldsymbol{P}\boldsymbol{w} - \boldsymbol{w}\rangle_{\partial\mathsf{T}_h}\\ &\quad -\langle \nu\mathrm{L}_h\boldsymbol{n} - \widetilde{p}_h\boldsymbol{n} - \tau\nu(\boldsymbol{u}_h - \widehat{\boldsymbol{u}}_h), \boldsymbol{w}\rangle_{\partial\mathsf{T}_h}.\end{aligned}$$

Since $\nu\mathrm{L}_h, \widetilde{p}_h$ and $\tau\nu(\boldsymbol{u}_h - \widehat{\boldsymbol{u}}_h)$ are polynomials, we can use the definition of $\mathbf{P}_M$ to rewrite the last equation as

$$\begin{aligned}(\widetilde{p}_h, \nabla\cdot\boldsymbol{w})_{\mathsf{D}_h} &= (\nu \mathrm{L}_h, \nabla\boldsymbol{w})_{\mathsf{T}_h} + \langle \tau\nu(\boldsymbol{u}_h - \widehat{\boldsymbol{u}}_h), \boldsymbol{P}\boldsymbol{w} - \mathbf{P}_M\boldsymbol{w}\rangle_{\partial\mathsf{T}_h}\\ &\quad -\langle \nu\mathrm{L}_h\boldsymbol{n} - \widetilde{p}_h\boldsymbol{n} - \tau\nu(\boldsymbol{u}_h - \widehat{\boldsymbol{u}}_h), \mathbf{P}_M\boldsymbol{w}\rangle_{\partial\mathsf{T}_h}.\end{aligned}$$

The last term vanishes thanks to (2.4e) with $\boldsymbol{\mu} = \mathbf{P}_M\boldsymbol{w}$ and the fact that $\boldsymbol{w} \in \boldsymbol{H}_0^1(\mathsf{D}_h)$. Thus,

$$(\widetilde{p}_h, \nabla\cdot\boldsymbol{w})_{\mathsf{D}_h} = (\nu \mathrm{L}_h, \nabla\boldsymbol{w})_{\mathsf{T}_h} + \langle \tau\nu(\boldsymbol{u}_h - \widetilde{\boldsymbol{u}}_h), \boldsymbol{P}\boldsymbol{w} - \mathbf{P}_M\boldsymbol{w}\rangle_{\partial\mathsf{T}_h}, \tag{2.10}$$

On the other hand, Proposition 3.9 in [18], states that

$$\max\left\{1, \sup_{\boldsymbol{w}\in\boldsymbol{H}_0^1(\mathsf{D}_h)\setminus\{\mathbf{0}\}} \frac{\|\boldsymbol{P}\boldsymbol{w} - \mathbf{P}_M\boldsymbol{w}\|_{\partial\mathsf{T}_h,\tau}}{\|\boldsymbol{w}\|_{\boldsymbol{H}^1(\mathsf{D}_h)}}\right\} \leq \max\left\{1, \max_{K\in\mathsf{T}_h}(\tau h_K)^{1/2}\right\}. \tag{2.11}$$

Combining (2.8), (2.10), Cauchy-Schwarz inequality and (2.11), we arrive at

$$\|\widetilde{p}_h\|_{\mathsf{D}_h} \leq \beta\nu M(\|\mathrm{L}_h\|_{\mathsf{D}_h} + \|\boldsymbol{u}_h - \widetilde{\boldsymbol{u}}_h\|_{\partial\mathsf{T}_h,\tau}) \leq \beta M 2\sqrt{6}\|\widetilde{p}_h\|_{\Gamma_h,l},$$

where the last inequality is provided by Lemma 2.2. Thus, the result follows from this estimate, discrete trace inequality (1.7) and Assumption (A.3).

□

2.3 Error estimates

In this section we summarize the main error estimates in this chapter. First, we make the following assumption that allows us to estimate the L^2-norm of $\boldsymbol{u}$ by using a duality argument.

For any given $\boldsymbol{\theta} \in \boldsymbol{L}^2(\Omega)$, let $(\Phi, \boldsymbol{\phi}, \phi)$ be the solution of

$$\Phi + \nabla\boldsymbol{\phi} = 0 \quad \text{in } \Omega, \tag{2.12a}$$
$$\nabla\cdot(\nu\Phi) - \nabla\phi = \boldsymbol{\theta} \quad \text{in } \Omega, \tag{2.12b}$$
$$-\nabla\cdot\boldsymbol{\phi} = 0 \quad \text{in } \Omega, \tag{2.12c}$$
$$\boldsymbol{\phi} = \mathbf{0} \quad \text{on } \partial\Omega. \tag{2.12d}$$

We suppose

Assumption B

$$\nu\|\Phi\|_{\mathrm{H}^1(\Omega)} + \nu\|\boldsymbol{\phi}\|_{\boldsymbol{H}^2(\Omega)} + \|\phi\|_{H^1(\Omega)} \leq C\|\boldsymbol{\theta}\|_\Omega. \tag{2.13}$$

This is satisfied, for example, for the two-dimensional case if the domain is convex [46] and for any convex polyhedron in three dimensions [26].

Theorem 2.4. *Suppose that Assumptions A hold and τ of order one. If $(\mathrm{L},\boldsymbol{u},\widetilde{p})\in H^{k+1}(\Omega)\times\boldsymbol{H}^{k+1}(\Omega)\times H^{k+1}(\Omega)$, then, for $h<1$ and $k\geq 1$, we have*

$$\|\mathrm{L}-\mathrm{L}_h\|_{\mathsf{D}_h}+\|\widetilde{\boldsymbol{g}}-\widetilde{\boldsymbol{g}}_h\|_{\Gamma_h,l^{-1}}+\nu^{-1}\|\widetilde{p}-\widetilde{p}_h\|_{\mathsf{D}_h}\lesssim C_{reg}\,h^{k+1}.$$

Moreover, if Assumption B holds, then $\|\boldsymbol{u}-\boldsymbol{u}_h\|_{\mathsf{D}_h}\lesssim C_{reg}\,h^{k+1}$ and

$$\|\mathbf{P}_M\boldsymbol{u}-\widehat{\boldsymbol{u}}_h\|_{\partial\mathsf{T}_h,h}+\|\boldsymbol{u}-\boldsymbol{u}_h^*\|_{\mathsf{D}_h}\lesssim C_{reg}\,h^{k+3/2}\left(R+R^{1/2}+h^{1/2}R+R^{3/2}\right).$$

Here, $R:=\max_{e\in\mathcal{E}_h^i}r_e$ (defined in section 1.1.2) $C_{reg}:=\big(|\mathrm{L}-\nu^{-1}\widetilde{p}\mathrm{I}|_{\mathrm{H}^{k+1}(\mathsf{D}_h)}+\tau|\boldsymbol{u}|_{\boldsymbol{H}^{k+1}(\mathsf{D}_h)}+|\mathrm{L}|_{\mathrm{H}^{k+1}(\mathsf{D}_h)}\big)$ and $\boldsymbol{u}_h^*$ is an element-by-element postprocessing of $\boldsymbol{u}_h$ computed as follows. For each element $K\in\mathsf{T}_h$, we seek $\boldsymbol{u}_h^*\in\boldsymbol{\mathcal{P}}_{k+1}^0(K):=\{\boldsymbol{w}\in\boldsymbol{\mathcal{P}}_{k+1}(K):\int_K\boldsymbol{w}=0\}$ such that

$$(\nabla\boldsymbol{u}_h^*,\nabla\boldsymbol{w}_h)_K=(\mathrm{L}_h,\nabla\boldsymbol{w}_h)_K\quad\forall\boldsymbol{w}_h\in\boldsymbol{\mathcal{P}}_{k+1}^0(K),\tag{2.14a}$$

$$\int_K\boldsymbol{u}_h^*=\int_K\boldsymbol{u}_h.\tag{2.14b}$$

In other words, if the solution is smooth enough then the L^2-norm of the errors in L, $\boldsymbol{u}$ and $\widetilde{p}$ are of order h^{k+1}, which is the same as in the case of a polyhedral domain [18]. In addition, the above estimate indicates that the error in the numerical trace $\widehat{\boldsymbol{u}}_h$ and the post processed solution $\boldsymbol{u}_h^*$ is of order h^{k+2} if R is of order h and only of order $h^{k+3/2}$ if R is of order one. For the latter case, our numerical experiments suggest an experimental order of convergence higher than of $h^{k+3/2}$. The same behavior has been observed for the Poisson's equation in curved domains [21].

2.4 Proofs

This section is devoted to prove the error estimates stated in Theorem 2.4. It follows from the standard procedure for analyzing HDG schemes using the projection-based approach. That is, a suitable projection operator is defined and then an energy argument helps to bound the projection of the errors of all variables except $\boldsymbol{u}$. A duality argument is employed to obtain an L^2-estimate of the projection of the error in $\boldsymbol{u}$. The main difference compared to [18] is the presence of additional terms at Γ_h due to the approximation of the boundary data (1.2).

2.4.1 An energy argument

First of all, let us recall the projection defined in [18] which will be used in our analysis. If $(\mathrm{L},\boldsymbol{u},\widetilde{p})\in\mathrm{H}^1(\mathsf{T}_h)\times\boldsymbol{H}^1(\mathsf{T}_h)\times H^1(\mathsf{T}_h)$, we take its projection $\mathit{\Pi}_h(\mathrm{L},\boldsymbol{u},\widetilde{p}):=(\Pi\mathrm{L},\boldsymbol{\mathit{\Pi}}\boldsymbol{u},\mathit{\Pi}\widetilde{p})$ as the element of $\mathrm{G}_h\times\boldsymbol{V}_h\times P_h$ defined as follows. On an arbitrary element K of the triangulation T_h, the values of the projected function on the simplex K are determined by requiring that

$$(\Pi\mathrm{L},\mathrm{G})_K=(\mathrm{L},\mathrm{G})_K\qquad\forall\,\mathrm{G}\in\mathrm{P}_{k-1}(K),\tag{2.15a}$$

$$(\boldsymbol{\mathit{\Pi}}\boldsymbol{u},\boldsymbol{v})_K=(\boldsymbol{u},\boldsymbol{v})_K\qquad\forall\,\boldsymbol{v}\in\boldsymbol{\mathcal{P}}_{k-1}(K),\tag{2.15b}$$

$$(\mathit{\Pi}\widetilde{p},q)_K=(\widetilde{p},q)_K\qquad\forall\,q\in\mathcal{P}_{k-1}(K),\tag{2.15c}$$

$$(\mathrm{tr}\;\Pi\mathrm{L},q)_K=(\mathrm{tr}\;\mathrm{L},q)_K\qquad\forall\,q\in\mathcal{P}_k(K),\tag{2.15d}$$

$$\langle\nu\Pi\mathrm{L}\boldsymbol{n}-\mathit{\Pi}\widetilde{p}\boldsymbol{n}-\tau\nu\boldsymbol{\mathit{\Pi}}\boldsymbol{u},\boldsymbol{\mu}\rangle_e=\langle\nu\mathrm{L}\boldsymbol{n}-\widetilde{p}\boldsymbol{n}-\tau\nu\boldsymbol{u},\boldsymbol{\mu}\rangle_e,\qquad\forall\,\boldsymbol{\mu}\in\boldsymbol{\mathcal{P}}_k(e)\tag{2.15e}$$

for all faces e of the simplex K. Thus, we define the projection of the errors $\mathrm{E}^{\mathrm{L}} := \Pi\mathrm{L} - \mathrm{L}_h$, $\boldsymbol{\varepsilon}^{\boldsymbol{u}} := \boldsymbol{\Pi}\boldsymbol{u} - \boldsymbol{u}_h$, $\varepsilon^p := \Pi\widetilde{p} - \widetilde{p}_h$, $\boldsymbol{\varepsilon}^{\hat{\boldsymbol{u}}} := \mathbf{P}_M\boldsymbol{u} - \widehat{\boldsymbol{u}}_h$; and the interpolation errors $\mathrm{I}^{\mathrm{L}} := \mathrm{L} - \Pi\mathrm{L}$, $\boldsymbol{I}^{\boldsymbol{u}} := \boldsymbol{u} - \boldsymbol{\Pi}\boldsymbol{u}$, $I^p := \widetilde{p} - \Pi\widetilde{p}$. If $(\mathrm{L}, \boldsymbol{u}, \widetilde{p}) \in \mathrm{H}^{k+1}(K) \times \boldsymbol{H}^{k+1}(K) \times H^{k+1}(K)$ on each element $K \in \mathsf{T}_h$, it is known (Theorem 2.1 in [18]) that the above defined projection satisfies the following properties:

$$\|\boldsymbol{I}^{\boldsymbol{u}}\|_K \lesssim h_K^{k+1}|\boldsymbol{u}|_{\boldsymbol{H}^{k+1}(K)} + h_K^{k+1}(\tau\nu)^{-1}|\nabla\cdot(\nu\mathrm{L} - \mathrm{I}\widetilde{p})|_{\mathrm{H}^k(K)}, \tag{2.16a}$$

$$\|\nu\mathrm{I}^{\mathrm{L}}\|_K + \|I^p\|_K \lesssim h_K^{k+1}|\nu\mathrm{L} - \widetilde{p}\mathrm{I}|_{\mathrm{H}^{k+1}(K)} + h_K^{k+1}\tau\nu|\boldsymbol{u}|_{\boldsymbol{H}^{k+1}(K)} + \tau\nu\|\boldsymbol{I}^{\boldsymbol{u}}\|_K. \tag{2.16b}$$

Moreover, by a standard scaling argument and the fact that $h_e^{\perp} \leq h_K$, we obtain

$$\|\mathrm{I}^{\mathrm{L}}\boldsymbol{n}\|_{e,h_e^{\perp}} \lesssim \|\mathrm{I}^{\mathrm{L}}\|_K, \quad \|\boldsymbol{I}^{\boldsymbol{u}}\|_{e,h_e^{\perp}} \lesssim \|\boldsymbol{I}^{\boldsymbol{u}}\|_K, \quad \text{and} \quad \|I^p\|_{e,h_e^{\perp}} \lesssim \|I^p\|_K. \tag{2.16c}$$

We observe that $\int_{\mathsf{D}_h}\varepsilon^p = 0$ for $k > 0$, thanks to (2.15c) and (2.4f). Since we are interested in a high order method, we assume $k > 0$ to avoid technicalities.

Let $\partial_{\boldsymbol{n}}(\mathrm{I}^{\mathrm{L}}\boldsymbol{n})$ be the directional derivative of each component of $\mathrm{I}^{\mathrm{L}}\boldsymbol{n}$. We define the following quantity that will appear in the right hand side of next estimates:

$$\Theta_{\mathrm{I}^{\mathrm{L}}} := \left(4R^2\|\partial_n(\mathrm{I}^{\mathrm{L}}\boldsymbol{n})\|^2_{\mathsf{D}_h^c,(h^{\perp})^2} + 12R\|\mathrm{I}^{\mathrm{L}}\boldsymbol{n}\|^2_{\Gamma_h,h^{\perp}} + 5\|\mathrm{I}^{\mathrm{L}}\|^2_{\mathsf{D}_h}\right)^{1/2}. \tag{2.17}$$

If $(\mathrm{L}, \boldsymbol{u}, \widetilde{p}) \in \mathrm{H}^{k+1}(\Omega) \times \boldsymbol{H}^{k+1}(\Omega) \times H^{k+1}(\Omega)$, by Lemma 3.8 in [21] and (2.16), we have

$$\Theta_{\mathrm{I}^{\mathrm{L}}} \lesssim h^{k+1}\left(|\mathrm{L} - \nu^{-1}\widetilde{p}\mathrm{I}|_{\mathrm{H}^{k+1}(\Omega)} + \tau|\boldsymbol{u}|_{\boldsymbol{H}^{k+1}(\Omega)} + |\mathrm{L}|_{\mathrm{H}^{k+1}(\Omega)}\right). \tag{2.18}$$

Lemma 2.5. *Let us suppose Assumptions A hold. Then*

$$\begin{aligned}
|\!|\!|\left(\mathrm{E}^{\mathrm{L}}, \boldsymbol{\varepsilon}^{\boldsymbol{u}} - \boldsymbol{\varepsilon}^{\hat{\boldsymbol{u}}}, \tilde{\boldsymbol{g}} - \tilde{\boldsymbol{g}}_h, \varepsilon^p\right)|\!|\!| &\leq \left(4\sqrt{3}\beta M + 1\right)\Theta_{\mathrm{I}^{\mathrm{L}}}, \quad \textit{where} \\
|\!|\!|\left(\mathrm{E}^{\mathrm{L}}, \boldsymbol{\varepsilon}^{\boldsymbol{u}} - \boldsymbol{\varepsilon}^{\hat{\boldsymbol{u}}}, \tilde{\boldsymbol{g}} - \tilde{\boldsymbol{g}}_h, \varepsilon^p\right)|\!|\!| &:= \big(\|\mathrm{E}^{\mathrm{L}}\|^2_{\mathsf{D}_h} + \|\boldsymbol{\varepsilon}^{\boldsymbol{u}} - \boldsymbol{\varepsilon}^{\hat{\boldsymbol{u}}}\|^2_{\partial\mathsf{T}_h,\tau} + \|\tilde{\boldsymbol{g}} - \tilde{\boldsymbol{g}}_h\|^2_{\Gamma_h,l^{-1}} \\
&\quad + \nu^{-2}\|\varepsilon^p\|^2_{\mathsf{D}_h}\big)^{1/2}.
\end{aligned}$$

We now proceed to detail the steps that lead to the statement of Lemma 2.5. As we will see, we will employ the ideas behind the proofs of Lemmas 2.2 and 2.3.

Step 1: The projection of the errors

The following lemma establishes the equations satisfied by the projection of the errors.

Lemma 2.6.

$$(\mathrm{E}^{\mathrm{L}}, \mathrm{G})_{\mathsf{T}_h} + (\boldsymbol{\varepsilon}^{\boldsymbol{u}}, \nabla\cdot\mathrm{G})_{\mathsf{T}_h} - \langle\boldsymbol{\varepsilon}^{\hat{\boldsymbol{u}}}, \mathrm{G}\boldsymbol{n}\rangle_{\partial\mathsf{T}_h} = -(\mathrm{I}^{\mathrm{L}}, \mathrm{G})_{\mathsf{T}_h}, \tag{2.19a}$$

$$-(\nabla\cdot(\nu\mathrm{E}^{\mathrm{L}}), \boldsymbol{v})_{\mathsf{T}_h} + (\nabla\varepsilon^p, \boldsymbol{v})_{\mathsf{T}_h} + \langle\tau\nu(\boldsymbol{\varepsilon}^{\boldsymbol{u}} - \boldsymbol{\varepsilon}^{\hat{\boldsymbol{u}}}), \boldsymbol{v}\rangle_{\partial\mathsf{T}_h} = 0, \tag{2.19b}$$

$$-(\boldsymbol{\varepsilon}^{\boldsymbol{u}}, \nabla q)_{\mathsf{T}_h} + \langle\boldsymbol{\varepsilon}^{\hat{\boldsymbol{u}}}, q\boldsymbol{n}\rangle_{\partial\mathsf{T}_h} = 0, \tag{2.19c}$$

$$\langle\boldsymbol{\varepsilon}^{\hat{\boldsymbol{u}}}, \boldsymbol{\mu}\rangle_{\Gamma_h} = \langle\tilde{\boldsymbol{g}} - \tilde{\boldsymbol{g}}_h, \boldsymbol{\mu}\rangle_{\Gamma_h}, \tag{2.19d}$$

$$\langle\hat{\mathrm{E}}\boldsymbol{n}, \boldsymbol{\mu}\rangle_{\partial\mathsf{T}_h\setminus\Gamma_h} = 0, \tag{2.19e}$$

$$(\varepsilon^p, 1)_{\mathsf{D}_h} = 0, \tag{2.19f}$$

for all $(\mathrm{G}, \boldsymbol{v}, q, \boldsymbol{\mu}) \in \mathrm{G}_h \times \boldsymbol{V}_h \times P_h \times \boldsymbol{M}_h$, *where*

$$\begin{aligned} \hat{\mathrm{E}}\boldsymbol{n} &:= \mathbf{P}_M(\nu \mathrm{L}\boldsymbol{n} - \widetilde{p}\boldsymbol{n} - \nu\widehat{\mathrm{L}}_h\boldsymbol{n} + \widehat{p}_h\boldsymbol{n}) \\ &= \nu\mathrm{E}^{\mathrm{L}}\boldsymbol{n} - \varepsilon^p\boldsymbol{n} - \tau\nu(\boldsymbol{\varepsilon}^{\boldsymbol{u}} - \boldsymbol{\varepsilon}^{\hat{\boldsymbol{u}}}) \text{ on } \partial\mathsf{T}_h. \end{aligned} \tag{2.19g}$$

Proof. All the equations, except (2.19d), follow directly from Lemma 3.1 in [18]. To show (2.19d), let $\boldsymbol{\mu} \in \boldsymbol{M}_h$. Thanks to (2.4d) and the fact that $\widetilde{\boldsymbol{g}} = \boldsymbol{u}$ on Γ_h, we get $\langle \boldsymbol{\varepsilon}^{\hat{\boldsymbol{u}}}, \boldsymbol{\mu}\rangle_{\Gamma_h} = \langle \mathbf{P}_M\boldsymbol{u} - \widehat{\boldsymbol{u}}_h, \boldsymbol{\mu}\rangle_{\Gamma_h} = \langle \boldsymbol{u}, \boldsymbol{\mu}\rangle_{\Gamma_h} - \langle \widehat{\boldsymbol{u}}_h, \boldsymbol{\mu}\rangle_{\Gamma_h} = \langle \widetilde{\boldsymbol{g}}, \boldsymbol{\mu}\rangle_{\Gamma_h} - \langle \widetilde{\boldsymbol{g}}_h, \boldsymbol{\mu}\rangle_{\Gamma_h}$.

□

Corollary 2.7. *Let* $\mathbb{T}_{\mathrm{L},h} := \nu^{-1}\langle \boldsymbol{\varepsilon}^{\hat{\boldsymbol{u}}}, \hat{\mathrm{E}}\boldsymbol{n}\rangle_{\Gamma_h}$. *Then,*

$$\|\mathrm{E}^{\mathrm{L}}\|^2_{\mathsf{D}_h} + \|\boldsymbol{\varepsilon}^{\boldsymbol{u}} - \boldsymbol{\varepsilon}^{\hat{\boldsymbol{u}}}\|^2_{\partial\mathsf{T}_h,\tau} = -(\mathrm{I}^{\mathrm{L}}, \mathrm{E}^{\mathrm{L}})_{\mathsf{T}_h} + \mathbb{T}_{\mathrm{L},h}.$$

Proof. It is consequence of previous lemma by taking $\mathrm{G} = \nu\mathrm{E}^{\mathrm{L}}$, $\boldsymbol{v} = \boldsymbol{\varepsilon}^{\boldsymbol{u}}$, $q = \varepsilon^p$, $\boldsymbol{\mu} = \boldsymbol{\varepsilon}^{\hat{\boldsymbol{u}}}$ and adding the equations.

□

If Ω were polygonal and the mesh is fitted to it, then $\widetilde{\boldsymbol{g}}$ would be equal to $\widetilde{\boldsymbol{g}}_h$. Thus, the right hand side of (2.19d) would be zero and, as a consequence, $\mathbb{T}_{\mathrm{L},h}$ would vanish, recovering Lemma 3.1 and Proposition 3.2 in [18].

Step 2: A bound for $\mathbb{T}_{\mathrm{L},h}$

Following the approach by [21], we need to rewrite the term $\mathbb{T}_{\mathrm{L},h}$ in a suitable manner.

Lemma 2.8.

$$\begin{aligned} \mathbb{T}_{\mathrm{L},h} \leq\ & - \|\tilde{\boldsymbol{g}} - \tilde{\boldsymbol{g}}_h\|^2_{\Gamma_h,l^{-1}} + \|\tilde{\boldsymbol{g}} - \tilde{\boldsymbol{g}}_h\|_{\Gamma_h,l^{-1}}\big\{\|\delta_{\mathrm{I}^{\mathrm{L}}}\|_{\Gamma_h,l} + \|\mathrm{I}^{\mathrm{L}}\boldsymbol{n}\|_{\Gamma_h,l} \\ & + \|\delta_{\mathrm{E}^{\mathrm{L}}}\|_{\Gamma_h,l} + \|\boldsymbol{\varepsilon}^{\boldsymbol{u}} - \boldsymbol{\varepsilon}^{\hat{\boldsymbol{u}}}\|_{\Gamma_h,\tau^2 l} + \nu^{-1}\|\varepsilon^p\|_{\Gamma_h,l}\big\}. \end{aligned}$$

Proof. Proceeding exactly as in Lemma 5.1 of [21], it is not difficult to see that, according to (1.1), (1.2) and (1.3), we can decompose $(\tilde{\boldsymbol{g}} - \tilde{\boldsymbol{g}}_h)(\boldsymbol{x}) = -l(\boldsymbol{x})\big\{\delta_{\mathrm{I}^{\mathrm{L}}} + \mathrm{I}^{\mathrm{L}}\boldsymbol{n} + \delta_{\mathrm{E}^{\mathrm{L}}} + \mathrm{E}^{\mathrm{L}}\boldsymbol{n}\big\}(\boldsymbol{x})$. Then, by (2.19g), we obtain

$$\hat{\mathrm{E}}\boldsymbol{n} = -\nu\left\{(\tilde{\boldsymbol{g}} - \tilde{\boldsymbol{g}}_h)/l + \delta_{\mathrm{I}^{\mathrm{L}}} + \mathrm{I}^{\mathrm{L}}\boldsymbol{n} + \delta_{\mathrm{E}^{\mathrm{L}}}\right\} - \varepsilon^p\boldsymbol{n} - \tau\nu(\boldsymbol{\varepsilon}^{\boldsymbol{u}} - \boldsymbol{\varepsilon}^{\hat{\boldsymbol{u}}}). \tag{2.20}$$

On the other hand, by the definition of $\mathbb{T}_{\mathrm{L},h}$ and (2.19d),

$$\mathbb{T}_{\mathrm{L},h} := \nu^{-1}\langle \boldsymbol{\varepsilon}^{\hat{\boldsymbol{u}}}, \hat{\mathrm{E}}\boldsymbol{n}\rangle_{\Gamma_h} = \nu^{-1}\langle \mathbf{P}_M(\tilde{\boldsymbol{g}} - \tilde{\boldsymbol{g}}_h), \hat{\mathrm{E}}\boldsymbol{n}\rangle_{\Gamma_h} = \nu^{-1}\langle (\tilde{\boldsymbol{g}} - \tilde{\boldsymbol{g}}_h), \hat{\mathrm{E}}\boldsymbol{n}\rangle_{\Gamma_h},$$

which, according to (2.20), leads to the decomposition $\mathbb{T}_{\mathrm{L},h} = \sum_{i=1}^6 \mathbb{T}^i_{\mathrm{L},h}$, where

$$\begin{aligned} \mathbb{T}^1_{\mathrm{L},h} &= -\langle (\tilde{\boldsymbol{g}} - \tilde{\boldsymbol{g}}_h)/l, (\tilde{\boldsymbol{g}} - \tilde{\boldsymbol{g}}_h)\rangle_{\Gamma_h}, & \mathbb{T}^2_{\mathrm{L},h} &= -\langle \tilde{\boldsymbol{g}} - \tilde{\boldsymbol{g}}_h, \delta_{\mathrm{I}^{\mathrm{L}}}\rangle_{\Gamma_h}, \\ \mathbb{T}^3_{\mathrm{L},h} &= -\langle \tilde{\boldsymbol{g}} - \tilde{\boldsymbol{g}}_h, \mathrm{I}^{\mathrm{L}}\boldsymbol{n}\rangle_{\Gamma_h}, & \mathbb{T}^4_{\mathrm{L},h} &= -\langle \tilde{\boldsymbol{g}} - \tilde{\boldsymbol{g}}_h, \delta_{\mathrm{E}^{\mathrm{L}}}\rangle_{\Gamma_h}, \\ \mathbb{T}^5_{\mathrm{L},h} &= -\langle \tilde{\boldsymbol{g}} - \tilde{\boldsymbol{g}}_h, \tau(\boldsymbol{\varepsilon}^{\boldsymbol{u}} - \boldsymbol{\varepsilon}^{\hat{\boldsymbol{u}}})\rangle_{\Gamma_h}, & \mathbb{T}^6_{\mathrm{L},h} &= -\nu^{-1}\langle \tilde{\boldsymbol{g}} - \tilde{\boldsymbol{g}}_h, \varepsilon^p\boldsymbol{n}\rangle_{\Gamma_h}. \end{aligned}$$

The result is obtained by applying Cauchy-Schwarz inequality to each of these terms.

□

Step 3: A first energy estimate

We recall the estimate in Lemma 5.2 of [21]:

$$\|l^{1/2}\delta_{\mathrm{I^L}}\|_e \leq 3^{-\frac{1}{2}} r_e \|h_e^{\perp}\partial_n(\mathrm{I^L}\boldsymbol{n})\|_{K^e_{ext}}. \tag{2.21}$$

Thus, gathering the result stated in Corollary 2.7, estimate in Lemma 2.8, inequality (2.21), (1.4) with $\mathrm{G} = \mathrm{E^L}$, Young's inequality, definition (2.17) and noticing that $\|\mathrm{I^L}\boldsymbol{n}\|^2_{\Gamma_h,l} \leq R\|\mathrm{I^L}\boldsymbol{n}\|^2_{\Gamma_h,h^\perp}$, we conclude:

Lemma 2.9. $\|\mathrm{E^L}\|^2_{\mathsf{D}_h} + \|\boldsymbol{\varepsilon}^{\boldsymbol{u}} - \boldsymbol{\varepsilon}^{\hat{\boldsymbol{u}}}\|^2_{\partial\mathsf{T}_h,\tau} + \|\tilde{\boldsymbol{g}} - \tilde{\boldsymbol{g}}_h\|^2_{\Gamma_h,l^{-1}} \leq \Theta^2_{\mathrm{I^L}} + 12\nu^{-2}\|\varepsilon^p\|^2_{\Gamma_h,l}$.

Comparing this estimate with the corresponding result in [18] for polyhedral domains, we see in our case the presence of the terms $\|\tilde{\boldsymbol{g}} - \tilde{\boldsymbol{g}}_h\|^2_{\Gamma_h,l^{-1}}$ and $12\nu^{-2}\|\varepsilon^p\|^2_{\Gamma_h,l}$ coming from $\mathbb{T}_{\mathrm{L},h}$. In other words, for a polyhedral domain, we would have $\mathbb{T}_{\mathrm{L},h} = 0$ and recover the estimates in [18]. We also observe that the estimate in Lemma 2.9 is similar to the one obtained in Lemma 2.2, except that the right hand side involves terms related to the interpolation operator instead of the source term and boundary data. Similarly, we must bound the term that contains ε^p and proceed as in Lemma 2.3.

Lemma 2.10. *If Assumption (A.3) holds, then* $\|\varepsilon^p\|_{\mathsf{D}_h} \leq 3\sqrt{2}\beta\nu M\Theta_{\mathrm{I^L}}$.

Proof. The proof of this lemma is very similar to that of Lemma 2.3. Since $\varepsilon^p \in L^2_0(\mathsf{D}_h)$, there exists $\beta > 0$ such that

$$\|\varepsilon^p\|_{\mathsf{D}_h} \leq \beta \sup_{\boldsymbol{w}\in\boldsymbol{H}^1_0(\mathsf{D}_h)\setminus\{\boldsymbol{0}\}} \frac{(\varepsilon^p, \nabla\cdot\boldsymbol{w})_{\mathsf{D}_h}}{\|\boldsymbol{w}\|_{\boldsymbol{H}^1(\mathsf{D}_h)}}. \tag{2.22}$$

On the other hand, similarly to the proof of Lemma 2.3, using (2.19e), we get

$$(\varepsilon^p, \nabla\cdot\boldsymbol{w})_{\mathsf{D}_h} = (\nu\mathrm{E^L}, \nabla\boldsymbol{w})_{\mathsf{T}_h} + \langle\tau\nu(\boldsymbol{\varepsilon}^{\boldsymbol{u}} - \boldsymbol{\varepsilon}^{\hat{\boldsymbol{u}}}), \boldsymbol{P}\boldsymbol{w} - \mathbf{P}_M\boldsymbol{w}\rangle_{\partial\mathsf{T}_h}, \tag{2.23}$$

for $\boldsymbol{w} \in \boldsymbol{H}^1_0(\mathsf{D}_h)$. Using Cauchy-Schwarz inequality in this expression, combining (2.22), (2.11), Lemma 2.9, trace inequality (1.7) and Assumption (A.4), the result follows.

□

If Ω were polyhedral, this result reduces to the estimate of Proposition 3.4 in [18].

Step 4: Conclusion of the proof of Lemma 2.5

Gathering the bounds obtained in Lemmas 2.9 and 2.10, we obtain the estimate stated in Lemma 2.5.

2.4.2 A duality argument

We recall ([18]) properties of the projection $\mathit{\Pi}_h$ that will be used to obtain estimates for the velocity. Let $(\Phi, \boldsymbol{\phi}, \phi) \in \mathrm{H}^1(\mathsf{T}_h) \times \boldsymbol{H}^1(\mathsf{T}_h) \times H^1(\mathsf{T}_h)$. Then, for all $(\mathrm{G}, \boldsymbol{v}, q) \in \mathrm{G}_h \times \boldsymbol{V}_h \times P_h$,

$$
\begin{aligned}
(\boldsymbol{v}, \nabla \cdot \Phi)_{\mathsf{T}_h} &= (\boldsymbol{v}, \nabla \cdot \Pi\Phi)_{\mathsf{T}_h} + \langle \boldsymbol{v}, (\Phi - \Pi\Phi)\boldsymbol{n}\rangle_{\partial\mathsf{T}_h}, && \text{(2.24a)}\\
(\mathrm{G}, \nabla\boldsymbol{\phi})_{\mathsf{T}_h} &= -(\nabla \cdot \mathrm{G}, \boldsymbol{\mathit{\Pi}}\boldsymbol{\phi})_{\mathsf{T}_h} + \langle \mathrm{G}\boldsymbol{n}, \boldsymbol{\phi}\rangle_{\partial\mathsf{T}_h}, && \text{(2.24b)}\\
(q, \nabla \cdot \boldsymbol{\phi})_{\mathsf{T}_h} &= -(\nabla q, \boldsymbol{\mathit{\Pi}}\boldsymbol{\phi})_{\mathsf{T}_h} + \langle q\boldsymbol{n}, \boldsymbol{\phi}\rangle_{\partial\mathsf{T}_h}, && \text{(2.24c)}\\
(\boldsymbol{v}, \nabla\phi)_{\mathsf{T}_h} &= (\boldsymbol{v}, \nabla \mathit{\Pi}\phi)_{\mathsf{T}_h} + \langle \boldsymbol{v}, (\phi - \mathit{\Pi}\phi)\boldsymbol{n}\rangle_{\partial\mathsf{T}_h}. && \text{(2.24d)}
\end{aligned}
$$

The main estimate of this section is the following.

Lemma 2.11. *Let $H(R,h) := h^{1/2}(1+\tau) + R + R^{1/2} + h^{1/2}\tau^{1/2}R + R^{3/2}$. If Assumptions A and B hold, and $h \le 1$, then*

$$
\|\boldsymbol{\varepsilon}^{\boldsymbol{u}}\|_{\mathsf{D}_h} \lesssim h^{1/2}\big(H(R,h)\Theta_{\mathrm{I^L}} + R\nu^{-1}\|I^p\|_{\mathsf{D}_h} + R\tau\|\boldsymbol{I}^{\boldsymbol{u}}\|_{\mathsf{D}_h}\big).
$$

We observe that, for a smooth solution, if τ and R are of order one, then $\|\boldsymbol{\varepsilon}^{\boldsymbol{u}}\|_{\mathsf{D}_h} \lesssim h^{k+3/2}$ since the interpolation errors are of order h^{k+1}. In the case of a polyhedral domain where Γ_h fits Γ, we would have $R = 0$, $\tilde{\boldsymbol{g}} = \tilde{\boldsymbol{g}}_h$. As a consequence, $\|\boldsymbol{\varepsilon}^{\boldsymbol{u}}\|_{\mathsf{D}_h}$ would be of order h^{k+2} which agrees with the estimates in [18]. We now detail the steps that construct the proof of Lemma 2.11.

Step 1: Estimate of the velocity

We first obtain an identity for the projection of the error in the velocity by using a duality argument.

Lemma 2.12. *Let $\mathbb{T}_{\boldsymbol{u},h} := \langle \hat{\mathrm{E}}\boldsymbol{n}, \boldsymbol{\phi}\rangle_{\Gamma_h} + \langle \boldsymbol{\varepsilon}^{\hat{\boldsymbol{u}}}, \nu\Phi\boldsymbol{n} - \phi\boldsymbol{n}\rangle_{\Gamma_h}$ and P_{k-1} the L^2-projection over the space of piecewise polynomials of degree at most $k-1$. Then,*

$$
(\boldsymbol{\varepsilon}^{\boldsymbol{u}}, \boldsymbol{\theta})_{\mathsf{T}_h} = \nu(\mathrm{L}_h - \mathrm{L}, \Pi\Phi - \Phi)_{\mathsf{T}_h} - \nu(\mathrm{I^L}, \Phi - \mathrm{P}_{k-1}\Phi)_{\mathsf{T}_h} + \mathbb{T}_{\boldsymbol{u},h}.
$$

Proof. Proceeding as in the proof of Lemma 3.6 of [18], but keeping the boundary terms since in our case they are not zero, we can write $(\boldsymbol{\varepsilon}^{\boldsymbol{u}}, \boldsymbol{\theta})_{\mathsf{T}_h} = \sum_{i=1}^{5} T_i$, where

$$
\begin{aligned}
T_1 &:= \nu(\mathrm{L}_h - \mathrm{L}, \Pi\Phi - \Phi)_{\mathsf{T}_h}, \quad T_2 := -\nu(\mathrm{I^L}, \Phi)_{\mathsf{T}_h},\\
T_3 &:= \langle \boldsymbol{\varepsilon}^{\boldsymbol{u}} - \boldsymbol{\varepsilon}^{\hat{\boldsymbol{u}}}, \nu(\Phi - \Pi\Phi)\boldsymbol{n} - (\phi - \mathit{\Pi}\phi)\boldsymbol{n} + \tau\nu(\boldsymbol{\phi} - \boldsymbol{\mathit{\Pi}}\boldsymbol{\phi})\rangle_{\partial\mathsf{T}_h},\\
T_4 &:= \langle \nu\mathrm{E^L}\boldsymbol{n} - \varepsilon^p\boldsymbol{n} - \tau\nu(\boldsymbol{\varepsilon}^{\boldsymbol{u}} - \boldsymbol{\varepsilon}^{\hat{\boldsymbol{u}}}), \boldsymbol{\phi}\rangle_{\partial\mathsf{T}_h}, \quad T_5 := \langle \boldsymbol{\varepsilon}^{\hat{\boldsymbol{u}}}, \nu\Phi\boldsymbol{n} - \phi\boldsymbol{n}\rangle_{\partial\mathsf{T}_h}.
\end{aligned}
$$

By the property of the projection (2.15a), we have that $T_2 = -\nu(\mathrm{I^L}, \Phi - \mathrm{P}_{k-1}\Phi)_{\mathsf{T}_h}$, and by (2.15e) with $\boldsymbol{\mu} = \boldsymbol{\varepsilon}^{\boldsymbol{u}} - \boldsymbol{\varepsilon}^{\hat{\boldsymbol{u}}}$, we have that $T_3 = 0$. Moreover, using the error equation (2.19e) we obtain that $T_4 = \langle \hat{\mathrm{E}}\boldsymbol{n}, \boldsymbol{\phi}\rangle_{\Gamma_h}$. Finally, since $\nu\Phi - \phi\mathrm{I} \in \mathrm{H}(\mathrm{div}, \Omega)$ and $\boldsymbol{\varepsilon}^{\hat{\boldsymbol{u}}}$ is single-valued, then $T_5 = \langle \boldsymbol{\varepsilon}^{\hat{\boldsymbol{u}}}, \nu\Phi\boldsymbol{n} - \phi\boldsymbol{n}\rangle_{\Gamma_h}$, which concludes the proof.

□

We point out that $\phi = 0$ on Γ, but not in Γ_h. Thus, if Γ and Γ_h were the same (as in the polyhedral case), then T_4 would be zero. Moreover, for a polyhedral domain Ω, T_5 would also vanish thanks to (2.19e) since $\widetilde{\boldsymbol{g}} = \widetilde{\boldsymbol{g}}_h$, recovering the equality stated in Lemma 3.6 of [18].

Step 2: A new expression for $\mathbb{T}_{\boldsymbol{u},h}$

As we did previously with $\mathbb{T}_{\mathrm{L},h}$, we proceed now to rewrite $\mathbb{T}_{\boldsymbol{u},h}$ in a suitable manner.

Lemma 2.13. *We have that* $\mathbb{T}_{\boldsymbol{u},h} = \sum_{i=1}^{10} \mathbb{T}^i_{\boldsymbol{u},h}$, *where*

$$\begin{aligned}
\mathbb{T}^1_{\boldsymbol{u},h} &= -\nu\langle(\tilde{\boldsymbol{g}} - \tilde{\boldsymbol{g}}_h)/l, \boldsymbol{\phi} + \ l\nabla\boldsymbol{\phi}\boldsymbol{n}\rangle_{\Gamma_h}, \quad \mathbb{T}^2_{\boldsymbol{u},h} = \nu\langle\tilde{\boldsymbol{g}} - \tilde{\boldsymbol{g}}_h, \nabla\boldsymbol{\phi}\boldsymbol{n} - \mathbf{P}_M(\nabla\boldsymbol{\phi}\boldsymbol{n})\rangle_{\Gamma_h},\\
\mathbb{T}^3_{\boldsymbol{u},h} &= -\nu\langle\delta_{\mathrm{I}^{\mathrm{L}}}, \boldsymbol{\phi}\rangle_{\Gamma_h}, \quad \mathbb{T}^4_{\boldsymbol{u},h} = -\nu\langle\mathrm{I}^{\mathrm{L}}\boldsymbol{n}, \boldsymbol{\phi} - \mathbf{P}_M\boldsymbol{\phi}\rangle_{\Gamma_h}, \quad \mathbb{T}^5_{\boldsymbol{u},h} = -\langle I^p\boldsymbol{n}, \mathbf{P}_M\boldsymbol{\phi}\rangle_{\Gamma_h},\\
\mathbb{T}^6_{\boldsymbol{u},h} &= -\nu\langle\mathbf{P}_M\tau\boldsymbol{I}^{\boldsymbol{u}}, \boldsymbol{\phi}\rangle_{\Gamma_h}, \quad \mathbb{T}^7_{\boldsymbol{u},h} = -\nu\langle\delta_{E^{\mathrm{L}}}, \boldsymbol{\phi}\rangle_{\Gamma_h}, \quad \mathbb{T}^8_{\boldsymbol{u},h} = -\langle\varepsilon^p\boldsymbol{n}, \boldsymbol{\phi}\rangle_{\Gamma_h},\\
\mathbb{T}^9_{\boldsymbol{u},h} &= -\nu\langle\tau(\boldsymbol{\varepsilon}^{\boldsymbol{u}} - \boldsymbol{\varepsilon}^{\hat{\boldsymbol{u}}}), \boldsymbol{\phi}\rangle_{\Gamma_h}, \quad \mathbb{T}^{10}_{\boldsymbol{u},h} = -\langle\tilde{\boldsymbol{g}} - \tilde{\boldsymbol{g}}_h, \mathbf{P}_M(\phi\boldsymbol{n})\rangle_{\Gamma_h}.
\end{aligned}$$

Proof. We recall (2.19g):

$$\hat{\mathrm{E}}\boldsymbol{n} = -\nu\left\{(\tilde{\boldsymbol{g}} - \tilde{\boldsymbol{g}}_h)/l + \delta_{\mathrm{I}^{\mathrm{L}}} + \mathrm{I}^{\mathrm{L}}\boldsymbol{n} + \delta_{\mathrm{E}^{\mathrm{L}}}\right\} - \varepsilon^p\boldsymbol{n} - \nu\tau(\boldsymbol{\varepsilon}^{\boldsymbol{u}} - \boldsymbol{\varepsilon}^{\hat{\boldsymbol{u}}}).$$

Then, since $\boldsymbol{\varepsilon}^{\hat{\boldsymbol{u}}} = \mathbf{P}_M(\tilde{\boldsymbol{g}} - \tilde{\boldsymbol{g}}_h)$ on Γ_h, we obtain

$$\begin{aligned}
\mathbb{T}_{\boldsymbol{u},h} &= \langle\hat{\mathrm{E}}\boldsymbol{n}, \boldsymbol{\phi}\rangle_{\Gamma_h} + \langle\boldsymbol{\varepsilon}^{\hat{\boldsymbol{u}}}, \nu\Phi\boldsymbol{n} - \phi\boldsymbol{n}\rangle_{\Gamma_h}\\
&= \nu\langle(\tilde{\boldsymbol{g}} - \tilde{\boldsymbol{g}}_h)/l, \ l\mathbf{P}_M(\Phi\boldsymbol{n}) - \boldsymbol{\phi}\rangle_{\Gamma_h} - \nu\langle\delta_{\mathrm{I}^{\mathrm{L}}}, \boldsymbol{\phi}\rangle_{\Gamma_h} - \nu\langle\mathrm{I}^{\mathrm{L}}\boldsymbol{n}, \boldsymbol{\phi}\rangle_{\Gamma_h}\\
&\quad -\nu\langle\delta_{\mathrm{E}^{\mathrm{L}}}, \boldsymbol{\phi}\rangle_{\Gamma_h} - \langle\varepsilon^p\boldsymbol{n}, \boldsymbol{\phi}\rangle_{\Gamma_h} - \nu\langle\tau(\boldsymbol{\varepsilon}^{\boldsymbol{u}} - \boldsymbol{\varepsilon}^{\hat{\boldsymbol{u}}}), \boldsymbol{\phi}\rangle_{\Gamma_h} - \langle\tilde{\boldsymbol{g}} - \tilde{\boldsymbol{g}}_h, \mathbf{P}_M(\phi\boldsymbol{n})\rangle_{\Gamma_h}.
\end{aligned}$$

Using the first equation of the dual problem (2.12a), adding and subtracting $l\nabla\boldsymbol{\phi}\boldsymbol{n}$,

$$\begin{aligned}
\nu\langle(\tilde{\boldsymbol{g}} - \tilde{\boldsymbol{g}}_h)/l, \ l\mathbf{P}_M(\Phi\boldsymbol{n}) - \boldsymbol{\phi}\rangle_{\Gamma_h} &= -\nu\langle(\tilde{\boldsymbol{g}} - \tilde{\boldsymbol{g}}_h)/l, \ l\nabla\boldsymbol{\phi}\boldsymbol{n} + \boldsymbol{\phi}\rangle_{\Gamma_h}\\
&\quad +\nu\langle\tilde{\boldsymbol{g}} - \tilde{\boldsymbol{g}}_h, \nabla\boldsymbol{\phi}\boldsymbol{n} - \mathbf{P}_M(\nabla\boldsymbol{\phi}\boldsymbol{n})\rangle_{\Gamma_h}.
\end{aligned}$$

On the other hand, adding and subtracting $\mathbf{P}_M\boldsymbol{\phi}$, and using equation (2.15e), we get $\nu\langle\mathrm{I}^{\mathrm{L}}\boldsymbol{n}, \boldsymbol{\phi}\rangle_{\Gamma_h} = \nu\langle\mathrm{I}^{\mathrm{L}}\boldsymbol{n}, \boldsymbol{\phi} - \mathbf{P}_M\boldsymbol{\phi}\rangle_{\Gamma_h} + \langle I^p\boldsymbol{n}, \mathbf{P}_M\boldsymbol{\phi}\rangle_{\Gamma_h} + \nu\langle\tau\boldsymbol{I}^{\boldsymbol{u}}, \mathbf{P}_M\boldsymbol{\phi}\rangle_{\Gamma_h}$. The result follows by gathering the above equalities.

□

Step 3: Estimate of $\mathbb{T}_{\boldsymbol{u},h}$

In order to obtain the estimate of $\mathbb{T}_{\boldsymbol{u},h}$, we need the following lemma, which provides bounds related to the solution of the dual problem (2.12a)-(2.12d) that will be used later.

Lemma 2.14. *Suppose that the elliptic regularity inequality (2.13) holds. Then*

$$\begin{aligned}
\nu\|\boldsymbol{\phi} - \mathbf{P}_M\boldsymbol{\phi}\|_{\Gamma_h,(h^\perp)^{-1}} &\lesssim h\|\boldsymbol{\theta}\|_\Omega, \quad \nu\|\nabla\boldsymbol{\phi}\boldsymbol{n} - \mathbf{P}_M(\nabla\boldsymbol{\phi}\boldsymbol{n})\|_{\Gamma_h,l} \lesssim hR\|\boldsymbol{\theta}\|_\Omega,\\
\nu\|\boldsymbol{\phi} + \ l\nabla\boldsymbol{\phi}\boldsymbol{n}\|_{\Gamma_h,l^{-3}} &\lesssim \|\boldsymbol{\theta}\|_\Omega, \quad \nu\|\boldsymbol{\phi}\|_{\Gamma_h,l^{-2}} \lesssim \|\boldsymbol{\theta}\|_\Omega, \quad \|\phi\boldsymbol{n}\|_{\Gamma_h,l} \lesssim h^{1/2}R^{1/2}\|\boldsymbol{\theta}\|_\Omega.
\end{aligned}$$

Proof. The first four estimates follow by applying Lemma 5.5 of [21] to each component of a tensor- or a vector-valued function. For the last one, we observe that for $e \in \mathcal{E}_h^\partial$, $\sum_{e\in\mathcal{E}_h^\partial} \|\phi\boldsymbol{n}\|^2_{e,l} \leq \sum_{e\in\mathcal{E}_h^\partial} r_e h_e^\perp \|\phi\|_e^2 \lesssim h\|\phi\|^2_{\Gamma_h} \max_{e\in\mathcal{E}_h^\partial} r_e$. Now, since $\phi \in H^1(\Omega)$, by trace inequality we have that $\|\phi\|_{\Gamma_h} \lesssim \|\phi\|_{\mathsf{D}_h} \leq \|\phi\|_\Omega$, and the result follows.

□

We are now ready to obtain the estimate of $\mathbb{T}_{\boldsymbol{u},h}$.

Lemma 2.15. *We have that*

$$|\mathbb{T}_{\boldsymbol{u},h}| \lesssim h^{1/2}\Big\{(R^{3/2}+h^{1/2}+R+R^{1/2}+h^{1/2}\tau^{1/2}R)\Theta_{\mathrm{I^L}} + R\nu^{-1}\|I^p\|_{\mathsf{D}_h} + R\tau\|\boldsymbol{I}^{\boldsymbol{u}}\|_{\mathsf{D}_h}\Big\}\|\boldsymbol{\theta}\|_{\Omega}.$$

Proof. By Lemma 2.13, we know that $\mathbb{T}_{\boldsymbol{u},h} = \sum_{i=1}^{10}\mathbb{T}^i_{\boldsymbol{u},h}$. We first apply the Cauchy-Schwarz inequality to each term $\mathbb{T}^i_{\boldsymbol{u},h}$. The result follows from estimate in (1.6), Lemma 2.14, Assumptions A, the fact that $\|I^p\boldsymbol{n}\|_{\Gamma_h,l^2} \leq Rh^{1/2}\|I^p\boldsymbol{n}\|_{\Gamma_h,h^\perp}$, the interpolation properties (2.16c) and Lemma 2.5 .

□

Step 4: Proof of Lemma 2.11

From Lemma 2.12, we have

$$(\boldsymbol{\varepsilon}^{\boldsymbol{u}},\boldsymbol{\theta})_{\mathsf{T}_h} \leq \|\mathrm{L}_h-\mathrm{L}\|_{\mathsf{D}_h}\|\nu\Pi\Phi-\nu\Phi\|_{\mathsf{D}_h} + \|\mathrm{I^L}\|_{\mathsf{D}_h}\|\nu\Phi-\nu\mathrm{P}_{k-1}\Phi\|_{\mathsf{D}_h} + |\mathbb{T}_{\boldsymbol{u},h}|.$$

According to the regularity Assumption B, (2.16a) implies that $\|\nu\Pi\Phi-\nu\Phi\|_{\mathsf{D}_h} \lesssim h(1+\tau h)\|\boldsymbol{\theta}\|_{\Omega}$. Also, by the approximation properties of the L^2-projection, we have $\|\nu\Phi-\nu\mathrm{P}_{k-1}\Phi\|_{\mathsf{D}_h} \lesssim h\|\boldsymbol{\theta}\|_{\Omega}$. We recall we are considering $k\geq 1$. Hence,

$$(\boldsymbol{\varepsilon}^{\boldsymbol{u}},\boldsymbol{\theta})_{\mathsf{T}_h} \lesssim h(1+\tau h)\left(\|\mathrm{E^L}\|_{\mathsf{D}_h}+\|\mathrm{I^L}\|_{\mathsf{D}_h}\right)\|\boldsymbol{\theta}\|_{\Omega} + |\mathbb{T}_{\boldsymbol{u},h}|.$$

Thus, using the estimate for $|\mathbb{T}_{\boldsymbol{u},h}|$ from Lemma 2.15, recalling that $\|\mathrm{E^L}\|_{\mathsf{D}_h} \leq \Theta_{\mathrm{I^L}}$ from Lemma 2.5, dividing by $\|\boldsymbol{\theta}\|_{\Omega}$, $\boldsymbol{\theta}\neq\mathbf{0}$, and considering the supremum over $\boldsymbol{\theta}$, we obtain the result.

2.4.3 Conclusion of the proof of Theorem 2.4

First of all, adding and subtracting $\Pi\mathrm{L}$ and $\Pi\widetilde{p}$, using the triangle inequality, Lemma 2.5 and recalling the definition of $\Theta_{\mathrm{I^L}}$ in (2.17), we get

$$\|\mathrm{L}-\mathrm{L}_h\|_{\mathsf{D}_h} + \|\tilde{\boldsymbol{g}}-\tilde{\boldsymbol{g}}_h\|_{\Gamma_h,l^{-1}} + \nu^{-1}\|\widetilde{p}-\widetilde{p}_h\|_{\mathsf{D}_h} \lesssim \Theta_{\mathrm{I^L}} + \nu^{-1}\|I^p\|_{\mathsf{D}_h}.$$

Moreover, if Assumption B holds, by adding and subtracting $\boldsymbol{\Pi}\boldsymbol{u}$, using triangle inequality and Lemma 2.11, we obtain

$$\|\boldsymbol{u}-\boldsymbol{u}_h\|_{\mathsf{D}_h} \lesssim h^{1/2}\big(H(R,h)\Theta_{\mathrm{I^L}} + R\nu^{-1}\|I^p\|_{\mathsf{D}_h} + R\tau\|\boldsymbol{I}^{\boldsymbol{u}}\|_{\mathsf{D}_h}\big) + \|\boldsymbol{I}^{\boldsymbol{u}}\|_{\mathsf{D}_h}.$$

Lemma 3.7 in [18] states that $\|\boldsymbol{\varepsilon}^{\widehat{\boldsymbol{u}}}\|_h \lesssim h\|\mathrm{I^L}\|_{\mathsf{D}_h} + h\|\mathrm{E^L}\|_{\mathsf{D}_h} + \|\boldsymbol{\varepsilon}^{\boldsymbol{u}}\|_{\mathsf{D}_h}$ which, together with Lemmas 2.5 and 2.11, implies

$$\|\mathbf{P}_M\boldsymbol{u}-\widehat{\boldsymbol{u}}_h\|_h \lesssim h^{1/2}\big((h^{1/2}+H(R,h))\Theta_{\mathrm{I^L}} + R\nu^{-1}\|I^p\|_{\mathsf{D}_h} + R\tau\|\boldsymbol{I}^{\boldsymbol{u}}\|_{\mathsf{D}_h}\big).$$

The error estimate $\|\boldsymbol{u}-\boldsymbol{u}_h^*\|_{\mathsf{D}_h} \leq \|\boldsymbol{\varepsilon}^{\boldsymbol{u}}\|_{\mathsf{D}_h} + Ch\|\mathrm{L}-\mathrm{L}_h\|_{\mathsf{D}_h} + Ch^{k+2}|\mathrm{L}|_{\mathrm{H}^{k+1}(\Omega)}$ can be found in [19] and, from Lemma 2.11, follows that

$$\begin{aligned}\|\boldsymbol{u}-\boldsymbol{u}_h^*\|_{\mathsf{D}_h} &\leq \|\boldsymbol{\varepsilon}^{\boldsymbol{u}}\|_{\mathsf{D}_h} + Ch\|\mathrm{L}-\mathrm{L}_h\|_{\mathsf{D}_h} + Ch^{k+2}|\mathrm{L}|_{\mathrm{H}^{k+1}(\Omega)}\\ &\lesssim h^{1/2}\big(H(R,h)\Theta_{\mathrm{I}^{\mathrm{L}}} + R\nu^{-1}\|I^p\|_{\mathsf{D}_h} + R\tau\|\boldsymbol{I}^{\boldsymbol{u}}\|_{\mathsf{D}_h}\big)\\ &\quad + h\|\mathrm{L}-\mathrm{L}_h\|_{\mathsf{D}_h} + h^{k+2}|\mathrm{L}|_{\mathrm{H}^{k+1}(\Omega)}.\end{aligned}$$

Finally, since τ is of order one, we have that $H(R,h) \lesssim R + R^{1/2} + h^{1/2}R + R^{3/2}$ and the estimates stated in Theorem 2.4 follow.

2.5 Approximation in D_h^c and recovering p_h

In this section we provide a way to extend the solution $(\mathrm{L}_h, \boldsymbol{u}_h, \widetilde{p}_h)$ of (2.4) to the non-meshed region D_h^c in the two-dimensional case. The case of three dimensions can be treated similarly. In addition, since the scheme (2.4) provides an approximation of $\widetilde{p}_h$, here we will explain a procedure to recover p_h. To that end, we write D_h^c as the union of disjoint regions. More precisely, let $e \in \mathcal{E}_h^{\partial}$ that belongs to $K^e \in \mathsf{T}_h$. For $j \in \{1,2\}$, we denote by $\boldsymbol{y}_j$, the j-th vertex of e and by $\overline{\boldsymbol{y}}_j$ its closest point in Γ. We remark that the closest point is unique if we assume

(D.6) the mesh in fine enough and Γ is $\mathcal{C}^2$.

We define $\widetilde{K}_{ext}^e$ as the region enclosed by Γ, e and the segments associated to $\boldsymbol{y}_1$ and $\boldsymbol{y}_2$, as Fig. 2.1 shows. Note that, the union of the regions K_{ext}^e defined in Section 1.1.2 is not equal to D_h^c, so we cannot use them to compute integrals over D_h^c and that is why we consider $\widetilde{K}_{ext}^e$ instead of K_{ext}^e.

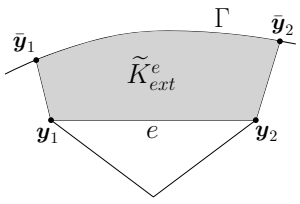

Figure 2.1: Example of points $\overline{\boldsymbol{y}}_j$ associated to the vertices $\boldsymbol{y}_j$ and region $\widetilde{K}_{ext}^e$.

Now, the polynomials $\mathrm{L}_h|_{K^e}$ and $\widetilde{p}_h|_{K^e}$ are extrapolated from K^e to $\widetilde{K}_{ext}^e$ and they constitute an approximation of L and $\widetilde{p}$ in $\widetilde{K}_{ext}^e$. We can also approximate $\boldsymbol{u}$ in $\widetilde{K}_{ext}^e$ by extrapolating $u_h|_{K^e}$, however we construct a better approximation based on the fact that L is the gradient of $\boldsymbol{u}$. Let $\boldsymbol{y} \in \widetilde{K}_{ext}^e$ and $\overline{\boldsymbol{y}}$ its closest point in Γ. Let $\boldsymbol{x} \in e$ be the intersection between e and the line determined by $\boldsymbol{y}$ and $\overline{\boldsymbol{y}}$. Then, denoting by $\boldsymbol{t}(\boldsymbol{x})$ the unit tangent vector of the segment joining $\boldsymbol{x}$ and $\boldsymbol{y}$, we can write $\boldsymbol{y} = \boldsymbol{x} + \eta\boldsymbol{t}(\boldsymbol{x})$ and $\bar{\boldsymbol{y}} := \boldsymbol{x} + \bar{\eta}\boldsymbol{t}(\boldsymbol{x})$, for some η and $\bar{\eta}$ positive. Thus, based on the procedure to obtain (1.1), we integrate $\mathrm{L} = \nabla\boldsymbol{u}$ along the segment connecting $\boldsymbol{y}$ and $\bar{\boldsymbol{y}}$, and propose the following approximation of the velocity in $\boldsymbol{y}$,

$$\boldsymbol{u}_h(\boldsymbol{y}) := \boldsymbol{g}(\bar{\boldsymbol{y}}) - \int_{\eta}^{\bar{\eta}} \mathrm{L}_h(\boldsymbol{y} + \boldsymbol{t}(\boldsymbol{x})s\,)\boldsymbol{t}(\boldsymbol{x})\,ds. \tag{2.26}$$

On the other hand, since $0 = \int_\Omega p = |\Omega|\,\overline{p}^{\mathsf{D}_h} + \int_{\mathsf{D}_h^c} \widetilde{p}$, we suggest the following approximation

$$\overline{p}^{\mathsf{D}_h} \approx \overline{p_h}^{\mathsf{D}_h} := -\frac{1}{|\Omega|}\int_{\mathsf{D}_h^c} \widetilde{p}_h, \tag{2.27}$$

thereby

$$p_h := \overline{p_h}^{\mathsf{D}_h} + \widetilde{p}_h \tag{2.28}$$

is an approximation of p. In the Appendix we explain how to approximate an integral over D_h^c.

Thus, we have defined approximations of L, $\widetilde{p}$ and $\boldsymbol{u}$ in $\mathsf{D}_h^c = \bigcup_{e\in\mathcal{E}_h^\partial} \widetilde{K}_{ext}^e$. Even though the variables L_h, $\widetilde{p}_h$ and $\boldsymbol{u}_h$ denote the approximations delivered by the HDG method in D_h, we use the same notation to represent the approximations in D_h^c proposed in this section.

Finally, from Lemmas 3.7 and 3.8 in [21], it can be obtained that

$$\begin{aligned}
\|\mathrm{L}-\mathrm{L}_h\|_{\mathsf{D}_h^c} &\lesssim \|\mathrm{I}^{\mathrm{L}}\|_{\mathsf{D}_h} + \|\mathrm{E}^{\mathrm{L}}\|_{\mathsf{D}_h} + h^{k+1}|\mathrm{L}|_{\mathrm{H}^{k+1}(\Omega)}, && \text{(2.29a)}\\
\|\boldsymbol{u}-\boldsymbol{u}_h\|_{\mathsf{D}_h^c} &\lesssim h\|\mathrm{L}-\mathrm{L}_h\|_{\mathsf{D}_h^c} \quad \text{and} && \text{(2.29b)}\\
\|\widetilde{p}-\widetilde{p}_h\|_{\mathsf{D}_h^c} &\lesssim \big(\|\mathrm{I}^p\|_{\mathsf{D}_h} + \|\varepsilon^p\|_{\mathsf{D}_h}\big) + h^{k+1}|\widetilde{p}|_{H^{k+1}(\mathsf{D}_h)}. && \text{(2.29c)}
\end{aligned}$$

Actually the estimates of Lemmas 3.7 and 3.8 in [21] were obtained based on a different projection of a point into Γ. However, if the closest projection is considered instead, the same results hold under minor modifications in the proofs.

Theorem 2.16. *Suppose assumptions of Theorem 2.4 hold, then*

$$\begin{aligned}
\|\mathrm{L}-\mathrm{L}_h\|_{\mathsf{D}_h^c} &\lesssim C_{reg}\, h^{k+1}, && \text{(2.30a)}\\
\|\boldsymbol{u}-\boldsymbol{u}_h\|_{\mathsf{D}_h^c} &\lesssim h\|\mathrm{L}-\mathrm{L}_h\|_{\mathsf{D}_h^c}, && \text{(2.30b)}\\
\|p-p_h\|_{\mathsf{D}_h} &\lesssim h^{k+1}\max\Big\{1,(\tau h)^{1/2}\Big\}\big(C_{reg}+|\widetilde{p}|_{H^{k+1}(\Omega)}\big) \quad \textit{and} && \text{(2.30c)}\\
\|p-p_h\|_{\mathsf{D}_h^c} &\lesssim h^{k+1}\max\Big\{1,(\tau h)^{1/2}\Big\}\big(C_{reg}+|\widetilde{p}|_{H^{k+1}(\Omega)}\big), && \text{(2.30d)}
\end{aligned}$$

where we recall that C_{reg} has been defined in Theorem 2.4.

Proof. The first two inequalities are obtained from (2.29), Lemma 2.5, estimates in (2.29) and the approximation properties (2.16). Now, by (2.2) and (2.28), we have that

$$\begin{aligned}
\|p-p_h\|_{\mathsf{D}_h} &\le \|\widetilde{p}-\widetilde{p}_h\|_{\mathsf{D}_h} + \|\overline{p}^{\mathsf{D}_h} - \overline{p_h}^{\mathsf{D}_h}\|_{\mathsf{D}_h}\\
&\le \|\widetilde{p}-\widetilde{p}_h\|_{\mathsf{D}_h} + |\mathsf{D}_h||\Omega|^{-1}\|\widetilde{p}-\widetilde{p}_h\|_{\mathsf{D}_h^c}.
\end{aligned}$$

This inequality, together with Theorem 2.4 and (2.29c) imply (2.30c).

Similarly $\|p-p_h\|_{\mathsf{D}_h^c} \le \|\widetilde{p}-\widetilde{p}_h\|_{\mathsf{D}_h^c} + |\mathsf{D}_h^c||\Omega|^{-1}\|\widetilde{p}-\widetilde{p}_h\|_{\mathsf{D}_h^c}$ and (2.30d) follows from (2.29c).

□

We remark that, if the solution of the problem is smooth enough, these estimates indicate that the L^2-norm of the error for L_h and p_h converge with optimal order h^{k+1} also in the region D_h^c. Moreover, $\boldsymbol{u}_h$ converges with order h^{k+2}. This additional power of h is due to the the fact that in (2.26) the length of the integration segment is of order h.

2.6 Numerical results

In this section we present two-dimensional numerical experiments to validate the theoretical orders of convergence of the approximations provided by the HDG method. In all our experiments, we use $\nu = 1$ and $\tau \equiv 1$, and compute the errors $e_p := \|p - p_h\|_\Omega$, $e_{\boldsymbol{u}} := \|\boldsymbol{u} - \boldsymbol{u}_h\|_\Omega$, $e_{\mathrm{L}} := \|\mathrm{L} - \mathrm{L}_h\|_\Omega$, $e_{\widehat{\boldsymbol{u}}} := \left(\sum_{K\in\mathsf{D}_h} h_K\|\mathbf{P}_M\boldsymbol{u} - \widehat{\boldsymbol{u}}_h\|_{\partial K}\right)^{1/2}$ and $e_{\boldsymbol{u}^*} := \left(\|\boldsymbol{u} - \boldsymbol{u}_h^*\|^2_{\mathsf{D}_h} + \|\boldsymbol{u} - \boldsymbol{u}_h\|^2_{\mathsf{D}_h^c}\right)^{1/2}$. In addition, for each variable, we calculate the experimental order of convergence e.o.c. $= -2\dfrac{\log\left(e_{\mathcal{T}_1}/e_{\mathcal{T}_2}\right)}{\log(N_{\mathcal{T}_1}/N_{\mathcal{T}_2})}$, where $e_{\mathcal{T}_1}$ and $e_{\mathcal{T}_2}$ are the errors associated to the corresponding variable considering two consecutive meshes with $N_{\mathcal{T}_1}$ and $N_{\mathcal{T}_2}$ elements, respectively.

2.6.1 Example 1: $\mathrm{dist}(\Gamma_h, \Gamma)$ of order h^2.

In this first example, we consider the annular domain $\Omega = \{(x, y) \in \mathbb{R}^2 : 0.5^2 < x^2 + y^2 < 2^2\}$. The computational boundary Γ_h is constructed by interpolating $\partial\Omega$ by a piecewise linear function and D_h is the domain enclosed by Γ_h. In this case all the assumptions are satisfied, except (D.3) because the domain is not convex. However, if we assume that the PDE is also valid in the $\mathsf{D}_h \cap \Omega^c$, under minor modification our analysis is also valid.

The source term $\boldsymbol{f}$ and boundary data $\boldsymbol{g}$ are such that the exact solution is

$$p(x, y) = \sin(x)\sin(y), \quad \boldsymbol{u}(x, y) = \begin{bmatrix} \sin(x)\sin(y) \\ \cos(x)\cos(y) \end{bmatrix}.$$

In Table 2.1 we observe optimal convergence rate for all the variables as Theorems 2.4 and 2.16 predict, i.e., order of h^{k+1} for the errors of e_p, $e_{\boldsymbol{u}}$ and e_{L}; and superconvergence with order h^{k+2} for the numerical trace of the velocity and post-processed solution, since in this case R is of order h. Moreover, in Fig. 2.2 we display the approximation of the second component of $\boldsymbol{u}$ for $k = 1$ and 2 obtained with meshes of sizes $N = 150$ and 2396 elements (first column).

2.6.2 Example 2: $\mathrm{dist}(\Gamma_h, \Gamma)$ of order h.

We consider $\Omega := \{(x, y) \in \mathbb{R}^2_+ : 1.4 < \sqrt{x^2 + y^2} < 2\}$ and the exact solution

$$p(x, y) = e^{x^2+y^2} - (e^{2^2} - e^{1.4^2})/(2^2 - 1.4^2), \quad \boldsymbol{u}(x, y) = \begin{bmatrix} \sin(3x)e^y \\ -3\cos(3x)e^y \end{bmatrix}.$$

The computational D_h is set in such a way that $r_e = 1$ for all $e \in \Gamma_h \setminus \{(x, y) : x = 0 \vee y = 0\}$ as seen in Fig. 2.3.

Table 2.2 shows optimal rate of convergence for the error all variables in Ω, that is, order $k + 1$ for the errors of the pressure p, the velocity $\boldsymbol{u}$ and the gradient of the velocity L. In addition, the rate of convergence of the errors $e_{\widehat{\boldsymbol{u}}}$ and $e_{\boldsymbol{u}^*}$ seems to be slightly larger than the order $k + 3/2$ predicted by Theorem 2.4.

k	N	e_p	order	$e_{\boldsymbol{u}}$	order	e_{L}	order	$e_{\widehat{\boldsymbol{u}}}$	order	$e_{\boldsymbol{u}^*}$	order
1	150	1.83e-02	–	2.01e-02	–	3.76e-02	–	7.68e-03	–	3.21e-03	–
	608	4.38e-03	2.04	5.10e-03	1.96	8.92e-03	2.06	1.04e-03	2.86	4.20e-04	2.91
	2396	1.05e-03	2.08	1.29e-03	2.00	2.23e-03	2.02	1.34e-04	2.99	5.51e-05	2.96
	5842	4.19e-04	2.07	5.32e-04	1.99	8.84e-04	2.07	3.35e-05	3.10	1.39e-05	3.10
	15480	1.57e-04	2.01	2.02e-04	1.98	3.35e-04	1.99	7.98e-06	2.94	3.28e-06	2.96
2	150	1.29e-03	–	1.35e-03	–	1.99e-03	–	2.79e-04	–	1.48e-04	–
	608	1.43e-04	3.14	1.62e-04	3.04	2.43e-04	3.00	1.75e-05	3.95	9.49e-06	3.93
	2396	1.70e-05	3.11	2.07e-05	3.00	3.02e-05	3.04	1.18e-06	3.93	6.05e-07	4.01
	5842	4.33e-06	3.07	5.44e-06	2.99	7.74e-06	3.06	1.99e-07	3.99	1.01e-07	4.01
	15480	1.01e-06	2.98	1.29e-06	2.96	1.82e-06	2.97	2.97e-08	3.91	1.49e-08	3.93
3	150	4.49e-05	–	5.54e-05	–	1.10e-04	–	9.42e-06	–	4.58e-06	–
	608	2.94e-06	3.90	3.80e-06	3.83	6.45e-06	4.05	3.19e-07	4.84	1.50e-07	4.88
	2396	1.81e-07	4.06	2.40e-07	4.03	3.99e-07	4.06	9.85e-09	5.07	5.08e-09	4.94
	5842	2.93e-08	4.09	3.98e-08	4.03	6.46e-08	4.08	1.05e-09	5.03	5.42e-10	5.02
	15480	4.27e-09	3.95	5.83e-09	3.94	9.48e-09	3.94	9.75e-11	4.87	5.01e-11	4.89

Table 2.1: History of convergence of Example 1.

k	N	e_p	order	$e_{\boldsymbol{u}}$	order	e_{L}	order	$e_{\widehat{\boldsymbol{u}}}$	order	$e_{\boldsymbol{u}^*}$	order
1	180	2.35e+00	–	1.13e-01	–	2.29e+00	–	1.96e-01	–	5.46e-02	–
	868	4.20e-01	2.19	2.05e-02	2.17	2.79e-01	2.67	2.62e-02	2.55	7.76e-03	2.48
	3780	9.37e-02	2.04	4.95e-03	1.93	6.90e-02	1.90	3.86e-03	2.61	1.15e-03	2.60
	15748	2.16e-02	2.06	1.24e-03	1.95	1.72e-02	1.95	5.35e-04	2.77	1.61e-04	2.76
	64260	5.05e-03	2.07	3.10e-04	1.96	4.23e-03	1.99	7.18e-05	2.86	2.18e-05	2.85
2	180	1.95e-01	–	5.49e-03	–	7.69e-02	–	1.22e-02	–	3.66e-03	–
	868	2.14e-02	2.81	4.76e-04	3.11	9.84e-03	2.61	1.03e-03	3.14	3.09e-04	3.14
	3780	2.28e-03	3.04	4.78e-05	3.13	1.22e-03	2.83	7.56e-05	3.55	2.28e-05	3.54
	15748	2.48e-04	3.11	5.45e-06	3.04	1.52e-04	2.92	5.20e-06	3.75	1.58e-06	3.74
	64260	2.76e-05	3.13	6.65e-07	2.99	1.87e-05	2.98	3.47e-07	3.85	1.06e-07	3.85
3	180	4.74e-02	–	1.77e-03	–	4.85e-02	–	3.17e-03	–	9.36e-04	–
	868	1.31e-03	4.57	2.02e-05	5.69	5.54e-04	5.69	5.75e-05	5.10	1.72e-05	5.08
	3780	6.97e-05	3.98	7.68e-07	4.45	3.51e-05	3.75	2.11e-06	4.50	6.34e-07	4.49
	15748	3.79e-06	4.08	3.20e-08	4.45	2.21e-06	3.87	7.28e-08	4.72	2.21e-08	4.70

Table 2.2: History of convergence of Example 2. Errors measured in the Computational domain D_h.

2.6.3 Example 3: Other choice of transferring paths.

As mentioned int the introduction, one of the advantages of the method is that the computational domain does not need to fit the actual domain and can be easily constructed by immersing Ω in a

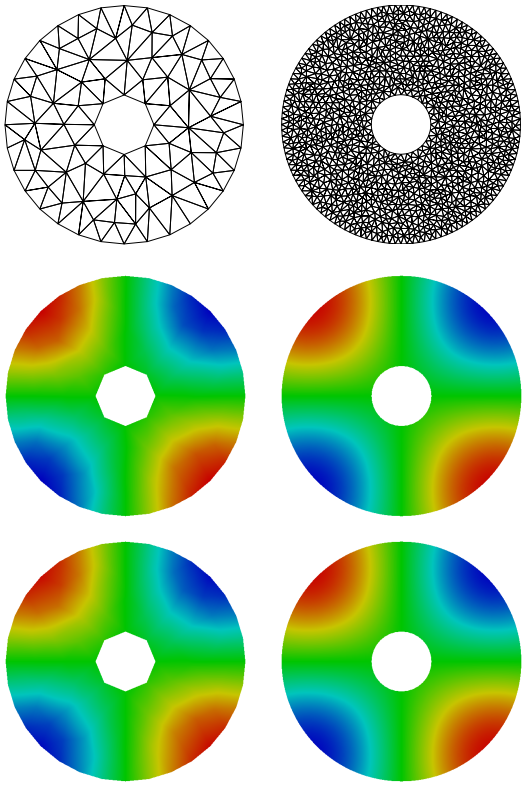

Figure 2.2: Approximation of the first component of $\boldsymbol{u}$ in Example 1. Columns: $N = 150$ and 2396. Rows: Polynomial of degree $k = 1$ and 2.

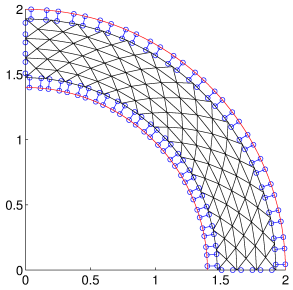

Figure 2.3: Domain Ω (red solid line) and D_h in Example 2. Transferring paths (blue solid lines) associated to the quadrature points when $k = 1$.

background mesh. In this case, for some domains, it is not convenient to use transferring paths normal to the boundary edges because the length of the paths might be large, affecting the magnitude of the errors. Instead, it is preferable to construct the transferring paths such that $\boldsymbol{x}$ and $\overline{\boldsymbol{x}}$ are as close as possible and hence they will not be necessarily normal to the boundary edges. That is why, in the last set of examples, we explore the capabilities of the method in a more general setting where some of the assumptions on the paths are not necessarily satisfied.

We consider a kidney-shaped domain whose boundary satisfies the equation $(2[(x+0.5)^2+y^2]-x-0.5)^2-[(x+0.5)^2+y^2]+0.1=0$ and a triangulation of a background domain $\mathcal{B}$ such that $\Omega\subset\mathcal{B}$. We set D_h as the union of all the elements inside Ω, as it is shown in Fig. 2.4 (most-left). In this case, the family of transferring paths is constructed by the procedure in Section 2.4.1 of [23]. We point out that now the tangent vector associated to a transferring path is not, in general, normal to a boundary edge. An example is depicted in Fig. 2.4. In this case, instead of (1.2), for $\boldsymbol{x}$ in a boundary edge e, we set

$$\widetilde{\boldsymbol{g}}_h(\boldsymbol{x}) := \boldsymbol{g}(\bar{\boldsymbol{x}}) - \int_0^{l(\boldsymbol{x})} \mathrm{L}_h(\boldsymbol{x}+\boldsymbol{t}(\boldsymbol{x})s\,)\boldsymbol{t}(\boldsymbol{x})\,ds, \tag{2.31}$$

where $\boldsymbol{t}(\boldsymbol{x})$ is the unit vector joining $\boldsymbol{x}$ and $\bar{\boldsymbol{x}}$.

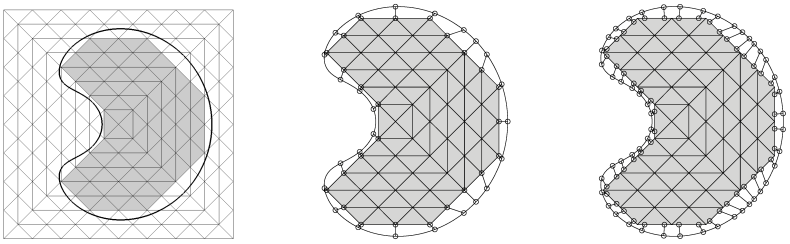

Figure 2.4: Left: Example of a domain Ω (kidney-shaped), background domain (square) and polygonal subdomain (gray). Middle: *transferring paths* (segments with starting and ending points marked with $\circ$) associated to boundary vertices. Right: *transferring paths* associated to two points on each boundary edge.

In all the simulations the source term $\boldsymbol{f}$ and boundary data $\boldsymbol{g}$ are such that the exact solution is

$$p(x,y)=\sin(x^2+y^2)-c_\Omega \quad \text{and} \quad \boldsymbol{u}(x,y)=\begin{bmatrix}\sin(x)\sin(y)\\ \cos(x)\cos(y)\end{bmatrix},$$

where $c_\Omega := \dfrac{1}{|\Omega|}\displaystyle\int_\Omega \sin(x^2+y^2)\,dx\,dy$ was computed numerically considering a extremely fine triangulation that fits the domain.

h-convergence

In Table 2.3 we observe, for $k=1$, convergence of order $k+1$ for the errors in p, $\boldsymbol{u}$ and L; and order higher than $k+3/2$ for the errors of the numerical trace and post-processed solution. This agrees with the estimates provided in Theorems 2.4 and 2.16. We recall that Theorem 2.16 predicts an order $h+3/2$ for the numerical trace and post-processed solution, but for an HDG method in polyhedral domains the order of convergence is $k+2$ for these variables. For the case $k=2$, the convergence rate deteriorates in the fourth mesh, but then the optimal order seems to be recovered. When $k=3$, optimal rates are also observed. In the last mesh $e_{\boldsymbol{u}^*}$ and $e_{\widehat{\boldsymbol{u}}}$ seem to be affected by round-off errors. On the other hand, Fig.2.5 shows the approximation of the first component of the tensor L obtained with $k=2$ and 712 elements. Here we display the computational domain, the approximations in D_h and D_h^c, and the two of them together in Ω.

k-convergence and condition number

Even though our estimates provide convergence with respect to the meshsize h, we numerically explore the performance of the method when the polynomial degree increases, since the constants in Assumptions A depend on k. Fig. 2.6 (left) shows the behavior of the log of errors for a fixed mesh with 154 elements. We observe that they linearly decrease for $k = 1$, 2, 3 and 4. For $k = 5$ they deteriorate but decrease again for $k = 6$.

On the other hand, we denote by κ the condition number of the global matrix. For comparison purpose, let κ_{poly} the condition number of the global matrix where the boundary data on Γ_h is being imposed exactly (we can do this since in this example we know the exact solution). We define the ratios $r^{\kappa} := \kappa/((k+1)^2h^{-2})$ and $r^{\kappa}_{poly} := \kappa_{poly}/((k+1)^2h^{-2})$. We observe in Fig. 2.6 (right) that r_{poly} remains constant, which means it behaves like a constant times $(k+1)^2h^{-2}$. However, r^{κ} increases with k. This fact shows one of the limitations of our method which has been also observed in the Poisson problem [21]. Developing efficient preconditioners is subject of future work. Meanwhile, we solve the system using UMFPACK [27], which is an LU factorization for sparse matrices that is a built-in function in MATLAB.

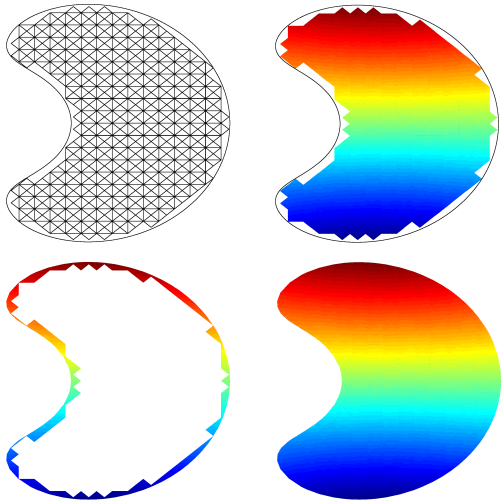

Figure 2.5: Approximation of the first component of L in Example 3 for $k = 2$ and 712 elements.

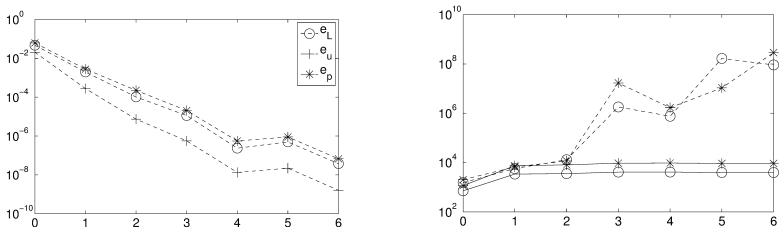

Figure 2.6: Left: Errors e_{L} ($\circ$), $e_{\boldsymbol{u}}$ ($+$) and e_p ($*$) versus $k = 0, ..., 6$ in semi-log scale, for 154 elements. Right: Ratios r^{κ} (dashed line) and r^{κ}_{poly} (solid line) in semi-log scale for 28 ($\circ$) and 154 ($*$) elements.

k	N	e_p	order	$e_{\boldsymbol{u}}$	order	e_{L}	order	$e_{\boldsymbol{u}^*}$	order	$e_{\widehat{\boldsymbol{u}}}$	order
1	28	1.82e−02	–	1.24e−03	–	1.10e−02	–	2.20e−03	–	3.10e−03	–
	154	2.78e−03	2.21	2.77e−04	1.75	1.97e−03	2.01	1.83e−03	0.22	3.74e−04	2.48
	712	8.09e−04	1.61	8.35e−05	1.57	4.77e−04	1.85	3.14e−05	5.31	6.71e−05	2.24
	3054	1.41e−04	2.40	2.06e−05	1.92	1.29e−04	1.80	3.24e−06	3.12	7.54e−06	3.00
	12579	3.44e−05	1.99	5.12e−06	1.97	3.31e−05	1.92	3.51e−07	3.14	8.55e−07	3.08
	50877	8.39e−06	2.02	1.28e−06	1.99	8.20e−06	2.00	4.43e−08	2.96	1.09e−07	2.95
2	28	2.21e−03	–	6.20e−05	–	7.75e−04	–	9.84e−05	–	1.18e−04	–
	154	2.25e−04	2.68	7.40e−06	2.49	1.03e−04	2.37	1.21e−05	2.46	2.20e−05	1.97
	712	2.84e−05	2.70	6.18e−07	3.24	1.73e−05	2.33	8.27e−07	3.50	1.73e−06	3.32
	3054	1.88e−05	0.57	1.88e−07	1.63	1.15e−05	0.56	2.38e−07	1.71	5.31e−07	1.62
	12579	8.11e−08	7.69	4.66e−09	5.23	6.97e−08	7.22	7.68e−10	8.11	1.85e−09	8.00
	50877	8.43e−09	3.24	5.82e−10	2.98	7.61e−09	3.17	4.60e−11	4.03	1.12e−10	4.01
3	28	1.33e−02	–	4.74e−04	–	5.33e−03	–	8.67e−04	–	1.06e−03	–
	154	2.06e−05	7.59	5.62e−07	7.90	1.13e−05	7.22	8.40e−07	8.14	1.43e−06	7.75
	712	9.09e−07	4.08	1.50e−08	4.73	5.43e−07	3.97	2.00e−08	4.88	4.04e−08	4.66
	3054	2.53e−08	4.92	3.05e−10	5.35	1.47e−08	4.95	2.98e−10	5.78	6.65e−10	5.64
	12579	1.40e−09	4.10	1.53e−11	4.23	1.13e−09	3.63	1.23e−11	4.51	3.00e−11	4.38
	50877	8.13e−11	4.07	1.36e−12	3.47	6.43e−11	4.10	1.46e−12	3.04	3.53e−12	3.06

Table 2.3: History of convergence of Example 3.

CHAPTER 3

Analysis of an HDG method for Oseen equations in curved domains

In this chapter we present a high order HDG method to numerically solve the Oseen equations in a region not necessarily polyhedral/polygonal. Since these equations are very similar to those of the Stokes problem, the structure of this chapter is very similar to the one of chapter 2.

3.1 Introduction

Let $\Omega \subset \mathbb{R}^d$ be a region not necessarily polygonal ($d = 2$) or polyhedral ($d = 3$), with compact, Lipschitz and piecewise $\mathcal{C}^2$ boundary $\Gamma := \partial\Omega$. The incompressible Oseen equations are given by the following set of equations:

$$\mathrm{L} - \nabla \boldsymbol{u} = 0 \quad \text{in } \Omega, \tag{3.1a}$$

$$-\nu \nabla \cdot \mathrm{L} + (\boldsymbol{\beta} \cdot \nabla)\boldsymbol{u} + \nabla p = \boldsymbol{f} \quad \text{in } \Omega, \tag{3.1b}$$

$$\nabla \cdot \boldsymbol{u} = 0 \quad \text{in } \Omega, \tag{3.1c}$$

$$\boldsymbol{u} = \boldsymbol{g} \quad \text{on } \Gamma, \tag{3.1d}$$

$$\int_\Omega p = 0, \tag{3.1e}$$

where $\boldsymbol{u}$ is the velocity of the fluid, p the pressure, $\nu > 0$ a constant viscosity, $\boldsymbol{f} \in [L^2(\Omega)]^d$ a source term and $\boldsymbol{g} \in [L^2(\Gamma)]^d$ the prescribed velocity at the boundary satisfying the compatibility condition $\int_\Gamma \boldsymbol{g} \cdot \boldsymbol{n} = 0$ ($\boldsymbol{n}$ is the outward unit normal to Ω). In addition, the convective velocity is assumed to satisfy $\boldsymbol{\beta} \in [W^{1,\infty}(\Omega)]^d$ and to be divergence free. The motivation to solve (3.1) arises from the steady–state Navier–Stokes equations, where the term $(\boldsymbol{u} \cdot \nabla)\boldsymbol{u}$ appears instead of $(\boldsymbol{\beta} \cdot \nabla)\boldsymbol{u}$. In fact, the solution of the Navier–Stokes equations can be obtained by using Picard's iteration that consists of solving (3.1) with $\boldsymbol{\beta}$ as the velocity obtained in the previous iteration. Observe that the unknowns in this problem are the same than in Stokes problem of chapter 2 and the only difference between these two problems is the term involving $\boldsymbol{\beta}$.

3.2 The HDG method

Following the treatment to the pressure introduced in the beginning of chapter 2, we begin by decomposing $p = \overline{p}^{\mathsf{D}_h} + \widetilde{p}$. We consider the HDG method [11] that seeks an approximation $(\mathrm{L}_h, \boldsymbol{u}_h, \widetilde{p}_h, \widehat{\boldsymbol{u}}_h)$ of the solution $(\mathrm{L}, \boldsymbol{u}, \widetilde{p}, \boldsymbol{u}|_{\mathcal{E}_h})$ in the space $\mathrm{G}_h \times \boldsymbol{V}_h \times P_h \times \boldsymbol{M}_h$ given by

$$\begin{aligned}
\mathrm{G}_h &= \{\mathrm{G} \in \mathrm{L}^2(\mathsf{T}_h) : \quad G|_K \in \mathrm{P}_k(K) \quad \forall K \in \mathsf{T}_h\}, && \text{(3.2a)}\\
\boldsymbol{V}_h &= \{\boldsymbol{v} \in \boldsymbol{L}^2(\mathsf{T}_h) : \quad \boldsymbol{v}|_K \in \boldsymbol{\mathcal{P}}_k(K) \quad \forall K \in \mathsf{T}_h\}, && \text{(3.2b)}\\
P_h &= \{q \in L^2(\mathsf{T}_h) : \quad q|_K \in \mathcal{P}_k(K) \quad \forall K \in \mathsf{T}_h\}, && \text{(3.2c)}\\
\boldsymbol{M}_h &= \{\boldsymbol{\mu} \in \boldsymbol{L}^2(\mathcal{E}_h) : \quad \boldsymbol{\mu}|_e \in \boldsymbol{\mathcal{P}}_k(e) \quad \forall e \in \mathcal{E}_h\}. && \text{(3.2d)}
\end{aligned}$$

As we will see in Section 3.2.1, this approximation is the only solution of

$$\begin{aligned}
(\mathrm{L}_h, \mathrm{G})_{\mathsf{T}_h} + (\boldsymbol{u}_h, \nabla \cdot \mathrm{G})_{\mathsf{T}_h} - \langle \widehat{\boldsymbol{u}}_h, \mathrm{G}\boldsymbol{n}\rangle_{\partial\mathsf{T}_h} &= 0, && \text{(3.3a)}\\
(\nu \mathrm{L}_h, \nabla \boldsymbol{v})_{\mathsf{T}_h} - (\boldsymbol{u}_h \otimes \boldsymbol{\beta}, \nabla \boldsymbol{v})_{\mathsf{T}_h} - (\widetilde{p}_h, \nabla \cdot \boldsymbol{v})_{\mathsf{T}_h} & && \text{(3.3b)}\\
-\langle \nu \widehat{\mathrm{L}}_h \boldsymbol{n} - \widehat{p}_h \boldsymbol{n} - \widehat{(\boldsymbol{u}_h \otimes \boldsymbol{\beta})}\boldsymbol{n}, \boldsymbol{v}\rangle_{\partial\mathsf{T}_h} &= (\boldsymbol{f}, \boldsymbol{v})_{\mathsf{T}_h}, &&\\
-(\boldsymbol{u}_h, \nabla q)_{\mathsf{T}_h} + \langle \widehat{\boldsymbol{u}}_h \cdot \boldsymbol{n}, q\rangle_{\partial\mathsf{T}_h} &= 0, && \text{(3.3c)}\\
\langle \widehat{\boldsymbol{u}}_h, \boldsymbol{\mu}\rangle_{\Gamma_h} &= \langle \tilde{\boldsymbol{g}}_h, \boldsymbol{\mu}\rangle_{\Gamma_h}, && \text{(3.3d)}\\
\langle \nu \widehat{\mathrm{L}}_h \boldsymbol{n} - \widehat{p}_h \boldsymbol{n} - \widehat{(\boldsymbol{u}_h \otimes \boldsymbol{\beta})}\boldsymbol{n}, \boldsymbol{\mu}\rangle_{\partial\mathsf{T}_h \setminus \Gamma_h} &= 0, && \text{(3.3e)}\\
(\widetilde{p}_h, 1)_{\mathsf{D}_h} &= 0, && \text{(3.3f)}
\end{aligned}$$

for all $(\mathrm{G}, \boldsymbol{v}, q, \boldsymbol{\mu}) \in \mathrm{G}_h \times \boldsymbol{V}_h \times P_h \times \boldsymbol{M}_h$, where

$$\nu \widehat{\mathrm{L}}_h \boldsymbol{n} - \widehat{p}_h \boldsymbol{n} - \widehat{(\boldsymbol{u}_h \otimes \boldsymbol{\beta})}\boldsymbol{n} = \nu \mathrm{L}_h \boldsymbol{n} - \widetilde{p}_h \boldsymbol{n} - (\widehat{\boldsymbol{u}}_h \otimes \boldsymbol{\beta})\boldsymbol{n} - \mathrm{S}(\boldsymbol{u}_h - \widehat{\boldsymbol{u}}_h) \qquad \text{on } \partial\mathsf{T}_h, \tag{3.3g}$$

and τ is a non-negative piecewise constant stabilization parameter defined on $\partial\mathsf{T}_h$. In order to simplify notation, we assume τ to be constant on $\partial\mathsf{T}_h$, and to satisfy

$$\tau\nu - \frac{1}{2}(\boldsymbol{\beta} \cdot \boldsymbol{n}) > c_\tau \qquad \text{on } \partial K, \tag{3.4}$$

for all $K \in \mathsf{T}_h$ and for some positive constant c_τ. Note that this assumption is equivalent to $\mathrm{S}_{\boldsymbol{\beta}} := \big(\mathrm{S} - \frac{1}{2}(\boldsymbol{\beta} \cdot \boldsymbol{n})\mathrm{I}\big)\big|_{\partial K}$ being positive definite.

3.2.1 Well-posedness of the method

In this section we show that the discrete scheme (3.3) with the approximated boundary data (1.2) is well-posed. The steps that will lead to this statement will be very similar to those needed to obtain the error estimates in Section 3.4. The main result of this section is the following.

Theorem 3.1. *Under the assumptions of Lemmas 3.2, 3.3 and 3.4 (stated and proved below), the scheme (3.3) with boundary data defined in (1.2) has a unique solution.*

The proof of Theorem 3.1 will be a consequence of Lemmas 3.2, 3.3 and 3.4. Before proving the lemmas, for $K \in \mathsf{T}_h$, let $\boldsymbol{\beta}_0 \in \boldsymbol{\mathcal{P}}_0(K)$ be the function such that

$$\langle (\boldsymbol{\beta} - \boldsymbol{\beta}_0) \cdot \boldsymbol{n}, 1\rangle_F = 0, \qquad \text{for all faces } F \text{ of } K,$$

and define $\boldsymbol{\delta\beta} := \boldsymbol{\beta} - \boldsymbol{\beta}_0$. Observe that $\boldsymbol{\beta}_0$ exists since $\nabla \cdot \boldsymbol{\beta} = 0$. Indeed, it corresponds to the lowest order Raviart–Thomas projection of $\boldsymbol{\beta}$. It also holds [10] that

$$\|\boldsymbol{\delta\beta}\|_K \leq C h_K \|\nabla \boldsymbol{\beta}\|_K, \qquad \forall K \in \mathsf{T}_h. \tag{3.5}$$

The following lemmas will lead to the well-posedness of the method.

Lemma 3.2. *Let $(\mathrm{L}_h, \boldsymbol{u}_h, \widetilde{p}_h, \widehat{\boldsymbol{u}}_h) \in \mathrm{G}_h \times \boldsymbol{V}_h \times P_h \times \boldsymbol{M}_h$ be the solution of (3.3) with the boundary data defined in (1.2). Let us suppose that $\boldsymbol{f} = \boldsymbol{0}$ and $\boldsymbol{g} = \boldsymbol{0}$. In addition, for every $e \in \mathcal{E}_h^{\partial}$, we assume that*

(A.1) $r_e^3 (C_{ext}^e)^2 (C_{inv}^e)^2 \leq 1/8$,

(A.2) $\nu^{-1} r_e h_e^{\perp} \left(\nu\tau - \frac{1}{2}(\boldsymbol{\beta} \cdot \boldsymbol{n}) \right) \leq 1/8$,

(A.3) $(C_{tr}^e)^2 r_e \gamma \leq 1/6$.

Then,

$$\begin{aligned} \|\mathrm{L}_h\|_{\mathsf{D}_h}^2 + \nu^{-1} \langle \mathrm{S}_{\boldsymbol{\beta}}(\boldsymbol{u}_h - \widehat{\boldsymbol{u}}_h), \boldsymbol{u}_h - \widehat{\boldsymbol{u}}_h \rangle_{\partial \mathsf{T}_h} + \|\widetilde{\boldsymbol{g}}_h\|_{\Gamma_h, l^{-1}}^2 \quad &\leq \quad 24 \nu^{-2} \|\widetilde{p}_h\|_{\Gamma_h, l}^2 \\ &\quad + \nu^{-2} \|\boldsymbol{\beta}\|_{L^\infty(\Omega)}^2 \|\boldsymbol{u}_h\|_{\mathsf{D}_h}^2. \end{aligned}$$

Note that these assumptions are very similar to those made when we wanted to prove the well–posedness of the discrete scheme in chapter 2. Actually, the only difference is in (A.2), where in this case the addirional term $\frac{1}{2}\boldsymbol{\beta} \cdot \boldsymbol{n}$ appears. The comments mentioned about these assumptions in the previous chapter are also valid here.

Proof. By taking $\mathrm{G} = \nu \mathrm{L}_h$, $\boldsymbol{v} = \boldsymbol{u}_h$ and $q = \widetilde{p}_h$ in the first three equations of (3.3), integrating by parts and adding them up we obtain

$$\begin{aligned} 0 \quad &= \quad \nu \|\mathrm{L}_h\|_{\mathsf{D}_h}^2 + \big(\nabla \cdot (\boldsymbol{u}_h \otimes \boldsymbol{\beta}), \boldsymbol{u}_h\big)_{\mathsf{T}_h} - \langle \nu \mathrm{L}_h \boldsymbol{n} - \widetilde{p}_h \boldsymbol{n}, \boldsymbol{u}_h \rangle_{\partial \mathsf{T}_h} \\ &\quad - \big\langle \big((\boldsymbol{u}_h - \widehat{\boldsymbol{u}}_h) \otimes \boldsymbol{\beta}\big)\boldsymbol{n} + \mathrm{S}(\boldsymbol{u}_h - \widehat{\boldsymbol{u}}_h), \boldsymbol{u}_h \big\rangle_{\partial \mathsf{T}_h}. \end{aligned} \tag{3.6}$$

Now, note that using (3.3e) with $\boldsymbol{\mu} = \widehat{\boldsymbol{u}}_h$, we have

$$\langle \nu \widehat{\mathrm{L}}_h \boldsymbol{n} - \widehat{p}_h \boldsymbol{n} - \widehat{(\boldsymbol{u}_h \otimes \boldsymbol{\beta})} \boldsymbol{n}, \widehat{\boldsymbol{u}}_h \rangle_{\partial \mathsf{T}_h} = \langle \nu \widehat{\mathrm{L}}_h \boldsymbol{n} - \widehat{p}_h \boldsymbol{n} - \widehat{(\boldsymbol{u}_h \otimes \boldsymbol{\beta})} \boldsymbol{n}, \widehat{\boldsymbol{u}}_h \rangle_{\Gamma_h},$$

which implies that

$$\begin{aligned} \langle \nu \mathrm{L}_h \boldsymbol{n} - \widetilde{p}_h \boldsymbol{n}, \widehat{\boldsymbol{u}}_h \rangle_{\partial \mathsf{T}_h} \quad &= \quad \langle (\widehat{\boldsymbol{u}}_h \otimes \boldsymbol{\beta}) \boldsymbol{n} + \mathrm{S}(\boldsymbol{u}_h - \widehat{\boldsymbol{u}}_h), \widehat{\boldsymbol{u}}_h \rangle_{\partial \mathsf{T}_h} \\ &\quad + \langle \nu \mathrm{L}_h \boldsymbol{n} - \widetilde{p}_h \boldsymbol{n} - (\widehat{\boldsymbol{u}}_h \otimes \boldsymbol{\beta}) \boldsymbol{n} - \mathrm{S}(\boldsymbol{u}_h - \widehat{\boldsymbol{u}}_h), \widehat{\boldsymbol{u}}_h \rangle_{\Gamma_h}. \end{aligned}$$

On the other hand, observe that for any tensor M and vectors $\boldsymbol{w}, \boldsymbol{y}, \boldsymbol{z}$, it holds

$$\nabla \cdot (\boldsymbol{w} \otimes \boldsymbol{z}) = (\nabla \cdot \boldsymbol{z}) \boldsymbol{w} + (\nabla \boldsymbol{w}) \boldsymbol{z}, \tag{3.7a}$$

$$(\mathsf{M}\boldsymbol{z}, \boldsymbol{w}) = (\mathsf{M}, \boldsymbol{w} \otimes \boldsymbol{z}), \tag{3.7b}$$

$$(\boldsymbol{w} \otimes \boldsymbol{y}) \boldsymbol{z} = (\boldsymbol{y} \cdot \boldsymbol{z}) \boldsymbol{w} \tag{3.7c}$$

We want to apply these properties to the term $\big(\nabla\cdot(\boldsymbol{u}_h\otimes\boldsymbol{\beta}),\boldsymbol{u}_h\big)_{\mathsf{T}_h}$. Since $\nabla\cdot\boldsymbol{\beta}=0$, we have

$$(\nabla\cdot(\boldsymbol{u}_h\otimes\boldsymbol{\beta}),\boldsymbol{u}_h)_{\mathsf{T}_h}=\big((\nabla\boldsymbol{u}_h)\beta,\boldsymbol{u}_h\big)_{\mathsf{T}_h}=(\nabla\boldsymbol{u}_h,\boldsymbol{u}_h\otimes\boldsymbol{\beta})_{\mathsf{T}_h}.$$

But, integrating by parts,

$$(\nabla\boldsymbol{u}_h,\boldsymbol{u}_h\otimes\boldsymbol{\beta})_{\mathsf{T}_h}=-(\nabla\cdot(\boldsymbol{u}_h\otimes\boldsymbol{\beta}),\boldsymbol{u}_h)_{\mathsf{T}_h}+\langle(\boldsymbol{u}_h\otimes\boldsymbol{\beta})\boldsymbol{n},\boldsymbol{u}_h\rangle_{\partial\mathsf{T}_h}.$$

Thus, we conclude that

$$(\nabla\cdot(\boldsymbol{u}_h\otimes\boldsymbol{\beta}),\boldsymbol{u}_h)_{\mathsf{T}_h}=\frac{1}{2}\langle(\boldsymbol{u}_h\otimes\boldsymbol{\beta})\boldsymbol{n},\boldsymbol{u}_h\rangle_{\partial\mathsf{T}_h},$$

and hence we can rewrite (3.6) as

$$\begin{aligned}
0 &= \nu\|\mathrm{L}_h\|^2_{\mathsf{D}_h}+\frac{1}{2}\langle(\boldsymbol{u}_h\otimes\boldsymbol{\beta})\boldsymbol{n},\boldsymbol{u}_h\rangle_{\partial\mathsf{T}_h}-\langle(\widehat{\boldsymbol{u}}_h\otimes\boldsymbol{\beta})\boldsymbol{n}+\mathrm{S}(\boldsymbol{u}_h-\widehat{\boldsymbol{u}}_h),\widehat{\boldsymbol{u}}_h\rangle_{\partial\mathsf{T}_h}\\
&\quad-\langle\nu\mathrm{L}_h\boldsymbol{n}-\widetilde{p}_h\boldsymbol{n}-(\widehat{\boldsymbol{u}}_h\otimes\boldsymbol{\beta})\boldsymbol{n}-\mathrm{S}(\boldsymbol{u}_h-\widehat{\boldsymbol{u}}_h),\widehat{\boldsymbol{u}}_h\rangle_{\Gamma_h}-\langle(\boldsymbol{u}_h\otimes\boldsymbol{\beta})\boldsymbol{n},\boldsymbol{u}_h\rangle_{\partial\mathsf{T}_h}\\
&\quad+\langle(\widehat{\boldsymbol{u}}_h\otimes\boldsymbol{\beta})\boldsymbol{n}+\mathrm{S}(\boldsymbol{u}_h-\widehat{\boldsymbol{u}}_h),\boldsymbol{u}_h\rangle_{\partial\mathsf{T}_h}\\
&= \nu\|\mathrm{L}_h\|^2_{\mathsf{D}_h}-\frac{1}{2}\langle(\boldsymbol{u}_h\otimes\boldsymbol{\beta})\boldsymbol{n},\boldsymbol{u}_h\rangle_{\partial\mathsf{T}_h}+\langle(\widehat{\boldsymbol{u}}_h\otimes\boldsymbol{\beta})\boldsymbol{n}+\mathrm{S}(\boldsymbol{u}_h-\widehat{\boldsymbol{u}}_h),\boldsymbol{u}_h-\widehat{\boldsymbol{u}}_h\rangle_{\partial\mathsf{T}_h}\\
&\quad-\langle\nu\mathrm{L}_h\boldsymbol{n}-\widetilde{p}_h\boldsymbol{n}-(\widehat{\boldsymbol{u}}_h\otimes\boldsymbol{\beta})\boldsymbol{n}-\mathrm{S}(\boldsymbol{u}_h-\widehat{\boldsymbol{u}}_h),\widehat{\boldsymbol{u}}_h\rangle_{\Gamma_h}.
\end{aligned}\tag{3.8}$$

Now, since for any vector $\boldsymbol{z}$ it holds that $(\boldsymbol{z}\otimes\boldsymbol{\beta})\boldsymbol{n}=(\boldsymbol{\beta}\cdot\boldsymbol{n})\boldsymbol{z}$, the definition of $\mathrm{S}_{\boldsymbol{\beta}}:=\mathrm{S}-\frac{1}{2}(\boldsymbol{\beta}\cdot\boldsymbol{n})\mathrm{I}$, and the fact that $\widehat{\boldsymbol{u}}_h$ is single valued on $\mathcal{E}_h^0$ and $(\boldsymbol{\beta}\cdot\boldsymbol{n})$ is continuous on $\mathcal{E}_h^0$, it is easy to see that

$$\begin{aligned}
-\frac{1}{2}\langle(\boldsymbol{u}_h\otimes\boldsymbol{\beta})\boldsymbol{n},\boldsymbol{u}_h\rangle_{\partial\mathsf{T}_h} &+ \langle(\widehat{\boldsymbol{u}}_h\otimes\boldsymbol{\beta})\boldsymbol{n}+\mathrm{S}(\boldsymbol{u}_h-\widehat{\boldsymbol{u}}_h),\boldsymbol{u}_h-\widehat{\boldsymbol{u}}_h\rangle_{\partial\mathsf{T}_h}\\
&= -\frac{1}{2}\langle(\widehat{\boldsymbol{u}}_h\otimes\boldsymbol{\beta})\boldsymbol{n},\widehat{\boldsymbol{u}}_h\rangle_{\partial\mathsf{T}_h}+\langle\mathrm{S}_{\boldsymbol{\beta}}(\boldsymbol{u}_h-\widehat{\boldsymbol{u}}_h),\boldsymbol{u}_h-\widehat{\boldsymbol{u}}_h\rangle_{\partial\mathsf{T}_h}\\
&= -\frac{1}{2}\langle(\widehat{\boldsymbol{u}}_h\otimes\boldsymbol{\beta})\boldsymbol{n},\widehat{\boldsymbol{u}}_h\rangle_{\Gamma_h}+\langle\mathrm{S}_{\boldsymbol{\beta}}(\boldsymbol{u}_h-\widehat{\boldsymbol{u}}_h),\boldsymbol{u}_h-\widehat{\boldsymbol{u}}_h\rangle_{\partial\mathsf{T}_h}.
\end{aligned}$$

Hence, (3.8) can be rewritten as

$$\begin{aligned}
\nu\|\mathrm{L}_h\|^2_{\mathsf{D}_h} &+ \langle\mathrm{S}_{\boldsymbol{\beta}}(\boldsymbol{u}_h-\widehat{\boldsymbol{u}}_h),\boldsymbol{u}_h-\widehat{\boldsymbol{u}}_h\rangle_{\partial\mathsf{T}_h}\\
&= \Big\langle\nu\mathrm{L}_h\boldsymbol{n}-\widetilde{p}_h\boldsymbol{n}-\frac{1}{2}(\widehat{\boldsymbol{u}}_h\otimes\boldsymbol{\beta})\boldsymbol{n}-\mathrm{S}(\boldsymbol{u}_h-\widehat{\boldsymbol{u}}_h),\widehat{\boldsymbol{u}}_h\Big\rangle_{\Gamma_h}.
\end{aligned}\tag{3.9}$$

Observe now that, according to (1.2) and (1.3), we can write

$$\mathrm{L}_h(\boldsymbol{x})\boldsymbol{n}=-l^{-1}(\boldsymbol{x})\widetilde{\boldsymbol{g}}_h(\boldsymbol{x})-\delta_{\mathrm{L}_h}(\boldsymbol{x}).\tag{3.10}$$

Replacing this in the right hand side of (3.9) and using (2.4d), we have

$$\begin{aligned}
\Big\langle\nu\mathrm{L}_h\boldsymbol{n}-\widetilde{p}_h\boldsymbol{n}-\frac{1}{2}(\widehat{\boldsymbol{u}}_h\otimes\boldsymbol{\beta})\boldsymbol{n} &- \mathrm{S}(\boldsymbol{u}_h-\widehat{\boldsymbol{u}}_h),\widehat{\boldsymbol{u}}_h\Big\rangle_{\Gamma_h}\\
&= -\nu\langle\widetilde{\boldsymbol{g}}_h l^{-1},\widetilde{\boldsymbol{g}}_h\rangle_{\Gamma_h}-\nu\langle\delta_{\mathrm{L}_h},\widetilde{\boldsymbol{g}}_h\rangle_{\Gamma_h}-\langle\widetilde{p}_h\boldsymbol{n},\widetilde{\boldsymbol{g}}_h\rangle_{\Gamma_h}\\
&\quad-\frac{1}{2}\langle(\widehat{\boldsymbol{u}}_h\otimes\boldsymbol{\beta})\boldsymbol{n},\mathbf{P}_M(\widetilde{\boldsymbol{g}}_h)\rangle_{\Gamma_h}-\langle\mathrm{S}_{\boldsymbol{\beta}}(\boldsymbol{u}_h-\widehat{\boldsymbol{u}}_h),\widetilde{\boldsymbol{g}}_h\rangle_{\Gamma_h}\\
&\quad-\frac{1}{2}\langle\big((\boldsymbol{u}_h-\widehat{\boldsymbol{u}}_h)\otimes\boldsymbol{\beta}\big)\boldsymbol{n},\mathbf{P}_M(\widetilde{\boldsymbol{g}}_h)\rangle_{\Gamma_h}\\
&= -\nu\langle\widetilde{\boldsymbol{g}}_h l^{-1},\widetilde{\boldsymbol{g}}_h\rangle_{\Gamma_h}-\nu\langle\delta_{\mathrm{L}_h},\widetilde{\boldsymbol{g}}_h\rangle_{\Gamma_h}-\langle\widetilde{p}_h\boldsymbol{n},\widetilde{\boldsymbol{g}}_h\rangle_{\Gamma_h}\\
&\quad-\frac{1}{2}\langle(\boldsymbol{u}_h\otimes\boldsymbol{\beta})\boldsymbol{n},\mathbf{P}_M(\widetilde{\boldsymbol{g}}_h)\rangle_{\Gamma_h}-\langle\mathrm{S}_{\boldsymbol{\beta}}(\boldsymbol{u}_h-\widehat{\boldsymbol{u}}_h),\widetilde{\boldsymbol{g}}_h\rangle_{\Gamma_h}.
\end{aligned}$$

Applying Cauchy-Schwarz and Young's inequalities with $\epsilon = 1/6$, we can rewrite (3.9) as

$$\begin{aligned}\nu\|\mathrm{L}_h\|^2_{\mathsf{D}_h} &+ \langle \mathrm{S}_{\boldsymbol{\beta}}(\boldsymbol{u}_h - \widehat{\boldsymbol{u}}_h), \boldsymbol{u}_h - \widehat{\boldsymbol{u}}_h\rangle_{\partial\mathsf{T}_h} + \frac{\nu}{3}\|\widetilde{\boldsymbol{g}}_h\|^2_{\Gamma_h,l^{-1}} \\ &\leq 3\nu\|\delta_{\mathrm{L}_h}\|^2_{\Gamma_h,l} + 3\nu^{-1}\|\widetilde{p}_h\|^2_{\Gamma_h,l} + 3\nu^{-1}\|\mathrm{S}_{\boldsymbol{\beta}}(\boldsymbol{u}_h - \widehat{\boldsymbol{u}}_h)\|^2_{\Gamma_h,l} \\ &\quad + \frac{3\nu^{-1}}{4}\|(\boldsymbol{\beta}\cdot\boldsymbol{n})\boldsymbol{u}_h\|^2_{\Gamma_h,l}. \end{aligned} \tag{3.11}$$

By (1.4), (1.7), Assumptions $(A.1)$ and $(A.2)$, the fact that $l \leq H_e^{\perp} = r_e h_e^{\perp}$ and $h_e^{\perp} \leq \gamma h_e$, we can bound the terms in the right hand side of (3.11):

$$\begin{aligned} 3\nu\|\delta_{\mathrm{L}_h}\|^2_{\Gamma_h,l} &= 3\nu\sum_{e\in\mathcal{E}_h^{\partial}}\|\delta_{\mathrm{L}_h}\|^2_{e,l} \leq 3\nu\sum_{e\in\mathcal{E}_h^{\partial}}\frac{1}{3}r_e^3(C_{ext}^e)^2(C_{inv}^e)^2\|\mathrm{L}_h\|^2_{K^e} \\ &\leq \frac{\nu}{8}\|\mathrm{L}_h\|^2_{\mathsf{D}_h}, \end{aligned} \tag{3.12}$$

$$\begin{aligned} 3\nu^{-1}\|\mathrm{S}_{\boldsymbol{\beta}}(\boldsymbol{u}_h - \widehat{\boldsymbol{u}}_h)\|^2_{\Gamma_h,l} &= 3\nu^{-1}\sum_{e\in\mathcal{E}_h^{\partial}}\langle l^{1/2}\mathrm{S}_{\boldsymbol{\beta}}(\boldsymbol{u}_h - \widehat{\boldsymbol{u}}_h), l^{1/2}\mathrm{S}_{\boldsymbol{\beta}}(\boldsymbol{u}_h - \widehat{\boldsymbol{u}}_h)\rangle_e \\ &\leq 3\sum_{e\in\mathcal{E}_h^{\partial}}\nu^{-1}r_e h_e^{\perp}\left(\tau\nu - \frac{1}{2}(\boldsymbol{\beta}\cdot\boldsymbol{n})\right)\langle \mathrm{S}_{\boldsymbol{\beta}}(\boldsymbol{u}_h - \widehat{\boldsymbol{u}}_h), \boldsymbol{u}_h - \widehat{\boldsymbol{u}}_h\rangle_e \\ &\leq \frac{3}{8}\langle \mathrm{S}_{\boldsymbol{\beta}}(\boldsymbol{u}_h - \widehat{\boldsymbol{u}}_h), \boldsymbol{u}_h - \widehat{\boldsymbol{u}}_h\rangle_{\partial\mathsf{T}_h}, \end{aligned} \tag{3.13}$$

$$\begin{aligned} \frac{3\nu^{-1}}{4}\|(\boldsymbol{\beta}\cdot\boldsymbol{n})\boldsymbol{u}_h\|^2_{\Gamma_h,l} &= \frac{3\nu^{-1}}{4}\sum_{e\in\mathcal{E}_h^{\partial}}\|(\boldsymbol{\beta}\cdot\boldsymbol{n})\boldsymbol{u}_h\|^2_{e,l} \leq \frac{3\nu^{-1}}{4}\sum_{e\in\mathcal{E}_h^{\partial}}\|\boldsymbol{\beta}\|^2_{L^\infty(\Omega)}r_e h_e^{\perp}\|\boldsymbol{u}_h\|^2_e \\ &\leq \frac{3\nu^{-1}}{4}\|\boldsymbol{\beta}\|^2_{L^\infty(\Omega)}\sum_{e\in\mathcal{E}_h^{\partial}}r_e h_e^{\perp}(C_{tr}^e)^2 h_e^{-1}\|\boldsymbol{u}_h\|^2_{K^e} \\ &\leq \frac{3\nu^{-1}}{4}\|\boldsymbol{\beta}\|^2_{L^\infty(\Omega)}\sum_{e\in\mathcal{E}_h^{\partial}}(C_{tr}^e)^2 r_e\gamma\|\boldsymbol{u}_h\|^2_{K^e} \\ &\leq \frac{\nu^{-1}}{8}\|\boldsymbol{\beta}\|^2_{L^\infty(\Omega)}\|\boldsymbol{u}_h\|^2_{\mathsf{D}_h}. \end{aligned} \tag{3.14}$$

Replacing these estimates in (3.11) and rearranging terms, we obtain

$$\begin{aligned}\frac{7\nu}{8}\|\mathrm{L}_h\|^2_{\mathsf{D}_h} + \frac{5}{8}\langle \mathrm{S}_{\boldsymbol{\beta}}(\boldsymbol{u}_h - \widehat{\boldsymbol{u}}_h), \boldsymbol{u}_h - \widehat{\boldsymbol{u}}_h\rangle_{\partial\mathsf{T}_h} + \frac{\nu}{3}\|\widetilde{\boldsymbol{g}}_h\|^2_{\Gamma_h,l^{-1}} &\leq 3\nu^{-1}\|\widetilde{p}_h\|^2_{\Gamma_h,l} \\ &\quad + \frac{\nu^{-1}}{8}\|\boldsymbol{\beta}\|^2_{L^\infty(\Omega)}\|\boldsymbol{u}_h\|^2_{\mathsf{D}_h}. \end{aligned}$$

Finally, since $\dfrac{1}{8} < \min\left\{\dfrac{7}{8}, \dfrac{5}{8}, \dfrac{1}{3}\right\}$, we have

$$\begin{aligned}\|\mathrm{L}_h\|^2_{\mathsf{D}_h} + \nu^{-1}\langle \mathrm{S}_{\boldsymbol{\beta}}(\boldsymbol{u}_h - \widehat{\boldsymbol{u}}_h), \boldsymbol{u}_h - \widehat{\boldsymbol{u}}_h\rangle_{\partial\mathsf{T}_h} + \|\widetilde{\boldsymbol{g}}_h\|^2_{\Gamma_h,l^{-1}} &\leq 24\nu^{-2}\|\widetilde{p}_h\|^2_{\Gamma_h,l} \\ &\quad + \nu^{-2}\|\boldsymbol{\beta}\|^2_{L^\infty(\Omega)}\|\boldsymbol{u}_h\|^2_{\mathsf{D}_h}, \end{aligned}$$

which concludes the proof. □

In order to deal with the terms at the right hand side of the estimate in Lemma 3.2, we need the next result.

Proposition 3.1. *It holds that*

$$\|\widehat{\boldsymbol{u}}_h\|_h \le C\big(h\|\mathrm{L}_h\|_{\mathsf{D}_h} + \|\boldsymbol{u}_h\|_{\mathsf{D}_h}\big).$$

Proof. Using (3.3a) we obtain that

$$\langle \widehat{\boldsymbol{u}}_h, \mathrm{G}\boldsymbol{n}\rangle_{\partial K} = (\mathrm{L}_h, \mathrm{G})_K + (\boldsymbol{u}_h, \nabla\cdot\mathrm{G})_K \qquad \forall\ \mathrm{G}\in \mathrm{P}_k(K).$$

Then, by a standard scaling argument,

$$h_K^{1/2}\|\widehat{\boldsymbol{u}}_h\|_{\partial K} \le C\big(h_K\|\mathrm{L}_h\|_K + \|\boldsymbol{u}_h\|_K\big).$$

Finally, we obtain the result by summing up over all $K\in\mathsf{T}_h$. □

We can now state the next lemma.

Lemma 3.3. *Let $\boldsymbol{P}:\boldsymbol{H}^1(\mathsf{T}_h)\to\boldsymbol{V}_h$ be any projection such that*

$$(\boldsymbol{P}\boldsymbol{w}-\boldsymbol{w},\boldsymbol{v})_K = 0, \qquad \forall\ \boldsymbol{v}\in\boldsymbol{\mathcal{P}}_{k-1}(K), \tag{3.15}$$

for all $K\in\mathsf{T}_h$. Define

$$\begin{aligned}
H_p^1 &= C\max\left\{\nu,\ \|\boldsymbol{\beta}_0\|_{L^\infty(\Omega)}\sup_{\boldsymbol{w}\in\boldsymbol{H}_0^1(\mathsf{D}_h)\setminus\{\boldsymbol{0}\}}\frac{\|\boldsymbol{P}\boldsymbol{w}\|_{\mathsf{T}_h}}{\|\boldsymbol{w}\|_{\boldsymbol{H}^1(\mathsf{D}_h)}},\ h|\boldsymbol{\beta}|_{W^{1,\infty}(\Omega)}\sup_{\boldsymbol{w}\in\boldsymbol{H}_0^1(\mathsf{D}_h)\setminus\{\boldsymbol{0}\}}\frac{\|\boldsymbol{P}\boldsymbol{w}\|_{\mathsf{D}_h}}{\|\boldsymbol{w}\|_{\boldsymbol{H}^1(\mathsf{D}_h)}}\right\},\\
H_p^2 &= C|\boldsymbol{\beta}|_{W^{1,\infty}(\Omega)}\max\left\{h\sup_{\boldsymbol{w}\in\boldsymbol{H}_0^1(\mathsf{D}_h)\setminus\{\boldsymbol{0}\}}\frac{\|\nabla\boldsymbol{P}\boldsymbol{w}\|_{\mathsf{T}_h}}{\|\boldsymbol{w}\|_{\boldsymbol{H}^1(\mathsf{D}_h)}},\ \sup_{\boldsymbol{w}\in\boldsymbol{H}_0^1(\mathsf{D}_h)\setminus\{\boldsymbol{0}\}}\frac{\|\boldsymbol{P}\boldsymbol{w}\|_{\mathsf{T}_h}}{\|\boldsymbol{w}\|_{\boldsymbol{H}^1(\mathsf{D}_h)}}\right\},\\
H_p^3 &= \sup_{\boldsymbol{w}\in\boldsymbol{H}_0^1(\mathsf{D}_h)\setminus\{\boldsymbol{0}\}}\frac{\|\boldsymbol{P}\boldsymbol{w}-\mathbf{P}_M\boldsymbol{w}\|_{\partial\mathsf{T}_h,\tau}}{\|\boldsymbol{w}\|_{\boldsymbol{H}^1(\mathsf{D}_h)}},
\end{aligned}$$

and $C_{\tau,\nu,\boldsymbol{\beta}} = \nu^{1/2}\tau^{-1/2}\left\{\tau^{1/2}\nu^{1/2}+\|\boldsymbol{\beta}\|_{L^\infty(\Omega)}^{1/2}\big(1+c_\tau^{-1/2}\|\boldsymbol{\beta}\|_{L^\infty(\Omega)}^{1/2}\big)\right\}$. Suppose that assumptions of Lemma 3.2 are satisfied and that for each $e\in\mathcal{E}_h^\partial$ it holds that

(A.4) $2\sqrt{6}\kappa\nu^{-1}\big(3H_p^1 + C_{\tau,\nu,\boldsymbol{\beta}}H_p^3\big)C_{tr}^e r_e^{1/2}\gamma^{1/2} < 1/2,$

where $\kappa>0$ is defined below. Then

$$\|\widetilde{p}_h\|_{\mathsf{D}_h} \le 2\kappa\left\{\nu^{-1}\|\boldsymbol{\beta}\|_{L^\infty(\Omega)}\big(3H_p^1 + C_{\tau,\nu,\boldsymbol{\beta}}H_p^3\big) + 2H_p^2\right\}\|\boldsymbol{u}_h\|_{\mathsf{D}_h}.$$

Proof. We adapt the proof of Proposition 3.4 in [18] to our setting. Since $\widetilde{p}_h\in L_0^2(\mathsf{D}_h)$, there exists $\kappa>0$, independent of h, such that

$$\|\widetilde{p}_h\|_{\mathsf{D}_h} \le \kappa\sup_{\boldsymbol{w}\in\boldsymbol{H}_0^1(\mathsf{D}_h)\setminus\{\boldsymbol{0}\}}\frac{(\widetilde{p}_h,\nabla\cdot\boldsymbol{w})_{\mathsf{D}_h}}{\|\boldsymbol{w}\|_{\boldsymbol{H}^1(\mathsf{D}_h)}}. \tag{3.16}$$

We will work now on the numerator. Integrating by parts, using the projection $\boldsymbol{P}$ and equation (3.3b) with $\boldsymbol{v} = \boldsymbol{P}\boldsymbol{w}$, we have

$$\begin{aligned}(\widetilde{p}_h, \nabla\cdot\boldsymbol{w})_{\mathsf{D}_h} &= (\nu \mathrm{L}_h, \nabla\boldsymbol{P}\boldsymbol{w})_{\mathsf{T}_h} - (\boldsymbol{u}_h\otimes\boldsymbol{\beta}, \nabla\boldsymbol{P}\boldsymbol{w})_{\mathsf{T}_h} - \langle \nu\mathrm{L}_h\boldsymbol{n}, \boldsymbol{P}\boldsymbol{w}\rangle_{\partial\mathsf{T}_h}\\ &\quad +\langle(\widehat{\boldsymbol{u}}_h\otimes\boldsymbol{\beta})\boldsymbol{n}, \boldsymbol{P}\boldsymbol{w}\rangle_{\partial\mathsf{T}_h} + \langle \mathrm{S}(\boldsymbol{u}_h - \widehat{\boldsymbol{u}}_h), \boldsymbol{P}\boldsymbol{w}\rangle_{\partial\mathsf{T}_h} + \langle \widetilde{p}_h\boldsymbol{n}, \boldsymbol{w}\rangle_{\partial\mathsf{T}_h}.\end{aligned}$$

Integrating by parts again, using the projections $\boldsymbol{P}$ and P_M, and rearranging terms, we obtain

$$\begin{aligned}(\widetilde{p}_h, \nabla\cdot\boldsymbol{w})_{\mathsf{D}_h} &= (\nu \mathrm{L}_h, \nabla\boldsymbol{w})_{\mathsf{T}_h} - \langle \nu\mathrm{L}_h\boldsymbol{n} - \widetilde{p}_h\boldsymbol{n}, \mathsf{P}_M\boldsymbol{w}\rangle_{\partial\mathsf{T}_h} - (\boldsymbol{u}_h\otimes\boldsymbol{\beta}, \nabla\boldsymbol{P}\boldsymbol{w})_{\mathsf{T}_h}\\ &\quad +\langle(\widehat{\boldsymbol{u}}_h\otimes\boldsymbol{\beta})\boldsymbol{n}, \boldsymbol{P}\boldsymbol{w}\rangle_{\partial\mathsf{T}_h} + \langle \mathrm{S}(\boldsymbol{u}_h - \widehat{\boldsymbol{u}}_h), \boldsymbol{P}\boldsymbol{w}\rangle_{\partial\mathsf{T}_h}.\end{aligned}$$

Taking $\boldsymbol{\mu} = \mathsf{P}_M\boldsymbol{w}$ in (3.3e), and since $\boldsymbol{w} = \boldsymbol{0}$ on Γ_h,

$$\langle \nu\mathrm{L}_h\boldsymbol{n} - \widetilde{p}_h\boldsymbol{n} - (\widehat{\boldsymbol{u}}_h\otimes\boldsymbol{\beta})\boldsymbol{n} - \mathrm{S}(\boldsymbol{u}_h - \widehat{\boldsymbol{u}}_h), \mathsf{P}_M\boldsymbol{w}\rangle_{\partial\mathsf{T}_h} = 0,$$

which implies that

$$\langle \nu\mathrm{L}_h\boldsymbol{n} - \widetilde{p}_h\boldsymbol{n}, \mathsf{P}_M\boldsymbol{w}\rangle_{\partial\mathsf{T}_h} = \langle(\widehat{\boldsymbol{u}}_h\otimes\boldsymbol{\beta})\boldsymbol{n} + \mathrm{S}(\boldsymbol{u}_h - \widehat{\boldsymbol{u}}_h), \mathsf{P}_M\boldsymbol{w}\rangle_{\partial\mathsf{T}_h}.$$

Since $(\boldsymbol{\beta}\cdot\boldsymbol{n})$ is continuous on $\mathcal{E}_h^0$, $\widehat{\boldsymbol{u}}_h$ is single valued on $\mathcal{E}_h^0$ and $\boldsymbol{w} = \boldsymbol{0}$ on Γ_h, then $\langle(\widehat{\boldsymbol{u}}_h\otimes\boldsymbol{\beta})\boldsymbol{n}, \mathsf{P}_M\boldsymbol{w}\rangle_{\partial\mathsf{T}_h} = 0$. Hence, we can rewrite our numerator as

$$\begin{aligned}(\widetilde{p}_h, \nabla\cdot\boldsymbol{w})_{\mathsf{D}_h} &= (\nu \mathrm{L}_h, \nabla\boldsymbol{w})_{\mathsf{T}_h} - (\boldsymbol{u}_h\otimes\boldsymbol{\beta}, \nabla\boldsymbol{P}\boldsymbol{w})_{\mathsf{T}_h} + \langle(\widehat{\boldsymbol{u}}_h\otimes\boldsymbol{\beta})\boldsymbol{n}, \boldsymbol{P}\boldsymbol{w}\rangle_{\partial\mathsf{T}_h}\\ &\quad +\langle \mathrm{S}(\boldsymbol{u}_h - \widehat{\boldsymbol{u}}_h), \boldsymbol{P}\boldsymbol{w} - \mathsf{P}_M\boldsymbol{w}\rangle_{\partial\mathsf{T}_h}.\end{aligned}$$

Let us bound the last term. Observe first that, for any given vector $\boldsymbol{z}$, it holds that $\|\boldsymbol{z}\|_{\partial K} \leq c_\tau^{-1/2}\langle \mathrm{S}_{\boldsymbol{\beta}}\boldsymbol{z}, \boldsymbol{z}\rangle_{\partial K}^{1/2}$, $\forall K\in\mathsf{T}_h$. In fact, thanks to (3.4), we have

$$\langle \mathrm{S}_{\boldsymbol{\beta}}\boldsymbol{z}, \boldsymbol{z}\rangle_{\partial K} = \left\langle \Big(\tau\nu - \frac{1}{2}(\boldsymbol{\beta}\cdot\boldsymbol{n})\Big)\boldsymbol{z}, \boldsymbol{z}\right\rangle_{\partial K} \geq c_\tau\langle\boldsymbol{z},\boldsymbol{z}\rangle_{\partial K} = c_\tau\|\boldsymbol{z}\|_{\partial K}^2.$$

Using the definition of $\mathrm{S}_{\boldsymbol{\beta}}$, we can split the last term into

$$\begin{aligned}\langle \mathrm{S}(\boldsymbol{u}_h - \widehat{\boldsymbol{u}}_h), \boldsymbol{P}\boldsymbol{w} - \mathsf{P}_M\boldsymbol{w}\rangle_{\partial\mathsf{T}_h} &= \langle \mathrm{S}_{\boldsymbol{\beta}}(\boldsymbol{u}_h - \widehat{\boldsymbol{u}}_h), \boldsymbol{P}\boldsymbol{w} - \mathsf{P}_M\boldsymbol{w}\rangle_{\partial\mathsf{T}_h}\\ &\quad +\frac{1}{2}\langle(\boldsymbol{\beta}\cdot\boldsymbol{n})(\boldsymbol{u}_h - \widehat{\boldsymbol{u}}_h), \boldsymbol{P}\boldsymbol{w} - \mathsf{P}_M\boldsymbol{w}\rangle_{\partial\mathsf{T}_h}.\end{aligned}$$

Using the Cauchy-Schwarz inequality and the definition of $\mathrm{S}_{\boldsymbol{\beta}}$ again, we have that

$$\begin{aligned}\langle \mathrm{S}_{\boldsymbol{\beta}}(\boldsymbol{u}_h &- \widehat{\boldsymbol{u}}_h), \boldsymbol{P}\boldsymbol{w} - \mathsf{P}_M\boldsymbol{w}\rangle_{\partial\mathsf{T}_h}\\ &\leq \sum_{K\in\mathsf{T}_h}\langle \mathrm{S}_{\boldsymbol{\beta}}(\boldsymbol{u}_h - \widehat{\boldsymbol{u}}_h), \mathrm{S}_{\boldsymbol{\beta}}(\boldsymbol{u}_h - \widehat{\boldsymbol{u}}_h)\rangle_{\partial K}^{1/2}\langle \boldsymbol{P}\boldsymbol{w} - \mathsf{P}_M\boldsymbol{w}, \boldsymbol{P}\boldsymbol{w} - \mathsf{P}_M\boldsymbol{w}\rangle_{\partial K}^{1/2}\\ &\leq \sum_{K\in\mathsf{T}_h}\tau^{-1/2}\max_{\boldsymbol{x}\in\partial K}\left|\tau\nu - \frac{1}{2}(\boldsymbol{\beta}(\boldsymbol{x})\cdot\boldsymbol{n})\right|^{1/2}\langle \mathrm{S}_{\boldsymbol{\beta}}(\boldsymbol{u}_h - \widehat{\boldsymbol{u}}_h), \boldsymbol{u}_h - \widehat{\boldsymbol{u}}_h\rangle_{\partial K}^{1/2}\|\boldsymbol{P}\boldsymbol{w} - \mathsf{P}_M\boldsymbol{w}\|_{\partial K,\tau}\\ &\leq \tau^{-1/2}\nu^{1/2}\Big(\tau^{1/2}\nu^{1/2} + \|\boldsymbol{\beta}\|_{L^\infty(\Omega)}^{1/2}\Big)\nu^{-1/2}\langle \mathrm{S}_{\boldsymbol{\beta}}\boldsymbol{u}_h - \widehat{\boldsymbol{u}}_h), \boldsymbol{u}_h - \widehat{\boldsymbol{u}}_h\rangle_{\partial\mathsf{T}_h}^{1/2}\|\boldsymbol{P}\boldsymbol{w} - \mathsf{P}_M\boldsymbol{w}\|_{\partial\mathsf{T}_h,\tau}.\end{aligned}$$

Analogously,

$$\begin{aligned}\frac{1}{2}|\langle(\boldsymbol{\beta}\cdot\boldsymbol{n})(\boldsymbol{u}_h &- \widehat{\boldsymbol{u}}_h), \boldsymbol{P}\boldsymbol{w} - \mathbf{P}_M\boldsymbol{w}\rangle_{\partial\mathsf{T}_h}| \\ &\le \frac{1}{2}\tau^{-1/2}\sum_{K\in\mathsf{T}_h}\max_{\boldsymbol{x}\in\partial K}|\boldsymbol{\beta}(\boldsymbol{x})\cdot\boldsymbol{n}|\|\boldsymbol{u}_h-\widehat{\boldsymbol{u}}_h\|_{\partial K}\|\boldsymbol{P}\boldsymbol{w}-\mathbf{P}_M\boldsymbol{w}\|_{\partial K,\tau} \\ &\le \tau^{-1/2}c_\tau^{-1/2}\|\boldsymbol{\beta}\|_{L^\infty(\Omega)}\sum_{K\in\mathsf{T}_h}\langle \mathrm{S}_{\boldsymbol{\beta}}(\boldsymbol{u}_h-\widehat{\boldsymbol{u}}_h),\boldsymbol{u}_h-\widehat{\boldsymbol{u}}_h\rangle_{\partial K}^{1/2}\|\boldsymbol{P}\boldsymbol{w}-\mathbf{P}_M\boldsymbol{w}\|_{\partial K,\tau} \\ &\le \tau^{-1/2}c_\tau^{-1/2}\nu^{1/2}\|\boldsymbol{\beta}\|_{L^\infty(\Omega)}\nu^{-1/2}\langle \mathrm{S}_{\boldsymbol{\beta}}(\boldsymbol{u}_h-\widehat{\boldsymbol{u}}_h),\boldsymbol{u}_h-\widehat{\boldsymbol{u}}_h\rangle_{\partial\mathsf{T}_h}^{1/2}\|\boldsymbol{P}\boldsymbol{w}-\mathbf{P}_M\boldsymbol{w}\|_{\partial\mathsf{T}_h,\tau}.\end{aligned}$$

Hence, combining the two estimates above, we obtain that

$$\begin{aligned}\langle \mathrm{S}(\boldsymbol{u}_h-\widehat{\boldsymbol{u}}_h),\boldsymbol{P}\boldsymbol{w} &- \mathbf{P}_M\boldsymbol{w}\rangle_{\partial\mathsf{T}_h} \\ &\le C_{\tau,\nu,\boldsymbol{\beta}}\nu^{-1/2}\langle \mathrm{S}_{\boldsymbol{\beta}}(\boldsymbol{u}_h-\widehat{\boldsymbol{u}}_h),\boldsymbol{u}_h-\widehat{\boldsymbol{u}}_h\rangle_{\partial\mathsf{T}_h}^{1/2}\|\boldsymbol{P}\boldsymbol{w}-\mathbf{P}_M\boldsymbol{w}\|_{\partial\mathsf{T}_h,\tau}.\end{aligned}$$

On the other hand, we can rewrite the third term as

$$\begin{aligned}\langle(\widehat{\boldsymbol{u}}_h\otimes\boldsymbol{\beta})\boldsymbol{n},\boldsymbol{P}\boldsymbol{w}\rangle_{\partial\mathsf{T}_h} &= \langle(\boldsymbol{\beta}\cdot\boldsymbol{n})\widehat{\boldsymbol{u}}_h,\boldsymbol{P}\boldsymbol{w}\rangle_{\partial\mathsf{T}_h} \\ &= \langle\widehat{\boldsymbol{u}}_h,(\boldsymbol{\beta}\cdot\boldsymbol{n})\boldsymbol{P}\boldsymbol{w}\rangle_{\partial\mathsf{T}_h} \\ &= \langle\widehat{\boldsymbol{u}}_h,(\boldsymbol{P}\boldsymbol{w}\otimes\boldsymbol{\beta})\boldsymbol{n}\rangle_{\partial\mathsf{T}_h} \\ &= \langle\widehat{\boldsymbol{u}}_h,(\boldsymbol{P}\boldsymbol{w}\otimes\boldsymbol{\beta}_0)\boldsymbol{n}\rangle_{\partial\mathsf{T}_h}+\langle\widehat{\boldsymbol{u}}_h,(\boldsymbol{P}\boldsymbol{w}\otimes\boldsymbol{\delta}\boldsymbol{\beta})\boldsymbol{n}\rangle_{\partial\mathsf{T}_h}.\end{aligned}$$

Then, thanks to (3.3a) with $\mathrm{G}=\boldsymbol{P}\boldsymbol{w}\otimes\boldsymbol{\beta}_0$, we have

$$\langle\widehat{\boldsymbol{u}}_h,(\boldsymbol{P}\boldsymbol{w}\otimes\boldsymbol{\beta}_0)\boldsymbol{n}\rangle_{\partial\mathsf{T}_h}=(\mathrm{L}_h,\boldsymbol{P}\boldsymbol{w}\otimes\boldsymbol{\beta}_0)_{\mathsf{T}_h}+(\boldsymbol{u}_h,\nabla\cdot(\boldsymbol{P}\boldsymbol{w}\otimes\boldsymbol{\beta}_0))_{\mathsf{T}_h}.$$

Thus, since $\boldsymbol{\delta}\boldsymbol{\beta}=\boldsymbol{\beta}-\boldsymbol{\beta}_0$ and using (3.7),

$$\begin{aligned}(\widetilde{p}_h,\nabla\cdot\boldsymbol{w})_{\mathsf{D}_h} &= (\nu\mathrm{L}_h,\nabla\boldsymbol{w})_{\mathsf{T}_h}-(\boldsymbol{u}_h\otimes\boldsymbol{\delta}\boldsymbol{\beta},\nabla\boldsymbol{P}\boldsymbol{w})_{\mathsf{T}_h}+(\mathrm{L}_h,\boldsymbol{P}\boldsymbol{w}\otimes\boldsymbol{\beta}_0)_{\mathsf{T}_h} \\ &\quad+\langle\widehat{\boldsymbol{u}}_h,(\boldsymbol{P}\boldsymbol{w}\otimes\boldsymbol{\delta}\boldsymbol{\beta})\boldsymbol{n}\rangle_{\partial\mathsf{T}_h}+\langle\mathrm{S}(\boldsymbol{u}_h-\widehat{\boldsymbol{u}}_h),\boldsymbol{P}\boldsymbol{w}-\mathbf{P}_M\boldsymbol{w}\rangle_{\partial\mathsf{T}_h}\end{aligned}$$

Using the Cauchy-Schwarz and trace inequalities, Proposition 3.1 and (3.5), we have

$$\begin{aligned}|(\widetilde{p}_h,\nabla\cdot\boldsymbol{w})_{\mathsf{D}_h}| &\le \nu\|\mathrm{L}_h\|_{\mathsf{D}_h}\|\nabla\boldsymbol{w}\|_{\mathsf{D}_h}+h|\boldsymbol{\beta}|_{W^{1,\infty}(\Omega)}\|\boldsymbol{u}_h\|_{\mathsf{D}_h}\|\nabla\boldsymbol{P}\boldsymbol{w}\|_{\mathsf{T}_h} \\ &\quad+\|\boldsymbol{\beta}_0\|_{L^\infty}\|\mathrm{L}_h\|_{\mathsf{T}_h}\|\boldsymbol{P}\boldsymbol{w}\|_{\mathsf{T}_h}+|\boldsymbol{\beta}|_{W^{1,\infty}(\Omega)}\|\widehat{\boldsymbol{u}}_h\|_h\|\boldsymbol{P}\boldsymbol{w}\|_{\mathsf{T}_h} \\ &\quad+C_{\tau,\nu,\boldsymbol{\beta}}\nu^{-1/2}\langle\mathrm{S}_{\boldsymbol{\beta}}(\boldsymbol{u}_h-\widehat{\boldsymbol{u}}_h),\boldsymbol{u}_h-\widehat{\boldsymbol{u}}_h\rangle_{\partial\mathsf{T}_h}^{1/2}\|\boldsymbol{P}\boldsymbol{w}-\mathbf{P}_M\boldsymbol{w}\|_{\partial\mathsf{T}_h,\tau} \\ &\le \nu\|\mathrm{L}_h\|_{\mathsf{D}_h}\|\boldsymbol{w}\|_{\boldsymbol{H}^1(\mathsf{D}_h)}+h|\boldsymbol{\beta}|_{W^{1,\infty}(\Omega)}\|\boldsymbol{u}_h\|_{\mathsf{D}_h}\|\nabla\boldsymbol{P}\boldsymbol{w}\|_{\mathsf{T}_h} \\ &\quad+\|\boldsymbol{\beta}_0\|_{L^\infty}\|\mathrm{L}_h\|_{\mathsf{D}_h}\|\boldsymbol{P}\boldsymbol{w}\|_{\mathsf{T}_h}+|\boldsymbol{\beta}|_{W^{1,\infty}(\Omega)}\big(h\|\mathrm{L}_h\|_{\mathsf{D}_h}+C\|\boldsymbol{u}_h\|_{\mathsf{D}_h}\big)\|\boldsymbol{P}\boldsymbol{w}\|_{\mathsf{T}_h} \\ &\quad+C_{\tau,\nu,\boldsymbol{\beta}}\nu^{-1/2}\langle\mathrm{S}_{\boldsymbol{\beta}}(\boldsymbol{u}_h-\widehat{\boldsymbol{u}}_h),\boldsymbol{u}_h-\widehat{\boldsymbol{u}}_h\rangle_{\partial\mathsf{T}_h}^{1/2}\|\boldsymbol{P}\boldsymbol{w}-\mathbf{P}_M\boldsymbol{w}\|_{\partial\mathsf{T}_h,\tau} \\ &\le C\left\{\nu+\|\boldsymbol{\beta}_0\|_{L^\infty}\frac{\|\boldsymbol{P}\boldsymbol{w}\|_{\mathsf{T}_h}}{\|\boldsymbol{w}\|_{\boldsymbol{H}^1(\mathsf{D}_h)}}+h|\boldsymbol{\beta}|_{W^{1,\infty}(\Omega)}\frac{\|\boldsymbol{P}\boldsymbol{w}\|_{\mathsf{T}_h}}{\|\boldsymbol{w}\|_{\boldsymbol{H}^1(\mathsf{D}_h)}}\right\}\|\mathrm{L}_h\|_{\mathsf{D}_h}\|\boldsymbol{w}\|_{\boldsymbol{H}^1(\mathsf{D}_h)} \\ &\quad+C|\boldsymbol{\beta}|_{W^{1,\infty}(\Omega)}\left\{h\frac{\|\nabla\boldsymbol{P}\boldsymbol{w}\|_{\mathsf{T}_h}}{\|\boldsymbol{w}\|_{\boldsymbol{H}^1(\mathsf{D}_h)}}+\frac{\|\boldsymbol{P}\boldsymbol{w}\|_{\mathsf{T}_h}}{\|\boldsymbol{w}\|_{\boldsymbol{H}^1(\mathsf{D}_h)}}\right\}\|\boldsymbol{u}_h\|_{\mathsf{D}_h}\|\boldsymbol{w}\|_{\boldsymbol{H}^1(\mathsf{D}_h)} \\ &\quad+C_{\tau,\nu,\boldsymbol{\beta}}\nu^{-1/2}\langle\mathrm{S}_{\boldsymbol{\beta}}(\boldsymbol{u}_h-\widehat{\boldsymbol{u}}_h),\boldsymbol{u}_h-\widehat{\boldsymbol{u}}_h\rangle_{\partial\mathsf{T}_h}^{1/2}\frac{\|\boldsymbol{P}\boldsymbol{w}-\mathbf{P}_M\boldsymbol{w}\|_{\partial\mathsf{T}_h,\tau}}{\|\boldsymbol{w}\|_{\boldsymbol{H}^1(\mathsf{D}_h)}}\|\boldsymbol{w}\|_{\boldsymbol{H}^1(\mathsf{D}_h)} \\ &\le 3H_p^1\|\mathrm{L}_h\|_{\mathsf{D}_h}\|\boldsymbol{w}\|_{\boldsymbol{H}^1(\mathsf{D}_h)}+2H_p^2\|\boldsymbol{u}_h\|_{\mathsf{D}_h}\|\boldsymbol{w}\|_{\boldsymbol{H}^1(\mathsf{D}_h)} \\ &\quad+C_{\tau,\nu,\boldsymbol{\beta}}H_p^3\nu^{-1/2}\langle\mathrm{S}_{\boldsymbol{\beta}}(\boldsymbol{u}_h-\widehat{\boldsymbol{u}}_h),\boldsymbol{u}_h-\widehat{\boldsymbol{u}}_h\rangle_{\partial\mathsf{T}_h}^{1/2}\|\boldsymbol{w}\|_{\boldsymbol{H}^1(\mathsf{D}_h)},\end{aligned}$$

which implies

$$\begin{aligned}\|\widetilde{p}_h\|_{\mathsf{D}_h} &\leq 3\kappa H_p^1\|\mathrm{L}_h\|_{\mathsf{D}_h}+2\kappa H_p^2\|\boldsymbol{u}_h\|_{\mathsf{D}_h}\\ &\quad +C_{\tau,\nu,\boldsymbol{\beta}}H_p^3\kappa\nu^{-1/2}\langle \mathrm{S}_{\boldsymbol{\beta}}(\boldsymbol{u}_h-\widehat{\boldsymbol{u}}_h),\boldsymbol{u}_h-\widehat{\boldsymbol{u}}_h\rangle_{\partial\mathsf{T}_h}^{1/2}.\end{aligned}$$

Applying Lemma 3.2, we obtain

$$\begin{aligned}\|\widetilde{p}_h\|_{\mathsf{D}_h} &\leq 3\kappa H_p^1\left\{2\sqrt{6}\nu^{-1}\|\widetilde{p}_h\|_{\Gamma_h,l}+\nu^{-1}\|\boldsymbol{\beta}\|_{L^\infty(\Omega)}\|\boldsymbol{u}_h\|_{\mathsf{D}_h}\right\}+2\kappa H_p^2\|\boldsymbol{u}_h\|_{\mathsf{D}_h}\\ &\quad +C_{\tau,\nu,\boldsymbol{\beta}}H_p^3\kappa\left\{2\sqrt{6}\nu^{-1}\|\widetilde{p}_h\|_{\Gamma_h,l}+\nu^{-1}\|\boldsymbol{\beta}\|_{L^\infty(\Omega)}\|\boldsymbol{u}_h\|_{\mathsf{D}_h}\right\}\\ &= \kappa\left\{3H_p^1\nu^{-1}\|\boldsymbol{\beta}\|_{L^\infty(\Omega)}+2H_p^2+C_{\tau,\nu,\boldsymbol{\beta}}H_p^3\nu^{-1}\|\boldsymbol{\beta}\|_{L^\infty(\Omega)}\right\}\|\boldsymbol{u}_h\|_{\mathsf{D}_h}\\ &\quad +2\sqrt{6}\kappa\nu^{-1}\big(3H_p^1+C_{\tau,\nu,\boldsymbol{\beta}}H_p^3\big)\|\widetilde{p}_h\|_{\Gamma_h,l}.\end{aligned}\tag{3.17}$$

Finally, using that $l\leq H_e^\perp=r_eh_e^\perp$ and $h_e^\perp\leq\gamma h_e$ and inequality (1.7),

$$\begin{aligned}\|\widetilde{p}_h\|_{\Gamma_h,l} &= \left\{\sum_{e\in\mathcal{E}_h^\partial}\|\widetilde{p}_h\|_{e,l}^2\right\}^{1/2}\leq\left\{\sum_{e\in\mathcal{E}_h^\partial}r_eh_e^\perp\|\widetilde{p}_h\|_e^2\right\}^{1/2}\\ &\leq \left\{\sum_{e\in\mathcal{E}_h^\delta}r_eh_e^\perp(C_{tr}^e)^2h_e^{-1}\|\widetilde{p}_h\|_{K^e}^2\right\}^{1/2}\leq\left\{\sum_{e\in\mathcal{E}_h^\delta}(C_{tr}^e)^2r_e\gamma\|\widetilde{p}_h\|_{K^e}^2\right\}^{1/2}.\end{aligned}\tag{3.18}$$

Using assumption (A.4) in the inequality above, we have that

$$2\sqrt{6}\kappa\nu^{-1}\big(3H_p^1+C_{\tau,\nu,\boldsymbol{\beta}}H_p^3\big)\|\widetilde{p}_h\|_{\Gamma_h,l}\leq\frac{1}{2}\|\widetilde{p}_h\|_{\mathsf{D}_h}.$$

The result follows by moving this term to the right hand side and multiplying by 2. □

Before going to the last result of this section, we would like to write the results we have obtained so far in a more convenient way. To do that, note first that, according to Proposition 3.11 in [11], H_p^1 and H_p^2 are of order $\mathcal{O}(1)$. In addition, from Proposition 3.9 in [19] we have that $H_p^3\leq\max\{1,(\tau h)^{1/2}\}$. As a consequence, if h is small enough, then H_p^3 is also of order $\mathcal{O}(1)$.
On the other hand, note that (3.18) together with assumption (A.3) imply that

$$\|\widetilde{p}_h\|_{\Gamma_h,l}\lesssim\|\widetilde{p}_h\|_{\mathsf{D}_h}.\tag{3.19}$$

Hence, from Lemma 3.3 we deduce that

$$\|\widetilde{p}_h\|_{\mathsf{D}_h}\lesssim\|\boldsymbol{u}_h\|_{\mathsf{D}_h}.\tag{3.20}$$

From this and Lemma 3.2, we obtain that

$$\|\mathrm{L}_h\|_{\mathsf{D}_h}+\nu^{-1/2}\langle\mathrm{S}_{\boldsymbol{\beta}}(\boldsymbol{u}_h-\widehat{\boldsymbol{u}}_h),\boldsymbol{u}_h-\widehat{\boldsymbol{u}}_h\rangle_{\partial\mathsf{T}_h}^{1/2}+\|\widetilde{\boldsymbol{g}}_h\|_{\Gamma_h,l^{-1}}\lesssim\|\boldsymbol{u}_h\|_{\mathsf{D}_h}.\tag{3.21}$$

Now, in order to state the final lemma of this section, we need some previous tools.

Assumption B For any given $\boldsymbol{\theta} \in \boldsymbol{L}^2(\Omega)$, let $(\Phi, \boldsymbol{\phi}, \phi)$ be the solution of

$$\Phi - \nabla\boldsymbol{\phi} = 0 \quad \text{in } \Omega, \tag{3.22a}$$
$$-\nu\nabla\cdot\Phi - \nabla\cdot(\boldsymbol{\phi}\otimes\boldsymbol{\beta}) - \nabla\phi = \boldsymbol{\theta} \quad \text{in } \Omega, \tag{3.22b}$$
$$-\nabla\cdot\boldsymbol{\phi} = 0 \quad \text{in } \Omega, \tag{3.22c}$$
$$\boldsymbol{\phi} = \mathbf{0} \quad \text{on } \partial\Omega. \tag{3.22d}$$

In order to estimate the L^2-norm of the error in $\boldsymbol{u}$, we assume

$$\nu\|\Phi\|_{\mathrm{H}^1(\Omega)} + \nu\|\boldsymbol{\phi}\|_{\boldsymbol{H}^2(\Omega)} + \|\phi\|_{H^1(\Omega)} \le C\|\boldsymbol{\theta}\|_\Omega. \tag{3.23}$$

Additionally, for any element $K \in \mathsf{T}_h$, we introduce the projection $\Pi_h^*(\Phi, \boldsymbol{\phi}, \phi) = (\Pi^*\Phi, \boldsymbol{\Pi}^*\boldsymbol{\phi}, \Pi^*\phi) \in \mathrm{P}_k(K)\times\boldsymbol{P}_k(K)\times P_k(K)$ such that

$$\nu(\Pi^*\Phi, \mathrm{G})_K + (\boldsymbol{\Pi}^*\boldsymbol{\phi}\otimes\boldsymbol{\beta}, \mathrm{G})_K = \nu(\Phi, \mathrm{G})_K + (\boldsymbol{\phi}\otimes\boldsymbol{\beta}, \mathrm{G})_K, \tag{3.24a}$$
$$(\boldsymbol{\Pi}^*\boldsymbol{\phi}, \boldsymbol{v})_K = (\boldsymbol{\phi}, \boldsymbol{v})_K, \tag{3.24b}$$
$$(\Pi^*\phi, q)_K = (\phi, q)_K, \tag{3.24c}$$
$$\langle \nu\Pi^*\Phi\boldsymbol{n} + \Pi^*\phi\boldsymbol{n} + (\boldsymbol{\Pi}^*\boldsymbol{\phi}\otimes\boldsymbol{\beta})\boldsymbol{n} - S\boldsymbol{\Pi}^*\boldsymbol{\phi}, \boldsymbol{\mu}\rangle_e = \langle \nu\Phi\boldsymbol{n} + \phi\boldsymbol{n} + (\boldsymbol{\phi}\otimes\boldsymbol{\beta})\boldsymbol{n} - S\boldsymbol{\phi}, \boldsymbol{\mu}\rangle_e, \tag{3.24d}$$

for all $(\mathrm{G}, \boldsymbol{v}, q, \boldsymbol{\mu}) \in \mathrm{P}_{k-1}(K)\times\boldsymbol{\mathcal{P}}_{k-1}(K)\times\mathcal{P}_{k-1}(K)\times\boldsymbol{\mathcal{P}}_k(e)$ and for all the faces e of K. If τ satisfies (3.4) and $\mathrm{tr}(\Phi) = 0$, then it holds (Theorem 2.5 in [11]) that the above defined projection satisfies the following properties:

$$\|\Pi^*\phi - \phi\|_K \lesssim Ch_K^{k+1}|\phi|_{k+1,K}, \tag{3.25a}$$
$$\|\boldsymbol{\Pi}^*\boldsymbol{\phi} - \boldsymbol{\phi}\|_K \lesssim (\tau\nu + 1 + h_K)h_K^{k+1}|\boldsymbol{\phi}|_{k+1,K} + h_K^{k+1}|\nabla\cdot(\nu\Phi + \phi\mathrm{I})|_{k,K}, \tag{3.25b}$$
$$\begin{aligned}\nu\|\Pi^*\Phi - \Phi\|_K \lesssim\ & \nu h_K^{k+1}|\Phi|_{k+1,K} + (\tau\nu + h_K)h_K^{k+1}|\boldsymbol{\phi}|_{k+1,K}\\ & + (\tau\nu + (1+\nu) + h_K)\|\boldsymbol{\Pi}^*\boldsymbol{\phi} - \boldsymbol{\phi}\|_K + \|\Pi^*\phi - \phi\|_K.\end{aligned} \tag{3.25c}$$

Now we can prove the next lemma.

Lemma 3.4. *Suppose assumptions of Lemmas 3.2 and 3.3, and Assumption B hold. Then, for h small enough, $\boldsymbol{u}_h = \mathbf{0}$.*

Proof. Given $\boldsymbol{\theta} \in L^2(\Omega)$, thanks to (3.22b), integrating by parts and using the equations defining Π_h^*, we have

$$\begin{aligned}(\boldsymbol{u}_h, \boldsymbol{\theta})_{\mathsf{T}_h} &= -(\boldsymbol{u}_h, \nu\nabla\cdot\Phi)_{\mathsf{T}_h} - (\boldsymbol{u}_h, \nabla\cdot(\boldsymbol{\phi}\otimes\boldsymbol{\beta}))_{\mathsf{T}_h} - (\boldsymbol{u}_h, \nabla\phi)_{\mathsf{T}_h}\\ &= (\nabla\boldsymbol{u}_h, \nu\Pi^*\Phi)_{\mathsf{T}_h} + (\nabla\boldsymbol{u}_h, \boldsymbol{\Pi}^*\boldsymbol{\phi}\otimes\boldsymbol{\beta})_{\mathsf{T}_h} + (\nabla\cdot\boldsymbol{u}_h, \Pi^*\phi)_{\mathsf{T}_h}\\ &\quad -\langle \boldsymbol{u}_h, \nu\Pi^*\Phi\boldsymbol{n} + \Pi^*\phi\boldsymbol{n} + (\boldsymbol{\Pi}^*\boldsymbol{\phi}\otimes\boldsymbol{\beta})\boldsymbol{n}\rangle_{\partial\mathsf{T}_h}\\ &= -(\boldsymbol{u}_h, \nu\nabla\cdot\Pi^*\Phi)_{\mathsf{T}_h} - (\boldsymbol{u}_h, \nabla\cdot(\boldsymbol{\Pi}^*\boldsymbol{\phi}\otimes\boldsymbol{\beta}))_{\mathsf{T}_h} - (\boldsymbol{u}_h, \nabla\Pi^*\phi)_{\mathsf{T}_h}\\ &\quad -\langle \boldsymbol{u}_h, \nu(\Phi - \Pi^*\Phi)\boldsymbol{n} + (\phi - \Pi^*\phi)\boldsymbol{n} + \big((\boldsymbol{\phi} - \boldsymbol{\Pi}^*\boldsymbol{\phi})\otimes\boldsymbol{\beta}\big)\boldsymbol{n}\rangle_{\partial\mathsf{T}_h}.\end{aligned}$$

We can rewrite the first term of the right hand side by using (3.3a) with $\mathrm{G} = \nu\Pi^*\Phi$:

$$-(\boldsymbol{u}_h, \nu\nabla\cdot\Pi^*\Phi)_{\mathsf{T}_h} = (\mathrm{L}_h, \nu\Pi^*\Phi)_{\mathsf{T}_h} - \langle \widehat{\boldsymbol{u}}_h, \nu\Pi^*\Phi\boldsymbol{n}\rangle_{\partial\mathsf{T}_h}.$$

Hence, adding and subtracting the term $(\mathrm{L}_h, \nu\Phi)_{\mathsf{T}_h}$ and using (3.22a), we have

$$\begin{aligned}(\boldsymbol{u}_h, \boldsymbol{\theta})_{\mathsf{T}_h} &= (\mathrm{L}_h, \nu\Pi^*\Phi - \nu\Phi)_{\mathsf{T}_h} + (\mathrm{L}_h, \nu\Phi)_{\mathsf{T}_h} - \langle \widehat{\boldsymbol{u}}_h, \nu\Pi^*\Phi\boldsymbol{n}\rangle_{\partial\mathsf{T}_h} \\ &\quad -(\boldsymbol{u}_h, \nabla\cdot(\boldsymbol{\Pi}^*\boldsymbol{\phi}\otimes\boldsymbol{\beta}))_{\mathsf{T}_h} - (\boldsymbol{u}_h, \nabla\Pi^*\phi)_{\mathsf{T}_h} \\ &\quad -\langle \boldsymbol{u}_h, \nu(\Phi-\Pi^*\Phi)\boldsymbol{n} + (\phi-\Pi^*\phi)\boldsymbol{n} + \big((\boldsymbol{\phi}-\boldsymbol{\Pi}^*\boldsymbol{\phi})\otimes\boldsymbol{\beta}\big)\boldsymbol{n}\rangle_{\partial\mathsf{T}_h} \\ &= (\mathrm{L}_h, \nu\Pi^*\Phi - \nu\Phi)_{\mathsf{T}_h} + (\mathrm{L}_h, \nu\nabla\boldsymbol{\phi})_{\mathsf{T}_h} - \langle \widehat{\boldsymbol{u}}_h, \nu\Pi^*\Phi\boldsymbol{n}\rangle_{\partial\mathsf{T}_h} \\ &\quad -(\boldsymbol{u}_h, \nabla\cdot(\boldsymbol{\Pi}^*\boldsymbol{\phi}\otimes\boldsymbol{\beta}))_{\mathsf{T}_h} - (\boldsymbol{u}_h, \nabla\Pi^*\phi)_{\mathsf{T}_h} \\ &\quad -\langle \boldsymbol{u}_h, \nu(\Phi-\Pi^*\Phi)\boldsymbol{n} + (\phi-\Pi^*\phi)\boldsymbol{n} + \big((\boldsymbol{\phi}-\boldsymbol{\Pi}^*\boldsymbol{\phi})\otimes\boldsymbol{\beta}\big)\boldsymbol{n}\rangle_{\partial\mathsf{T}_h}.\end{aligned} \tag{3.26}$$

Using now the identities (3.7) and equation (3.3b) with $\boldsymbol{v} = \boldsymbol{\Pi}^*\boldsymbol{\phi}$, we can write the fourth term of the right hand side as

$$\begin{aligned}(\boldsymbol{u}_h, \nabla\cdot(\boldsymbol{\Pi}^*\boldsymbol{\phi}\otimes\boldsymbol{\beta}))_{\mathsf{T}_h} &= (\nabla\boldsymbol{\Pi}^*\boldsymbol{\phi}, \boldsymbol{u}_h\otimes\boldsymbol{\beta})_{\mathsf{T}_h} \\ &= (\nu\mathrm{L}_h, \nabla\boldsymbol{\Pi}^*\boldsymbol{\phi})_{\mathsf{T}_h} - (\widetilde{p}_h, \nabla\cdot\boldsymbol{\Pi}^*\boldsymbol{\phi})_{\mathsf{T}_h} \\ &\quad -\langle \nu\mathrm{L}_h\boldsymbol{n} - \widetilde{p}_h\boldsymbol{n} - (\widehat{\boldsymbol{u}}_h\otimes\boldsymbol{\beta})\boldsymbol{n} - \mathrm{S}(\boldsymbol{u}_h - \widehat{\boldsymbol{u}}_h), \boldsymbol{\Pi}^*\boldsymbol{\phi}\rangle_{\partial\mathsf{T}_h}.\end{aligned}$$

Replacing this into (3.26), rearranging terms and integrating by parts, we have

$$\begin{aligned}(\boldsymbol{u}_h, \boldsymbol{\theta})_{\mathsf{T}_h} &= (\mathrm{L}_h, \nu\Pi^*\Phi - \nu\Phi)_{\mathsf{T}_h} - (\nu\nabla\cdot\mathrm{L}_h, \boldsymbol{\phi}-\boldsymbol{\Pi}^*\boldsymbol{\phi})_{\mathsf{T}_h} + \langle \nu\mathrm{L}_h\boldsymbol{n}, \boldsymbol{\phi}-\boldsymbol{\Pi}^*\boldsymbol{\phi}\rangle_{\partial\mathsf{T}_h} \\ &\quad -\langle \widehat{\boldsymbol{u}}_h, \nu\Pi^*\Phi\boldsymbol{n}\rangle_{\partial\mathsf{T}_h} + (\widetilde{p}_h, \nabla\cdot\boldsymbol{\Pi}^*\boldsymbol{\phi})_{\mathsf{T}_h} \\ &\quad +\langle \nu\mathrm{L}_h\boldsymbol{n} - \widetilde{p}_h\boldsymbol{n} - (\widehat{\boldsymbol{u}}_h\otimes\boldsymbol{\beta})\boldsymbol{n} - \mathrm{S}(\boldsymbol{u}_h - \widehat{\boldsymbol{u}}_h), \boldsymbol{\Pi}^*\boldsymbol{\phi}\rangle_{\partial\mathsf{T}_h} - (\boldsymbol{u}_h, \nabla\Pi^*\phi)_{\mathsf{T}_h} \\ &\quad -\langle \boldsymbol{u}_h, \nu(\Phi-\Pi^*\Phi)\boldsymbol{n} + (\phi-\Pi^*\phi)\boldsymbol{n} + \big((\boldsymbol{\phi}-\boldsymbol{\Pi}^*\boldsymbol{\phi})\otimes\boldsymbol{\beta}\big)\boldsymbol{n}\rangle_{\partial\mathsf{T}_h}\end{aligned}$$

Since $\nabla\cdot\boldsymbol{\phi} = \mathbf{0}$, $(\widetilde{p}_h, \nabla\cdot\boldsymbol{\Pi}^*\boldsymbol{\phi})_{\mathsf{T}_h} = (\widetilde{p}_h, \nabla\cdot(\boldsymbol{\Pi}^*\boldsymbol{\phi}-\boldsymbol{\phi}))_{\mathsf{T}_h}$. Using integration by parts, we can write

$$\begin{aligned}(\boldsymbol{u}_h, \boldsymbol{\theta})_{\mathsf{T}_h} &= (\mathrm{L}_h, \nu\Pi^*\Phi - \nu\Phi)_{\mathsf{T}_h} - (\nu\nabla\cdot\mathrm{L}_h, \boldsymbol{\phi}-\boldsymbol{\Pi}^*\boldsymbol{\phi})_{\mathsf{T}_h} + \langle \nu\mathrm{L}_h\boldsymbol{n}, \boldsymbol{\phi}-\boldsymbol{\Pi}^*\boldsymbol{\phi}\rangle_{\partial\mathsf{T}_h} \\ &\quad -\langle \widehat{\boldsymbol{u}}_h, \nu\Pi^*\Phi\boldsymbol{n}\rangle_{\partial\mathsf{T}_h} - (\nabla\widetilde{p}_h, \boldsymbol{\Pi}^*\boldsymbol{\phi}-\boldsymbol{\phi})_{\mathsf{T}_h} + \langle \widetilde{p}_h\boldsymbol{n}, \boldsymbol{\Pi}^*\boldsymbol{\phi}-\boldsymbol{\phi}\rangle_{\partial\mathsf{T}_h} \\ &\quad +\langle \nu\mathrm{L}_h\boldsymbol{n} - \widetilde{p}_h\boldsymbol{n} - (\widehat{\boldsymbol{u}}_h\otimes\boldsymbol{\beta})\boldsymbol{n} - \mathrm{S}(\boldsymbol{u}_h - \widehat{\boldsymbol{u}}_h), \boldsymbol{\Pi}^*\boldsymbol{\phi}\rangle_{\partial\mathsf{T}_h} - (\boldsymbol{u}_h, \nabla\Pi^*\phi)_{\mathsf{T}_h} \\ &\quad -\langle \boldsymbol{u}_h, \nu(\Phi-\Pi^*\Phi)\boldsymbol{n} + (\phi-\Pi^*\phi)\boldsymbol{n} + \big((\boldsymbol{\phi}-\boldsymbol{\Pi}^*\boldsymbol{\phi})\otimes\boldsymbol{\beta}\big)\boldsymbol{n}\rangle_{\partial\mathsf{T}_h}.\end{aligned}$$

The fifth term of the right hand side vanishes thanks to (3.24c). From (3.3e) with $\boldsymbol{\mu} = \mathbf{P}_M\boldsymbol{\phi}$, we obtain

$$\begin{aligned}\langle \nu\mathrm{L}_h\boldsymbol{n} - \widetilde{p}_h\boldsymbol{n} &- (\widehat{\boldsymbol{u}}_h\otimes\boldsymbol{\beta})\boldsymbol{n} - \mathrm{S}(\boldsymbol{u}_h - \widehat{\boldsymbol{u}}_h), \mathbf{P}_M\boldsymbol{\phi}\rangle_{\partial\mathsf{T}_h} \\ &= \langle \nu\mathrm{L}_h\boldsymbol{n} - \widetilde{p}_h\boldsymbol{n} - (\widehat{\boldsymbol{u}}_h\otimes\boldsymbol{\beta})\boldsymbol{n} - \mathrm{S}(\boldsymbol{u}_h - \widehat{\boldsymbol{u}}_h), \mathbf{P}_M\boldsymbol{\phi}\rangle_{\Gamma_h},\end{aligned}$$

and then, adding and subtracting this term,

$$\begin{aligned}(\boldsymbol{u}_h, \boldsymbol{\theta})_{\mathsf{T}_h} &= (\mathrm{L}_h, \nu\Pi^*\Phi - \nu\Phi)_{\mathsf{T}_h} - (\nu\nabla\cdot\mathrm{L}_h, \boldsymbol{\phi}-\boldsymbol{\Pi}^*\boldsymbol{\phi})_{\mathsf{T}_h} + \langle \nu\mathrm{L}_h\boldsymbol{n}, \boldsymbol{\phi}-\boldsymbol{\Pi}^*\boldsymbol{\phi}\rangle_{\partial\mathsf{T}_h} \\ &\quad -\langle \widehat{\boldsymbol{u}}_h, \nu\Pi^*\Phi\boldsymbol{n}\rangle_{\partial\mathsf{T}_h} + \langle \widetilde{p}_h\boldsymbol{n}, \boldsymbol{\Pi}^*\boldsymbol{\phi}-\boldsymbol{\phi}\rangle_{\partial\mathsf{T}_h} - (\boldsymbol{u}_h, \nabla\Pi^*\phi)_{\mathsf{T}_h} \\ &\quad +\langle \nu\mathrm{L}_h\boldsymbol{n} - \widetilde{p}_h\boldsymbol{n} - (\widehat{\boldsymbol{u}}_h\otimes\boldsymbol{\beta})\boldsymbol{n} - \mathrm{S}(\boldsymbol{u}_h - \widehat{\boldsymbol{u}}_h), \boldsymbol{\Pi}^*\boldsymbol{\phi}-\mathbf{P}_M\boldsymbol{\phi}\rangle_{\partial\mathsf{T}_h} \\ &\quad +\langle \nu\mathrm{L}_h\boldsymbol{n} - \widetilde{p}_h\boldsymbol{n} - (\widehat{\boldsymbol{u}}_h\otimes\boldsymbol{\beta})\boldsymbol{n} - \mathrm{S}(\boldsymbol{u}_h - \widehat{\boldsymbol{u}}_h), \mathbf{P}_M\boldsymbol{\phi}\rangle_{\Gamma_h} \\ &\quad -\langle \boldsymbol{u}_h, \nu(\Phi-\Pi^*\Phi)\boldsymbol{n} + (\phi-\Pi^*\phi)\boldsymbol{n} + \big((\boldsymbol{\phi}-\boldsymbol{\Pi}^*\boldsymbol{\phi})\otimes\boldsymbol{\beta}\big)\boldsymbol{n}\rangle_{\partial\mathsf{T}_h}.\end{aligned}$$

Cancelling some terms and using the projection $\mathbf{P}_M$, we get

$$\begin{aligned}(\boldsymbol{u}_h,\boldsymbol{\theta})_{\mathsf{T}_h} &= (\mathrm{L}_h,\nu\Pi^*\Phi-\nu\Phi)_{\mathsf{T}_h}-(\nu\nabla\cdot\mathrm{L}_h,\boldsymbol{\phi}-\boldsymbol{\Pi}^*\boldsymbol{\phi})_{\mathsf{T}_h}-\langle\widehat{\boldsymbol{u}}_h,\nu\Pi^*\Phi\boldsymbol{n}\rangle_{\partial\mathsf{T}_h}\\ &\quad-\langle(\widehat{\boldsymbol{u}}_h\otimes\boldsymbol{\beta})\boldsymbol{n},\boldsymbol{\Pi}^*\boldsymbol{\phi}-\mathbf{P}_M\boldsymbol{\phi}\rangle_{\partial\mathsf{T}_h}-\langle\mathrm{S}(\boldsymbol{u}_h-\widehat{\boldsymbol{u}}_h),\boldsymbol{\Pi}^*\boldsymbol{\phi}-\mathbf{P}_M\boldsymbol{\phi}\rangle_{\partial\mathsf{T}_h}\\ &\quad+\langle\nu\mathrm{L}_h\boldsymbol{n}-\widetilde{p}_h\boldsymbol{n}-(\widehat{\boldsymbol{u}}_h\otimes\boldsymbol{\beta})\boldsymbol{n}-\mathrm{S}(\boldsymbol{u}_h-\widehat{\boldsymbol{u}}_h),\mathbf{P}_M\boldsymbol{\phi}\rangle_{\Gamma_h}-(\boldsymbol{u}_h,\nabla\Pi^*\phi)_{\mathsf{T}_h}\\ &\quad-\langle\boldsymbol{u}_h,\nu(\Phi-\Pi^*\Phi)\boldsymbol{n}+(\phi-\Pi^*\phi)\boldsymbol{n}+\big((\boldsymbol{\phi}-\boldsymbol{\Pi}^*\boldsymbol{\phi})\otimes\boldsymbol{\beta}\big)\boldsymbol{n}\rangle_{\partial\mathsf{T}_h}.\end{aligned}\tag{3.27}$$

Adding and subtracting the term $\langle\widehat{\boldsymbol{u}}_h,\nu\Phi\boldsymbol{n}+(\boldsymbol{\phi}\otimes\boldsymbol{\beta})\boldsymbol{n}\rangle_{\partial\mathsf{T}_h}$, and using (3.24b), we can rewrite (3.27) as

$$\begin{aligned}(\boldsymbol{u}_h,\boldsymbol{\theta})_{\mathsf{T}_h} &= (\mathrm{L}_h,\nu\Pi^*\Phi-\nu\Phi)_{\mathsf{T}_h}-\langle\boldsymbol{u}_h-\widehat{\boldsymbol{u}}_h,\nu(\Phi-\Pi^*\Phi)\boldsymbol{n}+\big((\boldsymbol{\phi}-\boldsymbol{\Pi}^*\boldsymbol{\phi})\otimes\boldsymbol{\beta}\big)\boldsymbol{n}\rangle_{\partial\mathsf{T}_h}\\ &\quad-\langle\widehat{\boldsymbol{u}}_h,\nu\Phi\boldsymbol{n}+(\boldsymbol{\beta}\cdot\boldsymbol{n})(\boldsymbol{\phi}-\mathbf{P}_M\boldsymbol{\phi})\rangle_{\partial\mathsf{T}_h}-\langle\mathrm{S}(\boldsymbol{u}_h-\widehat{\boldsymbol{u}}_h),\boldsymbol{\Pi}^*\boldsymbol{\phi}-\mathbf{P}_M\boldsymbol{\phi}\rangle_{\partial\mathsf{T}_h}\\ &\quad+\langle\nu\mathrm{L}_h\boldsymbol{n}-\widetilde{p}_h\boldsymbol{n}-(\widehat{\boldsymbol{u}}_h\otimes\boldsymbol{\beta})\boldsymbol{n}-\mathrm{S}(\boldsymbol{u}_h-\widehat{\boldsymbol{u}}_h),\mathbf{P}_M\boldsymbol{\phi}\rangle_{\Gamma_h}-(\boldsymbol{u}_h,\nabla\Pi^*\phi)_{\mathsf{T}_h}\\ &\quad-\langle\boldsymbol{u}_h,(\phi-\Pi^*\phi)\boldsymbol{n}\rangle_{\partial\mathsf{T}_h}.\end{aligned}$$

Using (3.3c) with $q=\Pi^*\phi$ and the projection $\mathbf{P}_M$, we obtain

$$\begin{aligned}(\boldsymbol{u}_h,\boldsymbol{\theta})_{\mathsf{T}_h} &= -\langle\boldsymbol{u}_h-\widehat{\boldsymbol{u}}_h,\nu(\Phi-\Pi^*\Phi)\boldsymbol{n}+\big((\boldsymbol{\phi}-\boldsymbol{\Pi}^*\boldsymbol{\phi})\otimes\boldsymbol{\beta}\big)\boldsymbol{n}-\mathrm{S}(\boldsymbol{\phi}-\boldsymbol{\Pi}^*\boldsymbol{\phi})\rangle_{\partial\mathsf{T}_h}\\ &\quad+(\mathrm{L}_h,\nu\Pi^*\Phi-\nu\Phi)_{\mathsf{T}_h}-\langle\widehat{\boldsymbol{u}}_h,\nu\Phi\boldsymbol{n}+(\boldsymbol{\beta}\cdot\boldsymbol{n})(\boldsymbol{\phi}-\mathbf{P}_M\boldsymbol{\phi})\rangle_{\partial\mathsf{T}_h}\\ &\quad+\langle\nu\mathrm{L}_h\boldsymbol{n}-\widetilde{p}_h\boldsymbol{n}-(\widehat{\boldsymbol{u}}_h\otimes\boldsymbol{\beta})\boldsymbol{n}-\mathrm{S}(\boldsymbol{u}_h-\widehat{\boldsymbol{u}}_h),\mathbf{P}_M\boldsymbol{\phi}\rangle_{\Gamma_h}-\langle\widehat{\boldsymbol{u}}_h,\Pi^*\phi\boldsymbol{n}\rangle_{\partial\mathsf{T}_h}\\ &\quad-\langle\boldsymbol{u}_h,(\phi-\Pi^*\phi)\boldsymbol{n}\rangle_{\partial\mathsf{T}_h}.\end{aligned}$$

Note that, since $\widehat{\boldsymbol{u}}_h$ is single valued on $\mathcal{E}_h^0$ and $\phi\boldsymbol{n}$ is continuous on $\mathcal{E}_h^0$, then

$$\langle\widehat{\boldsymbol{u}}_h,\phi\boldsymbol{n}\rangle_{\partial\mathsf{T}_h}=\langle\widehat{\boldsymbol{u}}_h,\phi\boldsymbol{n}\rangle_{\Gamma_h}.$$

Analogously, $\langle\widehat{\boldsymbol{u}}_h,\nu\Phi\boldsymbol{n}+(\boldsymbol{\beta}\cdot\boldsymbol{n})(\boldsymbol{\phi}-\mathbf{P}_M\boldsymbol{\phi})\rangle_{\partial\mathsf{T}_h}=\langle\widehat{\boldsymbol{u}}_h,\nu\Phi\boldsymbol{n}+(\boldsymbol{\beta}\cdot\boldsymbol{n})(\boldsymbol{\phi}-\mathbf{P}_M\boldsymbol{\phi})\rangle_{\Gamma_h}$. Thus, adding and subtracting $\langle\widehat{\boldsymbol{u}}_h,\phi\boldsymbol{n}\rangle_{\partial\mathsf{T}_h}$ we have

$$\begin{aligned}(\boldsymbol{u}_h,\boldsymbol{\theta})_{\mathsf{T}_h} &= -\langle\boldsymbol{u}_h-\widehat{\boldsymbol{u}}_h,\nu(\Phi-\Pi^*\Phi)\boldsymbol{n}+(\phi-\Pi^*\phi)\boldsymbol{n}+\big((\boldsymbol{\phi}-\boldsymbol{\Pi}^*\boldsymbol{\phi})\otimes\boldsymbol{\beta}\big)\boldsymbol{n}-\mathrm{S}(\boldsymbol{\phi}-\boldsymbol{\Pi}^*\boldsymbol{\phi})\rangle_{\partial\mathsf{T}_h}\\ &\quad+(\mathrm{L}_h,\nu\Pi^*\Phi-\nu\Phi)_{\mathsf{T}_h}-\langle\widehat{\boldsymbol{u}}_h,\nu\Phi\boldsymbol{n}+\phi\boldsymbol{n}+(\boldsymbol{\beta}\cdot\boldsymbol{n})(\boldsymbol{\phi}-\mathbf{P}_M\boldsymbol{\phi})\rangle_{\Gamma_h}\\ &\quad+\langle\nu\mathrm{L}_h\boldsymbol{n}-\widetilde{p}_h\boldsymbol{n}-(\widehat{\boldsymbol{u}}_h\otimes\boldsymbol{\beta})\boldsymbol{n}-\mathrm{S}(\boldsymbol{u}_h-\widehat{\boldsymbol{u}}_h),\mathbf{P}_M\boldsymbol{\phi}\rangle_{\Gamma_h}.\end{aligned}$$

The first term vanishes thanks to (3.24d) with $\boldsymbol{\mu}=\boldsymbol{u}_h-\widehat{\boldsymbol{u}}_h$. Furthermore, from the third and fourth terms:

$$\begin{aligned}-\langle\widehat{\boldsymbol{u}}_h,\nu\Phi\boldsymbol{n} &+ \phi\boldsymbol{n}+(\boldsymbol{\beta}\cdot\boldsymbol{n})(\boldsymbol{\phi}-\mathbf{P}_M\boldsymbol{\phi})\rangle_{\Gamma_h}+\langle\nu\mathrm{L}_h\boldsymbol{n}-\widetilde{p}_h\boldsymbol{n}-(\widehat{\boldsymbol{u}}_h\otimes\boldsymbol{\beta})\boldsymbol{n}-\mathrm{S}(\boldsymbol{u}_h-\widehat{\boldsymbol{u}}_h),\mathbf{P}_M\boldsymbol{\phi}\rangle_{\Gamma_h}\\ &= \langle\nu\mathrm{L}_h\boldsymbol{n}-\widetilde{p}_h\boldsymbol{n}-\mathrm{S}(\boldsymbol{u}_h-\widehat{\boldsymbol{u}}_h),\boldsymbol{\phi}\rangle_{\Gamma_h}-\langle\widehat{\boldsymbol{u}}_h,\nu\Phi\boldsymbol{n}\rangle_{\Gamma_h}\\ &\quad-\langle\widehat{\boldsymbol{u}}_h,\phi\boldsymbol{n}\rangle_{\Gamma_h}-\langle\widehat{\boldsymbol{u}}_h,(\boldsymbol{\beta}\cdot\boldsymbol{n})\boldsymbol{\phi}\rangle_{\Gamma_h}.\end{aligned}$$

Hence,

$$\begin{aligned}(\boldsymbol{u}_h,\boldsymbol{\theta})_{\mathsf{T}_h} &= (\mathrm{L}_h,\nu\Pi^*\Phi-\nu\Phi)_{\mathsf{T}_h}+\langle\nu\mathrm{L}_h\boldsymbol{n}-\widetilde{p}_h\boldsymbol{n}-\mathrm{S}(\boldsymbol{u}_h-\widehat{\boldsymbol{u}}_h),\boldsymbol{\phi}\rangle_{\Gamma_h}\\ &\quad-\langle\widehat{\boldsymbol{u}}_h,\nu\Phi\boldsymbol{n}+\phi\boldsymbol{n}+(\boldsymbol{\phi}\otimes\boldsymbol{\beta})\boldsymbol{n}\rangle_{\Gamma_h}.\end{aligned}\tag{3.28}$$

Let us denote the last two terms of the right hand side of (3.28) by $\mathrm{T}_{\boldsymbol{u}}$. Then, note that we can rewrite $\mathrm{T}_{\boldsymbol{u}}$ as follows:

$$\begin{aligned}\mathrm{T}_{\boldsymbol{u}} &= \langle \nu \mathrm{L}_h \boldsymbol{n} - \widetilde{p}_h \boldsymbol{n} - \mathrm{S}_{\boldsymbol{\beta}}(\boldsymbol{u}_h - \widehat{\boldsymbol{u}}_h), \boldsymbol{\phi}\rangle_{\Gamma_h} - \langle \widehat{\boldsymbol{u}}_h, \nu \Phi \boldsymbol{n}\rangle_{\Gamma_h} - \langle \widehat{\boldsymbol{u}}_h, \phi \boldsymbol{n}\rangle_{\Gamma_h} \\ &\quad -\frac{1}{2}\langle (\boldsymbol{\beta}\cdot\boldsymbol{n})\boldsymbol{u}_h, \boldsymbol{\phi}\rangle_{\Gamma_h} - \frac{1}{2}\langle (\boldsymbol{\beta}\cdot\boldsymbol{n})\widehat{\boldsymbol{u}}_h, \boldsymbol{\phi}\rangle_{\Gamma_h}.\end{aligned}$$

We use now that $\widehat{\boldsymbol{u}}_h = \mathbf{P}_M(\widetilde{\boldsymbol{g}}_h)$ on Γ_h and (3.10), to obtain

$$\begin{aligned}\mathrm{T}_{\boldsymbol{u}} &= -\nu\langle \widetilde{\boldsymbol{g}}_h l^{-1}, \boldsymbol{\phi}\rangle_{\Gamma_h} - \nu\langle \delta_{\mathrm{L}_h}, \boldsymbol{\phi}\rangle_{\Gamma_h} - \langle \widetilde{p}_h \boldsymbol{n}, \boldsymbol{\phi}\rangle_{\Gamma_h} \\ &\quad -\langle \mathrm{S}_{\boldsymbol{\beta}}(\boldsymbol{u}_h - \widehat{\boldsymbol{u}}_h), \boldsymbol{\phi}\rangle_{\Gamma_h} - \langle \widetilde{\boldsymbol{g}}_h, \nu \mathbf{P}_M(\Phi\boldsymbol{n})\rangle_{\Gamma_h} - \langle \widetilde{\boldsymbol{g}}_h, \mathbf{P}_M(\phi\boldsymbol{n})\rangle_{\Gamma_h} \\ &\quad -\frac{1}{2}\langle (\boldsymbol{\beta}\cdot\boldsymbol{n})\boldsymbol{u}_h, \boldsymbol{\phi}\rangle_{\Gamma_h} - \frac{1}{2}\langle (\boldsymbol{\beta}\cdot\boldsymbol{n})\widehat{\boldsymbol{u}}_h, \boldsymbol{\phi}\rangle_{\Gamma_h}.\end{aligned} \tag{3.29}$$

We can associate the first and fifth terms. In addition, adding and subtracting $l\nabla\boldsymbol{\phi}\boldsymbol{n}$, and using (3.22a), we have

$$\begin{aligned}-\nu\langle \widetilde{\boldsymbol{g}}_h l^{-1}, \boldsymbol{\phi} + l\mathbf{P}_M(\Phi\boldsymbol{n})\rangle_{\Gamma_h} &= -\nu\langle \widetilde{\boldsymbol{g}}_h l^{-1}, \boldsymbol{\phi} + l\nabla\boldsymbol{\phi}\boldsymbol{n} - l\nabla\boldsymbol{\phi}\boldsymbol{n} + l\mathbf{P}_M(\Phi\boldsymbol{n})\rangle_{\Gamma_h} \\ &= -\nu\langle \widetilde{\boldsymbol{g}}_h l^{-1}, \boldsymbol{\phi} + l\nabla\boldsymbol{\phi}\boldsymbol{n}\rangle_{\Gamma_h} + \nu\left\langle \widetilde{\boldsymbol{g}}_h, \nabla\boldsymbol{\phi}\boldsymbol{n} - \mathbf{P}_M\big(\nabla\boldsymbol{\phi}\boldsymbol{n}\big)\right\rangle_{\Gamma_h}.\end{aligned}$$

Hence, replacing in (3.29) we obtain

$$\begin{aligned}\mathrm{T}_{\boldsymbol{u}} &= -\nu\langle \widetilde{\boldsymbol{g}}_h l^{-1}, \boldsymbol{\phi} + l\nabla\boldsymbol{\phi}\boldsymbol{n}\rangle_{\Gamma_h} + \nu\left\langle \widetilde{\boldsymbol{g}}_h, \nabla\boldsymbol{\phi}\boldsymbol{n} - \mathbf{P}_M\big(\nabla\boldsymbol{\phi}\boldsymbol{n}\big)\right\rangle_{\Gamma_h} \\ &\quad -\nu\langle \delta_{\mathrm{L}_h}, \boldsymbol{\phi}\rangle_{\Gamma_h} - \langle \widetilde{p}_h\boldsymbol{n}, \boldsymbol{\phi}\rangle_{\Gamma_h} - \langle \mathrm{S}_{\boldsymbol{\beta}}(\boldsymbol{u}_h - \widehat{\boldsymbol{u}}_h), \boldsymbol{\phi}\rangle_{\Gamma_h} \\ &\quad -\langle \widetilde{\boldsymbol{g}}_h, \mathbf{P}_M(\phi\boldsymbol{n})\rangle_{\Gamma_h} - \frac{1}{2}\langle (\boldsymbol{\beta}\cdot\boldsymbol{n})\boldsymbol{u}_h, \boldsymbol{\phi}\rangle_{\Gamma_h} - \frac{1}{2}\langle (\boldsymbol{\beta}\cdot\boldsymbol{n})\widehat{\boldsymbol{u}}_h, \boldsymbol{\phi}\rangle_{\Gamma_h}\end{aligned}$$

Note, from (2.4d), that $\|\widehat{\boldsymbol{u}}_h\|_{\Gamma_h} \le \|\widetilde{\boldsymbol{g}}_h\|_{\Gamma_h}$. Using this, the Cauchy-Schwarz inequality, (3.12), (3.19), (3.13), (3.14) and Lemma 2.14, we obtain

$$\begin{aligned}|\mathrm{T}_{\boldsymbol{u}}| &\lesssim \nu\|\widetilde{\boldsymbol{g}}_h\|_{\Gamma_h,l^{-1}}\|l^2(\boldsymbol{\phi} + l\nabla\boldsymbol{\phi}\boldsymbol{n})\|_{\Gamma_h,l^{-3}} + \nu\|\widetilde{\boldsymbol{g}}_h\|_{\Gamma_h,l^{-1}}\|\nabla\boldsymbol{\phi}\boldsymbol{n} - \mathbf{P}_M\big(\nabla\boldsymbol{\phi}\boldsymbol{n}\big)\|_{\Gamma_h,l} \\ &\quad +\nu\|l^{1/2}\delta_{\mathrm{L}_h}\|_{\Gamma_h,l}\|\boldsymbol{\phi}\|_{\Gamma_h,l^{-2}} + \nu^{-1}\|l^{1/2}\widetilde{p}_h\boldsymbol{n}\|_{\Gamma_h,l}\nu\|\boldsymbol{\phi}\|_{\Gamma_h,l^{-2}} \\ &\quad +\nu^{-1}\|l^{1/2}\mathrm{S}_{\boldsymbol{\beta}}(\boldsymbol{u}_h - \widehat{\boldsymbol{u}}_h)\|_{\Gamma_h,l}\nu\|\boldsymbol{\phi}\|_{\Gamma_h,l^{-2}} + \|\widetilde{\boldsymbol{g}}_h\|_{\Gamma_h,l^{-1}}\|\mathbf{P}_M(\phi\boldsymbol{n})\|_{\Gamma_h,l} \\ &\quad +\nu^{-1}\|l^{1/2}(\boldsymbol{\beta}\cdot\boldsymbol{n})\boldsymbol{u}_h\|_{\Gamma_h,l}\nu\|\boldsymbol{\phi}\|_{\Gamma_h,l^{-2}} + \nu^{-1}\|l^{3/2}(\boldsymbol{\beta}\cdot\boldsymbol{n})\widehat{\boldsymbol{u}}_h\|_{\Gamma_h,l^{-1}}\nu\|\boldsymbol{\phi}\|_{\Gamma_h,l^{-2}} \\ &\lesssim R^{1/2}h^{1/2}\left\{R^{3/2}h^{3/2} + R^{1/2}h^{1/2} + 1 + \nu^{-1}Rh\|\boldsymbol{\beta}\|_{L^\infty(\Omega)}\right\}\|\widetilde{\boldsymbol{g}}_h\|_{\Gamma_h,l^{-1}}\|\boldsymbol{\theta}\|_\Omega \\ &\quad +R^{1/2}h^{1/2}\|\mathrm{L}_h\|_{\mathsf{D}_h}\|\boldsymbol{\theta}\|_\Omega + R^{1/2}h^{1/2}\nu^{-1/2}\langle \mathrm{S}_{\boldsymbol{\beta}}(\boldsymbol{u}_h - \widehat{\boldsymbol{u}}_h), \boldsymbol{u}_h - \widehat{\boldsymbol{u}}_h\rangle^{1/2}_{\partial\mathsf{T}_h}\|\boldsymbol{\theta}\|_\Omega \\ &\quad +R^{1/2}h^{1/2}\|\widetilde{p}_h\|_{\mathsf{D}_h}\|\boldsymbol{\theta}\|_\Omega + R^{1/2}h^{1/2}\nu^{-1}\|\boldsymbol{\beta}\|_{L^\infty(\Omega)}\|\boldsymbol{u}_h\|_{\mathsf{D}_h}\|\boldsymbol{\theta}\|_\Omega.\end{aligned}$$

Using now (3.20) and (3.21),

$$|\mathrm{T}_{\boldsymbol{u}}| \lesssim h^{1/2}H_{\boldsymbol{u}}(R,h)\|\boldsymbol{u}_h\|_{\mathsf{D}_h}\|\boldsymbol{\theta}\|_\Omega, \tag{3.30}$$

where $H_{\boldsymbol{u}}(R,h) := R^{1/2}\left\{R^{3/2}h^{3/2} + R^{1/2}h^{1/2} + (1+Rh)\nu^{-1}\|\boldsymbol{\beta}\|_{L^\infty(\Omega)} + 4\right\}$. On the other hand, using the Cauchy-Schwarz inequality and (3.21),

$$\begin{aligned}(\mathrm{L}_h, \nu\Pi^*\Phi - \nu\Phi)_{\mathsf{T}_h} &\le \|\mathrm{L}_h\|_{\mathsf{D}_h}\nu\|\Pi^*\Phi - \Phi\|_{\mathsf{T}_h} \\ &\lesssim \|\boldsymbol{u}_h\|_{\mathsf{D}_h}\nu\|\Pi^*\Phi - \Phi\|_{\mathsf{T}_h}.\end{aligned} \tag{3.31}$$

Hence, since $(\boldsymbol{u}_h,\boldsymbol{\theta})_{\mathsf{T}_h} = (\mathrm{L}_h,\nu\Pi^*\Phi-\nu\Phi)_{\mathsf{T}_h} + \mathrm{T}_{\boldsymbol{u}}$, using (3.31), (3.30), the approximation properties of Π_h^*, the regularity estimate (3.23), we can divide by $\|\boldsymbol{\theta}\|_\Omega$, $\boldsymbol{\theta}\neq\mathbf{0}$ and take the supremum over $\boldsymbol{\theta}$ to obtain

$$\|\boldsymbol{u}_h\|_{\mathsf{D}_h} \leq h^{1/2}C^*\|\boldsymbol{u}_h\|_{\mathsf{D}_h}, \tag{3.32}$$

where $C^*>0$ collects the contributions of the right hand sides of (3.30) and (3.31). Since C^* contains only positive powers of h, from (3.32) we deduce that for h small enough, $\boldsymbol{u}_h=\mathbf{0}$. □

3.3 Error estimates

The main result of this chapter is the following.

Theorem 3.5. *Suppose that Assumptions A hold and τ is of order one. If $(\mathrm{L},\boldsymbol{u},\widetilde{p})\in H^{k+1}(\Omega)\times\boldsymbol{H}^{k+1}(\Omega)\times H^{k+1}(\Omega)$, then there exists $h_0>0$ such that for all $h<h_0$ and $k\geq 1$, we have*

$$\|\mathrm{L}-\mathrm{L}_h\|_{\mathsf{D}_h} + \|\widetilde{\boldsymbol{g}}-\widetilde{\boldsymbol{g}}_h\|_{\Gamma_h,l^{-1}} + \nu^{-1}\|\widetilde{p}-\widetilde{p}_h\|_{\mathsf{D}_h} \lesssim C_{\mathrm{L},\boldsymbol{g},p}h^{k+1}.$$

Moreover, if Assumption B holds, then $\|\boldsymbol{u}-\boldsymbol{u}_h\|_{\mathsf{D}_h}\lesssim C_{\boldsymbol{u}}h^{k+1}$ and

$$\|\mathbf{P}_M\boldsymbol{u}-\widehat{\boldsymbol{u}}_h\|_{\partial\mathsf{T}_h,h} + \|\boldsymbol{u}-\boldsymbol{u}_h^*\|_{\mathsf{D}_h} \lesssim \begin{cases} C_{\widehat{\boldsymbol{u}},\boldsymbol{u}^*}h^{k+3/2}, & \text{if } R \text{ is of order } 1,\\ \widetilde{C}_{\widehat{\boldsymbol{u}},\boldsymbol{u}^*}h^{k+2}, & \text{if } R \text{ is of order } h.\end{cases}$$

Here, $C_{\mathrm{L},\boldsymbol{g},p}$, $C_{\boldsymbol{u}}$, $C_{\widehat{\boldsymbol{u}},\boldsymbol{u}^*}$ and $\widetilde{C}_{\widehat{\boldsymbol{u}},\boldsymbol{u}^*}$ depend on the exact solutions L, $\boldsymbol{u}$ and $\widetilde{p}$, the parameters τ and ν, the convective veclocity $\boldsymbol{\beta}$, and on positive powers of h, and $\boldsymbol{u}_h^*$ is the postprocessed velocity defined by (2.14) in chapter 2.

The first two estimates in the Theorem above imply that the L^2-norm of the errors in L, $\boldsymbol{u}$ and $\widetilde{p}$ are of order h^{k+1} if the solution is smooth enough and if τ is chosen of order one, for instance. The same conclusion was obtained for the case of a polyhedral domain [11]. In addition, the third estimate shows that the error in the numerical trace $\widehat{u}_h$ and the postprocessed velocity $\boldsymbol{u}_h^*$ is of order $h^{k+3/2}$, which is half a power less than the error obtained in the case of a polyhedral domain [11]. However, our numerical experiments show an experimental order of h^{k+2} for these two variables, which suggests that our analysis might not be sharp. The same behavior has been observed for the Poisson's equation [21] and Stokes problem in curved domains (chapter 2).

3.4 Proofs

In this section we will prove the error estimates stated in Theorem 3.5 by following the standard procedure for analyzing HDG schemes, this is, the projection–based approach. A projection operator is defined and then, in the first part of the section, an energy argument is used to bound the projection of the errors of all the variables except $\boldsymbol{u}$. In the second part of the section, a duality argument is employed to obtain an estimate of the L^2-norm of the projection of the error in $\boldsymbol{u}$.

3.4.1 An energy argument

The first thing we need to introduce is the projection defined in [11] which will be used in our analysis. If $(\mathrm{L}, \boldsymbol{u}, \widetilde{p}) \in \mathrm{H}^1(\mathsf{T}_h) \times \boldsymbol{H}^1(\mathsf{T}_h) \times H^1(\mathsf{T}_h)$, we take its projection $\mathit{\Pi}_h(\mathrm{L}, \boldsymbol{u}, \widetilde{p}) := (\Pi\mathrm{L}, \boldsymbol{\mathit{\Pi}}\boldsymbol{u}, \mathit{\Pi}\widetilde{p})$ as the element of $\mathrm{G}_h \times \boldsymbol{V}_h \times P_h$ defined as follows. On an arbitrary element K of the triangulation T_h, the values of the projected function on the simplex K are determined by requiring that

$$(\nu\Pi\mathrm{L}, \mathrm{G})_K - (\boldsymbol{\mathit{\Pi}}\boldsymbol{u} \otimes \boldsymbol{\beta}, \mathrm{G})_K = (\nu\mathrm{L}, \mathrm{G})_K - (\boldsymbol{u} \otimes \boldsymbol{\beta}, \mathrm{G})_K, \tag{3.33a}$$

$$(\boldsymbol{\mathit{\Pi}}\boldsymbol{u}, \boldsymbol{v})_K = (\boldsymbol{u}, \boldsymbol{v})_K, \tag{3.33b}$$

$$(\mathit{\Pi}\widetilde{p}, q)_K = (\widetilde{p}, q)_K, \tag{3.33c}$$

$$\langle \nu\Pi\mathrm{L}\boldsymbol{n} - \mathit{\Pi}\widetilde{p}\boldsymbol{n} - (\mathsf{P}_M\boldsymbol{u} \otimes \boldsymbol{\beta})\boldsymbol{n} - \boldsymbol{\mathit{\Pi}}\boldsymbol{u}, \boldsymbol{\mu}\rangle_e = \langle \nu\mathrm{L}\boldsymbol{n} - \widetilde{p}\boldsymbol{n} - (\boldsymbol{u} \otimes \boldsymbol{\beta})\boldsymbol{n} - S\boldsymbol{u}, \boldsymbol{\mu}\rangle_e, \tag{3.33d}$$

for all $(\mathrm{G}, \boldsymbol{v}, q, \boldsymbol{\mu}) \in \mathrm{P}_{k-1}(K) \times \boldsymbol{\mathcal{P}}_{k-1}(K) \times \mathcal{P}_{k-1}(K) \times \boldsymbol{\mathcal{P}}_k(e)$ and for all faces e of the simplex K. Thus, we define the projection of the errors $\mathrm{E}^{\mathrm{L}} := \Pi\mathrm{L} - \mathrm{L}_h$, $\boldsymbol{\varepsilon}^{\boldsymbol{u}} := \boldsymbol{\mathit{\Pi}}\boldsymbol{u} - \boldsymbol{u}_h$, $\varepsilon^p := \mathit{\Pi}\widetilde{p} - \widetilde{p}_h$, $\boldsymbol{\varepsilon}^{\widehat{\boldsymbol{u}}} := \mathsf{P}_M\boldsymbol{u} - \widehat{\boldsymbol{u}}_h$; and the interpolation errors $\mathrm{I}^{\mathrm{L}} := \mathrm{L} - \Pi\mathrm{L}$, $\boldsymbol{I}^{\boldsymbol{u}} := \boldsymbol{u} - \boldsymbol{\mathit{\Pi}}\boldsymbol{u}$, $\boldsymbol{I}^{\boldsymbol{u}}_M := \boldsymbol{u} - \mathsf{P}_M\boldsymbol{u}$, $I^p := \widetilde{p} - \mathit{\Pi}\widetilde{p}$. If τ satisfies (3.4), $(\mathrm{L}, \boldsymbol{u}, \widetilde{p}) \in \mathrm{H}^{k+1}(K) \times \boldsymbol{H}^{k+1}(K) \times H^{k+1}(K)$ on each element $K \in \mathsf{T}_h$ and $\mathrm{tr}(\mathrm{L}) = 0$, it is known (Theorem 2.3 in [11]) that the above defined projection satisfies the following properties:

$$\|I^p\|_K \lesssim h_K^{k+1}|\widetilde{p}|_{H^{k+1}(K)}, \tag{3.34a}$$

$$\|\boldsymbol{I}^{\boldsymbol{u}}\|_K \lesssim (\tau\nu + h_K)h_K^{k+1}|\boldsymbol{u}|_{\boldsymbol{H}^{k+1}(K)} + h_K^{k+1}|\nabla \cdot (\nu\mathrm{L} - \widetilde{p}\mathrm{I})|_{\mathrm{H}^k(K)}, \tag{3.34b}$$

$$\begin{aligned}\nu\|\mathrm{I}^{\mathrm{L}}\|_K \lesssim\ & \nu h_K^{k+1}|\mathrm{L}|_{\mathrm{H}^{k+1}(K)} + (\tau\nu + h_K)h_K^{k+1}|\boldsymbol{u}|_{\boldsymbol{H}^{k+1}(K)} + \|I^p\|_K \\ & + \big(\tau\nu + (1+\nu)h_K\big)\|\boldsymbol{I}^{\boldsymbol{u}}\|_K.\end{aligned} \tag{3.34c}$$

Furthermore, Lemma 1.59 in [31] establishes that

$$\|\boldsymbol{I}^{\boldsymbol{u}}_M\|_{L^2(\Gamma_h)} \lesssim h^{k+1/2}|\boldsymbol{u}|_{\boldsymbol{H}^{k+1}(\Omega)}. \tag{3.34d}$$

Moreover, by a standard scaling argument and the fact that $h_e^{\perp} \leq h_K$, we obtain

$$\|\mathrm{I}^{\mathrm{L}}\boldsymbol{n}\|_{e,h_e^{\perp}} \lesssim \|\mathrm{I}^{\mathrm{L}}\|_K, \quad \|\boldsymbol{I}^{\boldsymbol{u}}\|_{e,h_e^{\perp}} \lesssim \|\boldsymbol{I}^{\boldsymbol{u}}\|_K, \quad \text{and} \quad \|I^p\|_{e,h_e^{\perp}} \lesssim \|I^p\|_K. \tag{3.35}$$

Let $\partial_{\boldsymbol{n}}(\mathrm{I}^{\mathrm{L}}\boldsymbol{n})$ be the directional derivative of each component of $\mathrm{I}^{\mathrm{L}}\boldsymbol{n}$. We define the following quantity that will appear in the right hand side of next estimates:

$$\Theta_{\mathrm{I}^{\mathrm{L}}} := \Big\{8R^2\|\partial_n(\mathrm{I}^{\mathrm{L}}\boldsymbol{n})\|^2_{\mathsf{D}_h^c,(h^{\perp})^2} + 24R\|\mathrm{I}^{\mathrm{L}}\boldsymbol{n}\|^2_{\Gamma_h,h^{\perp}} + 4\|\mathrm{I}^{\mathrm{L}}\|^2_{\mathsf{D}_h}\Big\}^{1/2}. \tag{3.36}$$

If $(\mathrm{L}, \boldsymbol{u}, \widetilde{p}) \in \mathrm{H}^{k+1}(\Omega) \times \boldsymbol{H}^{k+1}(\Omega) \times H^{k+1}(\Omega)$, by Lemma 3.8 in [21] and the approximation properties (3.34) of $\mathit{\Pi}_h$, we have

$$\Theta_{\mathrm{I}^{\mathrm{L}}} \lesssim C_1^{\mathrm{reg}} h^{k+1}, \tag{3.37}$$

where

$$\begin{aligned}C_1^{\mathrm{reg}} =\ & |\mathrm{L}|_{\mathrm{H}^{k+1}(\Omega)} + \nu^{-1}|\widetilde{p}|_{H^{k+1}(\Omega)} + \big(\tau + (\nu^{-1}+1)h\big)|\nu\mathrm{L} - \widetilde{p}\mathrm{I}|_{\mathrm{H}^{k+1}(\Omega)} \\ & + \big(\tau\nu + (1+\nu)h + 1\big)(\tau + \nu^{-1}h)|\boldsymbol{u}|_{\boldsymbol{H}^{k+1}(\Omega)}.\end{aligned}$$

Step 1: The projection of the errors

The following lemma establishes the equations satisfied by the projection of the errors.

Lemma 3.6.

$$
\begin{aligned}
(\mathrm{E}^{\mathrm{L}},\mathrm{G})_{\mathsf{T}_h}+(\boldsymbol{\varepsilon}^{\boldsymbol{u}},\nabla\cdot\mathrm{G})_{\mathsf{T}_h}-\langle\boldsymbol{\varepsilon}^{\widehat{\boldsymbol{u}}},\mathrm{G}\boldsymbol{n}\rangle_{\partial\mathsf{T}_h} &= -(\mathrm{I}^{\mathrm{L}},\mathrm{G})_{\mathsf{T}_h}, && (3.38a)\\
-(\nu\nabla\cdot\mathrm{E}^{\mathrm{L}},\boldsymbol{v})_{\mathsf{T}_h}+(\nabla\cdot(\boldsymbol{\varepsilon}^{\boldsymbol{u}}\otimes\boldsymbol{\beta}),\boldsymbol{v})_{\mathsf{T}_h}+(\nabla\varepsilon^{p},\boldsymbol{v})_{\mathsf{T}_h} & && (3.38b)\\
-\Big\langle\big((\boldsymbol{\varepsilon}^{\boldsymbol{u}}-\boldsymbol{\varepsilon}^{\widehat{\boldsymbol{u}}})\otimes\boldsymbol{\beta}\big)\boldsymbol{n}-\mathrm{S}(\boldsymbol{\varepsilon}^{\boldsymbol{u}}-\boldsymbol{\varepsilon}^{\widehat{\boldsymbol{u}}}),\boldsymbol{v}\Big\rangle_{\partial\mathsf{T}_h} &= 0, &&\\
-(\boldsymbol{\varepsilon}^{\boldsymbol{u}},\nabla q)_{\mathsf{T}_h}+\langle\boldsymbol{\varepsilon}^{\widehat{\boldsymbol{u}}},q\boldsymbol{n}\rangle_{\partial\mathsf{T}_h} &= 0, && (3.38c)\\
\langle\boldsymbol{\varepsilon}^{\widehat{\boldsymbol{u}}},\boldsymbol{\mu}\rangle_{\Gamma_h} &= \langle\tilde{\boldsymbol{g}}-\tilde{\boldsymbol{g}}_h,\boldsymbol{\mu}\rangle_{\Gamma_h}, && (3.38d)\\
\langle\nu\mathrm{E}^{\mathrm{L}}\boldsymbol{n}-\varepsilon^{p}\boldsymbol{n}-(\boldsymbol{\varepsilon}^{\widehat{\boldsymbol{u}}}\otimes\boldsymbol{\beta})\boldsymbol{n}-\mathrm{S}(\boldsymbol{\varepsilon}^{\boldsymbol{u}}-\boldsymbol{\varepsilon}^{\widehat{\boldsymbol{u}}}),\boldsymbol{\mu}\rangle_{\partial\mathsf{T}_h\setminus\Gamma_h} &= 0, && (3.38e)\\
(\varepsilon^{p},1)_{\mathsf{D}_h} &= 0, && (3.38f)
\end{aligned}
$$

for all $(\mathrm{G},\boldsymbol{v},q,\boldsymbol{\mu})\in\mathrm{G}_h\times\boldsymbol{V}_h\times P_h\times\boldsymbol{M}_h$.

Proof. Observe that if we insert (3.3g) in (3.3b) and (3.3e), we obtain

$$
\begin{aligned}
(\mathrm{L}_h,\mathrm{G})_{\mathsf{T}_h}+(\boldsymbol{u}_h,\nabla\cdot\mathrm{G})_{\mathsf{T}_h}-\langle\widehat{\boldsymbol{u}}_h,\mathrm{G}\boldsymbol{n}\rangle_{\partial\mathsf{T}_h} &= 0,\\
(\nu\mathrm{L}_h,\nabla\boldsymbol{v})_{\mathsf{T}_h}-(\boldsymbol{u}_h\otimes\boldsymbol{\beta},\nabla\boldsymbol{v})_{\mathsf{T}_h}-(\widetilde{p}_h,\nabla\cdot\boldsymbol{v})_{\mathsf{T}_h} &&\\
-\langle\nu\mathrm{L}_h\boldsymbol{n}-\widetilde{p}_h\boldsymbol{n}-(\widehat{\boldsymbol{u}}_h\otimes\boldsymbol{\beta})\boldsymbol{n}-\mathrm{S}(\boldsymbol{u}_h-\widehat{\boldsymbol{u}}_h),\boldsymbol{v}\rangle_{\partial\mathsf{T}_h} &= (\boldsymbol{f},\boldsymbol{v})_{\mathsf{T}_h},\\
-(\boldsymbol{u}_h,\nabla q)_{\mathsf{T}_h}+\langle\widehat{\boldsymbol{u}}_h\cdot\boldsymbol{n},q\rangle_{\partial\mathsf{T}_h} &= 0,\\
\langle\widehat{\boldsymbol{u}}_h,\boldsymbol{\mu}\rangle_{\Gamma_h} &= \langle\tilde{\boldsymbol{g}}_h,\boldsymbol{\mu}\rangle_{\Gamma_h},\\
\langle\nu\mathrm{L}_h\boldsymbol{n}-\widetilde{p}_h\boldsymbol{n}-(\widehat{\boldsymbol{u}}_h\otimes\boldsymbol{\beta})\boldsymbol{n}-\mathrm{S}(\boldsymbol{u}_h-\widehat{\boldsymbol{u}}_h),\boldsymbol{\mu}\rangle_{\partial\mathsf{T}_h\setminus\Gamma_h} &= 0,\\
(\widetilde{p}_h,1)_{\mathsf{D}_h} &= 0,
\end{aligned}
$$

for all $(\mathrm{G},\boldsymbol{v},q,\boldsymbol{\mu})\in\mathrm{G}_h\times\boldsymbol{V}_h\times P_h\times\boldsymbol{M}_h$. On the other hand, using the projection (3.33a)-(3.33d), the exact solution satisfies

$$
\begin{aligned}
(\mathrm{L},\mathrm{G})_{\mathsf{T}_h}+(\boldsymbol{\Pi}\boldsymbol{u},\nabla\cdot\mathrm{G})_{\mathsf{T}_h}-\langle\mathbf{P}_M\boldsymbol{u},\mathrm{G}\boldsymbol{n}\rangle_{\partial\mathsf{T}_h} &= 0,\\
(\nu\Pi\mathrm{L},\nabla\boldsymbol{v})_{\mathsf{T}_h}-(\boldsymbol{\Pi}\boldsymbol{u}\otimes\boldsymbol{\beta},\nabla\boldsymbol{v})_{\mathsf{T}_h}-(\Pi\widetilde{p},\nabla\cdot\boldsymbol{v})_{\mathsf{T}_h} &&\\
-\langle\nu\Pi\mathrm{L}\boldsymbol{n}-\Pi\widetilde{p}\boldsymbol{n}-(\mathbf{P}_M\boldsymbol{u}\otimes\boldsymbol{\beta})\boldsymbol{n}-\mathrm{S}(\boldsymbol{\Pi}\boldsymbol{u}-\mathbf{P}_M\boldsymbol{u}),\boldsymbol{v}\rangle_{\partial\mathsf{T}_h} &= (\boldsymbol{f},\boldsymbol{v})_{\mathsf{T}_h},\\
-(\boldsymbol{\Pi}\boldsymbol{u},\nabla q)_{\mathsf{T}_h}+\langle\mathbf{P}_M\boldsymbol{u}\cdot\boldsymbol{n},q\rangle_{\partial\mathsf{T}} &= 0,\\
\langle\mathbf{P}_M\boldsymbol{u},\boldsymbol{\mu}\rangle_{\Gamma_h} &= \langle\tilde{\boldsymbol{g}},\boldsymbol{\mu}\rangle_{\Gamma_h},\\
\langle\nu\Pi\mathrm{L}\boldsymbol{n}-\Pi\widetilde{p}\boldsymbol{n}-(\mathbf{P}_M\boldsymbol{u}\otimes\boldsymbol{\beta})\boldsymbol{n}-\mathrm{S}(\boldsymbol{\Pi}\boldsymbol{u}-\mathbf{P}_M\boldsymbol{u}),\boldsymbol{\mu}\rangle_{\partial\mathsf{T}_h\setminus\Gamma_h} &= 0,\\
(\widetilde{p},1)_{\mathsf{D}_h} &= 0,
\end{aligned}
$$

for all $(\mathrm{G}, \boldsymbol{v}, q, \boldsymbol{\mu}) \in \mathrm{G}_h \times \boldsymbol{V}_h \times P_h \times \boldsymbol{M}_h$. Subtracting these groups of equations we have

$$\begin{aligned}
(\mathrm{L} - \mathrm{L}_h, \mathrm{G})_{\mathsf{T}_h} + (\boldsymbol{\varepsilon}^{\boldsymbol{u}}, \nabla \cdot \mathrm{G})_{\mathsf{T}_h} - \langle \boldsymbol{\varepsilon}^{\widehat{\boldsymbol{u}}}, \mathrm{G}\boldsymbol{n} \rangle_{\partial \mathsf{T}_h} &= 0, \\
(\nu \mathrm{E}^{\mathrm{L}}, \nabla \boldsymbol{v})_{\mathsf{T}_h} - (\boldsymbol{\varepsilon}^{\boldsymbol{u}} \otimes \boldsymbol{\beta}, \nabla \boldsymbol{v})_{\mathsf{T}_h} - (\varepsilon^p, \nabla \cdot \boldsymbol{v})_{\mathsf{T}_h} & \\
-\langle \nu \mathrm{E}^{\mathrm{L}} \boldsymbol{n} - \varepsilon^p \boldsymbol{n} - (\boldsymbol{\varepsilon}^{\widehat{\boldsymbol{u}}} \otimes \boldsymbol{\beta})\boldsymbol{n} - \mathrm{S}(\boldsymbol{\varepsilon}^{\boldsymbol{u}} - \boldsymbol{\varepsilon}^{\widehat{\boldsymbol{u}}}), \boldsymbol{v} \rangle_{\partial \mathsf{T}_h} &= (\boldsymbol{f}, \boldsymbol{v})_{\mathsf{T}_h}, \\
-(\boldsymbol{\varepsilon}^{\boldsymbol{u}}, \nabla q)_{\mathsf{T}_h} + \langle \boldsymbol{\varepsilon}^{\widehat{\boldsymbol{u}}} \cdot \boldsymbol{n}, q \rangle_{\partial \mathsf{T}} &= 0, \\
\langle \boldsymbol{\varepsilon}^{\widehat{\boldsymbol{u}}}, \boldsymbol{\mu} \rangle_{\Gamma_h} &= \langle \tilde{\boldsymbol{g}} - \tilde{\boldsymbol{g}}_h, \boldsymbol{\mu} \rangle_{\Gamma_h}, \\
\langle \nu \mathrm{E}^{\mathrm{L}} \boldsymbol{n} - \varepsilon^p \boldsymbol{n} - (\boldsymbol{\varepsilon}^{\widehat{\boldsymbol{u}}} \otimes \boldsymbol{\beta})\boldsymbol{n} - \mathrm{S}(\boldsymbol{\varepsilon}^{\boldsymbol{u}} - \boldsymbol{\varepsilon}^{\widehat{\boldsymbol{u}}}), \boldsymbol{\mu} \rangle_{\partial \mathsf{T}_h \setminus \Gamma_h} &= 0, \\
(\varepsilon^p, 1)_{\mathsf{D}_h} &= 0,
\end{aligned}$$

for all $(\mathrm{G}, \boldsymbol{v}, q, \boldsymbol{\mu}) \in \mathrm{G}_h \times \boldsymbol{V}_h \times P_h \times \boldsymbol{M}_h$. Integrating by parts the first three terms of the second equation, cancelling and rearranging terms, we can rewrite that equation as

$$\begin{aligned}
-(\nu \nabla \cdot \mathrm{E}^{\mathrm{L}}, \boldsymbol{v})_{\mathsf{T}_h} + (\nabla \cdot (\boldsymbol{\varepsilon}^{\boldsymbol{u}} \otimes \boldsymbol{\beta}), \boldsymbol{v})_{\mathsf{T}_h} + (\nabla \varepsilon^p, \boldsymbol{v})_{\mathsf{T}_h} & \\
- \left\langle \big((\boldsymbol{\varepsilon}^{\boldsymbol{u}} - \boldsymbol{\varepsilon}^{\widehat{\boldsymbol{u}}}) \otimes \boldsymbol{\beta}\big)\boldsymbol{n} - \mathrm{S}(\boldsymbol{\varepsilon}^{\boldsymbol{u}} - \boldsymbol{\varepsilon}^{\widehat{\boldsymbol{u}}}), \boldsymbol{v} \right\rangle_{\partial \mathsf{T}_h} &= (\boldsymbol{f}, \boldsymbol{v})_{\mathsf{T}_h},
\end{aligned}$$

which ends the proof. □

Corollary 3.7. *Let* $\mathbb{T}_{\mathrm{L},h} := \left\langle \nu \mathrm{E}^{\mathrm{L}} \boldsymbol{n} - \varepsilon^p \boldsymbol{n} - \frac{1}{2}(\boldsymbol{\varepsilon}^{\widehat{\boldsymbol{u}}} \otimes \boldsymbol{\beta})\boldsymbol{n} - \mathrm{S}(\boldsymbol{\varepsilon}^{\boldsymbol{u}} - \boldsymbol{\varepsilon}^{\widehat{\boldsymbol{u}}}), \boldsymbol{\varepsilon}^{\widehat{\boldsymbol{u}}} \right\rangle_{\Gamma_h}$. *Then,*

$$\nu \|\mathrm{E}^{\mathrm{L}}\|^2_{\mathsf{D}_h} + \langle \mathrm{S}_{\boldsymbol{\beta}}(\boldsymbol{\varepsilon}^{\boldsymbol{u}} - \boldsymbol{\varepsilon}^{\widehat{\boldsymbol{u}}}), \boldsymbol{\varepsilon}^{\boldsymbol{u}} - \boldsymbol{\varepsilon}^{\widehat{\boldsymbol{u}}} \rangle_{\partial \mathsf{T}_h} = -(\mathrm{I}^{\mathrm{L}}, \nu \mathrm{E}^{\mathrm{L}})_{\mathsf{T}_h} + \mathbb{T}_{\mathrm{L},h}.$$

Proof. Taking $\mathrm{G} = \nu \mathrm{E}^{\mathrm{L}}$, $\boldsymbol{v} = \boldsymbol{\varepsilon}^{\boldsymbol{u}}$ and $q = \varepsilon^p$ in (3.38a), (3.38b) and (3.38c), respectively, adding up the resulting equations, cancelling and rearranging terms, we obtain

$$\begin{aligned}
\nu \|\mathrm{E}^{\mathrm{L}}\|^2_{\mathsf{D}_h} - \langle \boldsymbol{\varepsilon}^{\widehat{\boldsymbol{u}}}, \nu \mathrm{E}^{\mathrm{L}} \boldsymbol{n} - \varepsilon^p \boldsymbol{n} \rangle_{\partial \mathsf{T}_h} + (\nabla \cdot (\boldsymbol{\varepsilon}^{\boldsymbol{u}} \otimes \boldsymbol{\beta}), \boldsymbol{\varepsilon}^{\boldsymbol{u}})_{\mathsf{T}_h} & \\
- \left\langle \big((\boldsymbol{\varepsilon}^{\boldsymbol{u}} - \boldsymbol{\varepsilon}^{\widehat{\boldsymbol{u}}}) \otimes \boldsymbol{\beta}\big)\boldsymbol{n} - \mathrm{S}(\boldsymbol{\varepsilon}^{\boldsymbol{u}} - \boldsymbol{\varepsilon}^{\widehat{\boldsymbol{u}}}), \boldsymbol{\varepsilon}^{\boldsymbol{u}} \right\rangle_{\partial \mathsf{T}_h} &= -(\mathrm{I}^{\mathrm{L}}, \nu \mathrm{E}^{\mathrm{L}})_{\mathsf{T}_h}.
\end{aligned} \tag{3.39}$$

Thanks to (3.38e) with $\boldsymbol{\mu} = \boldsymbol{\varepsilon}^{\widehat{\boldsymbol{u}}}$, we note that

$$\langle \nu \mathrm{E}^{\mathrm{L}} \boldsymbol{n} - \varepsilon^p \boldsymbol{n} - (\boldsymbol{\varepsilon}^{\widehat{\boldsymbol{u}}} \otimes \boldsymbol{\beta})\boldsymbol{n} - \mathrm{S}(\boldsymbol{\varepsilon}^{\boldsymbol{u}} - \boldsymbol{\varepsilon}^{\widehat{\boldsymbol{u}}}), \boldsymbol{\varepsilon}^{\widehat{\boldsymbol{u}}} \rangle_{\partial \mathsf{T}_h} = \langle \nu \mathrm{E}^{\mathrm{L}} \boldsymbol{n} - \varepsilon^p \boldsymbol{n} - (\boldsymbol{\varepsilon}^{\widehat{\boldsymbol{u}}} \otimes \boldsymbol{\beta})\boldsymbol{n} - \mathrm{S}(\boldsymbol{\varepsilon}^{\boldsymbol{u}} - \boldsymbol{\varepsilon}^{\widehat{\boldsymbol{u}}}), \boldsymbol{\varepsilon}^{\widehat{\boldsymbol{u}}} \rangle_{\Gamma_h},$$

and hence

$$\begin{aligned}
\langle \nu \mathrm{E}^{\mathrm{L}} \boldsymbol{n} - \varepsilon^p \boldsymbol{n}, \boldsymbol{\varepsilon}^{\widehat{\boldsymbol{u}}} \rangle_{\partial \mathsf{T}_h} &= \langle \nu \mathrm{E}^{\mathrm{L}} \boldsymbol{n} - \varepsilon^p \boldsymbol{n} - (\boldsymbol{\varepsilon}^{\widehat{\boldsymbol{u}}} \otimes \boldsymbol{\beta})\boldsymbol{n} - \mathrm{S}(\boldsymbol{\varepsilon}^{\boldsymbol{u}} - \boldsymbol{\varepsilon}^{\widehat{\boldsymbol{u}}}), \boldsymbol{\varepsilon}^{\widehat{\boldsymbol{u}}} \rangle_{\Gamma_h} \\
&\quad + \langle (\boldsymbol{\varepsilon}^{\widehat{\boldsymbol{u}}} \otimes \boldsymbol{\beta})\boldsymbol{n} + \mathrm{S}(\boldsymbol{\varepsilon}^{\boldsymbol{u}} - \boldsymbol{\varepsilon}^{\widehat{\boldsymbol{u}}}), \boldsymbol{\varepsilon}^{\widehat{\boldsymbol{u}}} \rangle_{\partial \mathsf{T}_h}.
\end{aligned} \tag{3.40}$$

On the other hand, applying the properties (3.7) to the term $(\nabla \cdot (\boldsymbol{\varepsilon}^{\boldsymbol{u}} \otimes \boldsymbol{\beta}), \boldsymbol{\varepsilon}^{\boldsymbol{u}})_{\mathsf{T}_h}$ (proceeding in the same way as we did in the proof of Lemma 3.2), we conclude that

$$(\nabla \cdot (\boldsymbol{\varepsilon}^{\boldsymbol{u}} \otimes \boldsymbol{\beta}), \boldsymbol{\varepsilon}^{\boldsymbol{u}})_{\mathsf{T}_h} = \frac{1}{2} \langle (\boldsymbol{\varepsilon}^{\boldsymbol{u}} \otimes \boldsymbol{\beta})\boldsymbol{n}, \boldsymbol{\varepsilon}^{\boldsymbol{u}} \rangle_{\partial \mathsf{T}_h}. \tag{3.41}$$

Using (3.40) and (3.41), we can rewrite (3.39) as

$$\begin{aligned}
-(\mathrm{I}^{\mathrm{L}}, \nu \mathrm{E}^{\mathrm{L}})_{\mathsf{T}_h} &= \nu \|\mathrm{E}^{\mathrm{L}}\|^2_{\mathsf{D}_h} - \langle \nu \mathrm{E}^{\mathrm{L}} \boldsymbol{n} - \varepsilon^p \boldsymbol{n} - (\boldsymbol{\varepsilon}^{\widehat{\boldsymbol{u}}} \otimes \boldsymbol{\beta})\boldsymbol{n} - \mathrm{S}(\boldsymbol{\varepsilon}^{\boldsymbol{u}} - \boldsymbol{\varepsilon}^{\widehat{\boldsymbol{u}}}), \boldsymbol{\varepsilon}^{\widehat{\boldsymbol{u}}} \rangle_{\Gamma_h} \\
&\quad - \langle (\boldsymbol{\varepsilon}^{\widehat{\boldsymbol{u}}} \otimes \boldsymbol{\beta})\boldsymbol{n} + \mathrm{S}(\boldsymbol{\varepsilon}^{\boldsymbol{u}} - \boldsymbol{\varepsilon}^{\widehat{\boldsymbol{u}}}), \boldsymbol{\varepsilon}^{\widehat{\boldsymbol{u}}} \rangle_{\partial \mathsf{T}_h} + \frac{1}{2} \langle (\boldsymbol{\varepsilon}^{\boldsymbol{u}} \otimes \boldsymbol{\beta})\boldsymbol{n}, \boldsymbol{\varepsilon}^{\boldsymbol{u}} \rangle_{\partial \mathsf{T}_h} \\
&\quad - \left\langle \big((\boldsymbol{\varepsilon}^{\boldsymbol{u}} - \boldsymbol{\varepsilon}^{\widehat{\boldsymbol{u}}}) \otimes \boldsymbol{\beta}\big)\boldsymbol{n} - \mathrm{S}(\boldsymbol{\varepsilon}^{\boldsymbol{u}} - \boldsymbol{\varepsilon}^{\widehat{\boldsymbol{u}}}), \boldsymbol{\varepsilon}^{\boldsymbol{u}} \right\rangle_{\partial \mathsf{T}_h},
\end{aligned}$$

or equivalently, rearranging terms,

$$\begin{aligned}-(\mathrm{I}^{\mathrm{L}},\nu\mathrm{E}^{\mathrm{L}})_{\mathsf{T}_h} &= \nu\|\mathrm{E}^{\mathrm{L}}\|^2_{\mathsf{D}_h}-\frac{1}{2}\langle(\boldsymbol{\varepsilon}^{\boldsymbol{u}}\otimes\boldsymbol{\beta})\boldsymbol{n},\boldsymbol{\varepsilon}^{\boldsymbol{u}}\rangle_{\partial\mathsf{T}_h}+\langle(\boldsymbol{\varepsilon}^{\widehat{\boldsymbol{u}}}\otimes\boldsymbol{\beta})\boldsymbol{n}-\mathrm{S}(\boldsymbol{\varepsilon}^{\boldsymbol{u}}-\boldsymbol{\varepsilon}^{\widehat{\boldsymbol{u}}}),\boldsymbol{\varepsilon}^{\boldsymbol{u}}-\boldsymbol{\varepsilon}^{\widehat{\boldsymbol{u}}}\rangle_{\partial\mathsf{T}_h}\\ &- \langle\nu\mathrm{E}^{\mathrm{L}}\boldsymbol{n}-\varepsilon^p\boldsymbol{n}-(\boldsymbol{\varepsilon}^{\widehat{\boldsymbol{u}}}\otimes\boldsymbol{\beta})\boldsymbol{n}-\mathrm{S}(\boldsymbol{\varepsilon}^{\boldsymbol{u}}-\boldsymbol{\varepsilon}^{\widehat{\boldsymbol{u}}}),\boldsymbol{\varepsilon}^{\widehat{\boldsymbol{u}}}\rangle_{\Gamma_h}.\end{aligned}$$

Finally, using (3.7c) and since $(\boldsymbol{\beta}\cdot\boldsymbol{n})$ is continuous on $\mathcal{E}_h^0$ and $\boldsymbol{\varepsilon}^{\widehat{\boldsymbol{u}}}$ is single valued on $\mathcal{E}_h^0$, we have

$$\begin{aligned}-\frac{1}{2}\langle(\boldsymbol{\varepsilon}^{\boldsymbol{u}}\otimes\boldsymbol{\beta})\boldsymbol{n},\boldsymbol{\varepsilon}^{\boldsymbol{u}}\rangle_{\partial\mathsf{T}_h} &+ \langle(\boldsymbol{\varepsilon}^{\widehat{\boldsymbol{u}}}\otimes\boldsymbol{\beta})\boldsymbol{n}-\mathrm{S}(\boldsymbol{\varepsilon}^{\boldsymbol{u}}-\boldsymbol{\varepsilon}^{\widehat{\boldsymbol{u}}}),\boldsymbol{\varepsilon}^{\boldsymbol{u}}-\boldsymbol{\varepsilon}^{\widehat{\boldsymbol{u}}}\rangle_{\partial\mathsf{T}_h}\\ &= -\frac{1}{2}\langle(\boldsymbol{\varepsilon}^{\widehat{\boldsymbol{u}}}\otimes\boldsymbol{\beta})\boldsymbol{n},\boldsymbol{\varepsilon}^{\widehat{\boldsymbol{u}}}\rangle_{\partial\mathsf{T}_h}+\langle\mathrm{S}_{\boldsymbol{\beta}}(\boldsymbol{\varepsilon}^{\boldsymbol{u}}-\boldsymbol{\varepsilon}^{\widehat{\boldsymbol{u}}}),\boldsymbol{\varepsilon}^{\boldsymbol{u}}-\boldsymbol{\varepsilon}^{\widehat{\boldsymbol{u}}}\rangle_{\partial\mathsf{T}_h}\\ &= -\frac{1}{2}\langle(\boldsymbol{\varepsilon}^{\widehat{\boldsymbol{u}}}\otimes\boldsymbol{\beta})\boldsymbol{n},\boldsymbol{\varepsilon}^{\widehat{\boldsymbol{u}}}\rangle_{\Gamma_h}+\langle\mathrm{S}_{\boldsymbol{\beta}}(\boldsymbol{\varepsilon}^{\boldsymbol{u}}-\boldsymbol{\varepsilon}^{\widehat{\boldsymbol{u}}}),\boldsymbol{\varepsilon}^{\boldsymbol{u}}-\boldsymbol{\varepsilon}^{\widehat{\boldsymbol{u}}}\rangle_{\partial\mathsf{T}_h}.\end{aligned}$$

which concludes the proof. □

Step 2: A bound for $\mathbb{T}_{\mathrm{L},h}$

Following the approach by [21], we need to rewrite the term $\mathbb{T}_{\mathrm{L},h}$ in a suitable manner.

Lemma 3.8.

$$\begin{aligned}\mathbb{T}_{\mathrm{L},h}\leq &- \nu\|\tilde{\boldsymbol{g}}-\tilde{\boldsymbol{g}}_h\|^2_{\Gamma_h,l^{-1}}+\nu\|\tilde{\boldsymbol{g}}-\tilde{\boldsymbol{g}}_h\|_{\Gamma_h,l^{-1}}\Big\{\|\delta_{\mathrm{I}^{\mathrm{L}}}\|_{\Gamma_h,l}+\|\mathrm{I}^{\mathrm{L}}\boldsymbol{n}\|_{\Gamma_h,l}\\ &+ \|\delta_{\mathrm{E}^{\mathrm{L}}}\|_{\Gamma_h,l}+\nu^{-1}\|\varepsilon^p\|_{\Gamma_h,l}+\nu^{-1}\|\mathrm{S}_{\boldsymbol{\beta}}(\boldsymbol{\varepsilon}^{\boldsymbol{u}}-\boldsymbol{\varepsilon}^{\widehat{\boldsymbol{u}}})\|_{\Gamma_h,l}+\frac{1}{2}\nu^{-1}\|(\boldsymbol{\varepsilon}^{\boldsymbol{u}}\otimes\boldsymbol{\beta})\boldsymbol{n}\|_{\Gamma_h,l}\Big\}.\end{aligned}$$

Proof. Proceeding exactly as in Lemma 5.1 of [21], it is not difficult to see that we can decompose $(\tilde{\boldsymbol{g}}-\tilde{\boldsymbol{g}}_h)(\boldsymbol{x})=-l(\boldsymbol{x})\{\delta_{\mathrm{I}^{\mathrm{L}}}+\mathrm{I}^{\mathrm{L}}\boldsymbol{n}+\delta_{\mathrm{E}^{\mathrm{L}}}+\mathrm{E}^{\mathrm{L}}\boldsymbol{n}\}(\boldsymbol{x})$, which yields $\mathrm{E}^{\mathrm{L}}\boldsymbol{n}=-(\tilde{\boldsymbol{g}}-\tilde{\boldsymbol{g}}_h)(\boldsymbol{x})/l-\delta_{\mathrm{I}^{\mathrm{L}}}-\mathrm{I}^{\mathrm{L}}\boldsymbol{n}-\delta_{\mathrm{E}^{\mathrm{L}}}$. Hence, we can rewrite $\mathbb{T}_{\mathrm{L},h}$ as

$$\mathbb{T}_{\mathrm{L},h}=\left\langle-\nu\left\{(\tilde{\boldsymbol{g}}-\tilde{\boldsymbol{g}}_h)(\boldsymbol{x})/l+\delta_{\mathrm{I}^{\mathrm{L}}}+\mathrm{I}^{\mathrm{L}}\boldsymbol{n}+\delta_{\mathrm{E}^{\mathrm{L}}}\right\}-\varepsilon^p\boldsymbol{n}-\frac{1}{2}(\boldsymbol{\varepsilon}^{\widehat{\boldsymbol{u}}}\otimes\boldsymbol{\beta})\boldsymbol{n}-\mathrm{S}(\boldsymbol{\varepsilon}^{\boldsymbol{u}}-\boldsymbol{\varepsilon}^{\widehat{\boldsymbol{u}}}),\boldsymbol{\varepsilon}^{\widehat{\boldsymbol{u}}}\right\rangle_{\Gamma_h}.$$

Observe now that

$$-\left\langle\frac{1}{2}(\boldsymbol{\varepsilon}^{\widehat{\boldsymbol{u}}}\otimes\boldsymbol{\beta})\boldsymbol{n}+\mathrm{S}(\boldsymbol{\varepsilon}^{\boldsymbol{u}}-\boldsymbol{\varepsilon}^{\widehat{\boldsymbol{u}}}),\boldsymbol{\varepsilon}^{\widehat{\boldsymbol{u}}}\right\rangle_{\Gamma_h}=-\left\langle\frac{1}{2}(\boldsymbol{\varepsilon}^{\boldsymbol{u}}\otimes\boldsymbol{\beta})\boldsymbol{n}+\mathrm{S}_{\boldsymbol{\beta}}(\boldsymbol{\varepsilon}^{\boldsymbol{u}}-\boldsymbol{\varepsilon}^{\widehat{\boldsymbol{u}}}),\boldsymbol{\varepsilon}^{\widehat{\boldsymbol{u}}}\right\rangle_{\Gamma_h}.$$

Then, since $\boldsymbol{\varepsilon}^{\widehat{\boldsymbol{u}}}=\mathbf{P}_{\boldsymbol{M}}(\tilde{\boldsymbol{g}}-\tilde{\boldsymbol{g}}_h)$ on Γ_h, we can decompose $\mathbb{T}_{\mathrm{L},h}=\sum_{i=1}^7\mathbb{T}^i_{\mathrm{L},h}$, where

$$\begin{aligned}\mathbb{T}^1_{\mathrm{L},h} &= -\nu\langle(\tilde{\boldsymbol{g}}-\tilde{\boldsymbol{g}}_h)/l,(\tilde{\boldsymbol{g}}-\tilde{\boldsymbol{g}}_h)\rangle_{\Gamma_h}, & \mathbb{T}^2_{\mathrm{L},h} &= -\nu\langle\tilde{\boldsymbol{g}}-\tilde{\boldsymbol{g}}_h,\delta_{\mathrm{I}^{\mathrm{L}}}\rangle_{\Gamma_h},\\ \mathbb{T}^3_{\mathrm{L},h} &= -\nu\langle\tilde{\boldsymbol{g}}-\tilde{\boldsymbol{g}}_h,\mathrm{I}^{\mathrm{L}}\boldsymbol{n}\rangle_{\Gamma_h}, & \mathbb{T}^4_{\mathrm{L},h} &= -\nu\langle\tilde{\boldsymbol{g}}-\tilde{\boldsymbol{g}}_h,\delta_{\mathrm{E}^{\mathrm{L}}}\rangle_{\Gamma_h},\\ \mathbb{T}^5_{\mathrm{L},h} &= -\langle\tilde{\boldsymbol{g}}-\tilde{\boldsymbol{g}}_h,\varepsilon^p\boldsymbol{n}\rangle_{\Gamma_h}, & \mathbb{T}^6_{\mathrm{L},h} &= -\langle\tilde{\boldsymbol{g}}-\tilde{\boldsymbol{g}}_h,\mathrm{S}_{\boldsymbol{\beta}}(\boldsymbol{\varepsilon}^{\boldsymbol{u}}-\boldsymbol{\varepsilon}^{\widehat{\boldsymbol{u}}})\rangle_{\Gamma_h},\\ \mathbb{T}^7_{\mathrm{L},h} &= -\frac{1}{2}\langle\tilde{\boldsymbol{g}}-\tilde{\boldsymbol{g}}_h,(\boldsymbol{\varepsilon}^{\boldsymbol{u}}\otimes\boldsymbol{\beta})\boldsymbol{n}\rangle_{\Gamma_h}.\end{aligned}$$

The result follows from applying Cauchy-Schwarz inequality to each of these terms. □

Step 3: A first energy estimate

Gathering the result stated in Corollary 3.7, estimate in Lemma 3.8, inequality (1.6), (1.4) with $\mathrm{G} = \mathrm{E}^{\mathrm{L}}$, Young's inequality, definition (3.36), inequality (1.7), Assumptions A and noticing that $\|\mathrm{I}^{\mathrm{L}}\boldsymbol{n}\|^2_{\Gamma_h,l} \leq R\|\mathrm{I}^{\mathrm{L}}\boldsymbol{n}\|^2_{\Gamma_h,h^\perp}$ we conclude:

Lemma 3.9. *It holds that*

$$\begin{aligned}\|\mathrm{E}^{\mathrm{L}}\|^2_{\mathsf{D}_h} + \nu^{-1}\langle S_{\boldsymbol{\beta}}(\boldsymbol{\varepsilon}^{\boldsymbol{u}} - \boldsymbol{\varepsilon}^{\widehat{\boldsymbol{u}}}), \boldsymbol{\varepsilon}^{\boldsymbol{u}} - \boldsymbol{\varepsilon}^{\widehat{\boldsymbol{u}}}\rangle_{\partial\mathsf{T}_h} &+ \|\widetilde{\boldsymbol{g}} - \widetilde{\boldsymbol{g}}_h\|^2_{\Gamma_h,l^{-1}} \\ &\leq \Theta^2_{\mathrm{L}} + 24\nu^{-2}\|\varepsilon^p\|^2_{\Gamma_h,l} + \nu^{-2}\|\boldsymbol{\beta}\|^2_{L^\infty(\Omega)}\|\boldsymbol{\varepsilon}^{\boldsymbol{u}}\|^2_{\mathsf{D}_h}.\end{aligned}$$

Comparing this estimate with the corresponding result in [11] for polyhedral domains, we see in our case the presence of the terms $\|\widetilde{\boldsymbol{g}} - \widetilde{\boldsymbol{g}}_h\|^2_{\Gamma_h,l^{-1}}$, $24\nu^{-2}\|\varepsilon^p\|^2_{\Gamma_h,l}$ and $\nu^{-2}\|\boldsymbol{\beta}\|^2_{L^\infty(\Omega)}\|\boldsymbol{\varepsilon}^{\boldsymbol{u}}\|^2_{\mathsf{D}_h}$ coming from $\mathbb{T}_{\mathrm{L},h}$. In other words, for a polyhedral domain, we would have $\mathbb{T}_{\mathrm{L},h} = 0$ and recover the estimates in [11]. We also observe that the estimate in Lemma 3.9 is similar to the one obtained in Lemma 3.2, except that the right hand side involves terms related to the interpolation operator instead of the source term and boundary data.

Step 4: Estimate of the pressure

The next step is to bound the projection of the error of the pressure. In order to do that, we need a previous result (see Lemma 3.7 in [18]).

Lemma 3.10. *We have*

$$\|\boldsymbol{\varepsilon}^{\widehat{\boldsymbol{u}}}\|_h \leq C(h\|\mathrm{I}^{\mathrm{L}}\|_{\mathsf{D}_h} + h\|\mathrm{E}^{\mathrm{L}}\|_{\mathsf{D}_h} + \|\boldsymbol{\varepsilon}^{\boldsymbol{u}}\|_{\mathsf{D}_h}).$$

Now we can state the estimate for the pressure.

Lemma 3.11. *If Assumption (A.4) holds, then*

$$\begin{aligned}\|\varepsilon^p\|_{\mathsf{D}_h} \leq\ & \kappa\left\{\nu^{-1}\|\boldsymbol{\beta}\|_{L^\infty(\Omega)}\left(3H^1_p + C_{\tau,\nu,\boldsymbol{\beta}}H^3_p\right) + 2H^2_p\right\}\|\boldsymbol{\varepsilon}^{\boldsymbol{u}}\|_{\mathsf{D}_h} \\ &+\kappa\left(5H^1_p + C_{\tau,\nu,\boldsymbol{\beta}}H^3_p\right)\Theta_{\mathrm{I}^{\mathrm{L}}},\end{aligned}$$

where H^1_p, H^2_p, H^3_p and $C_{\tau,\nu,\boldsymbol{\beta}}$ were defined in Lemma 3.3.

Proof. We proceed in a similar way to the proof of Lemma 3.3. Since $\varepsilon^p \in L^2_0(\mathsf{D}_h)$, there exists $\kappa > 0$ such that

$$\|\varepsilon^p\|_{\mathsf{D}_h} \leq \kappa \sup_{\boldsymbol{w}\in\boldsymbol{H}^1_0(\mathsf{D}_h)\setminus\{\mathbf{0}\}} \frac{(\varepsilon^p, \nabla\cdot\boldsymbol{w})_{\mathsf{D}_h}}{\|\boldsymbol{w}\|_{\boldsymbol{H}^1(\mathsf{D}_h)}}. \tag{3.42}$$

We can write the numerator as

$$\begin{aligned}(\varepsilon^p, \nabla\cdot\boldsymbol{w})_{\mathsf{D}_h} =\ & (\nu\mathrm{E}^{\mathrm{L}}, \nabla\boldsymbol{w})_{\mathsf{T}_h} - (\boldsymbol{\varepsilon}^{\boldsymbol{u}}\otimes\boldsymbol{\delta\beta}, \nabla\boldsymbol{P}\boldsymbol{w})_{\mathsf{T}_h} \\ &+(\mathrm{L} - \mathrm{L}_h, \boldsymbol{P}\boldsymbol{w}\otimes\boldsymbol{\beta}_0)_{\mathsf{T}_h} + \langle\boldsymbol{\varepsilon}^{\widehat{\boldsymbol{u}}}, (\boldsymbol{P}\boldsymbol{w}\otimes\boldsymbol{\delta\beta})\boldsymbol{n}\rangle_{\partial\mathsf{T}_h} \\ &+\langle\mathrm{S}(\boldsymbol{\varepsilon}^{\boldsymbol{u}} - \boldsymbol{\varepsilon}^{\widehat{\boldsymbol{u}}}), \boldsymbol{P}\boldsymbol{w} - \mathbf{P}_M\boldsymbol{w}\rangle_{\partial\mathsf{T}_h},\end{aligned}$$

where the projection $\boldsymbol{P}$ is chosen as in Lemma 3.3. The result follows by applying the Cauchy-Schwarz inequality, the trace inequality (1.7), Lemma 3.9 and Assumption (A.4). □

If Ω were polyhedral, this result reduces to the estimate of Lemma 3.10 in [18]. Before going to the next subsection, we will obtain some conclusions that will be useful in what follows. Observe first, proceeding as we did in (3.19), that $\|\varepsilon^p\|_{\Gamma_h,l} \lesssim \|\varepsilon^p\|_{\mathsf{D}_h}$. Note also that the estimate of Lemma 2.10 can be rewritten as

$$\|\varepsilon^p\|_{\mathsf{D}_h} \lesssim \|\boldsymbol{\varepsilon}^{\boldsymbol{u}}\|_{\mathsf{D}_h} + \Theta_{\mathrm{I}^{\mathrm{L}}}. \tag{3.43}$$

Combining these expressions, from Lemma 2.9 we deduce that

$$\|\mathrm{E}^{\mathrm{L}}\|_{\mathsf{D}_h} + \nu^{-1/2}\langle \mathrm{S}_{\boldsymbol{\beta}}(\boldsymbol{\varepsilon}^{\boldsymbol{u}} - \boldsymbol{\varepsilon}^{\widehat{\boldsymbol{u}}}), \boldsymbol{\varepsilon}^{\boldsymbol{u}} - \boldsymbol{\varepsilon}^{\widehat{\boldsymbol{u}}}\rangle^{1/2}_{\partial\mathsf{T}_h} + \|\widetilde{\boldsymbol{g}} - \widetilde{\boldsymbol{g}}_h\|_{\Gamma_h,l^{-1}} \lesssim \Theta_{\mathrm{I}^{\mathrm{L}}} + \|\boldsymbol{\varepsilon}^{\boldsymbol{u}}\|_{\mathsf{D}_h}. \tag{3.44}$$

3.4.2 A duality argument

We proceed to obtain estimates for the velocity by carrying out a duality argument. First we need to define some terms that will appear in the estimates below. For any arbitrary $\boldsymbol{\phi}_h \in \boldsymbol{V}_h$, define

$$\begin{aligned} H_L &:= \nu \max\left\{ \sup_{\boldsymbol{\theta}\in L^2(\Omega)\setminus\{\mathbf{0}\}} \frac{\|\Pi^*\Phi - \Phi\|_{\mathsf{T}_h}}{\|\boldsymbol{\theta}\|_\Omega}, \sup_{\boldsymbol{\theta}\in L^2(\Omega)\setminus\{\mathbf{0}\}} \frac{\|\nabla(\boldsymbol{\phi}_h - \boldsymbol{\phi})\|_{\mathsf{T}_h}}{\|\boldsymbol{\theta}\|_\Omega} \right\}, \\ H_{\boldsymbol{\beta}} &:= \|\boldsymbol{\delta\beta}\|_{L^\infty(\Omega)} \sup_{\boldsymbol{\theta}\in L^2(\Omega)\setminus\{\mathbf{0}\}} \frac{\|\nabla\boldsymbol{\phi}_h\|_{\mathsf{T}_h}}{\|\boldsymbol{\theta}\|_\Omega}. \end{aligned}$$

Propositions 3.6 and 3.7 in [11] state that if $\mathrm{tr}(\mathrm{L}) = 0$, then

$$H_L \le C\nu C_{H_L} h^{\min\{k,1\}} \quad \text{and} \quad H_{\boldsymbol{\beta}} \le Ch|\boldsymbol{\beta}|_{W^{1,\infty}(\Omega)}, \tag{3.45}$$

where C_{H_L} is of order $\mathcal{O}(1)$ if h is small enough (see Proposition 3.6 in [11]). The main estimate of this section is the following result:

Lemma 3.12. *Let $H_{\boldsymbol{\varepsilon}^{\boldsymbol{u}}}(R,h) := h^{1/2} + R^2h^{3/2} + Rh^{1/2} + R^{1/2} + R^{3/2}h$. If Assumptions A and B hold, then there exists $h_0 > 0$ such that for all $h < h_0$,*

$$\begin{aligned} \|\boldsymbol{\varepsilon}^{\boldsymbol{u}}\|_{\mathsf{D}_h} \lesssim\ & h^{1/2}H_{\boldsymbol{\varepsilon}^{\boldsymbol{u}}}(R,h)\Theta_{\mathrm{I}^{\mathrm{L}}} + h^{1/2}\left\{\nu^{-1}R\|I^p\|_{\mathsf{D}_h} + (\tau R + h^{1/2})\|\boldsymbol{I}^{\boldsymbol{u}}\|_{\mathsf{D}_h}\right\} \\ & + \nu Rh\|\boldsymbol{\beta}\|_{L^\infty(\Omega)}\|\boldsymbol{I}^{\boldsymbol{u}}_M\|_{L^2(\Gamma_h)}. \end{aligned}$$

This lemma implies that $\|\boldsymbol{\varepsilon}^{\boldsymbol{u}}\|_{\mathsf{D}_h} \lesssim h^{k+3/2}$ if the solution is smooth enough and if τ and R are of order one, since the interpolation errors are of order h^{k+1}. In the case of a polyhedral domain where Γ_h fits Γ, we would have $R = 0$, $\widetilde{\boldsymbol{g}} = \widetilde{\boldsymbol{g}}_h$. As a consequence, $H_{\boldsymbol{\varepsilon}^{\boldsymbol{u}}}(R,h) = h^{1/2}$ and the estimate in Lemma 5.6 would read $\|\boldsymbol{\varepsilon}^{\boldsymbol{u}}\|_{\mathsf{D}_h} \lesssim h\big(\Theta_{\mathrm{I}^{\mathrm{L}}} + \|\boldsymbol{I}^{\boldsymbol{u}}\|_{\mathsf{D}_h}\big)$. Hence, $\|\boldsymbol{\varepsilon}^{\boldsymbol{u}}\|_{\mathsf{D}_h}$ would be of order h^{k+2}, which agrees with the estimate stated in Theorem 2.6 in [11] for the polyhedral case.

Step 1: Estimate of the velocity

We first obtain an identity for the projection of the error in the velocity by using a duality argument.

Lemma 3.13. *Let $\boldsymbol{\phi}_h$ be an arbitrary element of $\boldsymbol{V}_h$. Then $(\boldsymbol{\varepsilon}^{\boldsymbol{u}}, \boldsymbol{\theta})_{\mathsf{T}_h} = T_{\mathrm{L}} + T_{\boldsymbol{\beta}} + \mathbb{T}_{\boldsymbol{u},h}$, where*

$$\begin{aligned} T_{\mathrm{L}} &:= \big(\mathrm{L} - \mathrm{L}_h, \nu\Pi^*\Phi - \nu\Phi\big)_{\mathsf{T}_h} - \big(\nu\mathrm{L} - \nu\Pi\mathrm{L}, \nabla(\boldsymbol{\phi}_h - \boldsymbol{\phi})\big)_{\mathsf{T}_h}, \\ T_{\boldsymbol{\beta}} &:= \big((\boldsymbol{u} - \boldsymbol{\Pi u}) \otimes \boldsymbol{\delta\beta}, \nabla\boldsymbol{\phi}_h\big)_{\mathsf{T}_h}, \quad \textit{and} \\ \mathbb{T}_{\boldsymbol{u},h} &:= \langle \nu\mathrm{E}^{\mathrm{L}}\boldsymbol{n} - \varepsilon^p\boldsymbol{n} - S(\boldsymbol{\varepsilon}^{\boldsymbol{u}} - \boldsymbol{\varepsilon}^{\widehat{\boldsymbol{u}}}), \boldsymbol{\phi}\rangle_{\Gamma_h} - \langle \boldsymbol{\varepsilon}^{\widehat{\boldsymbol{u}}}, \nu\Phi\boldsymbol{n} + \phi\boldsymbol{n}\rangle_{\Gamma_h} - \langle (\boldsymbol{\varepsilon}^{\widehat{\boldsymbol{u}}} \otimes \boldsymbol{\beta})\boldsymbol{n}, \boldsymbol{\phi}\rangle_{\Gamma_h}. \end{aligned}$$

Proof. Proceeding as in the proof of Lemma 3.4 of [11], we can write $(\boldsymbol{\varepsilon^u},\boldsymbol{\theta})_{\mathsf{T}_h} = T_{\mathrm{L}} + T_{\boldsymbol{\beta}} + \Lambda$, where

$$\begin{aligned}\Lambda \;:=\; & -(\nu\nabla\cdot \mathrm{E}^{\mathrm{L}},\boldsymbol{\phi}-\boldsymbol{\Pi^*\phi})_{\mathsf{T}_h} + \langle \nu\mathrm{E}^{\mathrm{L}}\boldsymbol{n},\boldsymbol{\phi}-\boldsymbol{\Pi^*\phi}\rangle_{\partial\mathsf{T}_h} - \langle \boldsymbol{\varepsilon^{\widehat{u}}},\nu\Pi^*\Phi\boldsymbol{n}\rangle_{\partial\mathsf{T}_h}\\ & +\langle \nu\mathrm{E}^{\mathrm{L}}\boldsymbol{n}-\varepsilon^p\boldsymbol{n}-(\boldsymbol{\varepsilon^{\widehat{u}}}\otimes\boldsymbol{\beta})\boldsymbol{n}-\mathrm{S}(\boldsymbol{\varepsilon^u}-\boldsymbol{\varepsilon^{\widehat{u}}}),\boldsymbol{\Pi^*\phi}\rangle_{\partial\mathsf{T}_h} - (\nabla\varepsilon^p,\boldsymbol{\Pi^*\phi}-\boldsymbol{\phi})_{\mathsf{T}_h}\\ & +\langle\varepsilon^p\boldsymbol{n},\boldsymbol{\Pi^*\phi}-\boldsymbol{\phi}\rangle_{\partial\mathsf{T}_h} - (\boldsymbol{\varepsilon^u},\nabla\Pi^*\phi)_{\mathsf{T}_h}\\ & -\langle\boldsymbol{\varepsilon^u},\nu(\Phi-\Pi^*\Phi)\boldsymbol{n}+(\phi-\Pi^*\phi)\boldsymbol{n}+\big((\boldsymbol{\phi}-\boldsymbol{\Pi^*u})\otimes\boldsymbol{\beta}\big)\boldsymbol{n}\rangle_{\partial\mathsf{T}_h}.\end{aligned}$$

Using (3.38e) with $\boldsymbol{\mu}=\mathbf{P}_M\boldsymbol{\phi}$, we have that

$$\langle \nu\mathrm{E}^{\mathrm{L}}\boldsymbol{n}-\varepsilon^p\boldsymbol{n}-(\boldsymbol{\varepsilon^{\widehat{u}}}\otimes\boldsymbol{\beta})\boldsymbol{n}-\mathrm{S}(\boldsymbol{\varepsilon^u}-\boldsymbol{\varepsilon^{\widehat{u}}}),\mathbf{P}_M\boldsymbol{\phi}\rangle_{\partial\mathsf{T}_h} = \langle \nu\mathrm{E}^{\mathrm{L}}\boldsymbol{n}-\varepsilon^p\boldsymbol{n}-(\boldsymbol{\varepsilon^{\widehat{u}}}\otimes\boldsymbol{\beta})\boldsymbol{n}-\mathrm{S}(\boldsymbol{\varepsilon^u}-\boldsymbol{\varepsilon^{\widehat{u}}}),\mathbf{P}_M\boldsymbol{\phi}\rangle_{\Gamma_h}.$$

Then, adding and subtracting this term, we obtain

$$\begin{aligned}\Lambda \;=\; & -(\nu\nabla\cdot \mathrm{E}^{\mathrm{L}},\boldsymbol{\phi}-\boldsymbol{\Pi^*\phi})_{\mathsf{T}_h} + \langle \nu\mathrm{E}^{\mathrm{L}}\boldsymbol{n},\boldsymbol{\phi}-\boldsymbol{\Pi^*\phi}\rangle_{\partial\mathsf{T}_h} - \langle \boldsymbol{\varepsilon^{\widehat{u}}},\nu\Pi^*\Phi\boldsymbol{n}\rangle_{\partial\mathsf{T}_h}\\ & +\langle \nu\mathrm{E}^{\mathrm{L}}\boldsymbol{n}-\varepsilon^p\boldsymbol{n}-(\boldsymbol{\varepsilon^{\widehat{u}}}\otimes\boldsymbol{\beta})\boldsymbol{n}-\mathrm{S}(\boldsymbol{\varepsilon^u}-\boldsymbol{\varepsilon^{\widehat{u}}}),\boldsymbol{\Pi^*\phi}-\mathbf{P}_M\boldsymbol{\phi}\rangle_{\partial\mathsf{T}_h}\\ & -(\nabla\varepsilon^p,\boldsymbol{\Pi^*\phi}-\boldsymbol{\phi})_{\mathsf{T}_h} + \langle\varepsilon^p\boldsymbol{n},\boldsymbol{\Pi^*\phi}-\boldsymbol{\phi}\rangle_{\partial\mathsf{T}_h} - (\boldsymbol{\varepsilon^u},\nabla\Pi^*\phi)_{\mathsf{T}_h}\\ & -\langle\boldsymbol{\varepsilon^u},\nu(\Phi-\Pi^*\Phi)\boldsymbol{n}+(\phi-\Pi^*\phi)\boldsymbol{n}+\big((\boldsymbol{\phi}-\boldsymbol{\Pi^*u})\otimes\boldsymbol{\beta}\big)\boldsymbol{n}\rangle_{\partial\mathsf{T}_h}\\ & +\langle \nu\mathrm{E}^{\mathrm{L}}\boldsymbol{n}-\varepsilon^p\boldsymbol{n}-(\boldsymbol{\varepsilon^{\widehat{u}}}\otimes\boldsymbol{\beta})\boldsymbol{n}-\mathrm{S}(\boldsymbol{\varepsilon^u}-\boldsymbol{\varepsilon^{\widehat{u}}}),\mathbf{P}_M\boldsymbol{\phi}\rangle_{\Gamma_h}.\end{aligned}$$

Using the definition of the projections Π_h^* and $\mathbf{P}_M$, error equations and rearranging terms, we can rewrite Λ as

$$\begin{aligned}\Lambda \;=\; & -\langle\boldsymbol{\varepsilon^u}-\boldsymbol{\varepsilon^{\widehat{u}}},\nu(\Phi-\Pi^*\Phi)\boldsymbol{n}+\big((\boldsymbol{\phi}-\boldsymbol{\Pi^*\phi})\otimes\boldsymbol{\beta}\big)\boldsymbol{n}-\mathrm{S}(\boldsymbol{\phi}-\boldsymbol{\Pi^*\phi})\rangle_{\partial\mathsf{T}_h}\\ & -\langle\boldsymbol{\varepsilon^{\widehat{u}}},\Pi^*\phi\boldsymbol{n}\rangle_{\partial\mathsf{T}_h} - \langle\boldsymbol{\varepsilon^u},(\phi-\Pi\phi)\boldsymbol{n}\rangle_{\partial\mathsf{T}_h} - \langle\boldsymbol{\varepsilon^{\widehat{u}}},\nu\Phi\boldsymbol{n}+(\boldsymbol{\beta}\cdot\boldsymbol{n})(\boldsymbol{\phi}-\mathbf{P}_M\boldsymbol{\phi})\rangle_{\partial\mathsf{T}_h}\\ & +\langle \nu\mathrm{E}^{\mathrm{L}}\boldsymbol{n}-\varepsilon^p\boldsymbol{n}-(\boldsymbol{\varepsilon^{\widehat{u}}}\otimes\boldsymbol{\beta})\boldsymbol{n}-\mathrm{S}(\boldsymbol{\varepsilon^u}-\boldsymbol{\varepsilon^{\widehat{u}}}),\mathbf{P}_M\boldsymbol{\phi}\rangle_{\Gamma_h}.\end{aligned}$$

Since $\boldsymbol{\varepsilon^{\widehat{u}}}$ is single valued on $\mathcal{E}_h^0$ and $\nu\Phi\boldsymbol{n}+(\boldsymbol{\beta}\cdot\boldsymbol{n})(\boldsymbol{\phi}-\mathbf{P}_M\boldsymbol{\phi})$ is continuous on $\mathcal{E}_h^0$, then

$$\langle\boldsymbol{\varepsilon^{\widehat{u}}},\nu\Phi\boldsymbol{n}+(\boldsymbol{\beta}\cdot\boldsymbol{n})(\boldsymbol{\phi}-\mathbf{P}_M\boldsymbol{\phi})\rangle_{\partial\mathsf{T}_h} = \langle\boldsymbol{\varepsilon^{\widehat{u}}},\nu\Phi\boldsymbol{n}+(\boldsymbol{\beta}\cdot\boldsymbol{n})(\boldsymbol{\phi}-\mathbf{P}_M\boldsymbol{\phi})\rangle_{\Gamma_h}.$$

Analogously, $\langle\boldsymbol{\varepsilon^{\widehat{u}}},\phi\boldsymbol{n}\rangle_{\partial\mathsf{T}_h} = \langle\boldsymbol{\varepsilon^{\widehat{u}}},\phi\boldsymbol{n}\rangle_{\Gamma_h}$. Adding and subtracting this term, we rewrite Λ as

$$\begin{aligned}\Lambda \;=\; & -\langle\boldsymbol{\varepsilon^u}-\boldsymbol{\varepsilon^{\widehat{u}}},\nu(\Phi-\Pi^*\Phi)\boldsymbol{n}+(\phi-\Pi^*\phi)\boldsymbol{n}+\big((\boldsymbol{\phi}-\boldsymbol{\Pi^*\phi})\otimes\boldsymbol{\beta}\big)\boldsymbol{n}-\mathrm{S}(\boldsymbol{\phi}-\boldsymbol{\Pi^*\phi})\rangle_{\partial\mathsf{T}_h}\\ & +\langle \nu\mathrm{E}^{\mathrm{L}}\boldsymbol{n}-\varepsilon^p\boldsymbol{n}-(\boldsymbol{\varepsilon^{\widehat{u}}}\otimes\boldsymbol{\beta})\boldsymbol{n}-\mathrm{S}(\boldsymbol{\varepsilon^u}-\boldsymbol{\varepsilon^{\widehat{u}}}),\mathbf{P}_M\boldsymbol{\phi}\rangle_{\Gamma_h} - \langle\boldsymbol{\varepsilon^{\widehat{u}}},\nu\Phi\boldsymbol{n}\rangle_{\Gamma_h}\\ & -\langle\boldsymbol{\varepsilon^{\widehat{u}}},(\boldsymbol{\beta}\cdot\boldsymbol{n})(\boldsymbol{\phi}-\mathbf{P}_M\boldsymbol{\phi})\rangle_{\Gamma_h}.\end{aligned}$$

The first term of the right hand side vanishes thanks to (3.24d) with $\boldsymbol{\mu}=\boldsymbol{\varepsilon^u}-\boldsymbol{\varepsilon^{\widehat{u}}}$. Then, rearranging terms, we have

$$\Lambda = \langle \nu\mathrm{E}^{\mathrm{L}}\boldsymbol{n}-\varepsilon^p\boldsymbol{n}-\mathrm{S}(\boldsymbol{\varepsilon^u}-\boldsymbol{\varepsilon^{\widehat{u}}}),\boldsymbol{\phi}\rangle_{\Gamma_h} - \langle\boldsymbol{\varepsilon^{\widehat{u}}},\nu\Phi\boldsymbol{n}\rangle_{\Gamma_h} - \langle\boldsymbol{\varepsilon^{\widehat{u}}},\phi\boldsymbol{n}\rangle_{\Gamma_h} - \langle(\boldsymbol{\beta}\cdot\boldsymbol{n})\boldsymbol{\varepsilon^{\widehat{u}}},\boldsymbol{\phi}\rangle_{\Gamma_h},$$

which completes the proof. □

Step 2: A new expression for $\mathbb{T}_{\boldsymbol{u},h}$

As we did previously with $\mathbb{T}_{\mathrm{L},h}$, we proceed now to rewrite $\mathbb{T}_{\boldsymbol{u},h}$ in a suitable manner.

Lemma 3.14. *We have that* $\mathbb{T}_{\boldsymbol{u},h} = \sum_{i=1}^{13} \mathbb{T}^i_{\boldsymbol{u},h}$, *where*

$$\begin{aligned}
\mathbb{T}^1_{\boldsymbol{u},h} &= -\nu\langle(\widetilde{\boldsymbol{g}} - \widetilde{\boldsymbol{g}}_h)/l, \boldsymbol{\phi} + l\nabla\boldsymbol{\phi}\boldsymbol{n}\rangle_{\Gamma_h}, \quad \mathbb{T}^2_{\boldsymbol{u},h} = \nu\langle\widetilde{\boldsymbol{g}} - \widetilde{\boldsymbol{g}}_h, \nabla\boldsymbol{\phi}\boldsymbol{n} - \mathbf{P}_M(\nabla\boldsymbol{\phi}\boldsymbol{n})\rangle_{\Gamma_h},\\
\mathbb{T}^3_{\boldsymbol{u},h} &= -\nu\langle\delta_{\mathrm{I}^{\mathrm{L}}}, \boldsymbol{\phi}\rangle_{\Gamma_h}, \quad \mathbb{T}^4_{\boldsymbol{u},h} = -\nu\langle\mathrm{I}^{\mathrm{L}}\boldsymbol{n}, \boldsymbol{\phi} - \mathbf{P}_M\boldsymbol{\phi}\rangle_{\Gamma_h}, \quad \mathbb{T}^5_{\boldsymbol{u},h} = -\langle I^p\boldsymbol{n}, \mathbf{P}_M\boldsymbol{\phi}\rangle_{\Gamma_h},\\
\mathbb{T}^6_{\boldsymbol{u},h} &= -\nu\langle\mathbf{P}_M\tau\boldsymbol{I}^{\boldsymbol{u}}, \boldsymbol{\phi}\rangle_{\Gamma_h}, \quad \mathbb{T}^7_{\boldsymbol{u},h} = -\left\langle\left(\boldsymbol{I}^{\boldsymbol{u}}_M \otimes \boldsymbol{\beta}\right)\boldsymbol{n}, \mathbf{P}_M\boldsymbol{\phi}\right\rangle_{\Gamma_h}, \quad \mathbb{T}^8_{\boldsymbol{u},h} = -\nu\langle\delta_{E^{\mathrm{L}}}, \boldsymbol{\phi}\rangle_{\Gamma_h},\\
\mathbb{T}^9_{\boldsymbol{u},h} &= -\langle\varepsilon^p\boldsymbol{n}, \boldsymbol{\phi}\rangle_{\Gamma_h}, \quad \mathbb{T}^{10}_{\boldsymbol{u},h} = -\langle\mathrm{S}_{\boldsymbol{\beta}}(\boldsymbol{\varepsilon}^{\boldsymbol{u}} - \boldsymbol{\varepsilon}^{\widehat{\boldsymbol{u}}}), \boldsymbol{\phi}\rangle_{\Gamma_h}, \quad \mathbb{T}^{11}_{\boldsymbol{u},h} = -\langle\tilde{\boldsymbol{g}} - \tilde{\boldsymbol{g}}_h, \mathbf{P}_M(\phi\boldsymbol{n})\rangle_{\Gamma_h},\\
\mathbb{T}^{12}_{\boldsymbol{u},h} &= -\frac{1}{2}\left\langle\left(\boldsymbol{\varepsilon}^{\widehat{\boldsymbol{u}}} \otimes \boldsymbol{\beta}\right)\boldsymbol{n}, \boldsymbol{\phi}\right\rangle_{\Gamma_h}, \quad \mathbb{T}^{13}_{\boldsymbol{u},h} = -\frac{1}{2}\left\langle\left(\boldsymbol{\varepsilon}^{\boldsymbol{u}} \otimes \boldsymbol{\beta}\right)\boldsymbol{n}, \boldsymbol{\phi}\right\rangle_{\Gamma_h}.
\end{aligned}$$

Proof. Let us begin by noting that we can rewrite $\mathbb{T}_{\boldsymbol{u},h}$ as follows:

$$\begin{aligned}
\mathbb{T}_{\boldsymbol{u},h} &= \langle\nu\mathrm{E}^{\mathrm{L}}\boldsymbol{n} - \varepsilon^p\boldsymbol{n} - \mathrm{S}_{\boldsymbol{\beta}}(\boldsymbol{\varepsilon}^{\boldsymbol{u}} - \boldsymbol{\varepsilon}^{\widehat{\boldsymbol{u}}}), \boldsymbol{\phi}\rangle_{\Gamma_h} - \langle\boldsymbol{\varepsilon}^{\widehat{\boldsymbol{u}}}, \nu\Phi\boldsymbol{n}\rangle_{\Gamma_h} - \langle\boldsymbol{\varepsilon}^{\widehat{\boldsymbol{u}}}, \phi\boldsymbol{n}\rangle_{\Gamma_h}\\
&\quad -\frac{1}{2}\langle(\boldsymbol{\beta}\cdot\boldsymbol{n})\boldsymbol{\varepsilon}^{\boldsymbol{u}}, \boldsymbol{\phi}\rangle_{\Gamma_h} - \frac{1}{2}\langle(\boldsymbol{\beta}\cdot\boldsymbol{n})\boldsymbol{\varepsilon}^{\widehat{\boldsymbol{u}}}, \boldsymbol{\phi}\rangle_{\Gamma_h}
\end{aligned}$$

We use now that $\boldsymbol{\varepsilon}^{\widehat{\boldsymbol{u}}} = \mathbf{P}_M(\widetilde{\boldsymbol{g}} - \widetilde{\boldsymbol{g}}_h)$ on $\partial\mathsf{T}_h$ and the fact that $\mathrm{E}^{\mathrm{L}}\boldsymbol{n} = -(\widetilde{\boldsymbol{g}} - \widetilde{\boldsymbol{g}}_h)/l - \delta_{\mathrm{I}^{\mathrm{L}}} - \mathrm{I}^{\mathrm{L}}\boldsymbol{n} - \delta_{\mathrm{E}^{\mathrm{L}}}$ (as we already saw in the proof of Lemma 3.8), to obtain

$$\begin{aligned}
\mathbb{T}_{\boldsymbol{u},h} &= -\nu\langle(\widetilde{\boldsymbol{g}} - \widetilde{\boldsymbol{g}}_h)/l, \boldsymbol{\phi}\rangle_{\Gamma_h} - \nu\langle\delta_{\mathrm{I}^{\mathrm{L}}}, \boldsymbol{\phi}\rangle_{\Gamma_h} - \nu\langle\mathrm{I}^{\mathrm{L}}\boldsymbol{n}, \boldsymbol{\phi}\rangle_{\Gamma_h} - \nu\langle\delta_{\mathrm{E}^{\mathrm{L}}}, \boldsymbol{\phi}\rangle_{\Gamma_h}\\
&\quad -\langle\varepsilon^p\boldsymbol{n}, \boldsymbol{\phi}\rangle_{\Gamma_h} - \langle\mathrm{S}_{\boldsymbol{\beta}}(\boldsymbol{\varepsilon}^{\boldsymbol{u}} - \boldsymbol{\varepsilon}^{\widehat{\boldsymbol{u}}}), \boldsymbol{\phi}\rangle_{\Gamma_h} - \langle\tilde{\boldsymbol{g}} - \tilde{\boldsymbol{g}}_h, \nu\mathbf{P}_M(\Phi\boldsymbol{n})\rangle_{\Gamma_h}\\
&\quad -\langle\widetilde{\boldsymbol{g}} - \widetilde{\boldsymbol{g}}_h, \mathbf{P}_M(\phi\boldsymbol{n})\rangle_{\Gamma_h} - \frac{1}{2}\langle(\boldsymbol{\beta}\cdot\boldsymbol{n})\boldsymbol{\varepsilon}^{\boldsymbol{u}}, \boldsymbol{\phi}\rangle_{\Gamma_h} - \frac{1}{2}\langle(\boldsymbol{\beta}\cdot\boldsymbol{n})\boldsymbol{\varepsilon}^{\widehat{\boldsymbol{u}}}, \boldsymbol{\phi}\rangle_{\Gamma_h}.
\end{aligned} \tag{3.46}$$

We can associate the first and seventh terms. In addition, adding and subtracting $l\nabla\boldsymbol{\phi}\boldsymbol{n}$, and using (3.22a), we have

$$\begin{aligned}
-\nu\langle(\widetilde{\boldsymbol{g}} - \widetilde{\boldsymbol{g}}_h)/l, \boldsymbol{\phi}\rangle_{\Gamma_h} + l\mathbf{P}_M(\Phi\boldsymbol{n})\rangle_{\Gamma_h} &= -\nu\langle(\widetilde{\boldsymbol{g}} - \widetilde{\boldsymbol{g}}_h)/l, \boldsymbol{\phi} + l\nabla\boldsymbol{\phi}\boldsymbol{n} - l\nabla\boldsymbol{\phi}\boldsymbol{n} + l\mathbf{P}_M(\Phi\boldsymbol{n})\rangle_{\Gamma_h}\\
&= -\nu\langle(\widetilde{\boldsymbol{g}} - \widetilde{\boldsymbol{g}}_h)/l, \boldsymbol{\phi} + l\nabla\boldsymbol{\phi}\boldsymbol{n}\rangle_{\Gamma_h} + \nu\left\langle\widetilde{\boldsymbol{g}} - \widetilde{\boldsymbol{g}}_h, \nabla\boldsymbol{\phi}\boldsymbol{n} - \mathbf{P}_M\big(\nabla\boldsymbol{\phi}\boldsymbol{n}\big)\right\rangle_{\Gamma_h}.
\end{aligned}$$

On the other hand, using (3.24d) with $\boldsymbol{\mu} = \mathbf{P}_M\boldsymbol{\phi}$, we can write

$$\begin{aligned}
\nu\langle\mathrm{I}^{\mathrm{L}}\boldsymbol{n}, \boldsymbol{\phi}\rangle_{\Gamma_h} &= \nu\langle\mathrm{I}^{\mathrm{L}}\boldsymbol{n}, \boldsymbol{\phi} - \mathbf{P}_M\boldsymbol{\phi}\rangle_{\Gamma_h} + \nu\langle\mathrm{I}^{\mathrm{L}}\boldsymbol{n}, \mathbf{P}_M\boldsymbol{\phi}\rangle_{\Gamma_h}\\
&= \nu\langle\mathrm{I}^{\mathrm{L}}\boldsymbol{n}, \boldsymbol{\phi} - \mathbf{P}_M\boldsymbol{\phi}\rangle_{\Gamma_h} + \langle I^p\boldsymbol{n}, \mathbf{P}_M\boldsymbol{\phi}\rangle_{\Gamma_h} + \langle\mathrm{S}\boldsymbol{I}^{\boldsymbol{u}}, \mathbf{P}_M\boldsymbol{\phi}\rangle_{\Gamma_h}\\
&\quad + \left\langle\left(\boldsymbol{I}^{\boldsymbol{u}}_M \otimes \boldsymbol{\beta}\right)\boldsymbol{n}, \mathbf{P}_M\boldsymbol{\phi}\right\rangle_{\Gamma_h}.
\end{aligned}$$

Finally, replacing these two expressions in (3.46), we obtain

$$\begin{aligned}
\mathbb{T}_{\boldsymbol{u},h} &= -\nu\langle(\widetilde{\boldsymbol{g}} - \widetilde{\boldsymbol{g}}_h)/l, \boldsymbol{\phi} + l\nabla\boldsymbol{\phi}\boldsymbol{n}\rangle_{\Gamma_h} + \nu\left\langle\widetilde{\boldsymbol{g}} - \widetilde{\boldsymbol{g}}_h, \nabla\boldsymbol{\phi}\boldsymbol{n} - \mathbf{P}_M\big(\nabla\boldsymbol{\phi}\boldsymbol{n}\big)\right\rangle_{\Gamma_h} - \nu\langle\delta_{\mathrm{I}^{\mathrm{L}}}, \boldsymbol{\phi}\rangle_{\Gamma_h}\\
&\quad -\nu\langle\mathrm{I}^{\mathrm{L}}\boldsymbol{n}, \boldsymbol{\phi} - \mathbf{P}_M\boldsymbol{\phi}\rangle_{\Gamma_h} - \langle I^p\boldsymbol{n}, \mathbf{P}_M\boldsymbol{\phi}\rangle_{\Gamma_h} - \langle\mathrm{S}\boldsymbol{I}^{\boldsymbol{u}}, \mathbf{P}_M\boldsymbol{\phi}\rangle_{\Gamma_h}\\
&\quad -\left\langle\left(\boldsymbol{I}^{\boldsymbol{u}}_M \otimes \boldsymbol{\beta}\right)\boldsymbol{n}, \mathbf{P}_M\boldsymbol{\phi}\right\rangle_{\Gamma_h} - \nu\langle\delta_{\mathrm{E}^{\mathrm{L}}}, \boldsymbol{\phi}\rangle_{\Gamma_h} - \langle\varepsilon^p\boldsymbol{n}, \boldsymbol{\phi}\rangle_{\Gamma_h} - \langle\mathrm{S}_{\boldsymbol{\beta}}(\boldsymbol{\varepsilon}^{\boldsymbol{u}} - \boldsymbol{\varepsilon}^{\widehat{\boldsymbol{u}}}), \boldsymbol{\phi}\rangle_{\Gamma_h}\\
&\quad -\langle\widetilde{\boldsymbol{g}} - \widetilde{\boldsymbol{g}}_h, \mathbf{P}_M(\phi\boldsymbol{n})\rangle_{\Gamma_h} - \frac{1}{2}\langle(\boldsymbol{\beta}\cdot\boldsymbol{n})\boldsymbol{\varepsilon}^{\boldsymbol{u}}, \boldsymbol{\phi}\rangle_{\Gamma_h} - \frac{1}{2}\langle(\boldsymbol{\beta}\cdot\boldsymbol{n})\boldsymbol{\varepsilon}^{\widehat{\boldsymbol{u}}}, \boldsymbol{\phi}\rangle_{\Gamma_h},
\end{aligned}$$

which completes the proof. □

Step 3: Estimate of $\mathbb{T}_{\boldsymbol{u},h}$, T_{L} and $T_{\boldsymbol{\beta}}$

The next lemma establishes the estimate of $\mathbb{T}_{\boldsymbol{u},h}$, T_{L} and $T_{\boldsymbol{\beta}}$.

Lemma 3.15. *It holds that*

$$\begin{aligned}
|\mathbb{T}_{\boldsymbol{u},h}| &\lesssim h^{1/2}H_{\boldsymbol{\varepsilon}^{\boldsymbol{u}}}(R,h)\Theta_{\mathrm{I}^{\mathrm{L}}}\|\boldsymbol{\theta}\|_{\Omega} + h^{1/2}\left\{R^2h^{3/2}+Rh^{1/2}+R^{1/2}+R^{3/2}h+R\right\}\|\boldsymbol{\varepsilon}^{\boldsymbol{u}}\|_{\mathsf{D}_h}\|\boldsymbol{\theta}\|_{\Omega}\\
&\quad+\left\{\nu^{-1}Rh^{1/2}\|I^p\|_{\mathsf{D}_h}+\tau Rh^{1/2}\|\boldsymbol{I}^{\boldsymbol{u}}\|_{\mathsf{D}_h}+\nu Rh\|\boldsymbol{\beta}\|_{L^\infty(\Omega)}\|\boldsymbol{I}^{\boldsymbol{u}}_M\|_{L^2(\Gamma_h)}\right\}\|\boldsymbol{\theta}\|_{\Omega},\\
|T_{\mathrm{L}}| &\lesssim H_L\Theta_{\mathrm{I}^{\mathrm{L}}}\|\boldsymbol{\theta}\|_{\Omega}+H_L\|\boldsymbol{\varepsilon}^{\boldsymbol{u}}\|_{\mathsf{D}_h}\|\boldsymbol{\theta}\|_{\Omega},\ \textit{and}\\
|T_{\boldsymbol{\beta}}| &\leq H_{\boldsymbol{\beta}}\|\boldsymbol{I}^{\boldsymbol{u}}\|_{\mathsf{D}_h}\|\boldsymbol{\theta}\|_{\Omega}.
\end{aligned}$$

Proof. The bound for $\mathbb{T}_{\boldsymbol{u},h}$ is similar to the last part of Lemma 3.4, when we bounded the term $\mathrm{T}_{\boldsymbol{u}}$. By Lemma 3.14, we know that $\mathbb{T}_{\boldsymbol{u},h}=\sum_{i=1}^{13}\mathbb{T}^i_{\boldsymbol{u},h}$. We first apply the Cauchy-Schwarz inequality to each term $\mathbb{T}^i_{\boldsymbol{u},h}$. The first estimate follows from estimate in (2.21), Lemma 2.14, Assumption A, the fact that $\|I^p\boldsymbol{n}\|_{\Gamma_h,l^2}\leq Rh^{1/2}\|I^p\boldsymbol{n}\|_{\Gamma_h,h^\perp}$, the interpolation properties (3.35) and estimates (3.43) and (3.44).
On the other hand, from the definition of T_{L}, using Cauchy-Schwarz inequality and estimate (3.44) we have

$$\begin{aligned}
|T_{\mathrm{L}}| &\leq \left|(\mathrm{L}-\mathrm{L}_h,\nu\Pi^*\Phi-\nu\Phi)_{\mathsf{T}_h}\right|+\left|(\nu\mathrm{L}-\nu\Pi\mathrm{L},\nabla(\phi_h-\phi))_{\mathsf{T}_h}\right|\\
&\leq \nu\Big(\|\mathrm{E}^{\mathrm{L}}\|_{\mathsf{D}_h}+\|\mathrm{I}^{\mathrm{L}}\|_{\mathsf{D}_h}\Big)\|\Pi^*\Phi-\Phi\|_{\mathsf{T}_h}+\nu\|\mathrm{I}^{\mathrm{L}}\|_{\mathsf{D}_h}\|\nabla(\phi_h-\phi)\|_{\mathsf{T}_h}\\
&= \nu\Big(\|\Pi^*\Phi-\Phi\|_{\mathsf{T}_h}+\|\nabla(\phi_h-\phi)\|_{\mathsf{T}_h}\Big)\|\mathrm{I}^{\mathrm{L}}\|_{\mathsf{D}_h}+\nu\|\mathrm{E}^{\mathrm{L}}\|_{\mathsf{D}_h}\|\Pi^*\Phi-\Phi\|_{\mathsf{T}_h}\\
&\lesssim \nu\left\{\frac{\|\Pi^*\Phi-\Phi\|_{\mathsf{T}_h}}{\|\boldsymbol{\theta}\|_{\Omega}}+\frac{\|\nabla(\phi_h-\phi)\|_{\mathsf{T}_h}}{\|\boldsymbol{\theta}\|_{\Omega}}\right\}\|\mathrm{I}^{\mathrm{L}}\|_{\mathsf{D}_h}\|\boldsymbol{\theta}\|_{\Omega}+\frac{\|\Pi^*\Phi-\Phi\|_{\mathsf{T}_h}}{\|\boldsymbol{\theta}\|_{\Omega}}\|\boldsymbol{\varepsilon}^{\boldsymbol{u}}\|_{\mathsf{D}_h}\|\boldsymbol{\theta}\|_{\Omega}\\
&\lesssim H_L\Theta_{\mathrm{I}^{\mathrm{L}}}\|\boldsymbol{\theta}\|_{\Omega}+H_L\|\boldsymbol{\varepsilon}^{\boldsymbol{u}}\|_{\mathsf{D}_h}\|\boldsymbol{\theta}\|_{\Omega}.
\end{aligned}$$

Analogously,

$$|T_{\boldsymbol{\beta}}|=\left|\left((\boldsymbol{u}-\boldsymbol{\Pi}\boldsymbol{u})\otimes\boldsymbol{\delta\beta},\nabla\boldsymbol{\phi}_h\right)_{\mathsf{T}_h}\right|\leq\|\boldsymbol{\delta\beta}\|_{L^\infty(\Omega)}\|\boldsymbol{I}^{\boldsymbol{u}}\|_{\mathsf{D}_h}\|\nabla\boldsymbol{\phi}_h\|_{\mathsf{T}_h}\leq H_{\boldsymbol{\beta}}\|\boldsymbol{I}^{\boldsymbol{u}}\|_{\mathsf{D}_h}\|\boldsymbol{\theta}\|_{\Omega},$$

which ends the proof. □

Step 4: Proof of Lemma 2.11

Dividing the identity of Lemma 3.13 by $\|\boldsymbol{\theta}\|_{\Omega},\boldsymbol{\theta}\neq\mathbf{0}$, taking the supremum over $\boldsymbol{\theta}$ and using the estimates of Lemma 3.15, we obtain

$$\begin{aligned}
\|\boldsymbol{\varepsilon}^{\boldsymbol{u}}\|_{\mathsf{D}_h} &\lesssim \left\{H_L+h^{1/2}H_{\boldsymbol{\varepsilon}^{\boldsymbol{u}}}(R,h)\right\}\Theta_{\mathrm{I}^{\mathrm{L}}}+\nu^{-1}Rh^{1/2}\|I^p\|_{\mathsf{D}_h}\\
&\quad+\left\{(\tau Rh^{1/2}+H_{\boldsymbol{\beta}})\|\boldsymbol{I}^{\boldsymbol{u}}\|_{\mathsf{D}_h}+\nu Rh\|\boldsymbol{\beta}\|_{L^\infty(\Omega)}\|\boldsymbol{I}^{\boldsymbol{u}}_M\|_{L^2(\Gamma_h)}\right\}\\
&\quad+\left\{H_L+R^2h^2+Rh+R^{1/2}h^{1/2}+R^{3/2}h^{3/2}+Rh^{1/2}\right\}\|\boldsymbol{\varepsilon}^{\boldsymbol{u}}\|_{\mathsf{D}_h}.
\end{aligned}$$

According to (3.45), for h small enough and $k \geq 1$ we have $H_L \lesssim h$ and $H_{\boldsymbol{\beta}} \lesssim h$. In such a case, the term multiplying $\|\boldsymbol{\varepsilon}^{\boldsymbol{u}}\|_{\mathsf{D}_h}$ contains only positive powers of h and hence, for h small enough, that term is less than $1/2$. Thus, rearranging terms, we obtain

$$\begin{aligned}\|\boldsymbol{\varepsilon}^{\boldsymbol{u}}\|_{\mathsf{D}_h} \lesssim\ & h^{1/2} H_{\boldsymbol{\varepsilon}^{\boldsymbol{u}}}(R,h)\Theta_{\mathrm{IL}} + h^{1/2}\left\{\nu^{-1}R\|I^p\|_{\mathsf{D}_h} + (\tau R + h^{1/2})\|\boldsymbol{I}^{\boldsymbol{u}}\|_{\mathsf{D}_h}\right\} \\ & + \nu R h \|\boldsymbol{\beta}\|_{L^\infty(\Omega)}\|\boldsymbol{I}^{\boldsymbol{u}}_M\|_{L^2(\Gamma_h)}.\end{aligned}$$

3.4.3 Conclusion of the proof of Theorem 3.5

First of all, adding and subtracting $\Pi\mathrm{L}$ and $I\widetilde{p}$, using the triangle inequality, estimates (3.43) and (3.44), and recalling the definition of Θ_{IL} in (3.36), we get

$$\|\mathrm{L} - \mathrm{L}_h\|_{\mathsf{D}_h} + \|\widetilde{\boldsymbol{g}} - \widetilde{\boldsymbol{g}}_h\|_{\Gamma_h,l^{-1}} + \nu^{-1}\|\widetilde{p} - \widetilde{p}_h\|_{\mathsf{D}_h} \lesssim \Theta_{\mathrm{IL}} + \|\boldsymbol{\varepsilon}^{\boldsymbol{u}}\|_{\mathsf{D}_h} + \nu^{-1}\|I^p\|_{\mathsf{D}_h}.$$

Moreover, if Assumption B holds, by adding and subtracting $\boldsymbol{I\!I}\,\boldsymbol{u}$, using triangle inequality and Lemma 3.12, we obtain

$$\begin{aligned}\|\boldsymbol{u} - \boldsymbol{u}_h\|_{\mathsf{D}_h} \lesssim\ & h^{1/2} H_{\boldsymbol{\varepsilon}^{\boldsymbol{u}}}(R,h)\Theta_{\mathrm{IL}} + \nu^{-1}Rh^{1/2}\|I^p\|_{\mathsf{D}_h} \\ & + (\tau R h^{1/2} + h + 1)\|\boldsymbol{I}^{\boldsymbol{u}}\|_{\mathsf{D}_h} + \nu R h\|\boldsymbol{\beta}\|_{L^\infty(\Omega)}\|\boldsymbol{I}^{\boldsymbol{u}}_M\|_{L^2(\Gamma_h)}.\end{aligned}$$

Lemma 3.7 in [18] states that $\|\boldsymbol{\varepsilon}^{\widehat{\boldsymbol{u}}}\|_h \lesssim h\|\mathrm{I}^{\mathrm{L}}\|_{\mathsf{D}_h} + h\|\mathrm{E}^{\mathrm{L}}\|_{\mathsf{D}_h} + \|\boldsymbol{\varepsilon}^{\boldsymbol{u}}\|_{\mathsf{D}_h}$. This, together with the definition of Θ_{IL}, estimate (3.44) and Lemma 3.12, implies

$$\begin{aligned}\|\mathbf{P}_M\boldsymbol{u} - \widehat{\boldsymbol{u}}_h\|_h \lesssim\ & h^{1/2}\left\{(h^{1/2} + (1+h)H_{\boldsymbol{\varepsilon}^{\boldsymbol{u}}}(R,h)\right\}\Theta_{\mathrm{IL}} + h^{1/2}(1+h)\nu^{-1}R\|I^p\|_{\mathsf{D}_h} \\ & + h^{1/2}(1+h)\left\{(\tau R + h^{1/2})\|\boldsymbol{I}^{\boldsymbol{u}}\|_{\mathsf{D}_h} + \nu R h^{1/2}\|\boldsymbol{\beta}\|_{L^\infty(\Omega)}\|\boldsymbol{I}^{\boldsymbol{u}}_M\|_{L^2(\Gamma_h)}\right\}.\end{aligned}$$

The error estimate $\|\boldsymbol{u} - \boldsymbol{u}^*_h\|_{\mathsf{D}_h} \leq \|\boldsymbol{\varepsilon}^{\boldsymbol{u}}\|_{\mathsf{D}_h} + Ch\|\mathrm{L} - \mathrm{L}_h\|_{\mathsf{D}_h} + Ch^{k+2}|\mathrm{L}|_{\mathrm{H}^{k+1}(\Omega)}$ can be found in [19] and, from Lemma 3.12, follows that

$$\begin{aligned}\|\boldsymbol{u} - \boldsymbol{u}^*_h\|_{\mathsf{D}_h} \lesssim\ & h^{1/2} H_{\boldsymbol{\varepsilon}^{\boldsymbol{u}}}(R,h)\Theta_{\mathrm{IL}} + h^{1/2}\left\{\nu^{-1}R\|I^p\|_{\mathsf{D}_h} + (\tau R + h^{1/2})\|\boldsymbol{I}^{\boldsymbol{u}}\|_{\mathsf{D}_h}\right\} \\ & + h^{1/2}\left\{h^{1/2}\Big(\nu R\|\boldsymbol{\beta}\|_{L^\infty(\Omega)}\|\boldsymbol{I}^{\boldsymbol{u}}_M\|_{L^2(\Gamma_h)} + \|\mathrm{L} - \mathrm{L}_h\|_{\mathsf{D}_h} + h|\mathrm{L}|_{\mathrm{H}^{k+1}(\Omega)}\Big)\right\}.\end{aligned}$$

Hence, since τ is of order one, we observe that if R is of order one, then $H_{\boldsymbol{\varepsilon}^{\boldsymbol{u}}}(R,h)$ is also of order one, whereas if R is of order h, $H_{\boldsymbol{\varepsilon}^{\boldsymbol{u}}}(R,h)$ is of order $h^{1/2}$. The estimates of Theorem 3.5 follow from the fact that Θ_{IL} and the interpolation errors are of order h^{k+1}.

3.5 Numerical results

In this section we present two-dimensional numerical experiments to validate the theoretical orders of convergence of the approximations provided by the HDG method. In order to satisfy (3.4), in all our experiments we choose $\tau = \dfrac{1}{2\nu}\max_{\boldsymbol{x}\in\mathsf{T}_h}\boldsymbol{\beta}(\boldsymbol{x})\cdot\boldsymbol{n} + 1$. We compute the errors $e_p := \|p - p_h\|_\Omega$, $e_{\boldsymbol{u}} := \|\boldsymbol{u} - \boldsymbol{u}_h\|_\Omega$,

$e_{\mathrm{L}} := \|\mathrm{L} - \mathrm{L}_h\|_\Omega$, $e_{\widehat{\boldsymbol{u}}} := \left\{ \sum_{K\in\mathsf{D}_h} h_K \|\mathbf{P}_M \boldsymbol{u} - \widehat{\boldsymbol{u}}_h\|_{\partial K} \right\}^{1/2}$ and $e_{\boldsymbol{u}^*} := \left\{ \|\boldsymbol{u} - \boldsymbol{u}_h^*\|^2_{\mathsf{D}_h} + \|\boldsymbol{u} - \boldsymbol{u}_h\|^2_{\mathsf{D}_h^c} \right\}^{1/2}$ and, in addition, for each variable, we calculate the experimental order of convergence e.o.c. $= -2\dfrac{\log\left(e_{\mathcal{T}_1}/e_{\mathcal{T}_2}\right)}{\log(N_{\mathcal{T}_1}/N_{\mathcal{T}_2})}$, where $e_{\mathcal{T}_1}$ and $e_{\mathcal{T}_2}$ are the errors associated to the corresponding variable considering two consecutive meshes with $N_{\mathcal{T}_1}$ and $N_{\mathcal{T}_2}$ elements, respectively.

3.5.1 Example 1: $\mathrm{dist}(\Gamma_h, \Gamma)$ of order h^2

In this example, we consider the circular domain $\Omega = \{(x,y) \in \mathbb{R}^2 : x^2 + y^2 < 0.75^2\}$. The computational boundary Γ_h is constructed by interpolating $\partial\Omega$ by a piecewise linear function and D_h is the domain enclosed by Γ_h. In this case all the assumptions are satisfied.

The source term $\boldsymbol{f}$ and boundary data $\boldsymbol{g}$ are such that the exact solution is

$$p(x,y) = \sin(x^2+y^2) + \frac{\cos(0.75^2) - 1}{0.75^2}, \quad \boldsymbol{u}(x,y) = \begin{bmatrix} \sin(x)\sin(y) \\ \cos(x)\cos(y) \end{bmatrix},$$

and the convective velocity is chosen to be $\boldsymbol{\beta}(x,y) = \begin{bmatrix} 1 \\ 1 \end{bmatrix}$. We will also consider different values of ν to see how it affects the results. Tables 3.1, 3.2 and 3.3 show the results for $\nu = 1, 0.1$ and 0.01, resp. In this case, since we are interpolating the curved boundary with a piecewise linear computational boundary, the predicted results by the theory are order h^{k+1} for the pressure, velocity and its gradient, whereas the numerical trace and postprocessed velocity are predicted to converge with order h^{k+2}. We observe that those predicted orders are attained when $\nu = 1$, but the experimental orders deteriorate when ν decreases. This might happen because negative powers of ν appear in some of the estimates of the errors (see section 3.4.3).

3.5.2 Example 2: $\mathrm{dist}(\Gamma_h, \Gamma)$ of order h

In this example we consider $\Omega := \left\{(x,y) \in \mathbb{R}^2_+ : 1.4 < \sqrt{x^2+y^2} < 2\right\}$ and the exact solution

$$p(x,y) = e^{x^2+y^2} - (e^{2^2} - e^{1.4^2})/(2^2 - 1.4^2), \quad \boldsymbol{u}(x,y) = \begin{bmatrix} \sin(3x)e^y \\ -3\cos(3x)e^y \end{bmatrix}.$$

The convective velocity $\boldsymbol{\beta}$ and the viscosity ν are chosen as in Example 1. The computational domain D_h is set in such a way that $r_e = 1, \forall e \in \Gamma_h \setminus \{(x,y) : x = 0 \vee y = 0\}$. According to Theorem 3.5, the predicted orders of convergence for this example are h^{k+1} for the pressure, velocity and its gradient, and $h^{k+3/2}$ for the numerical trace and the postprocessed velocity. In Tables 3.4, 3.5 and 3.6 we observe the same behavior of the experimental orders of convergence for the different values of ν that we observed in Example 1, this is, the orders predicted by the theory are attained when $\nu = 1$, but deteriorate when ν becomes smaller.

k	N	e_p	order	$e_{\boldsymbol{u}}$	order	e_{L}	order	$e_{\widehat{\boldsymbol{u}}}$	order	$e_{\boldsymbol{u}^*}$	order
1	60	2.94e-02	–	3.66e-03	–	2.97e-02	–	6.95e-03	–	1.95e-03	–
	129	9.48e-03	2.96	1.35e-03	2.60	1.32e-02	2.11	1.78e-03	3.55	4.83e-04	3.65
	234	4.43e-03	2.55	7.09e-04	2.17	7.46e-03	1.92	7.21e-04	3.04	1.91e-04	3.12
	485	2.27e-03	1.83	3.54e-04	1.91	3.85e-03	1.81	2.64e-04	2.75	7.10e-05	2.71
	918	1.15e-03	2.12	1.75e-04	2.21	1.95e-03	2.13	9.52e-05	3.20	2.53e-05	3.24
	1764	5.69e-04	2.17	8.85e-05	2.08	1.01e-03	2.00	3.53e-05	3.04	9.47e-06	3.01
	3546	2.82e-04	2.01	4.46e-05	1.96	5.21e-04	1.91	1.33e-05	2.80	3.60e-06	2.77
	7089	1.44e-04	1.93	2.24e-05	1.99	2.63e-04	1.97	4.79e-06	2.94	1.32e-06	2.90
	14291	7.20e-05	1.98	1.11e-05	1.99	1.33e-04	1.96	1.72e-06	2.93	4.72e-07	2.93
2	60	6.99e-04	–	1.23e-04	–	8.35e-04	–	1.20e-04	–	4.77e-05	–
	129	1.51e-04	4.00	2.61e-05	4.05	1.90e-04	3.87	1.41e-05	5.59	6.62e-06	5.16
	234	4.79e-05	3.87	9.32e-06	3.46	7.05e-05	3.33	3.71e-06	4.49	1.87e-06	4.25
	485	1.47e-05	3.23	2.94e-06	3.16	2.27e-05	3.11	8.56e-07	4.02	4.30e-07	4.03
	918	5.31e-06	3.20	1.09e-06	3.11	8.36e-06	3.12	2.34e-07	4.06	1.20e-07	4.01
	1764	2.00e-06	2.98	4.15e-07	2.96	3.16e-06	2.98	6.46e-08	3.94	3.34e-08	3.91
	3546	7.40e-07	2.85	1.51e-07	2.90	1.17e-06	2.84	1.80e-08	3.66	9.15e-09	3.71
	7089	2.55e-07	3.08	5.25e-08	3.05	4.08e-07	3.05	4.46e-09	4.03	2.25e-09	4.05
	14291	9.16e-08	2.92	1.88e-08	2.93	1.47e-07	2.91	1.19e-09	3.76	5.89e-10	3.82
3	60	6.42e-05	–	6.71e-06	–	5.12e-05	–	5.65e-06	–	2.06e-06	–
	129	8.83e-06	5.18	1.01e-06	4.95	7.58e-06	4.99	5.17e-07	6.25	2.03e-07	6.06
	234	1.87e-06	5.21	2.77e-07	4.34	1.94e-06	4.57	9.09e-08	5.84	3.94e-08	5.50
	485	3.97e-07	4.26	7.19e-08	3.70	4.84e-07	3.81	1.64e-08	4.69	7.74e-09	4.47
	918	1.06e-07	4.15	1.76e-08	4.42	1.20e-07	4.38	2.96e-09	5.38	1.33e-09	5.51
	1764	2.79e-08	4.07	4.37e-09	4.26	3.04e-08	4.20	5.35e-10	5.23	2.35e-10	5.32
	3546	7.65e-09	3.71	1.15e-09	3.83	8.17e-09	3.76	1.10e-10	4.53	4.62e-11	4.66
	7089	1.88e-09	4.05	2.91e-10	3.96	2.07e-09	3.96	1.96e-11	4.98	8.42e-12	4.92
	14291	4.87e-10	3.85	7.29e-11	3.95	5.28e-10	3.90	3.65e-12	4.80	1.53e-12	4.87

Table 3.1: History of convergence of Example 1 with $\nu = 1$.

3.5.3 Example 3: Other choice of transferring paths

As we did in section 2.6.3 of chapter 2, we want to see if our method works even though some of the assumtions are not necessarily satisfied. We consider again a kidney-shaped domain whose boundary satisfies the equation

$$(2[(x+0.5)^2+y^2]-x-0.5)^2-[(x+0.5)^2+y^2]+0.1=0$$

and a triangulation of a background domain $\mathcal{B}$ such that $\Omega \subset \mathcal{B}$. We set D_h as the union of all the elements inside Ω. The family of transferring paths is constructed by the procedure in Section 2.4.1 of [23] and, as we did in section 2.6.3, instead of (1.2), we use the boundary data 2.31.

k	N	e_p	order	$e_{\boldsymbol{u}}$	order	e_{L}	order	$e_{\widehat{\boldsymbol{u}}}$	order	$e_{\boldsymbol{u}^*}$	order
1	60	2.30e-02	–	6.47e-03	–	1.06e-01	–	2.36e-02	–	6.15e-03	–
	129	7.36e-03	2.98	2.24e-03	2.77	5.76e-02	1.59	7.78e-03	2.90	2.01e-03	2.93
	234	3.64e-03	2.36	1.09e-03	2.44	3.66e-02	1.53	3.54e-03	2.65	9.16e-04	2.64
	485	1.88e-03	1.81	4.94e-04	2.16	2.14e-02	1.47	1.45e-03	2.44	3.74e-04	2.46
	918	9.91e-04	2.01	2.26e-04	2.46	1.23e-02	1.73	5.95e-04	2.79	1.53e-04	2.81
	1764	5.03e-04	2.08	1.08e-04	2.26	7.10e-03	1.69	2.46e-04	2.71	6.40e-05	2.67
	3546	2.54e-04	1.95	5.22e-05	2.08	3.96e-03	1.68	1.00e-04	2.57	2.66e-05	2.52
	7089	1.33e-04	1.86	2.52e-05	2.11	2.14e-03	1.78	3.88e-05	2.73	1.05e-05	2.68
	14291	6.77e-05	1.93	1.21e-05	2.09	1.13e-03	1.81	1.47e-05	2.77	3.99e-06	2.76
2	60	5.95e-04	–	2.29e-04	–	3.19e-03	–	5.07e-04	–	1.93e-04	–
	129	1.35e-04	3.87	4.29e-05	4.38	9.10e-04	3.28	7.52e-05	4.99	3.23e-05	4.68
	234	4.35e-05	3.81	1.48e-05	3.56	3.74e-04	2.98	2.24e-05	4.07	1.03e-05	3.82
	485	1.34e-05	3.23	4.31e-06	3.39	1.34e-04	2.81	5.53e-06	3.84	2.62e-06	3.76
	918	4.89e-06	3.17	1.51e-06	3.29	5.51e-05	2.79	1.64e-06	3.82	8.08e-07	3.69
	1764	1.87e-06	2.94	5.40e-07	3.15	2.27e-05	2.72	4.90e-07	3.69	2.46e-07	3.64
	3546	7.01e-07	2.82	1.86e-07	3.05	8.96e-06	2.66	1.44e-07	3.51	7.12e-08	3.55
	7089	2.44e-07	3.04	6.15e-08	3.20	3.30e-06	2.88	3.77e-08	3.87	1.87e-08	3.85
	14291	8.87e-08	2.89	2.11e-08	3.05	1.24e-06	2.79	1.05e-08	3.65	5.11e-09	3.70
3	60	6.39e-05	–	1.01e-05	–	1.77e-04	–	2.53e-05	–	8.41e-06	–
	129	8.76e-06	5.19	1.38e-06	5.20	3.34e-05	4.35	2.81e-06	5.74	1.01e-06	5.54
	234	1.83e-06	5.26	3.64e-07	4.48	1.03e-05	3.94	5.68e-07	5.37	2.26e-07	5.02
	485	3.77e-07	4.34	9.14e-08	3.79	2.99e-06	3.40	1.11e-07	4.47	4.96e-08	4.16
	918	1.02e-07	4.10	2.11e-08	4.59	8.34e-07	4.00	2.21e-08	5.06	9.57e-09	5.16
	1764	2.73e-08	4.03	5.02e-09	4.40	2.31e-07	3.93	4.31e-09	5.01	1.83e-09	5.07
	3546	7.52e-09	3.70	1.28e-09	3.92	6.65e-08	3.57	9.31e-10	4.39	3.82e-10	4.48
	7089	1.85e-09	4.05	3.15e-10	4.04	1.78e-08	3.81	1.73e-10	4.85	7.30e-11	4.78
	14291	4.82e-10	3.84	7.75e-11	4.01	4.72e-09	3.78	3.33e-11	4.71	1.38e-11	4.76

Table 3.2: History of convergence of Example 1 with $\nu = 0.1$.

In all the simulations the source term $\boldsymbol{f}$ and boundary data $\boldsymbol{g}$ are such that the exact solution is

$$p(x,y) = \sin(x^2+y^2) - c_\Omega \quad \text{and} \quad \boldsymbol{u}(x,y) = \begin{bmatrix} \sin(x)\sin(y) \\ \cos(x)\cos(y) \end{bmatrix},$$

where $c_\Omega := \dfrac{1}{|\Omega|}\displaystyle\int_\Omega \sin(x^2+y^2)\,dx\,dy$ was computed numerically considering a extremely fine triangulation that fits the domain.

The results of this experiment are displayed in tables 3.7, 3.8 and 3.9, for the case of $\nu = 1$, $\nu = 0.1$ and $\nu = 0.01$, respectively. We observe that when $k = 2$, the results seem to oscilate, as well as we

k	N	e_p	order	$e_{\boldsymbol{u}}$	order	e_{L}	order	$e_{\widehat{\boldsymbol{u}}}$	order	$e_{\boldsymbol{u}^*}$	order
1	60	1.86e-02	–	9.38e-03	–	1.46e-01	–	3.72e-02	–	9.64e-03	–
	129	5.98e-03	2.97	3.57e-03	2.53	9.08e-02	1.24	1.40e-02	2.56	3.65e-03	2.54
	234	3.11e-03	2.20	1.81e-03	2.28	6.42e-02	1.16	6.98e-03	2.33	1.83e-03	2.31
	485	1.56e-03	1.90	8.26e-04	2.16	4.36e-02	1.06	3.23e-03	2.11	8.26e-04	2.19
	918	7.97e-04	2.10	3.89e-04	2.36	2.90e-02	1.27	1.51e-03	2.39	3.87e-04	2.38
	1764	4.03e-04	2.09	1.83e-04	2.31	1.94e-02	1.23	7.02e-04	2.34	1.79e-04	2.37
	3546	2.01e-04	2.00	8.75e-05	2.11	1.26e-02	1.23	3.27e-04	2.19	8.32e-05	2.19
	7089	1.06e-04	1.84	4.21e-05	2.11	8.02e-03	1.31	1.49e-04	2.27	3.87e-05	2.21
	14291	5.42e-05	1.92	1.92e-05	2.24	4.98e-03	1.36	6.43e-05	2.39	1.68e-05	2.38
2	60	4.60e-04	–	3.98e-04	–	4.94e-03	–	1.15e-03	–	3.86e-04	–
	129	1.11e-04	3.71	9.53e-05	3.73	1.96e-03	2.42	2.73e-04	3.76	9.25e-05	3.73
	234	4.17e-05	3.30	3.58e-05	3.29	9.10e-04	2.58	9.61e-05	3.51	3.43e-05	3.33
	485	1.20e-05	3.41	9.57e-06	3.62	3.66e-04	2.50	2.52e-05	3.67	9.00e-06	3.67
	918	4.29e-06	3.23	3.26e-06	3.37	1.67e-04	2.47	8.07e-06	3.58	3.01e-06	3.43
	1764	1.62e-06	2.98	1.10e-06	3.32	7.70e-05	2.36	2.57e-06	3.50	9.88e-07	3.42
	3546	5.99e-07	2.85	3.42e-07	3.35	3.42e-05	2.32	7.29e-07	3.61	2.91e-07	3.50
	7089	2.09e-07	3.04	1.08e-07	3.32	1.45e-05	2.47	2.07e-07	3.63	8.73e-08	3.48
	14291	7.63e-08	2.87	3.44e-08	3.28	6.23e-06	2.42	5.78e-08	3.64	2.54e-08	3.52
3	60	5.05e-05	–	1.39e-05	–	3.18e-04	–	5.09e-05	–	1.38e-05	–
	129	7.11e-06	5.12	1.85e-06	5.27	6.76e-05	4.05	6.96e-06	5.20	1.78e-06	5.36
	234	1.59e-06	5.03	4.95e-07	4.42	2.28e-05	3.65	1.64e-06	4.86	4.50e-07	4.61
	485	3.27e-07	4.34	1.25e-07	3.77	7.55e-06	3.03	3.56e-07	4.19	1.09e-07	3.88
	918	9.16e-08	3.99	3.04e-08	4.44	2.44e-06	3.54	7.80e-08	4.76	2.62e-08	4.49
	1764	2.52e-08	3.95	7.19e-09	4.41	7.86e-07	3.47	1.72e-08	4.64	5.90e-09	4.56
	3546	7.04e-09	3.65	1.83e-09	3.92	2.64e-07	3.13	4.10e-09	4.10	1.44e-09	4.04
	7089	1.74e-09	4.04	4.42e-10	4.10	8.25e-08	3.36	8.70e-10	4.48	3.26e-10	4.29
	14291	4.57e-10	3.81	1.05e-10	4.09	2.53e-08	3.37	1.88e-10	4.37	7.14e-11	4.33

Table 3.3: History of convergence of Example 1 with $\nu = 0.01$.

observed for this case in the context of Stokes problem (2). On the other hand, when $\nu = 1$, the orders of convergence of the pressure, velocity and its gradient are $k+1$, and around $k+3/2$ for the numerical trace and postprocessed velocity. These results deteriorate when ν decreases and, for instance, table 3.9 shows that the order of convergence of the gradient of the velocity is lower than 2 when $k = 1$.

k	N	e_p	order	$e_{\boldsymbol{u}}$	order	e_{L}	order	$e_{\widehat{\boldsymbol{u}}}$	order	$e_{\boldsymbol{u}^*}$	order
1	180	2.30e+00	–	8.38e-02	–	2.09e+00	–	1.71e-01	–	4.73e-02	–
	868	4.32e-01	2.12	1.21e-02	2.46	2.93e-01	2.50	2.44e-02	2.47	7.18e-03	2.40
	3780	9.72e-02	2.03	2.44e-03	2.18	7.27e-02	1.89	3.73e-03	2.56	1.11e-03	2.54
	15748	2.25e-02	2.05	5.46e-04	2.09	1.81e-02	1.95	5.28e-04	2.74	1.58e-04	2.72
	64260	5.28e-03	2.06	1.31e-04	2.03	4.47e-03	1.99	7.16e-05	2.84	2.17e-05	2.83
2	180	2.04e-01	–	5.96e-03	–	1.04e-01	–	1.27e-02	–	3.80e-03	–
	868	2.19e-02	2.84	4.63e-04	3.25	1.30e-02	2.65	1.06e-03	3.16	3.18e-04	3.15
	3780	2.33e-03	3.05	3.90e-05	3.36	1.55e-03	2.89	7.81e-05	3.54	2.35e-05	3.54
	15748	2.54e-04	3.11	3.83e-06	3.25	1.84e-04	2.99	5.40e-06	3.74	1.64e-06	3.73
	64260	2.82e-05	3.13	4.31e-07	3.11	2.18e-05	3.03	3.60e-07	3.85	1.10e-07	3.84
3	180	4.70e-02	–	1.77e-03	–	4.78e-02	–	3.19e-03	–	9.42e-04	–
	868	1.28e-03	4.59	1.97e-05	5.72	6.15e-04	5.53	5.45e-05	5.17	1.63e-05	5.16
	3780	6.86e-05	3.97	7.13e-07	4.51	3.78e-05	3.79	2.02e-06	4.48	6.06e-07	4.48
	15748	3.75e-06	4.08	2.72e-08	4.58	2.33e-06	3.91	7.04e-08	4.70	2.13e-08	4.69

Table 3.4: History of convergence of Example 2 with $\nu = 1$.

k	N	e_p	order	$e_{\boldsymbol{u}}$	order	e_{L}	order	$e_{\widehat{\boldsymbol{u}}}$	order	$e_{\boldsymbol{u}^*}$	order
1	180	1.62e+00	–	2.66e-01	–	7.19e+00	–	6.26e-01	–	1.74e-01	–
	868	3.66e-01	1.89	4.59e-02	2.23	1.39e+00	2.09	1.32e-01	1.98	3.89e-02	1.91
	3780	8.43e-02	2.00	8.63e-03	2.27	4.45e-01	1.55	2.58e-02	2.22	7.65e-03	2.21
	15748	1.97e-02	2.04	1.46e-03	2.49	1.31e-01	1.71	4.28e-03	2.52	1.28e-03	2.50
	64260	4.72e-03	2.03	2.39e-04	2.57	3.59e-02	1.84	6.36e-04	2.71	1.92e-04	2.70
2	180	1.75e-01	–	2.48e-02	–	4.90e-01	–	5.58e-02	–	1.66e-02	–
	868	2.04e-02	2.73	2.49e-03	2.92	8.32e-02	2.25	6.53e-03	2.73	1.94e-03	2.73
	3780	2.22e-03	3.01	2.11e-04	3.35	1.23e-02	2.60	5.99e-04	3.25	1.79e-04	3.24
	15748	2.46e-04	3.09	1.62e-05	3.60	1.66e-03	2.81	4.73e-05	3.56	1.42e-05	3.55
	64260	2.79e-05	3.10	1.18e-06	3.72	2.11e-04	2.93	3.39e-06	3.75	1.03e-06	3.74
3	180	5.41e-02	–	1.80e-02	–	4.43e-01	–	3.41e-02	–	1.01e-02	–
	868	1.28e-03	4.76	1.47e-04	6.11	4.53e-03	5.82	4.29e-04	5.56	1.27e-04	5.57
	3780	6.83e-05	3.98	5.84e-06	4.39	3.23e-04	3.59	1.80e-05	4.31	5.36e-06	4.31
	15748	3.71e-06	4.08	2.15e-07	4.63	2.17e-05	3.79	6.75e-07	4.60	2.03e-07	4.59

Table 3.5: History of convergence of Example 2 with $\nu = 0.1$.

3.5.4 Example 4: Solving the steady–state incompressible Navier–Stokes equations through Picard's iteration.

In this example, which is not covered by the error estimates of our work, we explore the performance of the method in solving the steady–state incompressible Navier–Stokes equations, which can be written

k	N	e_p	order	$e_{\boldsymbol{u}}$	order	e_{L}	order	$e_{\widehat{\boldsymbol{u}}}$	order	$e_{\boldsymbol{u}^*}$	order
1	180	1.55e+00	–	3.94e-01	–	1.07e+01	–	9.81e-01	–	2.74e-01	–
	868	3.79e-01	1.79	8.86e-02	1.90	2.97e+00	1.63	2.50e-01	1.74	7.35e-02	1.67
	3780	8.98e-02	1.96	2.24e-02	1.87	1.29e+00	1.13	6.75e-02	1.78	1.99e-02	1.77
	15748	1.99e-02	2.11	5.14e-03	2.07	5.21e-01	1.27	1.60e-02	2.02	4.77e-03	2.00
	64260	4.39e-03	2.15	1.05e-03	2.27	1.91e-01	1.43	3.32e-03	2.24	9.95e-04	2.23
2	180	1.94e-01	–	4.49e-02	–	9.93e-01	–	9.94e-02	–	2.90e-02	–
	868	2.33e-02	2.69	5.55e-03	2.66	1.82e-01	2.16	1.41e-02	2.49	4.18e-03	2.46
	3780	2.55e-03	3.01	6.39e-04	2.94	3.72e-02	2.16	1.78e-03	2.81	5.30e-04	2.81
	15748	2.64e-04	3.18	6.84e-05	3.13	7.14e-03	2.31	2.03e-04	3.05	6.08e-05	3.04
	64260	2.72e-05	3.23	6.51e-06	3.34	1.24e-03	2.49	2.00e-05	3.29	6.04e-06	3.28
3	180	3.60e-02	–	3.45e-02	–	9.02e-01	–	7.04e-02	–	2.05e-02	–
	868	1.70e-03	3.88	4.67e-04	5.47	1.36e-02	5.33	1.25e-03	5.12	3.71e-04	5.10
	3780	9.43e-05	3.93	2.62e-05	3.91	1.37e-03	3.12	7.65e-05	3.80	2.27e-05	3.80
	15748	4.68e-06	4.21	1.28e-06	4.23	1.23e-04	3.38	3.95e-06	4.15	1.18e-06	4.14

Table 3.6: History of convergence of Example 2 with $\nu = 0.01$.

k	N	e_p	order	$e_{\boldsymbol{u}}$	order	e_{L}	order	$e_{\boldsymbol{u}^*}$	order	$e_{\widehat{\boldsymbol{u}}}$	order
1	28	5.79e-02	–	1.06e-03	–	1.83e-02	–	3.03e-03	–	7.88e-04	–
	154	9.50e-03	2.12	2.00e-04	1.96	4.30e-03	1.70	5.68e-04	1.97	1.52e-04	1.93
	712	1.48e-03	2.43	6.93e-05	1.38	1.22e-03	1.65	6.95e-05	2.74	2.28e-05	2.47
	3054	2.72e-04	2.33	1.53e-05	2.07	2.91e-04	1.97	8.30e-06	2.92	2.79e-06	2.89
	12579	4.49e-05	2.54	3.61e-06	2.04	6.36e-05	2.15	9.19e-07	3.11	3.08e-07	3.11
	50877	1.04e-05	2.09	8.86e-07	2.01	1.54e-05	2.03	1.23e-07	2.88	4.09e-08	2.89
2	28	3.72e-03	–	1.20e-04	–	1.47e-03	–	1.62e-04	–	5.09e-05	–
	154	3.79e-04	2.68	1.22e-05	2.69	1.82e-04	2.45	2.67e-05	2.11	8.59e-06	2.09
	712	3.73e-05	3.03	7.57e-07	3.63	2.28e-05	2.71	1.66e-06	3.63	5.35e-07	3.63
	3054	2.98e-05	0.31	2.72e-07	1.41	1.86e-05	0.28	5.98e-07	1.40	1.91e-07	1.41
	12579	1.19e-07	7.80	2.93e-09	6.40	1.12e-07	7.23	2.54e-09	7.71	8.09e-10	7.72
	50877	1.19e-08	3.30	3.38e-10	3.09	1.13e-08	3.28	1.47e-10	4.08	4.68e-11	4.08
3	28	6.34e-02	–	2.30e-03	–	2.63e-02	–	3.63e-03	–	1.21e-03	–
	154	4.01e-05	8.64	1.04e-06	9.04	2.18e-05	8.32	1.98e-06	8.82	6.46e-07	8.84
	712	1.32e-06	4.46	2.12e-08	5.09	7.91e-07	4.33	4.45e-08	4.96	1.44e-08	4.97
	3054	4.00e-08	4.81	3.72e-10	5.55	2.48e-08	4.75	7.48e-10	5.61	2.39e-10	5.63
	12579	1.93e-09	4.28	1.35e-11	4.69	1.33e-09	4.14	2.85e-11	4.62	8.90e-12	4.65
	50877	1.49e-10	3.67	8.47e-13	3.96	7.67e-11	4.08	1.99e-12	3.81	6.37e-13	3.77

Table 3.7: History of convergence of Example 3 with $\nu = 1$.

k	N	e_p	order	$e_{\boldsymbol{u}}$	order	e_{L}	order	$e_{\boldsymbol{u}^*}$	order	$e_{\widehat{\boldsymbol{u}}}$	order
1	28	3.98e-02	–	4.52e-03	–	8.45e-02	–	1.37e-02	–	3.51e-03	–
	154	8.44e-03	1.82	1.20e-03	1.56	2.65e-02	1.36	3.73e-03	1.52	1.04e-03	1.43
	712	1.77e-03	2.04	3.12e-04	1.76	1.01e-02	1.26	6.97e-04	2.19	2.24e-04	2.00
	3054	2.67e-04	2.60	3.74e-05	2.91	2.51e-03	1.92	7.78e-05	3.01	2.56e-05	2.98
	12579	4.13e-05	2.64	5.48e-06	2.71	5.79e-04	2.07	8.65e-06	3.10	2.87e-06	3.09
	50877	9.92e-06	2.04	1.10e-06	2.30	1.47e-04	1.97	1.24e-06	2.79	4.10e-07	2.79
2	28	8.39e-04	–	2.22e-04	–	3.05e-03	–	2.94e-04	–	9.39e-05	–
	154	1.13e-04	2.35	2.84e-05	2.41	4.78e-04	2.17	6.03e-05	1.86	1.95e-05	1.85
	712	1.98e-05	2.28	2.53e-06	3.16	1.02e-04	2.01	5.30e-06	3.18	1.70e-06	3.18
	3054	7.34e-06	1.36	6.20e-07	1.93	4.56e-05	1.11	1.36e-06	1.87	4.34e-07	1.88
	12579	1.07e-07	5.97	7.54e-09	6.23	8.57e-07	5.61	1.78e-08	6.12	5.63e-09	6.14
	50877	1.11e-08	3.25	5.27e-10	3.81	9.29e-08	3.18	1.08e-09	4.02	3.41e-10	4.02
3	28	2.87e-04	–	9.61e-05	–	1.14e-03	–	1.55e-04	–	5.12e-05	–
	154	4.52e-05	2.17	9.42e-06	2.72	2.07e-04	2.00	1.66e-05	2.62	5.47e-06	2.62
	712	1.52e-06	4.43	2.32e-07	4.84	7.49e-06	4.33	5.15e-07	4.53	1.67e-07	4.56
	3054	3.68e-08	5.11	2.93e-09	6.00	2.18e-07	4.86	6.24e-09	6.06	1.99e-09	6.08
	12579	1.85e-09	4.23	9.39e-11	4.86	1.24e-08	4.05	2.62e-10	4.48	8.19e-11	4.51
	50877	9.77e-11	4.21	2.95e-12	4.95	7.16e-10	4.08	8.37e-12	4.93	2.62e-12	4.92

Table 3.8: History of convergence of Example 3 with $\nu = 0.1$.

as the following first order system:

$$\mathrm{L} - \nabla \boldsymbol{u} = 0 \quad \text{in } \Omega, \tag{3.47a}$$

$$-\nu \nabla \cdot \mathrm{L} + \nabla \cdot (\boldsymbol{u} \otimes \boldsymbol{u}) + \nabla p = \boldsymbol{f} \quad \text{in } \Omega, \tag{3.47b}$$

$$\nabla \cdot \boldsymbol{u} = 0 \quad \text{in } \Omega, \tag{3.47c}$$

$$\boldsymbol{u} = \boldsymbol{g} \quad \text{on } \Gamma, \tag{3.47d}$$

$$\int_\Omega p = 0. \tag{3.47e}$$

To do that, we carry out an iterative process. For a fixed mesh, we solve first a Stokes problem and compute the postprocessed velocity, that we denote by $\boldsymbol{u}_h^{*,0}$. Then, for $n = 0, 1, 2, \ldots$, we solve the Oseen equations, using $\boldsymbol{\beta} := \boldsymbol{u}_h^{*,n}$, and compute the postprocessed velocity, denoted by $\boldsymbol{u}_h^{*,n+1}$, until the relative error satisfies $\dfrac{\|\boldsymbol{u}_h^{*,n+1} - \boldsymbol{u}_h^{*,n}\|}{\|\boldsymbol{u}_h^{*,n}\|} < \mathrm{tol}$, where tol is a prescribed value. Once that precision is achieved, we move to the next mesh.

We consider the circular domain $\Omega = \{(x, y) \in \mathbb{R}^2 : x^2 + y^2 < 0.75^2\}$, and the computational domain is constructed by interpolating $\partial\Omega$ by a piecewise linear function, as we did in Example 1. Note that,

k	N	e_p	order	$e_{\boldsymbol{u}}$	order	e_{L}	order	$e_{\boldsymbol{u}^*}$	order	$e_{\widehat{\boldsymbol{u}}}$	order
1	28	3.05e-02	–	6.31e-03	–	1.32e-01	–	1.83e-02	–	4.63e-03	–
	154	8.41e-03	1.51	2.60e-03	1.04	5.73e-02	0.98	7.56e-03	1.04	2.15e-03	0.90
	712	3.53e-03	1.13	1.32e-03	0.88	3.42e-02	0.67	3.37e-03	1.05	1.07e-03	0.91
	3054	3.50e-04	3.18	1.53e-04	2.97	1.02e-02	1.67	3.87e-04	2.97	1.25e-04	2.95
	12579	3.79e-05	3.14	1.87e-05	2.97	2.94e-03	1.76	4.78e-05	2.96	1.57e-05	2.93
	50877	8.56e-06	2.13	3.43e-06	2.42	9.56e-04	1.61	8.75e-06	2.43	2.88e-06	2.43
2	28	6.83e-04	–	2.49e-04	–	4.23e-03	–	4.19e-04	–	1.38e-04	–
	154	1.12e-04	2.12	6.89e-05	1.51	1.16e-03	1.52	1.52e-04	1.19	5.01e-05	1.19
	712	7.98e-05	0.44	4.56e-05	0.54	1.70e-03	−0.50	1.01e-04	0.53	3.21e-05	0.58
	3054	6.13e-06	3.52	4.74e-06	3.11	2.59e-04	2.58	1.12e-05	3.02	3.63e-06	2.99
	12579	8.63e-08	6.02	4.20e-08	6.68	4.46e-06	5.74	1.10e-07	6.54	3.49e-08	6.56
	50877	8.98e-09	3.24	3.08e-09	3.74	6.19e-07	2.83	8.49e-09	3.66	2.71e-09	3.66
3	28	2.22e-04	–	1.23e-04	–	1.73e-03	–	2.24e-04	–	7.19e-05	–
	154	8.00e-05	1.20	5.36e-05	0.97	1.38e-03	0.27	1.18e-04	0.75	3.84e-05	0.74
	712	1.22e-06	5.46	7.07e-07	5.65	2.36e-05	5.31	1.59e-06	5.62	5.11e-07	5.64
	3054	2.83e-08	5.17	1.23e-08	5.57	8.70e-07	4.54	2.68e-08	5.61	8.64e-09	5.60
	12579	1.78e-09	3.91	8.05e-10	3.85	8.94e-08	3.22	2.18e-09	3.55	6.92e-10	3.57
	50877	8.63e-11	4.33	2.18e-11	5.16	5.38e-09	4.02	6.25e-11	5.09	1.96e-11	5.10

Table 3.9: History of convergence of Example 3 with $\nu = 0.01$.

according to the error estimates stated in Theorem 3.5, the orders of convergence of the velocity and postprocessed velocity when solving Oseen equations are h^{k+1} and h^{k+2}, resp. This implies that the orders of convergence of the respective divergences are h^k and h^{k+1}. This means that $\|\nabla \cdot \boldsymbol{u}_h^*\|_{\mathsf{D}_h}$ converges to zero more quickly than $\|\nabla \cdot \boldsymbol{u}_h\|_{\mathsf{D}_h}$, even though neither $\nabla \cdot \boldsymbol{u}_h^*$ nor $\nabla \cdot \boldsymbol{u}_h^*$ are exactly null (as equation (3.47c) requires). This is why we use $\boldsymbol{\beta} = \boldsymbol{u}_h^{*,n}$ instead of $\boldsymbol{\beta} = \boldsymbol{u}_h^n$ in the n–th iteration. The orders of convergence of the velocity and postprocessed velocity, together with their divergences and the rest of the variables are displayed in Table 3.10. We observe that the results are the optimal for the pressure, velocity and its gradient. Additionally, the expected order h^{k+2} for the numerical trace and postprocessed velocity is also attained.

k	N	iter	e_p	order	$e_{\boldsymbol{u}}$	order	$\|\nabla\cdot\boldsymbol{u}_h\|_{\mathsf{D}_h}$	order	e_{L}	order	$e_{\widehat{\boldsymbol{u}}}$	order	$e^*_{\boldsymbol{u}}$	order	$\|\nabla\cdot\boldsymbol{u}^*_h\|_{\mathsf{D}_h}$	order
1	60	5	9.96e-03	–	3.55e-03	–	7.65e-02	–	1.02e-02	–	2.30e-03	–	6.53e-04	–	1.49e-03	–
	129	4	3.42e-03	2.79	1.46e-03	2.32	4.67e-02	1.29	4.13e-03	2.37	5.70e-04	3.65	1.49e-04	3.87	5.95e-04	2.39
	234	4	1.65e-03	2.44	7.99e-04	2.03	3.41e-02	1.05	2.20e-03	2.11	2.23e-04	3.16	5.61e-05	3.27	3.28e-04	2.00
	485	4	8.27e-04	1.90	3.98e-04	1.91	2.40e-02	0.96	1.11e-03	1.88	8.05e-05	2.79	2.05e-05	2.77	1.65e-04	1.88
	918	3	4.08e-04	2.21	2.02e-04	2.13	1.73e-02	1.03	5.51e-04	2.20	2.83e-05	3.27	7.19e-06	3.28	8.18e-05	2.21
	1764	3	2.06e-04	2.09	1.03e-04	2.05	1.22e-02	1.06	2.83e-04	2.05	1.04e-05	3.08	2.65e-06	3.06	4.35e-05	1.93
	3546	3	1.02e-04	2.02	5.20e-05	1.96	8.57e-03	1.01	1.43e-04	1.95	3.80e-06	2.87	9.73e-07	2.86	2.18e-05	1.98
	7089	2	5.13e-05	1.98	2.61e-05	1.99	6.12e-03	0.97	7.19e-05	1.98	1.36e-06	2.96	3.54e-07	2.92	1.10e-05	1.97
2	60	4	4.27e-04	–	1.23e-04	–	3.10e-03	–	4.21e-04	–	5.81e-05	–	1.92e-05	–	1.11e-04	–
	129	3	1.01e-04	3.77	3.13e-05	3.57	1.28e-03	2.31	9.66e-05	3.85	8.04e-06	5.17	2.71e-06	5.11	2.99e-05	3.42
	234	3	3.36e-05	3.68	1.13e-05	3.41	6.67e-04	2.19	3.57e-05	3.34	2.02e-06	4.65	7.36e-07	4.38	1.18e-05	3.11
	485	3	9.89e-06	3.36	3.73e-06	3.05	3.17e-04	2.04	1.16e-05	3.09	4.30e-07	4.24	1.69e-07	4.03	3.81e-06	3.12
	918	2	3.67e-06	3.11	1.40e-06	3.08	1.67e-04	2.01	4.14e-06	3.22	1.16e-07	4.11	4.50e-08	4.15	1.45e-06	3.03
	1764	2	1.37e-06	3.03	5.32e-07	2.96	8.88e-05	1.93	1.50e-06	3.10	3.10e-08	4.04	1.20e-08	4.05	5.53e-07	2.94
	3546	2	5.22e-07	2.75	1.97e-07	2.85	4.59e-05	1.89	5.59e-07	2.83	8.85e-09	3.59	3.31e-09	3.68	2.04e-07	2.85
	7089	2	1.78e-07	3.10	6.88e-08	3.03	2.27e-05	2.03	1.94e-07	3.05	2.15e-09	4.09	8.11e-10	4.06	7.25e-08	2.99
3	60	3	5.75e-05	–	9.39e-06	–	3.44e-04	–	4.00e-05	–	5.15e-06	–	1.34e-06	–	1.20e-05	–
	129	2	7.94e-06	5.17	1.52e-06	4.76	8.93e-05	3.52	5.25e-06	5.31	4.69e-07	6.26	1.19e-07	6.34	1.71e-06	5.10
	234	2	1.70e-06	5.18	3.98e-07	4.50	3.31e-05	3.34	1.08e-06	5.30	6.82e-08	6.48	1.65e-08	6.63	3.71e-07	5.13
	485	2	3.39e-07	4.42	9.40e-08	3.96	1.05e-05	3.14	2.15e-07	4.44	9.89e-09	5.30	2.49e-09	5.18	6.98e-08	4.58
	918	1	9.24e-08	4.08	2.47e-08	4.19	4.04e-06	3.01	5.66e-08	4.19	1.98e-09	5.05	4.69e-10	5.24	1.94e-08	4.02
	1764	1	2.52e-08	3.98	6.54e-09	4.07	1.53e-06	2.97	1.50e-08	4.06	3.88e-10	4.99	8.96e-11	5.07	5.31e-09	3.96
	3546	1	6.96e-09	3.68	1.75e-09	3.78	5.65e-07	2.85	4.19e-09	3.66	8.12e-11	4.48	1.83e-11	4.55	1.50e-09	3.63
	7089	1	1.69e-09	4.09	4.33e-10	4.02	1.98e-07	3.03	1.02e-09	4.08	1.39e-11	5.10	3.20e-12	5.04	3.66e-10	4.07

Table 3.10: History of convergence of Example 4. Circular domain.

CHAPTER 4

Dispersion analysis of HDG methods

In this chapter we carry out a dispersion analysis of HDG methods applied to the Helmholtz equation. The focus is to particularly study the SFH (Single Face HDG) method, which consists in setting the stabilization parameter τ of the HDG method equal to zero in all but one edge of every mesh element.

4.1 Introduction

In many physical and engineering applications involving wave propagation, the mathematical model is governed by the Helmholtz system

$$ik\boldsymbol{u} + \nabla\phi = \mathbf{0} \quad \text{in } \Omega, \tag{4.1a}$$

$$ik\phi + \nabla\cdot\boldsymbol{u} = f \quad \text{in } \Omega, \tag{4.1b}$$

$$\phi = 0 \quad \text{on } \partial\Omega, \tag{4.1c}$$

where $0 \neq k \in \mathbb{C}$ is the wavenumber, $\Omega \subset \mathbb{R}^2$, $\boldsymbol{u} : \Omega \to \mathbb{R}^2$ is a vector unknown, $\phi : \Omega \to \mathbb{R}$ is a scalar unknown, and $f \in L^2(\Omega)$ is a given source term. For example, in acoustics, $\boldsymbol{u}$ represents linearized velocity and ϕ represents pressure. When solving this kind of problems using a numerical method, differences are observed between the discrete and exact wavenumbers. In this chapter we present a dispersion analysis for HDG methods, where the focus is to study the Single Face HDG (SFH) method. The main result of this chapter is that the SFH method does indeed exhibit rates comparable to the HRT method for a particular choice of τ. The particular nonzero value of τ to be specified on the single facet to obtain rates comparable to the HRT method is displayed, together with the accompanying convergence rate, in the last row of Table 4.1. The rates obtained with other commonly used values of τ are also given in Table 4.1 for comparison.

4.2 The HDG method

Let $\{\mathcal{T}_h\}_{h>0}$ be a family triangulations of the domain Ω and denote by $\mathcal{E}_h$ the set of all the edges of a triangulation $\mathcal{T}_h$. Let $\boldsymbol{n}_K$ be the outward unit normal of a triangle K, writing $\boldsymbol{n}$ instead of $\boldsymbol{n}_K$ when

Table 4.1: Summary of convergence rates of wavenumber errors from [40] (first 3 rows) and this paper (remaining rows). The "0"s indicate that the errors observed were close to machine precision. The row in bold shows SFH rates comparable to the mixed HRT method. All the stated rates are based on observations for $p = 0, 1, 2, 3$. The rates for the lowest order case were obtained from a closed-form expression, whereas the rates for the higher order cases were obtained by numerically solving a small nonlinear system.

Method	τ	Rates		
		Dispersive error	Dissipative error	Total error
LDG-H	1	$2p+3$	$2p+2$	$2p+2$
LDG-H	$\sqrt{3}i/2$	$2p+2$	0	$2p+2$
HRT	–	$2p+3$	0	$2p+3$
SFH	1	$2p+3$	$2p+2$	$2p+2$
SFH	i	$2p+2$	0	$2p+2$
SFH	$\boldsymbol{i/kh}$	$\boldsymbol{2p+3}$	**0**	$\boldsymbol{2p+3}$
SFH	$1/kh$	$2p+3$	$2p+3$	$2p+3$
LDG-H	i	$2p+2$	0	$2p+2$
LDG-H	1	$2p+3$	$2p+2$	$2p+2$
LDG-H	i/kh	$2p+1$	0	$2p+1$
LDG-H	$1/kh$	$2p+1$	$2p+1$	$2p+1$

there is no confusion. In addition, for a given domain D, let $\mathcal{P}_p(D)$ denote the space of polynomials of degree at most p defined on D. Next, define the following discrete spaces:

$$\begin{aligned} V_h &= \left\{\boldsymbol{v} \in [L^2(\Omega)]^2 : \boldsymbol{v}|_K \in [\mathcal{P}_p(K)]^2,\ \forall K \in \mathcal{T}_h\right\}, \\ W_h &= \left\{\psi \in L^2(\Omega) : \psi|_K \in \mathcal{P}_p(K),\ \forall K \in \mathcal{T}_h\right\}, \\ M_h &= \left\{\widehat{\psi} \in L^2(\mathcal{E}_h) : \widehat{\psi}|_e \in \mathcal{P}_p(e),\ \forall e \in \mathcal{E}_h \text{ and } \widehat{\psi}|_{\partial\Omega} = 0\right\}. \end{aligned}$$

The standard HDG method, i.e., the LDG-H method [17], produces an approximation $(\boldsymbol{u}_h, \phi_h, \widehat{\phi}_h)$ of the exact solution $(\boldsymbol{u}, \phi, \phi|_{\mathcal{E}_h})$ in the space $V_h \times W_h \times M_h$ that satisfies

$$\sum_{K\in\mathcal{T}_h} ik(\boldsymbol{u}_h, \boldsymbol{v}_h)_K - (\phi_h, \boldsymbol{\nabla}\cdot\boldsymbol{v}_h)_K + \langle\widehat{\phi}_h, \boldsymbol{v}_h\cdot\boldsymbol{n}\rangle_{\partial K} = 0, \tag{4.2a}$$

$$\sum_{K\in\mathcal{T}_h} (\boldsymbol{\nabla}\cdot\boldsymbol{u}_h, \psi_h)_K + \langle\tau(\phi_h - \widehat{\phi}_h), \psi_h\rangle_{\partial K} + ik(\phi_h, \psi_h)_K = (f, \psi_h)_\Omega, \tag{4.2b}$$

$$\sum_{K\in\mathcal{T}_h} \langle\boldsymbol{u}_h\cdot\boldsymbol{n} + \tau(\phi_h - \widehat{\phi}_h), \widehat{\psi}_h\rangle_{\partial K} = 0, \tag{4.2c}$$

for all $\boldsymbol{v}_h \in V_h$, $\psi_h \in W_h$ and $\widehat{\psi}_h \in M_h$, where τ is a nonzero stabilization function defined on $\partial\mathcal{T}_h := \{\partial K : K \in \mathcal{T}_h\}$. Here $(\cdot,\cdot)_K$ and $\langle\cdot,\cdot\rangle_{\partial K}$ denote the inner products of $L^2(K)$ and $L^2(\partial K)$, respectively. It is traditional to choose $\tau \geq 0$, but for wave problems, as noted in [40], it may often be advantageous to choose τ in the complex plane. Hence, we will not require that τ is non-negative.

Let τ_K denote the value of τ on ∂K. While $\tau_K : \partial K \to \mathbb{C}$ is a single-valued function on each K, note that on each edge shared by two triangular elements, τ is generally double valued. We shall assume

that the restriction of τ_K to each edge of K is a constant function. When τ_K, for every K in $\mathcal{T}_h$, is such that τ_K is zero on all edges except one, we obtain the SFH method.

In the next section, we will work with the condensed form of the method. The HDG method was designed specifically to have this condensability feature. The condensed form is obtained by statically condensing out $\boldsymbol{u}_h$ and ϕ_h to get a single equation for the interface variable $\widehat{\phi}_h$. We refer to [17] for a general description of this form. We will focus on the condensed form of the lowest order SFH method next.

4.3 Dispersion analysis of the lowest order SFH method

In order to perform the dispersion analysis of the method (4.2), we follow the approach laid out in [30, 40]. Consider an infinite triangulation made of isosceles right triangles K with hypotenuse of length $\sqrt{2}h$ and vertical and horizontal edges of length h, as shown in Fig. 4.1. On this infinite grid, we will now derive the condensed form.

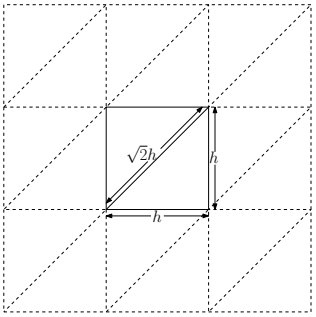

Figure 4.1: Sketch of the mesh.

4.3.1 Condensed element matrix

We consider the SFH method associated to (4.2), where the stabilization parameter τ is taken to be zero on all vertical and horizontal edges of every triangle. We first analyze the lowest order case ($p = 0$). As we shall see, it is possible to obtain a series expansion of the wavenumber error in closed form in the $p = 0$ case. Later, we shall numerically study the high order cases.

Let K be a triangle with edges e_1 (hypotenuse), e_2(horizontal) and e_3(vertical). For the polynomial spaces $[\mathcal{P}_0(K)]^2$, $\mathcal{P}_0(K)$, $\mathcal{P}_0(e_1)$, $\mathcal{P}_0(e_2)$ and $\mathcal{P}_0(e_3)$, we consider the Dubiner basis functions (see [47]), which for the lowest order case are given by

$$\boldsymbol{u}_1 = \begin{bmatrix} \sqrt{2} \\ 0 \end{bmatrix}, \boldsymbol{u}_2 = \begin{bmatrix} 0 \\ \sqrt{2} \end{bmatrix}, \phi_0 = \sqrt{2}\,, \widehat{\phi}_1 = 1, \widehat{\phi}_2 = 1\,, \text{and}\,, \widehat{\phi}_3 = 1,$$

respectively. For elements with the orientation of K_1 displayed in Fig. 4.3, the element matrix associated to (4.2), in the $[\boldsymbol{u}_1, \boldsymbol{u}_2, \phi_0, \widehat{\phi}_1, \widehat{\phi}_2, \widehat{\phi}_3]$-ordering, can be written in block form as

$$M = \begin{bmatrix} M_{11} & M_{12} \\ M_{21} & M_{22} \end{bmatrix},$$

where

$$M_{11} = \begin{bmatrix} ikh^2 & 0 & 0 \\ 0 & ikh^2 & 0 \\ 0 & 0 & -(ikh^2 + 2\sqrt{2}\tau h) \end{bmatrix}, \quad M_{12} = \begin{bmatrix} \sqrt{2}h & 0 & -\sqrt{2}h \\ -\sqrt{2}h & \sqrt{2}h & 0 \\ 2\tau h & 0 & 0, \end{bmatrix},$$

$$M_{21} = M_{12}^T, \qquad M_{22} = \begin{bmatrix} -\sqrt{2}\tau h & 0 & 0 \\ 0 & 0 & 0 \\ 0 & 0 & 0 \end{bmatrix}.$$

For elements with the orientation of K_2, also displayed in Fig. 4.3, the matrices M_{11} and M_{22} are the same, whereas due to the change of the normal vectors, the matrix M_{12} is given by

$$M_{12} = \begin{bmatrix} -\sqrt{2}h & 0 & \sqrt{2}h \\ \sqrt{2}h & -\sqrt{2}h & 0 \\ 2\tau h & 0 & 0 \end{bmatrix},$$

and $M_{21} = M_{12}^T$.

The condensation of all interior degrees of freedom is accomplished by taking the Schur complement $S = M_{22} - M_{21}M_{11}^{-1}M_{12}$. In both cases (of K_1 and K_2), the Schur complement is given by the matrix

$$S = \begin{bmatrix} \dfrac{4\tau^2 h}{ikh + 2\sqrt{2}\tau} + \dfrac{4i}{k} - \sqrt{2}\tau h & \dfrac{-2i}{k} & \dfrac{-2i}{k} \\ \dfrac{-2i}{k} & \dfrac{2i}{k} & 0 \\ \dfrac{-2i}{k} & 0 & \dfrac{2i}{k} \end{bmatrix},$$

a 3×3 matrix corresponding to the three interface (non-condensable) degrees of freedom, one per edge. Note that while performing this calculation, we have assumed that M_{11} is invertible, which is equivalent to assuming that

$$2\sqrt{2}\tau + ikh \neq 0. \tag{4.3}$$

We proceed with the derivation of the dispersion relations by making this assumption throughout.

4.3.2 Dispersion relation in the lowest order case

The above-mentioned infinite triangulation has three different types of interface degrees of freedom: the ones associated to the diagonal edges (first type), the horizontal edges (second type) and the

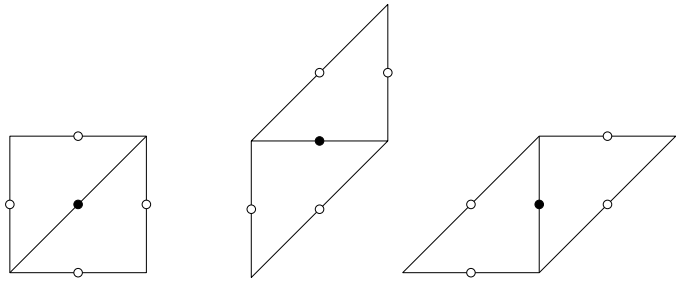

Figure 4.2: The three types of stencils for $p = 0$.

vertical edges (third type), as displayed in Fig. 4.2. We denote by C_1, C_2 and C_3 the infinite set of stencil centers for the three types of stencils present in this case. Then, we obtain an infinite system of equations for the numerical trace values $\widehat{\phi}_{1,\boldsymbol{p}_1}$, $\widehat{\phi}_{2,\boldsymbol{p}_2}$ and $\widehat{\phi}_{3,\boldsymbol{p}_3}$ at all $\boldsymbol{p}_1 \in C_1$, $\boldsymbol{p}_2 \in C_2$ and $\boldsymbol{p}_3 \in C_3$. Since we are interested in how this infinite system propagates plane wave solutions, we consider the ansatz

$$\widehat{\phi}_{j,\boldsymbol{p}_j} = a_j \exp(i\boldsymbol{k}^h \cdot \boldsymbol{p}_j), \tag{4.4}$$

where a_1, a_2 and a_3 are constants and the components of discrete wave vector $\boldsymbol{k}^h = (k_1^h, k_2^h)$ are given by $k_1^h := k^h \cos(\theta)$ and $k_2^h := k^h \sin(\theta)$. Here k^h is the unknown discrete wavenumber corresponding to the exact wavenumber k, and θ is the angle of propagation of the plane wave solution. We now proceed to determine an expression that relates k^h and k. Since we have three types of degrees of freedom, we need to construct three equations, but we will only explain the details of the construction of the first one, associated to diagonal edges: Let's denote by $\boldsymbol{e}_1$ and $\boldsymbol{e}_2$ the cartesian vectors, and suppose that the point P is located at the position $\boldsymbol{p}_1$.

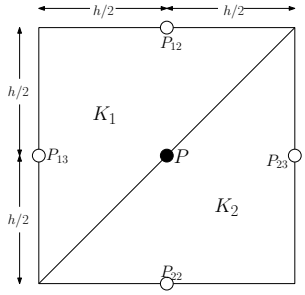

Figure 4.3: Positions of the degrees of freedom in the stencil of the first type.

Then, as seen in Fig. 4.3, the relative position of the point P_{12} (the location in K_1 of the degree of freedom of the second type) from P is $\boldsymbol{p}_1 + \frac{h}{2}\boldsymbol{e}_2$, and the relative position of the point P_{13} (the location in K_1 of the degree of freedom of the third type) from P is $\boldsymbol{p}_1 - \frac{h}{2}\boldsymbol{e}_1$. Hence, the contribution of K_1 to the first equation is given by

$$S_{11}\widehat{\phi}_{1,\boldsymbol{p}_1} + S_{12}\widehat{\phi}_{2,\boldsymbol{p}_1+\frac{h}{2}\boldsymbol{e}_2} + S_{13}\widehat{\phi}_{3,\boldsymbol{p}_1-\frac{h}{2}\boldsymbol{e}_1}.$$

Proceeding in the same way, the contribution of K_2 to the same equation is given by

$$S_{11}\widehat{\phi}_{1,\boldsymbol{p}_1} + S_{12}\widehat{\phi}_{2,\boldsymbol{p}_1-\frac{h}{2}\boldsymbol{e}_2} + S_{13}\widehat{\phi}_{3,\boldsymbol{p}_1+\frac{h}{2}\boldsymbol{e}_1}.$$

Since plane waves are exact solutions to the Helmholtz equation with zero sources, the right hand side (f) of the equation is zero. Thus, we can write the first equation as

$$\begin{aligned} 2S_{11}\widehat{\phi}_{1,\boldsymbol{p}_1} + S_{12}\big(\widehat{\phi}_{2,\boldsymbol{p}_1+\frac{h}{2}\boldsymbol{e}_2} + \widehat{\phi}_{2,\boldsymbol{p}_1-\frac{h}{2}\boldsymbol{e}_2}\big) \\ + S_{13}\big(\widehat{\phi}_{3,\boldsymbol{p}_1-\frac{h}{2}\boldsymbol{e}_1} + \widehat{\phi}_{3,\boldsymbol{p}_1+\frac{h}{2}\boldsymbol{e}_1}\big) = 0. \end{aligned} \tag{4.5}$$

Since $\widehat{\phi}_{j,\boldsymbol{p}_j}$ is given by (4.4) and

$$\widehat{\phi}_{i,\boldsymbol{p}_j\pm\frac{h}{2}\boldsymbol{e}_l} = a_i \exp\Big(i\boldsymbol{k}^h \cdot \big(\boldsymbol{p}_j \pm \frac{h}{2}\boldsymbol{e}_l\big)\Big),$$

we observe that we can simplify (4.5) to get

$$\begin{aligned} 0 &= 2S_{11}a_1 + S_{12}\left\{\exp\Big(\frac{hi}{2}\boldsymbol{k}^h\cdot\boldsymbol{e}_2\Big)+\exp\Big(-\frac{hi}{2}\boldsymbol{k}^h\cdot\boldsymbol{e}_2\Big)\right\}a_2 \\ &\quad +S_{13}\left\{\exp\Big(-\frac{hi}{2}\boldsymbol{k}^h\cdot\boldsymbol{e}_1\Big)+\exp\Big(\frac{hi}{2}\boldsymbol{k}^h\cdot\boldsymbol{e}_1\Big)\right\}a_3 \\ &= 2S_{11}a_1 + S_{12}\left\{\exp\Big(\frac{hi}{2}k^h\sin(\theta)\Big)+\exp\Big(-\frac{hi}{2}k^h\sin(\theta)\Big)\right\}a_2 \\ &\quad +S_{13}\left\{\exp\Big(-\frac{hi}{2}k^h\cos(\theta)\Big)+\exp\Big(\frac{hi}{2}k^h\cos(\theta)\Big)\right\}a_3. \end{aligned}$$

Using that $\exp(i\alpha)=\cos(\alpha)+i\sin(\alpha)$ for any $\alpha\in\mathbb{R}$, and some well known properties of complex numbers, we can write our equation as

$$2S_{11}a_1 + 2S_{12}\cos\Big(\frac{h}{2}k^h\cos(\theta)\Big)a_2 + 2S_{13}\cos\Big(\frac{h}{2}k^h\sin(\theta)\Big)a_3 = 0.$$

Finally, substituting

$$S_{11}=\frac{4\tau^2 h}{ikh+2\sqrt{2}\tau}+\frac{4i}{k}-\sqrt{2}\tau h,\quad S_{12}=S_{13}=\frac{-2i}{k},$$

multiplying the equation by $\frac{k}{2}(ikh+2\sqrt{2}\tau)$, and rearranging terms, we obtain

$$\begin{aligned}\Big\{(4i-\sqrt{2}\tau kh)(ikh+2\sqrt{2}\tau)+4\tau^2 kh\Big\}a_1 - 2i(ikh+2\sqrt{2}\tau)c_2a_2 \\ - 2i(ikh+2\sqrt{2}\tau)c_1a_3 = 0,\end{aligned}$$

where $c_j=\cos(hk_j^h/2)$, $j=1,2$, and

$$k_1^h = k^h\cos(\theta),\qquad k_2^h = k^h\sin(\theta). \tag{4.6}$$

This is the equation for the first type of degrees of freedom. The other two equations may be derived in the same way.

The three equations together form a system

$$F\begin{bmatrix}a_1\\a_2\\a_3\end{bmatrix}=0$$

where F is the so-called *dispersion matrix*, given by

$$F=\begin{bmatrix}(4i-\sqrt{2}\tau kh)(ikh+2\sqrt{2}\tau)+4\tau^2kh & -2i(ikh+2\sqrt{2}\tau)c_2 & -2i(ikh+2\sqrt{2}\tau)c_1\\ -c_2 & 1 & 0\\ -c_1 & 0 & 1\end{bmatrix}.$$

Its determinant is

$$\det(F) = -2i(2\sqrt{2}\tau+ikh)(c_1^2+c_2^2)+(2\sqrt{2}\tau+ikh)(4i-\sqrt{2}\tau kh)+4\tau^2kh.$$

We are interested in non-trivial solutions of this system. Hence we conclude that the *dispersion relation* relating k^h to k in the SFH method is

$$\det(F)=0. \tag{4.7}$$

Note that since the entries of F depend on k^h, the above forms a nonlinear equation for the discrete wavenumber k^h.

4.3.3 Asymptotic expansion of the wavenumber error

To get useful qualitative information about k^h, we must further manipulate (4.7). By virtue of (4.3), we may multiply (4.7) by $-[2i(2\sqrt{2}\tau + ikh)]^{-1}$ and simplify to obtain

$$c_1^2 + c_2^2 + \frac{i\left\{\left(2\sqrt{2}\tau + ikh\right)(4i - \sqrt{2}\tau kh) + 4\tau^2 kh\right\}}{2\left(2\sqrt{2}\tau + ikh\right)} = 0. \tag{4.8}$$

The identity $i\left\{\left(2\sqrt{2}\tau + ikh\right)(4i - \sqrt{2}\tau kh) + 4\tau^2 kh\right\} = (\sqrt{2}(kh)^2 - 8\sqrt{2})\tau - 4ikh$ now motivates us to set

$$R = -\frac{\left(\sqrt{2}(kh)^2 - 8\sqrt{2}\right)\tau - 4ikh}{2\left(2\sqrt{2}\tau + ikh\right)},$$

and rewrite (4.8) as

$$\begin{aligned} 0 &= c_1^2 + c_2^2 - R \\ &= (c_1^2 - 1) + (c_2^2 - 1) + (2 - R) \\ &= (c_1^2 - 1) + (c_2^2 - 1) + (2 - R)\left(\cos^2\theta + \sin^2\theta\right) \\ &= \left\{(c_1^2 - 1) + (2 - R)\cos^2(\theta)\right\} + \left\{(c_2^2 - 1) + (2 - R)\sin^2(\theta)\right\}. \end{aligned}$$

Thus, we identify two sufficient conditions for $\det(F) = 0$ to hold, namely

$$c_1 = (1 - d_1)^{1/2}, \qquad c_2 = (1 - d_2)^{1/2}, \tag{4.9}$$

where $d_1 = (2 - R)\cos^2(\theta)$ and $d_2 = (2 - R)\sin^2(\theta)$.

The two sufficient conditions take similar forms. As we shall see now, they are simple enough to understand by Taylor expansion. In analogy with (4.6), let

$$k_1 = k\cos(\theta), \qquad\qquad k_2 = k\sin(\theta).$$

By (4.9) and the definitions of c_j, d_j, we have

$$k_j^h h = 2\cos^{-1}(\sqrt{1 - d_j}), \qquad\qquad d_j = \frac{\sqrt{2}\tau(k_j h)^2}{4\sqrt{2}\tau + 2i(kh)}.$$

As $kh \to 0$, clearly $d_j \to 0$, so using the Taylor expansion of arccosine near 1, we obtain

$$\begin{aligned} k_1^h h &= \cos(\theta)(kh) - \frac{i\sqrt{2}\cos(\theta)}{8\tau}(kh)^2 + \frac{8\tau^2\cos^3(\theta) - 9\cos(\theta)}{192\tau^2}(kh)^3 + O(kh)^4 \\ k_2^h h &= \sin(\theta)(kh) - \frac{i\sqrt{2}\sin(\theta)}{8\tau}(kh)^2 + \frac{8\tau^2\sin^3(\theta) - 9\sin(\theta)}{192\tau^2}(kh)^3 + O(kh)^4 \end{aligned}$$

These relations, together with $k^h = (k_1^h)^2 + (k_2^h)^2$, yield

$$\boxed{k^h h - kh = \frac{i}{4\sqrt{2}\tau}(kh)^2 + \frac{2\tau^2\cos(4\theta) + 6\tau^2 - 9}{192\tau^2}(kh)^3 + O(kh)^4} \tag{4.10}$$

as $kh \to 0$. This is the main result of this subsection.

The series expansion (4.10) immediately shows that the wavenumber error is of order 2 (equalling $2p + 2$ when $p = 0$) for any nonzero τ. Next, note how τ appears in the first and second terms of the expansion (4.10). In the first term, it only appears in the denominator (while in the second term it appears in equal degrees in the denominator and numerator). This leads us to an important observation: If we set

$$\tau = \frac{i}{kh} \tag{4.11}$$

in (4.10), then we should obtain the higher rate of convergence $|k^h h - kh| = O(kh)^3$ as $kh \to 0$. Moreover, we see that all terms in the series expansion of $k^h h - kh$, except the first, have even powers of τ so $\mathrm{Im}(k^h h - kh) = 0$, if τ is set by (4.11) or any real multiple of it, i.e., the dissipative errors should vanish. We will gather numerical confirmation of these statements in the next subsection.

Actually, if we set

$$\tau = O\left(\frac{i}{(kh)^s}\right) \tag{4.12}$$

with any $s \geq 1$ in (4.10), we continue to obtain $|k^h h - kh| = O(kh)^3$ (since the rate is now limited by the second term on the right hand side of (4.10)). Thus our analysis also shows that the dispersion analysis for the staggered DG method [14] is comparable to the mixed method. In fact, [13] showed that as $\tau \to \infty$, the resulting HDG method is closely related to the staggered DG method. Therefore, in our numerical studies, we shall also include the case (4.12) for a few values of s.

4.3.4 Numerical computation of k^h for the lowest order SFH method

Since the above-derived error expansion is only asymptotic, we now proceed to check the practical size of wavenumber errors by direct numerical computation. We solve the nonlinear dispersion relation (4.7) numerically to find k^h. Recall that $k^h \equiv k^h(\theta)$ is a function of the propagation angle θ. In all the cases we present below, we consider $\theta \in \Theta = \{j\pi/40 : j = 1, \ldots, 20\}$. The exact wavenumber is set so that $kh \in \left\{\pi/2^{j+2} : j = 0, \ldots, 8\right\}$. (Note that the dependence on k occurs in the form of dependence on kh in the dispersion relations.) Define

$$\epsilon_{\text{disp}} = \max_{\theta\in\Theta} |\mathrm{Re}(k^h(\theta)h) - kh|, \qquad \epsilon_{\text{dissip}} = \max_{\theta\in\Theta} |\mathrm{Im}(k^h(\theta)h)|,$$
$$\epsilon_{\text{total}} = \max_{\theta\in\Theta} |k^h(\theta)h - kh|.$$

We report the numerically computed values of these numbers for the following cases.

Case 1: $\tau = i$**.** Equation (4.7) can now be simplified to the form

$$\det(F) = 2(2\sqrt{2} + kh)(c_1^2 + c_2^2) - (2\sqrt{2} + kh)(4 - \sqrt{2}kh) - 4kh = 0.$$

This is the form used in our nonlinear solve. For small kh, equation specifies values of $c_1^2 + c_2^2$ that admit real solutions for k^h. The values of k^h found by the numerical root finder, reported in Table 4.2, confirms that ϵ_{dissip} is 0 up to machine precision. The total error ϵ_{total} appears to go to 0 at the rate $O(kh)^2$, as expected from the asymptotic expansion (4.10).

Table 4.2: Results for $\tau = i$ and $\tau = 1$ in the lowest order SFH method.

	$\tau = i$						$\tau = 1$					
kh	ϵ_{disp}	rate	ϵ_{dissip}	rate	ϵ_{total}	rate	ϵ_{disp}	rate	ϵ_{dissip}	rate	ϵ_{total}	rate
$\pi/2^2$	8.34e-02	-	4.42e-16	-	8.34e-02	-	1.25e-02	-	1.13e-01	-	1.13e-01	-
$\pi/2^3$	2.37e-02	1.82	7.56e-16	-	2.37e-02	1.82	1.57e-03	2.99	2.75e-02	2.03	2.75e-02	2.04
$\pi/2^4$	6.34e-03	1.90	1.03e-15	-	6.34e-03	1.90	1.97e-04	3.00	6.83e-03	2.01	6.83e-03	2.01
$\pi/2^5$	1.64e-03	1.95	2.90e-15	-	1.64e-03	1.95	2.46e-05	3.00	1.70e-03	2.00	1.70e-03	2.00
$\pi/2^6$	4.18e-04	1.97	9.54e-15	-	4.18e-04	1.97	3.08e-06	3.00	4.26e-04	2.00	4.26e-04	2.00
$\pi/2^7$	1.05e-04	1.99	1.16e-14	-	1.05e-04	1.99	3.85e-07	3.00	1.06e-04	2.00	1.06e-04	2.00
$\pi/2^8$	2.65e-05	1.99	3.55e-14	-	2.65e-05	1.99	4.81e-08	3.00	2.66e-05	2.00	2.66e-05	2.00
$\pi/2^9$	6.64e-06	2.00	2.92e-14	-	6.64e-06	2.00	6.02e-09	3.00	6.66e-06	2.00	6.66e-06	2.00
$\pi/2^{10}$	1.66e-06	2.00	1.96e-13	-	1.66e-06	2.00	7.52e-10	3.00	1.66e-06	2.00	1.66e-06	2.00

Table 4.3: Results for $\tau = \dfrac{i}{kh}$ and $\tau = \dfrac{1}{kh}$ in the lowest order SFH method.

	$\tau = \frac{i}{kh}$						$\tau = \frac{1}{kh}$					
kh	ϵ_{disp}	rate	ϵ_{dissip}	rate	ϵ_{total}	rate	ϵ_{disp}	rate	ϵ_{dissip}	rate	ϵ_{total}	rate
$\pi/2^2$	6.60e-02	-	6.09e-16	-	6.60e-02	-	6.18e-03	-	9.01e-02	-	9.03e-02	-
$\pi/2^3$	9.11e-03	2.86	1.40e-15	-	9.11e-03	2.86	2.12e-03	1.55	1.09e-02	3.05	1.11e-02	3.02
$\pi/2^4$	1.17e-03	2.96	1.60e-15	-	1.17e-03	2.96	3.03e-04	2.80	1.34e-03	3.02	1.38e-03	3.01
$\pi/2^5$	1.47e-04	2.99	2.79e-15	-	1.47e-04	2.99	3.90e-05	2.96	1.67e-04	3.01	1.72e-04	3.00
$\pi/2^6$	1.84e-05	3.00	6.20e-15	-	1.84e-05	3.00	4.92e-06	2.99	2.09e-05	3.00	2.15e-05	3.00
$\pi/2^7$	2.31e-06	3.00	2.42e-14	-	2.31e-06	3.00	6.16e-07	3.00	2.61e-06	3.00	2.69e-06	3.00
$\pi/2^8$	2.88e-07	3.00	1.29e-14	-	2.88e-07	3.00	7.70e-08	3.00	3.27e-07	3.00	3.36e-07	3.00
$\pi/2^9$	3.60e-08	3.00	1.89e-14	-	3.60e-08	3.00	9.63e-09	3.00	4.08e-08	3.00	4.20e-08	3.00
$\pi/2^{10}$	4.50e-09	3.00	8.42e-14	-	4.50e-09	3.00	1.20e-09	3.00	5.10e-09	3.00	5.24e-09	3.00

Table 4.4: Results for $\tau = \dfrac{i}{(kh)^3}$ and $\tau = \dfrac{i}{(kh)^4}$ in the lowest order SFH method.

	$\tau = \frac{i}{(kh)^3}$						$\tau = \frac{i}{(kh)^4}$					
kh	ϵ_{disp}	rate	ϵ_{dissip}	rate	ϵ_{total}	rate	ϵ_{disp}	rate	ϵ_{dissip}	rate	ϵ_{total}	rate
$\pi/2^2$	3.94e-02	-	6.70e-16	-	3.94e-02	-	2.95e-02	-	3.47e-16	-	2.95e-02	-
$\pi/2^3$	8.95e-04	5.46	8.27e-16	-	8.95e-04	5.46	1.91e-03	3.95	8.12e-16	-	1.91e-03	3.95
$\pi/2^4$	2.65e-04	1.76	5.59e-16	-	2.65e-04	1.76	3.10e-04	2.64	1.20e-15	-	3.10e-04	2.64
$\pi/2^5$	3.79e-05	2.81	1.73e-15	-	3.79e-05	2.81	3.93e-05	2.96	4.71e-15	-	3.93e-05	2.96
$\pi/2^6$	4.88e-06	3.00	3.10e-15	-	4.89e-06	2.96	4.92e-06	3.00	6.33e-15	-	4.92e-06	3.00
$\pi/2^7$	6.14e-07	3.00	3.05e-15	-	6.14e-07	3.00	6.17e-07	3.00	1.50e-14	-	6.17e-07	3.00
$\pi/2^8$	7.70e-08	3.00	1.62e-14	-	7.68e-08	3.00	8.28e-08	2.89	1.62e-14	-	8.28e-08	2.89
$\pi/2^9$	8.94e-09	3.10	5.30e-14	-	8.95e-09	3.10	-	-	-	-	-	-

Case 2: $\tau = 1$**.** In this case the determinant simplifies to

$$\det(F) = \left\{2kh(c_1^2 + c_2^2) - 4k\right\} + i\left\{-4\sqrt{2}(c_1^2 + c_2^2) + 8\sqrt{2} - 2(kh)^2\right\},$$

and its no longer clear that solutions of the dispersion relation are real. Searching for roots in the complex plane, we computed k^h. These results are compiled in Table 4.2. Clearly, the dissipative errors seem to dominate in this case. As before, $\epsilon_{\text{total}} = O(kh)^2$.

Case 3: $\tau = i/kh$**.** This is the interesting value of τ found in (4.11). Here the determinant simplifies to

$$\det(F) = \left(\frac{2\sqrt{2}}{kh} + kh\right)\left(2(c_1^2 + c_2^2) - 4 + \sqrt{2}\right) - \frac{4}{kh}.$$

The results are now in Table 4.3. As expected from our discussions following the asymptotic expansion (4.10), the dissipative errors are zero to machine precision and moreover, we obtain the higher rate of convergence of $O(kh)^3$ for the total error. Moreover, the same behavior is observed when choosing τ as in (4.12), as we see in Table 4.4 for the specific values $\tau = i/(kh)^3$ and $\tau = i/(kh)^4$.

Case 4: $\tau = 1/kh$**.** This case differs from the previous case only by a scalar multiple. Hence, reviewing the expansion (4.10), we expect to obtain higher order convergence for the total error in this case also. The determinant in this case is

$$\det(F) = 2\left(\frac{2\sqrt{2}}{kh} + ikh\right)(c_1^2 + c_2^2) - \left(\frac{2\sqrt{2}}{kh} + ikh\right)(4i - \sqrt{2}) + \frac{4}{kh}.$$

The results, displayed in Table 4.3, show that although ϵ_{dissip} is no longer zero, the total error ϵ_{total} goes to zero at the faster rate $O(kh)^3$.

4.4 Wavenumber errors in the higher order SFH method

In order to go beyond the $p = 0$ case, we will use the technique of [40]. The main idea is to obtain an analogue of (4.7) with a larger matrix F. This will then be numerically solved for the discrete wavenumber $k^h = k^h(\theta)$. As we did in the lowest order case, we will use the same infinite lattice of isosceles right triangles, and the ansatz that the degrees of freedom interpolate a plane wave traveling in the θ direction with wavenumber k^h.

4.4.1 The dispersion relation

We describe the technique in detail for a method with L different node types. Recall that the lowest order SFH method had three node types. The first order SFH method, with $p = 1$, will have six node types. As p increases, L will increase as well. Let us denote the solution value at a node of the l^{th} type, $1 \le l \le L$, located at $\boldsymbol{r}h \in \mathbb{R}^2$, by $\psi_{l,\boldsymbol{r}}$. With our ansatz that these solution values interpolate a plane wave, we have that

$$\psi_{l,\boldsymbol{r}} = a_l e^{i\boldsymbol{k}^h \cdot \boldsymbol{r}h},$$

for some constants a_l.

We will now construct the equation of a fixed stencil within the lattice. Suppose that it corresponds to a node of the t^{th} type, $1 \le t \le L$, that is located at $\boldsymbol{j}h$. For $1 \le l \le L$, define the set $J_{t,l} = \{\boldsymbol{r} \in \mathbb{R}^2 : \boldsymbol{r}$ is a node of type s located at $(\boldsymbol{j}+\boldsymbol{r})h\}$. For $\boldsymbol{r} \in J_{t,l}$, denote the stencil coefficient of the node at location $(\boldsymbol{j}+\boldsymbol{r})h$ by $D_{t,l,\boldsymbol{r}}$. Since plane waves are exact solutions to the Helmholtz equation with zero sources, the stencil's equation is

$$\sum_{l=1}^{L} \sum_{\boldsymbol{r} \in J_{t,l}} D_{t,l,\boldsymbol{r}} \psi_{l,\boldsymbol{j}+\boldsymbol{r}} = 0.$$

Finally, we remove all dependence on $\boldsymbol{j}$ in this equation by dividing by $e^{ik^h \cdot \boldsymbol{j}h}$, so there are L equations in total, with the t^{th} equation given by

$$\sum_{l=1}^{L} a_l \sum_{\boldsymbol{r} \in J_{t,l}} D_{t,l,\boldsymbol{r}} e^{i\boldsymbol{k}^h \cdot \boldsymbol{r}h} = 0. \tag{4.13}$$

Thus, we can now define the $L \times L$ matrix $F(k^h)$ by

$$[F(k^h)]_{t,l} = \sum_{\boldsymbol{r} \in J_{t,l}} D_{t,l,\boldsymbol{r}} e^{ik^h[\cos(\theta),\sin(\theta)]\cdot \boldsymbol{r}h},$$

and observe that (4.13) has a non-trivial solution $a_1, \ldots, a_L$ if and only if k^h is such that

$$\det(F(k^h)) = 0. \tag{4.14}$$

This is the analogue of (4.7) for higher p. We need to solve it to determine k^h for any given θ.

4.4.2 Numerical computation of k^h for the higher order SFH method.

We will use the same values for the exact wavenumber kh and the angle θ as in the lowest order case, namely, $\theta \in \{j\pi/40 : j = 1, \ldots, 20\}$ and $kh \in \{\pi/2^{j+2} : j = 0, \ldots, 8\}$. We also measure the errors ϵ_{disp}, ϵ_{dissip} and ϵ_{total}, defined before. Due to the increased complexity, we are unable to write down analytical expressions for the determinant in each case, as we did in Section 4.3.4. The results for $p = 1, 2$ and 3 are shown in Tables 4.5–4.7, Tables 4.8–4.10 and Tables 4.11–4.13, respectively. We continue to consider the *standard case* of $\tau = 1$, in addition to the nonstandard cases of $\tau = i$, $\tau = i/kh$ and $\tau = 1/kh$. Recall that the latter two cases were motivated by the asymptotic expansion (4.10) in the lowest order case. The tabulated results show that these choices continue to remain superior in the higher order case also.

Taken together, these results and those of Section 4.3.4, indicate that for $\tau = i/kh$, the dissipative error is zero, and the total error goes to zero at the rate

$$\epsilon_{\text{total}} = O(kh)^{2p+3}, \qquad kh \to 0$$

for $p = 0, 1, 2$ and 3. For the remaining values of τ considered, we get convergence of the total error at one less rate. These are the rates we summarized in the introduction (see Table 4.1). To our knowledge, *the SFH method with $\tau = i/kh$ is the only DG method to give such rates comparable to the mixed (HRT) method.*

Table 4.5: Results for $\tau = i$ and $\tau = 1$ for the SFH method with $p = 1$.

	$\tau = i$						$\tau = 1$					
kh	ϵ_{disp}	rate	ϵ_{dissip}	rate	ϵ_{total}	rate	ϵ_{disp}	rate	ϵ_{dissip}	rate	ϵ_{total}	rate
$\pi/2^2$	2.37e-03	-	4.96e-16	-	2.37e-03	-	3.71e-04	-	2.69e-03	-	2.72e-03	-
$\pi/2^3$	1.62e-04	3.87	1.64e-15	-	1.62e-04	3.87	1.14e-05	5.02	1.73e-04	3.96	1.74e-04	3.97
$\pi/2^4$	1.05e-05	3.94	3.39e-15	-	1.05e-05	3.94	3.55e-07	5.01	1.09e-05	3.99	1.09e-05	3.99
$\pi/2^5$	6.72e-07	3.97	5.61e-15	-	6.72e-07	3.97	1.11e-08	5.00	6.84e-07	4.00	6.84e-07	4.00
$\pi/2^6$	4.24e-08	3.99	8.49e-15	-	4.24e-08	3.99	3.46e-10	5.00	4.28e-08	4.00	4.28e-08	4.00
$\pi/2^7$	2.66e-09	3.99	1.75e-14	-	2.66e-09	3.99	1.09e-11	4.99	2.67e-09	4.00	2.67e-09	4.00
$\pi/2^8$	1.67e-10	4.00	3.11e-14	-	1.67e-10	4.00	4.51e-13	4.59	1.67e-10	4.00	1.67e-10	4.00
$\pi/2^9$	1.04e-11	4.00	8.21e-14	-	1.04e-11	4.00	4.93e-13	-	1.04e-11	4.00	1.05e-11	4.00
$\pi/2^{10}$	9.22e-13	3.50	3.07e-13	-	9.72e-13	-	6.43e-13	-	7.39e-13	3.82	9.00e-13	-

Table 4.6: Results for $\tau = \dfrac{i}{kh}$ and $\tau = \dfrac{1}{kh}$ for the SFH method with $p = 1$.

	$\tau = \dfrac{i}{kh}$						$\tau = \dfrac{1}{kh}$					
kh	ϵ_{disp}	rate	ϵ_{dissip}	rate	ϵ_{total}	rate	ϵ_{disp}	rate	ϵ_{dissip}	rate	ϵ_{total}	rate
$\pi/2^2$	1.91e-03	-	7.29e-16	-	1.91e-03	-	2.21e-04	-	2.13e-03	-	2.14e-03	-
$\pi/2^3$	6.58e-05	4.86	2.68e-15	-	6.58e-05	4.86	1.99e-06	6.79	6.84e-05	4.96	6.84e-05	4.97
$\pi/2^4$	2.11e-06	4.96	4.09e-15	-	2.11e-06	4.96	9.17e-08	4.44	2.15e-06	4.99	2.15e-06	4.99
$\pi/2^5$	6.62e-08	4.99	7.82e-15	-	6.62e-08	4.99	3.09e-09	4.89	6.72e-08	5.00	6.72e-08	5.00
$\pi/2^6$	2.07e-09	5.00	8.19e-15	-	2.07e-09	5.00	9.84e-11	4.97	2.10e-09	5.00	2.10e-09	5.00
$\pi/2^7$	6.48e-11	5.00	1.99e-14	-	6.48e-11	5.00	3.06e-12	5.01	6.56e-11	5.00	6.56e-11	5.00
$\pi/2^8$	1.95e-12	5.05	2.33e-14	-	1.95e-12	5.05	1.95e-13	3.97	2.06e-12	4.99	2.07e-12	4.99
$\pi/2^9$	3.56e-13	-	4.39e-14	-	3.57e-13	-	4.05e-13	-	8.88e-14	-	4.08e-13	-
$\pi/2^{10}$	1.03e-12	-	1.60e-13	-	1.03e-12	-	5.19e-13	-	3.31e-13	-	5.21e-13	-

Table 4.7: Results for $\tau = \dfrac{i}{(kh)^3}$ and $\tau = \dfrac{i}{(kh)^4}$ in the SFH method with $p = 1$.

	$\tau = \dfrac{i}{(kh)^3}$						$\tau = \dfrac{i}{(kh)^4}$					
kh	ϵ_{disp}	rate	ϵ_{dissip}	rate	ϵ_{total}	rate	ϵ_{disp}	rate	ϵ_{dissip}	rate	ϵ_{total}	rate
$\pi/2^2$	1.22e-03	-	4.80e-16	-	1.22e-03	-	9.65e-04	-	4.51e-16	-	9.65e-04	-
$\pi/2^3$	9.70e-06	6.97	1.78e-15	-	9.70e-06	6.97	3.32e-06	8.12	1.73e-15	-	3.32e-06	8.12
$\pi/2^4$	5.74e-08	7.40	5.05e-15	-	5.74e-08	7.40	9.06e-08	5.19	3.42e-15	-	9.06e-08	5.19
$\pi/2^5$	2.74e-09	4.39	3.66e-15	-	2.73e-09	4.39	3.13e-09	4.86	6.76e-15	-	3.13e-09	4.86
$\pi/2^6$	9.56e-11	4.84	6.23e-15	-	9.56e-11	4.84	7.99e-11	5.29	1.92e-14	-	7.99e-11	5.29
$\pi/2^7$	6.54e-12	3.87	2.07e-14	-	6.54e-12	3.87	4.18e-10	-	2.35e-14	-	4.18e-10	-

Table 4.8: Results for $\tau = i$ and $\tau = 1$ for the SFH with $p = 2$.

	$\tau = i$						$\tau = 1$					
kh	ϵ_{disp}	rate	ϵ_{dissip}	rate	ϵ_{total}	rate	ϵ_{disp}	rate	ϵ_{dissip}	rate	ϵ_{total}	rate
$\pi/2^2$	2.35e-05	-	1.55e-15	-	2.35e-05	-	2.67e-06	-	2.51e-05	-	2.53e-05	-
$\pi/2^3$	3.87e-07	5.92	1.25e-15	-	3.87e-07	5.92	2.11e-08	6.98	4.02e-07	5.97	4.03e-07	5.97
$\pi/2^4$	6.20e-09	5.97	2.96e-15	-	6.20e-09	5.97	1.66e-10	7.00	6.32e-09	5.99	6.32e-09	5.99
$\pi/2^5$	9.79e-11	5.98	3.78e-15	-	9.79e-11	5.98	1.29e-12	7.00	9.89e-11	6.00	9.89e-11	6.00
$\pi/2^6$	1.50e-12	6.03	1.41e-14	-	1.50e-12	6.03	6.21e-14	-	1.56e-12	5.99	1.56e-12	5.99
$\pi/2^7$	1.54e-13	-	3.98e-14	-	1.54e-13	-	1.02e-13	-	5.40e-14	-	1.02e-13	-

Table 4.9: Results for $\tau = \dfrac{i}{kh}$ and $\tau = \dfrac{1}{kh}$ for the SFH with $p = 2$.

	$\tau = \frac{i}{kh}$						$\tau = \frac{1}{kh}$					
kh	ϵ_{disp}	rate	ϵ_{dissip}	rate	ϵ_{total}	rate	ϵ_{disp}	rate	ϵ_{dissip}	rate	ϵ_{total}	rate
$\pi/2^2$	1.88e-05	-	1.16e-15	-	1.88e-05	-	1.77e-06	-	1.98e-05	-	1.99e-05	-
$\pi/2^3$	1.58e-07	6.90	1.90e-15	-	1.58e-07	6.90	5.35e-09	8.37	1.58e-07	6.97	1.58e-07	6.97
$\pi/2^4$	1.26e-09	6.97	2.80e-15	-	1.26e-09	6.97	2.50e-11	7.74	1.24e-09	6.99	1.24e-09	6.99
$\pi/2^5$	9.87e-12	6.99	1.30e-14	-	9.87e-12	6.99	1.64e-13	-	9.71e-12	7.00	9.71e-12	7.00
$\pi/2^6$	1.16e-13	-	1.92e-14	-	1.16e-13	-	8.44e-14	-	8.54e-14	-	1.18e-13	-
$\pi/2^7$	8.72e-14	-	1.79e-14	-	8.90e-14	-	1.40e-13	-	3.30e-14	-	1.44e-13	-

Table 4.10: Results for $\tau = \dfrac{i}{(kh)^3}$ and $\tau = \dfrac{i}{(kh)^4}$ in the SFH method with $p = 2$.

	$\tau = \frac{i}{(kh)^3}$						$\tau = \frac{i}{(kh)^4}$					
kh	ϵ_{disp}	rate	ϵ_{dissip}	rate	ϵ_{total}	rate	ϵ_{disp}	rate	ϵ_{dissip}	rate	ϵ_{total}	rate
$\pi/2^2$	1.21e-05	-	9.32e-16	-	1.21e-05	-	9.62e-06	-	1.26e-15	-	9.62e-06	-
$\pi/2^3$	2.68e-08	8.81	1.55e-15	-	2.68e-08	8.81	1.20e-08	9.64	1.86e-15	-	1.20e-08	9.64
$\pi/2^4$	6.71e-11	8.64	2.79e-15	-	6.71e-11	8.64	2.86e-11	8.72	2.73e-15	-	2.86e-11	8.72
$\pi/2^5$	8.34e-13	6.33	3.62e-15	-	8.34e-13	6.33	4.06e-12	2.82	6.09e-15	-	4.06e-12	2.82
$\pi/2^6$	1.35e-12	-	1.27e-14	-	1.35e-12	-	5.88e-11	-	7.91e-15	-	5.88e-11	-

Table 4.11: Results for $\tau = i$ and $\tau = 1$ for the SFH with $p = 3$.

	$\tau = i$						$\tau = 1$					
kh	ϵ_{disp}	rate	ϵ_{dissip}	rate	ϵ_{total}	rate	ϵ_{disp}	rate	ϵ_{dissip}	rate	ϵ_{total}	rate
$\pi/2^2$	1.20e-07	-	2.70e-15	-	1.20e-07	-	1.12e-08	-	1.25e-07	-	1.26e-07	-
$\pi/2^3$	4.87e-10	7.94	2.80e-15	-	4.87e-10	7.94	2.23e-11	8.98	4.99e-10	7.97	4.99e-10	7.98
$\pi/2^4$	1.94e-12	7.97	4.62e-15	-	1.94e-12	7.97	3.29e-14	-	1.96e-12	7.99	1.96e-12	7.99
$\pi/2^5$	6.06e-14	-	1.35e-14	-	6.06e-14	-	1.03e-13	-	1.16e-14	-	1.03e-13	-

Table 4.12: Results for $\tau = \dfrac{i}{kh}$ and $\tau = \dfrac{1}{kh}$ for the SFH with $p = 3$.

	$\tau = \frac{i}{kh}$						$\tau = \frac{1}{kh}$					
kh	ϵ_{disp}	rate	ϵ_{dissip}	rate	ϵ_{total}	rate	ϵ_{disp}	rate	ϵ_{dissip}	rate	ϵ_{total}	rate
$\pi/2^2$	9.61e-08	-	9.47e-16	-	9.61e-08	-	7.89e-09	-	9.84e-08	-	9.88e-08	-
$\pi/2^3$	1.98e-10	8.92	2.71e-15	-	1.98e-10	8.92	7.60e-12	10.02	1.96e-10	8.97	1.96e-10	8.98
$\pi/2^4$	3.95e-13	8.97	3.44e-15	-	3.95e-13	8.97	5.99e-14	-	3.81e-13	9.01	3.85e-13	8.99
$\pi/2^5$	6.25e-14	-	5.77e-15	-	6.26e-14	-	2.50e-14	-	8.20e-15	-	2.52e-14	-

Table 4.13: Results for $\tau = \dfrac{i}{(kh)^3}$ and $\tau = \dfrac{i}{(kh)^4}$ in the SFH method with $p = 3$.

	$\tau = \frac{i}{(kh)^3}$						$\tau = \frac{i}{(kh)^4}$					
kh	ϵ_{disp}	rate	ϵ_{dissip}	rate	ϵ_{total}	rate	ϵ_{disp}	rate	ϵ_{dissip}	rate	ϵ_{total}	rate
$\pi/2^2$	6.14e-08	-	1.34e-15	-	6.14e-08	-	4.91e-08	-	1.32e-15	-	4.91e-08	-
$\pi/2^3$	3.51e-11	1.08	3.55e-15	-	3.51e-11	1.08	1.68e-11	1.15	2.81e-15	-	1.68e-11	1.15
$\pi/2^4$	5.41e-14	9.34	2.61e-15	-	5.41e-14	9.34	3.45e-13	5.60	3.93e-15	-	3.45e-13	5.60
$\pi/2^5$	5.00e-13	-	5.66e-15	-	5.00e-13	-	4.46e-14	2.95	1.06e-14	-	4.46e-14	2.95

4.5 Results for LDG-H method

In this section we consider (4.2) with τ set to the same nonzero positive constant on every edge and numerically explore the relation between k^h and k. This was already done in [40] for $p = 0, 1$ and $\tau = 1, \sqrt{3}i/2$. A natural question that arises, in view of the previously described results on SFH method, is whether the LDG-H exhibits better rates if the new-found parameter $\tau = i/kh$ is used.

To answer this, we compute the wavenumber errors of the LDG-H method for the same four values of τ we have been considering in Section 4.3–4.4 for $p = 0, 1, 2$ and 3. The results are in Tables 4.14–4.21. We find that for the imaginary values of τ, the dissipative errors are zero. However, the best rates for the total error that we could observe was $O(hp)^{2p+2}$, one order less than the best rates observed for the SFH method. We also note that the values of $\tau = i/kh$ and $\tau = 1/kh$ that gave better rates for the SFH method, do not give good rates for the LDG-H method, which is expected since the LDG-H method with $\tau = O(1/(kh))$ is not optimal [19, 43].

All the rates observed individually in Tables 4.14–4.21 are summarized together in Table 4.1 of the introduction, where the cases from other sections are also included to facilitate comparison.

Table 4.14: Results for $\tau = i$ and $\tau = 1$ for the LDG-H with $p = 0$.

	$\tau = i$						$\tau = 1$					
kh	ϵ_{disp}	rate	ϵ_{dissip}	rate	ϵ_{total}	rate	ϵ_{disp}	rate	ϵ_{dissip}	rate	ϵ_{total}	rate
$\pi/2^2$	1.41e-01	-	6.39e-16	-	1.41e-01	-	6.16e-02	-	1.74e-01	-	1.84e-01	-
$\pi/2^3$	3.08e-02	2.20	1.77e-15	-	3.08e-02	2.20	8.73e-03	2.82	4.80e-02	1.85	4.88e-02	1.92
$\pi/2^4$	7.23e-03	2.09	1.44e-15	-	7.23e-03	2.09	1.13e-03	2.95	1.23e-02	1.96	1.24e-02	1.98
$\pi/2^5$	1.75e-03	2.04	1.55e-15	-	1.75e-03	2.04	1.42e-04	2.99	3.11e-03	1.99	3.11e-03	1.99
$\pi/2^6$	4.32e-04	2.02	3.44e-15	-	4.32e-04	2.02	1.79e-05	3.00	7.78e-04	2.00	7.79e-04	2.00
$\pi/2^7$	1.07e-04	2.01	1.60e-14	-	1.07e-04	2.01	2.23e-06	3.00	1.95e-04	2.00	1.95e-04	2.00
$\pi/2^8$	2.67e-05	2.01	2.29e-14	-	2.67e-05	2.01	2.79e-07	3.00	4.87e-05	2.00	4.87e-05	2.00
$\pi/2^9$	6.67e-06	2.00	3.00e-14	-	6.67e-06	2.00	3.49e-08	3.00	1.22e-05	2.00	1.22e-05	2.00
$\pi/2^{10}$	1.67e-06	2.00	1.01e-13	-	1.67e-06	2.00	4.36e-09	3.00	3.04e-06	2.00	3.04e-06	2.00

Table 4.15: Results for $\tau = \dfrac{i}{kh}$ and $\tau = \dfrac{1}{kh}$ for the LDG-H with $p = 0$.

	$\tau = \frac{i}{kh}$						$\tau = \frac{1}{kh}$					
kh	ϵ_{disp}	rate	ϵ_{dissip}	rate	ϵ_{total}	rate	ϵ_{disp}	rate	ϵ_{dissip}	rate	ϵ_{total}	rate
$\pi/2^2$	2.39e-01	-	7.28e-16	-	2.39e-01	-	7.97e-02	-	1.93e-01	-	2.09e-01	-
$\pi/2^3$	1.51e-01	0.67	1.46e-15	-	1.51e-01	0.67	3.33e-02	1.26	8.83e-02	1.13	9.43e-02	1.15
$\pi/2^4$	7.98e-02	0.92	1.37e-15	-	7.98e-02	0.92	1.59e-02	1.07	4.30e-02	1.04	4.59e-02	1.04
$\pi/2^5$	4.05e-02	0.98	3.07e-15	-	4.05e-02	0.98	7.84e-03	1.02	2.14e-02	1.01	2.28e-02	1.01
$\pi/2^6$	2.03e-02	0.99	7.53e-15	-	2.03e-02	0.99	3.91e-03	1.00	1.07e-02	1.00	1.14e-02	1.00
$\pi/2^7$	1.02e-02	1.00	1.09e-14	-	1.02e-02	1.00	1.95e-03	1.00	5.33e-03	1.00	5.68e-03	1.00
$\pi/2^8$	5.08e-03	1.00	2.73e-14	-	5.08e-03	1.00	9.76e-04	1.00	2.67e-03	1.00	2.84e-03	1.00
$\pi/2^9$	2.54e-03	1.00	6.68e-14	-	2.54e-03	1.00	4.88e-04	1.00	1.33e-03	1.00	1.42e-03	1.00
$\pi/2^{10}$	1.27e-03	1.00	6.10e-14	-	1.27e-03	1.00	2.44e-04	1.00	6.67e-04	1.00	7.10e-04	1.00

Table 4.16: Results for $\tau = i$ and $\tau = 1$ for the LDG-H with $p = 1$.

	$\tau = i$						$\tau = 1$					
kh	ϵ_{disp}	rate	ϵ_{dissip}	rate	ϵ_{total}	rate	ϵ_{disp}	rate	ϵ_{dissip}	rate	ϵ_{total}	rate
$\pi/2^2$	2.90e-03	-	4.80e-16	-	2.90e-03	-	7.69e-04	-	4.82e-03	-	4.88e-03	-
$\pi/2^3$	1.79e-04	4.02	1.40e-15	-	1.79e-04	4.02	2.37e-05	5.02	3.16e-04	3.93	3.17e-04	3.95
$\pi/2^4$	1.11e-05	4.01	3.01e-15	-	1.11e-05	4.01	7.36e-07	5.01	1.99e-05	3.98	2.00e-05	3.99
$\pi/2^5$	6.89e-07	4.01	4.10e-15	-	6.89e-07	4.01	2.30e-08	5.00	1.25e-06	4.00	1.25e-06	4.00
$\pi/2^6$	4.29e-08	4.00	4.50e-15	-	4.29e-08	4.00	7.18e-10	5.00	7.82e-08	4.00	7.82e-08	4.00
$\pi/2^7$	2.68e-09	4.00	4.00e-14	-	2.68e-09	4.00	2.24e-11	5.00	4.89e-09	4.00	4.89e-09	4.00
$\pi/2^8$	1.67e-10	4.00	3.54e-14	-	1.67e-10	4.00	9.13e-13	4.62	3.05e-10	4.00	3.05e-10	4.00
$\pi/2^9$	1.04e-11	4.01	5.14e-14	-	1.04e-11	4.01	6.05e-13	-	1.91e-11	4.00	1.91e-11	4.00
$\pi/2^{10}$	1.47e-12	-	1.14e-13	-	1.47e-12	-	9.16e-13	-	1.20e-12	3.99	1.49e-12	3.68

Table 4.17: Results for $\tau = \frac{i}{kh}$ and $\tau = \frac{1}{kh}$ for the LDG-H with $p = 1$.

	$\tau = \frac{i}{kh}$						$\tau = \frac{1}{kh}$					
kh	ϵ_{disp}	rate	ϵ_{dissip}	rate	ϵ_{total}	rate	ϵ_{disp}	rate	ϵ_{dissip}	rate	ϵ_{total}	rate
$\pi/2^2$	4.47e-03	-	4.63e-16	-	4.47e-03	-	9.86e-04	-	5.57e-03	-	5.65e-03	-
$\pi/2^3$	6.80e-04	2.71	1.59e-15	-	6.80e-04	2.71	8.79e-05	3.49	6.40e-04	3.12	6.46e-04	3.13
$\pi/2^4$	8.90e-05	2.93	1.36e-15	-	8.90e-05	2.93	9.98e-06	3.14	7.81e-05	3.03	7.88e-05	3.04
$\pi/2^5$	1.13e-05	2.98	5.10e-15	-	1.13e-05	2.98	1.22e-06	3.04	9.71e-06	3.01	9.78e-06	3.01
$\pi/2^6$	1.41e-06	3.00	6.11e-15	-	1.41e-06	3.00	1.51e-07	3.01	1.21e-06	3.00	1.22e-06	3.00
$\pi/2^7$	1.76e-07	3.00	1.98e-14	-	1.76e-07	3.00	1.89e-08	3.00	1.51e-07	3.00	1.53e-07	3.00
$\pi/2^8$	2.21e-08	3.00	5.99e-14	-	2.21e-08	3.00	2.36e-09	3.00	1.89e-08	3.00	1.91e-08	3.00
$\pi/2^9$	2.76e-09	3.00	5.11e-14	-	2.76e-09	3.00	2.94e-10	3.00	2.36e-09	3.00	2.38e-09	3.00
$\pi/2^{10}$	3.45e-10	3.00	1.77e-13	-	3.45e-10	3.00	3.74e-11	2.98	2.96e-10	3.00	2.98e-10	3.00

Table 4.18: Results for $\tau = i$ and $\tau = 1$ for the LDG-H with $p = 2$.

	$\tau = i$						$\tau = 1$					
kh	ϵ_{disp}	rate	ϵ_{dissip}	rate	ϵ_{total}	rate	ϵ_{disp}	rate	ϵ_{dissip}	rate	ϵ_{total}	rate
$\pi/2^2$	2.64e-05	-	8.49e-16	-	2.64e-05	-	5.58e-06	-	4.54e-05	-	4.58e-05	-
$\pi/2^3$	4.12e-07	6.01	2.82e-15	-	4.12e-07	6.01	4.45e-08	6.97	7.33e-07	5.95	7.34e-07	5.96
$\pi/2^4$	6.39e-09	6.01	7.56e-15	-	6.39e-09	6.01	3.50e-10	6.99	1.15e-08	5.99	1.16e-08	5.99
$\pi/2^5$	9.94e-11	6.01	7.11e-15	-	9.94e-11	6.01	2.72e-12	7.01	1.81e-10	6.00	1.81e-10	6.00
$\pi/2^6$	1.63e-12	5.93	5.96e-15	-	1.63e-12	5.93	3.44e-14	6.30	2.83e-12	6.00	2.83e-12	6.00
$\pi/2^7$	1.22e-13	-	7.05e-14	-	1.22e-13	-	1.28e-13	-	6.86e-14	-	1.36e-13	-

Table 4.19: Results for $\tau = \frac{i}{kh}$ and $\tau = \frac{1}{kh}$ for the LDG-H with $p = 2$.

	$\tau = \frac{i}{kh}$						$\tau = \frac{1}{kh}$					
kh	ϵ_{disp}	rate	ϵ_{dissip}	rate	ϵ_{total}	rate	ϵ_{disp}	rate	ϵ_{dissip}	rate	ϵ_{total}	rate
$\pi/2^2$	$4.04e{-}05$	-	$1.34e{-}15$	-	$4.04e{-}05$	-	7.23e-06	-	5.26e-05	-	5.31e-05	-
$\pi/2^3$	$1.54e{-}06$	4.72	$1.40e{-}15$	-	$1.54e{-}06$	4.72	1.68e-07	5.42	1.49e-06	5.14	1.50e-06	5.14
$\pi/2^4$	$5.03e{-}08$	4.93	$3.88e{-}15$	-	$5.03e{-}08$	4.93	4.85e-09	5.12	4.54e-08	5.04	4.57e-08	5.04
$\pi/2^5$	$1.59e{-}09$	4.98	$1.35e{-}14$	-	$1.59e{-}09$	4.98	1.48e-10	5.03	1.41e-09	5.01	1.42e-09	5.01
$\pi/2^6$	$4.98e{-}11$	5.00	$1.27e{-}14$	-	$4.98e{-}11$	5.00	4.61e-12	5.01	4.40e-11	5.00	4.43e-11	5.00
$\pi/2^7$	$1.80e{-}12$	4.79	$3.33e{-}14$	-	$1.80e{-}12$	4.79	1.63e-13	4.82	1.41e-12	4.96	1.41e-12	4.97

Table 4.20: Results for $\tau = i$ and $\tau = 1$ for the LDG-H with $p = 3$.

	$\tau = i$						$\tau = 1$					
kh	ϵ_{disp}	rate	ϵ_{dissip}	rate	ϵ_{total}	rate	ϵ_{disp}	rate	ϵ_{dissip}	rate	ϵ_{total}	rate
$\pi/2^2$	1.30e-07	-	1.54e-15	-	1.30e-07	-	2.34e-08	-	2.27e-07	-	2.28e-07	-
$\pi/2^3$	5.08e-10	8.00	1.87e-15	-	5.08e-10	8.00	4.68e-11	8.97	9.10e-10	7.96	9.11e-10	7.97
$\pi/2^4$	2.00e-12	7.99	5.43e-15	-	2.00e-12	7.99	1.14e-13	8.68	3.58e-12	7.99	3.58e-12	7.99
$\pi/2^5$	7.71e-14	-	9.44e-15	-	7.75e-14	-	5.68e-14	-	1.91e-14	-	5.99e-14	-

Table 4.21: Results for $\tau = \dfrac{i}{kh}$ and $\tau = \dfrac{1}{kh}$ for the LDG-H with $p = 3$.

	$\tau = \frac{i}{kh}$						$\tau = \frac{1}{kh}$					
kh	ϵ_{disp}	rate	ϵ_{dissip}	rate	ϵ_{total}	rate	ϵ_{disp}	rate	ϵ_{dissip}	rate	ϵ_{total}	rate
$\pi/2^2$	1.98e-07	–	8.52e-16	–	1.98e-07	–	3.04e-08	–	2.63e-07	–	2.65e-07	–
$\pi/2^3$	1.87e-09	6.72	2.35e-15	-	1.87e-09	6.72	1.78e-10	7.41	1.86e-09	7.15	1.87e-09	7.15
$\pi/2^4$	1.53e-11	6.94	9.38e-15	-	1.53e-11	6.94	1.28e-12	7.12	1.41e-11	7.04	1.42e-11	7.04
$\pi/2^5$	6.20e-14	-	1.05e-14	-	6.20e-14	-	7.77e-14	-	1.16e-13	-	1.27e-13	-

Conclusions and future works

Conclusions

In the first part of this thesis we applied and analyzed a high order HDG method for the Stokes equations, and then we did the same for the Oseen equations. In both cases, a curved domain was considered. The curved domain was approximated by a polyhedral subdomain. We showed that, under certain assumptions, the numerical schemes were well–posed and provide orders of convergence $k+1$ for the pressure, velocity and its gradient; and order $k+3/2$ for the numerical trace of the velocity and for the element–by–element post–processed velocity. We also provided numerical results validating the error estimates and showing that the method performs optimally even though some of the assumptions cannot be totally guaranteed. In addition, we used Oseen equations to perform a Picard's iteration and numerically solve the incompressible Navier–Stokes equations, and the method also provided optimal orders of convergence. We observe that one of the adventages of our approach is that the mesh does not need fit the domain which is convenient for complicated geometries or evolving boundary. In addition, it can be easily coupled to a standard HDG code for polygonal domains and handling the curved boundary reduces to compute line integrals of locally extrapolated polynomials.

In the second part of the thesis we carried out a dispersion analysis of HDG methods. In particular, we focused on the Single Face HDG (SFH) method, and an analytic expansion for the wavenumber error was obtained for the lowest order case. That expansion showed that the rates achieved by this method with a specific value of the stabilization parameter τ are the same than those of the Hybrid Raviart–Thomas (HRT) method. The numerical experiments validate this behavior also for higher orders.

Future work

According to the work done in the context of curved domains, we have the following future works:

1. The development of a suitable preconditioner to the linear system: we think that the main limitation of our technique is the bad conditioning of the linear system when the polynomial degree increases.

2. Symmetrizing the method: when the global system is assembled, the resultant matrix is not symmetric, and hence the system cannot be solved with some of the well known efficient methods such as conjugate gradient.

3. Analysis of Navier–Stokes equations: since our numerical experiments in chapter 3 showed optimal results when solving Navier–Stokes equations, it is natural to think in carrying out the theoretical analysis of the application of our technique to that problem.

4. Application to more problems: related to the previous item, it would be interesting to continue applying our technique to other interesting problems in the context of Fluid Mechanics.

In turn, in the context of dispersion analysis, the following topics are considered to be done in the future:

1. Other problems: there are many other equations describing wave propagation whose dispersion properties have not been studied yet (Maxwell, acoustic wave equation, among others).

2. Study of equations modelling seismic waves and tsunamis: since Chile is a highly seismic country, it is particularly interesting to study the dispersion properties HDG methods applied to equations modelling seismic waves and tsunamis.

Conclusiones y trabajos futuros

Conclusiones

En la primera parte de esta tesis aplicamos y analizamos un método HDG de alto orden para las euaciones de Stokes, y luego hicimos lo mismo para las ecuaciones de Oseen. En ambos casos, se consideró un dominio curvo. Este dominio es aproximado por un subdominio poliédrico. Mostramos que, bajo ciertos supuestos, los esquemas numéricos están bien planteados y entregan órdenes de convergencia $k+1$ para la presión, velocidad y su gradiente; y orden $k+3/2$ para la traza numérica de la velocidad y para la velocidad postprocesada, calculada elemento a elemento. También mostramos ensayos numéricos en los que se validan las estimaciones de los errores, y en los que se ve que el método se comporta de manera óptima aún en casos en que algunos de los supuestos no pueden ser completamente garantizados. Además, usamos las ecuaciones de Oseen para realizar la iteración de Picard con el fin de resolver las ecuaciones de Navier–Stokes incompresibles, y el método también entregó órdenes de convergencia óptimos. Observamos que una de las ventajas de nuestro método es que la malla no necesita ajustarse al dominio, lo cual es conveniente cuando se trabaja con geometrías complicadas o con fronteras que evolucionan en el tiempo. Además, puede ser fácilmente acoplado con un código HDG para dominios poligonales y la manipulación de la frontera curva se reduce al cálculo de integrales de línea de polinomios extrapolados localmente.

En la segunda parte de esta tesis llevamos a cabo un análisis de dispersión de métodos HDG. En particular, nos enfocamos en el método *Single Face HDG* (SFH), y para el orden más bajo se pudo obtener una expansión analítica para el error del número de onda. Esa expansión mostró que las tasas logradas por este método para un valor específico del parámetro de estabilización τ son las mismas que las del método Raviart–Thomas híbrido (HRT). Los experimentos numéricos validan este comportamiento también para órdenes más altos.

Trabajos futuros

De acuerdo al trabajo realizado en el contexto de dominios curvos, tenemos los siguientes trabajos futuros:

1. El desarrollo de un precondicionador adecuado: pensamos que la principal limitación de nuestra técnica es el mal condicionamiento de la matriz del sistema lineal cuando el grado polinomial aumenta.

2. Simetrizar el método: cuando el sistema global es ensambado, la matriz resultante no es simétrica, y por lo tanto, el sistema no puede ser resuelto usando alguno de los métodos eficientes bien conocidos, como por ejemplo el gradiente conjugado.

3. Análisis de las ecuaciones de Navier–Stokes: dado que nuestros experimentos numéricos en el capítulo 3 muestran resultados óptimos cuando se resuleven las ecuaciones de Navier–Stokes, resulta natural pensar en llevar a cabo el análisis teórico de la aplicación de nuestra técnica a ese problema.

4. Aplicación a más problemas: relacionado con el punto anterior, sería interesante continuar aplicando nuestra técnica a otros problemas interesantes en el contexto de la Mecánica de Fluidos.

A su vez, en el contexto de análisis de dispersion, los siguientes temas están considerados para ser hechos en el futuro:

1. Otros problemas: hay muchas otras ecuaciones que describen propagación de ondas cuyas propiedades dispersivas no han sido estudiadas todavía (Maxwell, ecuación de la onda acústica, entre otras).

2. Estudio de ecuaciones que modelan ondas sísmicas y tsunamis: dado que Chile es un país altamente sísmico, resulta particularmente interesante estudiar las propiedades dispersivas de métodos HDG aplicados a ecuaciones que modelan ondas sísmicas y tsunamis.

Appendices

APPENDIX A

HDG implementation

The HDG method (2.4) can be implemented similarly to the standard HDG method for polygonal domains [52]. The boundary data $\widetilde{\boldsymbol{g}}_h$ defined in (1.2) produces a slight modification in the global system, as we will see. We first construct the local matrices associated to an element $K \in \mathsf{T}_h$ and the boundary data will be imposed after the global matrix is assembled. To fix ideas we briefly describe the two dimensional case. Let $K \in \mathsf{T}_h$ with edges e_1, e_2 and e_3, $N_{\mathrm{L}} = \dim(\mathrm{P}_k(K))$, $N_{\boldsymbol{u}} = \dim(\boldsymbol{\mathcal{P}}_k(K))$, $N_p = \dim(\mathcal{P}_k(K))$ and $N_{\widehat{\boldsymbol{u}}_h} = \dim(\boldsymbol{\mathcal{P}}_k(e_1)) = \dim(\boldsymbol{\mathcal{P}}_k(e_2)) = \dim(\boldsymbol{\mathcal{P}}_k(e_3))$. Let $\{\Psi_j\}_{j=1}^{N_{\mathrm{L}}}$, $\{\boldsymbol{\psi}_j\}_{j=1}^{N_{\boldsymbol{u}}}$, $\{\psi_j\}_{j=1}^{N_p}$ and $\{\boldsymbol{\xi}_j^{e_l}\}_{j=1}^{N_{\widehat{\boldsymbol{u}}_h}}$ ($l = 1$, 2 and 3) the basis function of $\mathrm{P}_k(K)$, $\boldsymbol{\mathcal{P}}_k(K)$, $\mathcal{P}_k(K)$ and $\mathcal{P}_k(e_l)$, respectively. In our numerical experiments we considered Dubiner basis [47] for the polynomial spaces in K and Legendre basis for the polynomial space on the edges. We write now the unknowns restricted to K as linear combination of the basis functions, i.e., $\mathrm{L}_h|_K = \sum_{j=1}^{N_{\mathrm{L}}} \alpha_j^K \Psi_j$, $\boldsymbol{u}_h|_K = \sum_{j=1}^{N_{\boldsymbol{u}}} \beta_j^K \boldsymbol{\psi}_j$, $\widetilde{p}_h|_K = \sum_{j=1}^{N_p} \gamma_j^K \psi_j$ and $\widehat{\boldsymbol{u}}_h|_{e_l} = \sum_{j=1}^{N_{\widehat{\boldsymbol{u}}_h}} \lambda_j^{e_l} \boldsymbol{\xi}_j^{e_l}$. We decompose $\widetilde{p}_h|_K = \overline{p_h}^K + \rho_h$, where $\overline{p_h}^K \in \mathcal{P}_0(K)$ and $\rho_h \in \mathcal{P}_k(K) \cap L_0^2(K)$. Since Dubiner basis are orthogonal on K and ψ_1 is a constant, then $\rho_h = \sum_{j=2}^{N_p} \gamma_j^K \psi_j$. Thus, the system associated to (2.4a)-(2.4c) is of the form

$$\mathbf{A}^K \begin{bmatrix} \boldsymbol{\alpha}^K \\ \boldsymbol{\beta}^K \\ \boldsymbol{\gamma}^K \end{bmatrix} = \mathbf{E}^K \begin{bmatrix} \boldsymbol{\lambda}^{e_1} \\ \boldsymbol{\lambda}^{e_2} \\ \boldsymbol{\lambda}^{e_3} \end{bmatrix} + \mathbf{F}^K, \quad \text{where } \mathbf{A}^K \in \mathbb{R}^{N_T \times N_T}, \mathbf{E}^K \in \mathbb{R}^{N_T \times 3N_{\widehat{\boldsymbol{u}}_h}}, \tag{A.1}$$

$\mathbf{F}^K \in \mathbb{R}^{N_T}$ and $N_T := N_{\mathrm{L}} + N_{\boldsymbol{u}} + N_p$. On the other hand, the local contribution of the global equation (2.4g) can be written in the following matrix form

$$\mathbf{B}^K \begin{bmatrix} \boldsymbol{\alpha}^K \\ \boldsymbol{\beta}^K \\ \boldsymbol{\gamma}^K \end{bmatrix} - \mathbf{H}^K \overline{p_h}^K = \boldsymbol{\Lambda}^K \begin{bmatrix} \boldsymbol{\lambda}^{e_1} \\ \boldsymbol{\lambda}^{e_2} \\ \boldsymbol{\lambda}^{e_3} \end{bmatrix}, \text{ where } \mathbf{B}^K \in \mathbb{R}^{3N_{\widehat{\boldsymbol{u}}_h} \times N_T}, \mathbf{H}^K \in \mathbb{R}^{3N_{\widehat{\boldsymbol{u}}_h}} \tag{A.2}$$

and $\boldsymbol{\Lambda}^K \in \mathbb{R}^{3N_{\widehat{\boldsymbol{u}}_h} \times 3N_{\widehat{\boldsymbol{u}}_h}}$. Since the matrix on the left hand side of (A.1) is invertible, we express the unknowns $\boldsymbol{\alpha}^K$, $\boldsymbol{\beta}^K$ and $\boldsymbol{\gamma}^K$ in terms of $\boldsymbol{\lambda}^{e_l}$ and substitute them in (A.2) to obtain a local system of

the form

$$\mathbf{M}^K \begin{bmatrix} \boldsymbol{\lambda}^{e_1} \\ \boldsymbol{\lambda}^{e_2} \\ \boldsymbol{\lambda}^{e_3} \end{bmatrix} + \mathbf{H}^K \overline{p_h}^K = \mathbf{b}^K, \quad \text{where } \mathbf{M}^K \in \mathbb{R}^{N_{\widehat{\boldsymbol{u}}_h} \times N_{\widehat{\boldsymbol{u}}_h}} \text{ and } \mathbf{b}^K \in \mathbb{R}^{N_{\widehat{\boldsymbol{u}}_h}}. \tag{A.3}$$

Now, let N_e and N_K be the number of edges and elements of the triangulation. We denote by $\boldsymbol{\lambda}^l$ $(l = 1, \ \ldots \ , N_e)$ the global unknowns associated to the l-th edge. We define the global vectors $\boldsymbol{\lambda} = [(\boldsymbol{\lambda}^1)^t, ..., (\boldsymbol{\lambda}^{N_e})^t]^t$ and $\boldsymbol{\sigma} = [\overline{p}_h^{K_1}, ..., \overline{p}_h^{K_{N_K}}]^t$. Thus, once the above local matrices are computed, we assembly on the edges of the triangulation and obtain the global system of the form

$$\begin{bmatrix} \mathbf{M} & \mathbf{H} \end{bmatrix} \begin{bmatrix} \boldsymbol{\lambda} \\ \boldsymbol{\sigma} \end{bmatrix} = \mathbf{b}, \quad \text{where} \quad \mathbf{M} \in \mathbb{R}^{(N_e N_{\widehat{\boldsymbol{u}}_h}) \times (N_e N_{\widehat{\boldsymbol{u}}_h})}, \mathbf{H} \in \mathbb{R}^{(N_e N_{\widehat{\boldsymbol{u}}_h}) \times N_K} \tag{A.4}$$

and $\mathbf{b} \in \mathbb{R}^{(N_e N_{\widehat{\boldsymbol{u}}_h})}$. In addition, equation (2.4f) can be written as $[|K_1| \quad \ldots \quad |K_{N_K}|]\boldsymbol{\sigma} = 0$, which, together with (A.4) and the boundary condition, fully determines $\boldsymbol{\lambda}$ and $\boldsymbol{\sigma}$.

We proceed now to impose the boundary condition. Let $e \in \mathcal{E}_h^{\partial}$ and K^e the triangle where it belongs. We assume that the only boundary edge of K is e and denote by e_1 and e_2 the other two edges. If K had two boundary edges the procedure is analogous. From (2.4d) and (2.31) we have that

$$\boldsymbol{\Lambda}^e \boldsymbol{\lambda}^e = \mathbf{b}^{\boldsymbol{g}} - \mathbf{J}^e \boldsymbol{\alpha}^{K^e},$$

where

$$\mathbf{b}^{\boldsymbol{g}} := \left\{ \int_e \int_0^{l(\boldsymbol{x})} \boldsymbol{g}(\bar{\boldsymbol{x}}(\boldsymbol{x})) \cdot \boldsymbol{\xi}_i^e(\boldsymbol{x}) \, ds \, d\boldsymbol{x} \right\}_{i=1}^{N_{\widehat{\boldsymbol{u}}_h}}$$

and

$$\mathbf{J}^e := \left\{ \int_e \int_0^{l(\boldsymbol{x})} \boldsymbol{\Psi}_j(\boldsymbol{x} + s\boldsymbol{t}(\boldsymbol{x})) \boldsymbol{t}(\boldsymbol{x}) \cdot \boldsymbol{\xi}_i^e(\boldsymbol{x}) \, ds \, d\boldsymbol{x} \right\}_{i=1}^{N_{\widehat{\boldsymbol{u}}_h}}.$$

Here, we see how the basis functions $\boldsymbol{\Psi}_j$ (defined in K) are being evaluated (extrapolated) along the path $\boldsymbol{x} + s\boldsymbol{t}(\boldsymbol{x})$. From (A.1) we write $\boldsymbol{\alpha}^K$ in terms of $\boldsymbol{\lambda}^{e_1}$, $\boldsymbol{\lambda}^{e_2}$ and $\boldsymbol{\lambda}^e$, say $\boldsymbol{\alpha}^K = \mathbf{K} \begin{bmatrix} \boldsymbol{\lambda}^{e_1} \\ \boldsymbol{\lambda}^{e_2} \\ \boldsymbol{\lambda}^e \end{bmatrix} + \mathbf{r}$, and obtain the system

$$\left[\begin{bmatrix} \boldsymbol{\Theta}_{N_{\widehat{\boldsymbol{u}}_h} \times 3N_{\widehat{\boldsymbol{u}}_h}} & \boldsymbol{\Theta}_{N_{\widehat{\boldsymbol{u}}_h} \times 3N_{\widehat{\boldsymbol{u}}_h}} & \boldsymbol{\Lambda}^e \end{bmatrix} + \mathbf{J}^e \mathbf{K} \right] \begin{bmatrix} \boldsymbol{\lambda}^{e_1} \\ \boldsymbol{\lambda}^{e_2} \\ \boldsymbol{\lambda}^e \end{bmatrix} = \mathbf{b}^{\boldsymbol{g}} - \mathbf{J}^e \mathbf{r}. \tag{A.5}$$

Finally, we substitute the rows in (A.4) associated to the global degrees of freedom of the edge e by the equations in (A.5). This resulting global system is not symmetric (unless $\mathbf{J}^e = \boldsymbol{\Theta}$). If Ω were polygonal, then $\mathbf{J}^e = \boldsymbol{\Theta}$ and the (A.5) becomes $\boldsymbol{\Lambda}^e \boldsymbol{\lambda}^e = \mathbf{b}^{\boldsymbol{g}}$ which is one of the ways to impose Dirichlet boundary conditions.

APPENDIX B

Integration over curved regions

In order to compute the approximation $\overline{p_h}^{\mathsf{D}_h}$ and errors in D_h^c, integrals over $\widetilde{K}_{ext}^e$ must be calculated. We write $\widetilde{K}_{ext}^e$ as a union of three disjoint regions T_1, T_2 and S as Fig. B.1 shows. The same quadrature rules considered in the calculation of the local matrices of the method are used now in the triangles T_1 and T_2. Now, let e_S and Γ_S denote the straight and curved part of the boundary of S, resp. For a point $\boldsymbol{x}$ in Γ_h, we construct $\sigma_{\boldsymbol{n}_S}(\boldsymbol{x})$, where $\boldsymbol{n}_S$ is the unit normal of e_S pointing to Γ_S. Thus, for a smooth enough function q defined on S, we approximate

$$\int_S q(\boldsymbol{x})d\boldsymbol{x} = \int_{e_S}\int_0^{l(\boldsymbol{x})} q(\boldsymbol{x}+t\boldsymbol{n}_S)\boldsymbol{n}_S\,dt\,d\boldsymbol{x}$$

using one-dimensional quadrature on both integrals.

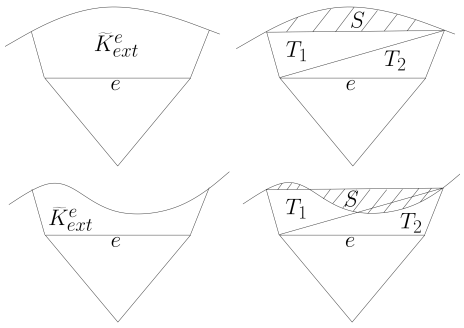

Figure B.1: Examples of $\widetilde{K}_{ext}^e$ divided in triangles T_1 and T_2, and a region S (dashed area).

References

[1] M. Ainsworth, *Discrete dispersion relation for hp-version finite element approximation at high wave number*, SIAM Journal on Numerical Analysis, 42 (2004), pp. 553–575.

[2] ——, *Dispersive and dissipative behaviour of high order discontinuous Galerkin finite element methods*, J. Comput. Phys., 198 (2004), pp. 106–130.

[3] M. Ainsworth, P. Monk, and W. Muniz, *Dispersive and dissipative properties of discontinuous Galerkin finite element methods for the second order wave equation*, Journal of Scientific Computing, 27 (2006), pp. 5–40.

[4] R. Araya, M. Solano, and P. Vega, *Analysis of an adaptive HDG method for the Brinkman problem*, IMA Journal of Numerical Analysis, (2018), p. dry031.

[5] I. M. Babuška and S. A. Sauter, *Is the pollution effect of the FEM avoidable for the Helmholtz equation considering high wave numbers?*, SIAM Journal on Numerical Analysis, 34 (1997), pp. 2392–2423.

[6] J. W. Barret and C. M. Elliot, *Fitted and unfitted finite-element methods for elliptic equations with smooth interfaces*, IMA Journal of Numerical Analysis, 7 (1987), pp. 283–300.

[7] J. H. Bramble, T. Dupont, and V. Thomée, *Projection methods for Dirichlet's problem in approximating polygonal domains with boundary-value corrections*, Mathematics of Computation, 26 (1972), pp. 869–879.

[8] J. H. Bramble and J. T. King, *A robust finite element method for nonhomogeneous Dirichlet problems in domains with curved boundaries*, Mathematics of Computation, 63 (1994), pp. 1–17.

[9] J. H. Bramble and J. T. King, *A finite element method for interface problems in domains with smooth boundaries and interfaces*, Advances in Computational Mathematics, 6 (1996), pp. 109–138.

[10] F. Brezzi and M. Fortin, *Mixed and Hybrid Finite Element Methods*, Springer-Verlag, Berlin, Heidelberg, 1991.

[11] A. Cesmelioglu, B. Cockburn, N. C. Nguyen, and J. Peraire, *Analysis of HDG methods for Oseen Equations*, Journal of Scientific Computing, 55 (2013), pp. 392–431.

[12] A. Cesmelioglu, B. Cockburn, and W. Qiu, *Analysis of a hybridizable discontinuous Galerkin method for the steady-state incompressible Navier–Stokes equations*, Math. Comput., 86 (2017), pp. 1643–1670.

[13] E. Chung, B. Cockburn, and G. Fu, *The staggered DG method is the limit of a hybridizable DG method*, SIAM Journal on Numerical Analysis, 52 (2014), pp. 915–932.

[14] E. Chung and B. Engquist, *Optimal discontinuous Galerkin methods for the acoustic wave equation in higher dimensions*, SIAM Journal on Numerical Analysis, 47 (2009), pp. 3820–3848.

[15] B. Cockburn, B. Dong, and J. Guzmán, *A superconvergent LDG-hybridizable Galerkin method for second-order elliptic problems*, Mathematics of Computation, 77 (2008), pp. 1887–1916.

[16] B. Cockburn and J. Gopalakrishnan, *The derivation of hybridizable discontinuous Galerkin methods for Stokes flow*, SIAM Journal on Numerical Analysis, 47 (2009), pp. 1092–1125.

[17] B. Cockburn, J. Gopalakrishnan, and R. Lazarov, *Unified hybridization of discontinuous Galerkin, mixed, and continuous Galerkin methods for second order elliptic problems*, SIAM Journal on Numerical Analysis, 47 (2009), pp. 1319–1365.

[18] B. Cockburn, J. Gopalakrishnan, N. C. Nguyen, J. Peraire, and F.-J. Sayas, *Analysis of HDG methods for Stokes flow*, Mathematics of Computation, 80 (2011), pp. 723–760.

[19] B. Cockburn, J. Gopalakrishnan, and F.-J. Sayas, *A projection-based error analysis of HDG methods*, Mathematics of Computation, 79 (2010), pp. 1351–1367.

[20] B. Cockburn, D. Gupta, and F. Reitich, *Boundary-conforming discontinuous Galerkin methods via extensions from subdomains*, Journal of Scientific Computing, 42 (2009), pp. 144–184.

[21] B. Cockburn, W. Qiu, and M. Solano, *A priori error analysis for HDG methods using extensions from subdomains to achieve boundary conformity*, Mathematics of Computation, 83 (2014), pp. 665–699.

[22] B. Cockburn and F.-J. Sayas, *Divergence-conforming HDG methods for Stokes flows*, Mathematics of Computation, 83 (2014), pp. 1571–1598.

[23] B. Cockburn and M. Solano, *Solving Dirichlet boundary-value problems on curved domains by extensions from subdomains*, SIAM Journal on Scientific Computing, 34 (2012), pp. A497–A519.

[24] B. Cockburn and M. Solano, *Solving convection-diffusion problems on curved domains by extensions from subdomains*, Journal of Scientific Computing, 59 (2014), pp. 512–543.

[25] J. Cui and W. Zhang, *An analysis of HDG methods for the Helmholtz equation*, IMA Journal of Numerical Analysis, 34 (2014), pp. 279–295.

[26] M. Dauge, *Stationary Stokes and Navier–Stokes systems on two- or three-dimensional domains with corners. Part I. Linearized Equations*, SIAM Journal on Mathematical Analysis, 20 (1989), pp. 74–97.

[27] T. A. Davis, *Algorithm 832: UMFPACK v4.3—An unsymmetric-pattern multifrontal method*, ACM Trans. Math. Softw., 30 (2004), pp. 196–199.

[28] J. D. De Basabe, M. K. Sen, and M. F. Wheeler, *The interior penalty discontinuous Galerkin method for elastic wave propagation: grid dispersion*, Geophysical Journal International, 175 (2008), pp. 83–93.

[29] K. Deckelnick, A. Günther, and M. Hinze, *Finite element approximation of Dirichlet boundary control for elliptic PDEs on two- and three-dimensional curved domains*, SIAM Journal on Control and Optimization, 48 (2009), pp. 2798–2819.

[30] A. Deraemaeker, I. M. Babuška, and P. Bouillard, *Dispersion and pollution of the FEM solution for the Helmholtz equation in one, two and three dimensions*, International Journal for Numerical Methods in Engineering, 46 (1999), pp. 471–499.

[31] D. A. Di Pietro and A. Ern, *Mathematical aspects of discontinuous Galerkin methods*, vol. 69 of Mathématiques & Applications, Springer–Verlag, Berlin–Heilderber, 2012.

[32] H. Dong, B. Wang, Z. Xie, and L.-L. Wang, *An unfitted hybridizable discontinuous Galerkin method for the Poisson interface problem and its error analysis*, IMA Journal of Numerical Analysis, 37 (2017), pp. 444–476.

[33] G. Fu, Y. Jin, and W. Qiu, *Parameter-free superconvergent h(div)-conforming HDG methods for the Brinkman equations*, IMA Journal of Numerical Analysis, (2018), p. dry001.

[34] G. N. Gatica and F. A. Sequeira, *Analysis of an augmented HDG method for a class of quasi-newtonian Stokes flows*, Journal of Scientific Computing, 65 (2015), pp. 1270–1308.

[35] ——, *A priori and a posteriori error analyses of an augmented HDG method for a class of quasi-newtonian Stokes flows*, Journal of Scientific Computing, 69 (2016), pp. 1192–1250.

[36] ——, *Analysis of the HDG method for the Stokes–Darcy coupling*, Numerical Methods for Partial Differential Equations, 33 (2017), pp. 885–917.

[37] L. F. Gatica and F. A. Sequeira, *A priori and a posteriori error analyses of an HDG method for the Brinkman problem*, Computers and Mathematics with Applications, 75 (2018), pp. 1191 – 1212.

[38] G. Giorgiani, S. Fernández-Méndez, and A. Huerta, *Hybridizable discontinuous Galerkin p-adaptivity for wave propagation problems*, International Journal for Numerical Methods in Fluids, 72 (2013), pp. 1244–1262.

[39] C. J. Gittelson and R. Hiptmair, *Dispersion analysis of plane wave discontinuous Galerkin methods*, International Journal for Numerical Methods in Engineering, 98 (2014), pp. 313–323.

[40] J. Gopalakrishnan, S. Lanteri, N. Olivares, and R. Perrussel, *Stabilization in relation to wavenumber in HDG methods*, Advanced Modeling and Simulation in Engineering Sciences, 2 (2015), p. 13.

[41] J. Gopalakrishnan, I. Muga, and N. Olivares, *Dispersive and dissipative errors in the DPG method with scaled norms for the Helmholtz equation*, SIAM J. Sci. Comput., 36 (2014), pp. A20–A39.

[42] J. Gopalakrishnan, M. Solano, and F. Vargas, *Dispersion analysis of HDG methods*, Journal of Scientific Computing, 77 (2018), pp. 1703–1735.

[43] R. Griesmaier and P. Monk, *Error analysis for a hybridizable discontinuous Galerkin method for the Helmholtz equation*, Journal of Scientific Computing, 49 (2011), pp. 291–310.

[44] J. Guzmán, M. A. Sánchez, and M. Sarkis, *Higher-order finite element methods for elliptic problems with interfaces*, ESAIM: M2AN, 50 (2016), pp. 1561–1583.

[45] F. Q. Hu, M. Hussaini, and P. Rasetarinera, *An analysis of the discontinuous Galerkin method for wave propagation problems*, Journal of Computational Physics, 151 (1999), pp. 921–946.

[46] R. Kellogg and J. Osborn, *A regularity result for the Stokes problem in a convex polygon*, Journal of Functional Analysis, 21 (1976), pp. 397 – 431.

[47] R. C. Kirby, *Singularity-free evaluation of collapsed-coordinate orthogonal polynomials*, ACM Trans. Math. Softw., 37 (2010), pp. 5:1–5:16.

[48] M. Lenoir, *Optimal isoparametric finite elements and error estimates for domains involving curved boundaries*, SIAM Journal on Numerical Analysis, 23 (1986), pp. 562–580.

[49] R. J. LeVeque and Z. Li, *Immersed interface methods for Stokes flow with elastic boundaries or surface tension*, SIAM J. Sci. Comput., 18 (1997), pp. 709–735.

[50] J. Li, J. M. Melenk, B. I. Wohlmuth, and J. Zou, *Optimal convergence of higher order finite element methods for elliptic interface problems*, Appl. Numer. Math., 60 (2010), pp. 19–37.

[51] Y. Mori, *Convergence proof of the velocity field for a Stokes flow immersed boundary method*, Communications on Pure and Applied Mathematics, 61 (2008), pp. 1213–1263.

[52] N. C. Nguyen, J. Peraire, and B. Cockburn, *A hybridizable discontinuous Galerkin method for Stokes flow*, Computer Methods in Applied Mechanics and Engineering, 199 (2010), pp. 582 – 597.

[53] ——, *An implicit high-order hybridizable discontinuous Galerkin method for the incompressible Navier–Stokes equations*, Journal of Computational Physics, 230 (2011), pp. 1147 – 1170.

[54] J. Nitsche, *Über ein variationsprinzip zur lösung von Dirichlet-problemen bei verwendung von teilräumen, die keinen randbedingungen unterworfen sind*, Abhandlungen aus dem Mathematischen Seminar der Universität Hamburg, 36 (1971), pp. 9–15.

[55] R. Oyarzúa, M. Solano, and P. Zúñiga, *A high order mixed-FEM for diffusion problems on curved domains.* https://www.ci2ma.udec.cl/publicaciones/prepublicaciones/prepublicacion.php?id=323, 2018.

[56] J. Peraire, N. C. Nguyen, and B. Cockburn, *A hybridizable discontinuous Galerkin method for the compressible Euler and Navier–Stokes equations*, in 48th AIAA Aerospace Sciences Meeting Including the New Horizons Forum and Aerospace Exposition, 12 2010.

[57] ——, *A hybridizable discontinuous Galerkin method for the compressible Euler and Navier–Stokes equations*, in 48th AIAA Aerospace Sciences Meeting Including the New Horizons Forum and Aerospace Exposition, 12 2010.

[58] C. S. Peskin, *Flow patterns around heart valves: A numerical method*, Journal of Computational Physics, 10 (1972), pp. 252 – 271.

[59] D. Peterseim and S. Sauter, *The composite mini elementâĂŤcoarse mesh computation of Stokes flows on complicated domains*, SIAM Journal on Numerical Analysis, 46 (2008), pp. 3181–3206.

[60] D. Peterseim and S. A. Sauter, *Finite element methods for the Stokes problem on complicated domains*, Computer Methods in Applied Mechanics and Engineering, 200 (2011), pp. 2611 – 2623.

[61] W. Qiu and K. Shi, *A superconvergent HDG method for the incompressible Navier–Stokes equations on general polyhedral meshes*, IMA Journal of Numerical Analysis, 36 (2016), pp. 1943–1967.

[62] W. Qiu, M. Solano, and P. Vega, *A high order HDG method for curved-interface problems via approximations from straight triangulations*, Journal of Scientific Computing, 69 (2016), pp. 1384–1407.

[63] S. Rhebergen and G. N. Wells, *A hybridizable discontinuous Galerkin method for the Navier–Stokes equations with pointwise divergence-free velocity field*, Journal of Scientific Computing, 76 (2018), pp. 1484–1501.

[64] S. Sherwin, *Dispersion Analysis of the Continuous and Discontinuous Galerkin Formulations*, Springer Berlin Heidelberg, Berlin, Heidelberg, 2000, pp. 425–431.

[65] M. Solano and F. vargas, *A high order HDG method for Stokes flow in curved domains.* https://www.ci2ma.udec.cl/publicaciones/prepublicaciones/prepublicacion.php?id=227, 2016.

[66] ——, *Analysis of an HDG method for Oseen equations in curved domains.* https://www.ci2ma.udec.cl/publicaciones/prepublicaciones, 2018.

[67] V. Thomée, *Polygonal domain approximation in Dirichlet's problem*, IMA Journal of Applied Mathematics, 11 (1973), pp. 33–44.